1-1-2003

Modeling groundwater flow and transport of contaminants at the Cherokee Former Manufactured Gas Plant site, Iowa

Rahul Biyani
Iowa State University

Modeling groundwater flow and transport of contaminants at the Cherokee Former Manufactured Gas Plant site, Iowa

by

Rahul Biyani

A thesis submitted to the graduate faculty

in partial fulfillment of the requirements for the degree of

MASTER OF SCIENCE

Major: Civil Engineering (Geotechnical Engineering)

Program of Study Committee:
Bruce Kjartanson, Co-major Professor
Say Kee Ong, Co-major Professor
Johanshir Golchin
William W. Simpkins

Iowa State University

Ames, Iowa

2003

Graduate College
Iowa State University

This is to certify that the master's thesis of

Rahul Biyani

has met the requirements of Iowa State University

Signatures have been redacted for privacy

DEDICATION

To

My parents

&

Vaishali

for their invaluable love, support and encouragement

TABLE OF CONTENTS

ACKNOWLEDGEMENTS

I would like to thank my major professors, Dr. Bruce Kjartanson and Dr. Say Kee Ong, for their immense support and guidance. I am thankful to Dr. Greg Stenback for his timely advices and useful comments. I acknowledge my thesis committee members, Dr. Johanshir Golchin and Dr. William Simpkins for giving support and valuable time. Special thanks to Shane Rogers for inspiring me to do research, sharing information and discussing concepts.

ABSTRACT

Improper disposal of wastes by former MGP sites has resulted in serious environmental threats today. Some of the main contaminants from MGP activities include tar, benzene, toluene, ethylbenzene and xylenes (BTEX), polycyclic aromatic hydrocarbons (PAH), metals and cynides. During the last decade, monitored natural attenuation (MNA) has become one of the widely accepted choices among researchers and regulators for the clean up of such contaminated sites.

The objectives of this study were to develop protocols for the use of Geoprobe direct push technologies (DPT) to characterize the geology and hydrogeology at FMGP sites, compare the capabilities of several publicly available groundwater flow and contaminant transport models (BIOSCREEN, BIOPLUME III and MODFLOW/MODPATH/RT3D) and select a model with the best overall capabilities to model groundwater flow, contaminant transport and to estimate the field-scale biodegradation rates for the implementation of natural attenuation at the Cherokee, Iowa FMGP site.

DPT pre-packed screen monitoring wells and dual tube direct push equipment were found to provide results that were equivalent to conventional 2-inch monitoring wells for groundwater sampling and hydraulic conductivity. Use of DPT electrical conductivity probes allowed geological stratigraphy to be easily mapped and provided detailed information of a pinch zone that restricted the groundwater flow at the site. Comparison of different groundwater and transport model showed MODFLOW/MODPATH/RT3D is a more versatile model due to its ability to model the flow and transport in 3-D and provide stable groundwater head and contaminant

concentration results. Biodegradation rates were computed using analytical and numerical (modeling) methods for selected compounds. Biodegradation rates for BTEX and PAH estimated by analytical method varied from 0.00019 d^{-1} to 0.0022 d^{-1} and 0.00003 d^{-1} to 0.0003 d^{-1}, respectively. Biodegradation rates calculated for toluene and phenanthrene by numerical method were 0.03 d^{-1} and 0.006 d^{-1}. Rates calculated by these two methods were different because of incomplete source characterization and insufficient groundwater sampling locations. A sensitivity analysis of the RT3D model showed that biodegradation rate is the most sensitive parameter.

CHAPTER 1 INTRODUCTION

1.1. Background

" The first gas light in the United States was lit in 1796 by M. Ambiose Co., which experimented with coal gas illumination in Philadelphia" (Hatheway, 1997). In 1816, Baltimore, Maryland became the first American city to establish a manufactured gas plant (MGP) to supply its residences, streets, and businesses with commercial manufactured gas (Warnes, 1919). Thereafter a steady demand for manufactured gas led to the installation of gas works in most towns of 10,000 or more residents and in some cases in towns with less population also.

At around 1900, the discovery of low cost carburetted water gas resulted in the expansion of manufactured gas usage even to smaller towns. But carburetted water gas plants soon suffered from severe shortages and price hikes of coke, a smokeless fuel. Coke was later substituted by coal to run the industry. The result of using coal was that 'water gas' tars became emulsified with water far beyond the contents tolerated (4-6 percent) by the tar distillers. Manufacturers started disposing of this useless by-product in the environment, causing harm to aquatic life, contamination of drinking water, destruction of crops and other associated health problems (Hatheway, 1997).

Regulatory bodies soon made the discharge of toxic tars to the environment more stringent. The rise of environmental concerns along with the discovery of large and reliable natural gas fields weakened the market for manufactured gas. As a result, most of the manufactured gas plants stopped operations by 1966 (Hatheway, 2000). In 1970, the first National Air Pollution Control Act was passed. These air pollution regulations further closed down the remaining gas manufacturing plants by 1990.

Although almost all of the MGP sites have been closed, they have left behind a legacy of impacted soil, groundwater and sediment. Most of the contamination at these sites resulted from leaking gas holders, oil tanks, tar cisterns, spills, and leachate from unlined holding ponds (Mueller et al., 1989; Fischer et al., 1999).

Contaminants include tar residues and sludges dominated by various trace elements, volatile organic compounds (VOCs), monoaromatic hydrocarbons (MAHs), and polycyclic aromatic hydrocarbons (PAHs) (Luthy et al., 1994). The major contaminants of importance at former MGP sites are PAHs and benzene, toluene, ethylbenzene and xylenes (BTEX).

PAHs are ubiquitous environmental pollutants of natural or anthropogenic origin (Dietmar et al., 2000). They are of concern because some of them are carcinogens and mutagens (World Health Organization, 1983). The hydrophobic nature, low biodegradability and low volatility of PAH make them more challenging to remediate than BTEX.

In 1980, U.S. Congress passed the Comprehensive Environmental Response, Compensation and Liability Act (CERCLA) for the clean up of contaminated sites. Fourteen former manufactured gas plant (FMGP) sites were included in the National Priority List. The average remediation cost of a FMGP site, as per survey of 269 sites, across the United States, conducted by GEI Consultants Inc., in December 2001, varied from $1.9 million in EPA Region 9 (southwest) to $19.3 million in EPA Region 10 (Northwest) (O'Neil, 2001). The large cost associated with remediation of FMGP sites as well as the technical limitations due to the variety and quantity of contaminants make the remediation process difficult.

Monitored natural attenuation (MNA) has evolved in the last decade as a viable and cost effective remediation alternative at a number of sites where the risk of exposure to contaminants is within acceptable limits. This technique, which is also referred to as natural assimilation, intrinsic bioremediation, natural recovery or passive remediation, relies on natural processes without human intervention to reduce contaminant concentrations in soil and groundwater. Important mechanisms causing contaminant flow and attenuation are advection, dispersion, sorption, dissolution from a residual source, and abiotic and biological transformations (biodegradation) (Rifai et al., 1995). Using indigenous microorganisms, the biodegradation process may destroy hazardous chemicals by converting them into innocuous byproducts, under both aerobic and anerobic conditions. MNA rely on

accurate hydrogeological, chemical and biological site characterizations, detailed data analysis, modeling of fate and transport of the contaminants and long term monitoring (Boulding, 1993a, 1993b; EPA, 1997a) to demonstrate adequate public and environmental protection.

The major challenge in evaluating natural attenuation at a site is not to show that the amount of contaminants is decreasing with distance and time but whether the transformation processes yield an Environmentally Acceptable Concentration (EAC) within a reasonable time frame (Golchin et al., 2000). These processes become important when natural attenuation does not reduce the concentration levels of contaminants reaching the receptor below hazardous levels set by regulatory agencies. In such situations, natural attenuation at a site may be enhanced by removing and treating, destroying or immobilizing contaminants (Golchin et al., 2000). This remediation approach is called Monitored Enhanced Natural Attenuation (MENA).

MENA involves long term monitoring of contaminants. Sometimes monitoring could go for years before the plume reaches steady state conditions. Since MNA or MENA is a fairly new remediation approach, there is not much literature available on its application for FMGP contaminated sites. The following chapters in this thesis focus on the development of various protocols for site characterization and modeling the fate and transport of contaminants at a FMGP site in Cherokee, Iowa.

1.2. Research Objectives

The objectives of this research are as follows:

1. Develop protocols for the use of Geoprobe direct push technologies to allow adequate development of geological and hydrogeological conceptual site models and optimizing groundwater monitoring for a MNA remedial approach.
2. Compare the capabilities of several publicly available groundwater flow/contaminant transport models (BIOSCREEN, BIOPLUME III and MODFLOW/MODPATH/RT3D) and select the model with the best overall capabilities for assessment of natural attenuation process at FMGP sites.

3. Use the selected model to model the groundwater flow, contaminant transport and to estimate the field-scale biodegradation rates at a specific site. Compare these rates to laboratory-scale biodegradation rates obtained in parallel studies by others or to published results.

Work related to objectives 1 and 3 is being carried out at the Cherokee FMGP site and by using past data obtained at the Cherokee site.

1.3. Tasks

The above objectives will be achieved by performing the following tasks:

Objective 1

1. Build a geological conceptual site model using the geologic data collected in the field with electrical conductivity probes and soil core boring data.
2. Build a hydrogeological conceptual site model using monitoring well water levels and direct push technology (DPT) hydraulic conductivity values calculated from the data obtained by conducting slug tests in new DPT pre-packed monitoring wells and Geoprobe dual tube direct push mechanisms.
3. Characterize the site soils using geotechnical index tests and organic carbon tests on soil cores obtained with DPT.
4. Conduct groundwater sampling using DPT to obtain groundwater PAH and BTEX concentrations and compare them with historical values. These comparisons will later aid in evaluating natural attenuation as an effective remedial tool.
5. Using the above work carried out at the Cherokee FMGP site, develop protocols for the application of DPT technologies for characterization and groundwater monitoring for a natural attenuation remedial strategy.

Objective 2

1. Identify the required input data for various groundwater flow / contaminant transport models and determine if the available data are sufficient to obtain input parameters. Otherwise, determine how the input parameters can be estimated.
2. Assess how the estimation could affect the efficacy of the modeled results.

3. Assess the capabilities of models to handle complexities in geology and hydrogeology at the site.
4. Assess the capabilities of models to produce stable groundwater flow and contaminant transport results.
5. Assess how the source terms are modeled for FMGP sites.
6. Assess the role of parameter sensitivity analysis.
7. Assess matching of historical data to the plumes.
8. Assess how the models forecast the plume migration or dissipation.
9. Select the model with the best overall capabilities.

Objective 3

1. Using the selected model and input data obtained from the field and laboratory, calibrate the model against historical data, evaluate the biodegradation rate and natural attenuation constants of several PAH and BTEX compounds.
2. Compare the rate constants with those estimated from laboratory studies conducted by others or in the literature and with analytical solutions.

1.4. Organization of Thesis

Chapter 1 gives a brief overview of the thesis. Chapter 2 is a literature review discusses environmental issues associated with FMGP sites. The contaminants of importance, their properties, site characterization techniques and several FMGP and petroleum site case histories are discussed. In addition, a comparison of different models for groundwater flow and fate and contaminant transport studies is given. Chapter 3 describes the protocols formulated for site characterization activities, their application at site and analyzes the results to define the geology and the hydrogeology at Cherokee FMGP site. Chapter 4 describes the modeling of the fate and transport of the contaminants at the Cherokee FMGP site. Chapter 5 discusses the results and gives conclusions of site characterization activities, fate and transport modeling of contaminants and compares the results with the actual observations at the Cherokee FMGP site. Site related data are placed in the appendices.

1.5. References

Boulding, J.R., 1993a. Subsurface Characterization and Monitoring Techniques, A Desk Reference Guide, Volume I: Solids and Groundwater. EPA/625/R-93/003a. Office of Research and Development, United States Environmental Protection Agency, Washington, DC.

Boulding, J.R., 1993b. Subsurface Characterization and Monitoring Techniques, A Desk Reference Guide, Volume I: The Vadose Zone, Field Screening and Analytical Methods. EPA/625/R-93/003b. Office of Research and Development, United States Environmental Protection Agency, Washington, DC.

Dietmar, K., Seifert, M., Vaananen, V., and Niessner, R., 2000. Determination of Polycyclic Aromatic Hydrocarbons in Contaminated Water and Soil Samples by Immunological and Chromatographic Methods. Environmental Science and Technology, 34 (10), 2035-2041.

EPA, 1997. Use of Monitored Natural Attenuation at Superfund, RCRA Corrective Action, and Underground Storage Tank Sites, OSWER Directive Number: 9200.4-17. United States Environmental Protection Agency, Office of Solid Waste and Emergency Response, Washington DC.

Fischer, C.L.J., Schmitter, R.D., O' Neil, E., 1999. Manufactured Gas Plants: The Environment Legacy. <http://www.hsrc.org/hsrc/html/tosc/sswtosc/mgp.html - introduction>. Publication of Hazardous Substance Research Center, Atlanta, GA. (Date accessed: March 29, 2002).

Golchin, J., Stenback, G.A., Kjartanson, B.H., and Ong, S.K., 2000. A Streamlined Process for Contaminated Site Closure. Proceedings, 13th Annual International Symposium on Site Remediation Technologies and Environmental Management Practices in the Utility Industry, December 4-7, Lake Buena Vista (Orlando), FL.

Hatheway, A.W., 1997. Manufactured Gas Plants: Yesterday's Pride, Today's Liability. Civil Engineering, ASCE, 67(11), 38-41.

Hatheway, A.W., 2000. Site and Waste Characterization and Remedial Engineering of Former Manufacturing Gas Plants and other Coal Tar Sites. http://www.hatheway.net. (Date accessed: March 15, 2002).

Luthy, R.G., Dzombak, D. A., Peters, C.A., Roy, S.B., Ramaswamy, A., Nakles, D.V., and Nott, B.R., 1994. Remediating Tar-Contaminated Soils at Manufacturing Gas Plant Sites. Environmental Science and Technology, 28 (6): 266-276.

Mueller, J.G., Chapman, P.J., Pritchard, P.H., 1989. Creosote-Contaminated Sites-Their Potential for Bioremediation. Environmental Science and Technology, 23: 1197-1201.

O'Neil, M., 2001. Some EPA Region More Costly Than Others? <http://www.geiconsultants.com/newsletters/PDF/MGP12_01.pdf>. Survey Report by GEI Consultants, Winchester, MD. (Date accessed: April 30, 2002).

Rifai, H.S., Newell, C.J., Miller, R., Taffinder, S., and Rounsaville, M., 1995. Simulation of Natural Attenuation with Multiple Electron Acceptors. In Intrinsic Bioremediation, R.E. Hinchee, J.T. Wilson and D.C. Downey (eds.), Battelle Press, Columbus, OH. 53-58.

Warnes, A.R., 1919. Coal Tar and Some of Its Products. Sir Isaac Pitman and Sons, Ltd; London.

World Health Organization, 1983. IARC Monographs on the Evaluation of Carcinogenic Risk of Chemicals to Humans. Polynuclear Aromatic Compounds, Part 1, Chemical, Environmental and Experimental Data, Vol. 32. International Agency for Research on Cancer, Lyon, France.

CHAPTER 2 LITERATURE REVIEW

2.1. FMGP Sites: An Environmental Concern

In the early 20th century, MGP became a major source of energy for lighting and heating (Hatheway, 1997). It was estimated that at the peak of the industry in the 1920's and 1930's, there were more than 10,000 MGPs in operation throughout North America and Europe (Ackerman et al., year not known). However, the growing availability of low-cost natural gas delivered by a network of pipelines in the mid-twentieth century led to its replacement (Srivastava, 1997; Larsen, 1997; Fischer et al., 1999; Edison Electric Institute, 1984).

Most of the unused or abandoned manufactured gas plants got demolished and the property sold to the gas and electric utility companies. The utility companies became responsible for the liabilities associated with the former MGP sites. It is estimated that during their use from 1880 to 1950, MGPs produced approximately 15 trillion cubic feet of gas and approximately 11 billion gallons of tar as a by-product (Srivastava, 1997) and thereby, resulted in thousands of acres of contaminated land and millions of gallons of impacted water. Many of the wastes generated and dumped during the manufacturing of gas contained substances now recognized as hazardous, including some chemicals known or suspected to cause cancer. Waste disposal practices at former MGPs have created serious environmental problems today. By-products from the gas plants were discharged into the nearest water body or into on- or off-site shallow pits, tar wells or lagoons. Historical spills or leaks that occurred during gas generation, purification, and storage had enhanced the environmental concerns. In general, the wastes released from these plants contaminated soils, sediments, and surface and groundwater at or near the manufacturing facilities (GZA, 1998). Typical impacted area ranged from half an acre to over 100 acres. It is estimated that cleaning up or containing the waste could cost between $25-75 billion to the utility industries in the next thirty years (Murarka, 1995).

Apart from health and environmental issues, former MGP sites also represent a vast amount of unused and under-developed land. The federal brownfields communities encourage investigation, remediation, and redevelopment of such sites. But before starting the remediation and redevelopment work at former MGP sites, these sites must be investigated to delineate onsite and potential offsite environmental impacts. An extensive investigation needs to be made to determine the waste materials at the sites and to decide remediation technologies that can be utilized to clean up the various contaminated media (Fischer et al., 1999).

2.2. Chemicals of Concern and Remediation Challenges at MGP sites

The common waste products found at former MGPs are tars, oils, lampblack, benzene, toluene, ethylbenzene, and xylene (BTEX), volatile organic compounds (VOCs), semi-volatile organic compounds (SVOCs), phenolics, polynuclear aromatic hydrocarbons (PAHs), cyanides, thiocyanates, metals (arsenic, chromium, copper, lead, nickel, and zinc), ammoniates, nitrates, sludges, ash, coke, ammonia, lime wastes, inorganic spent oxides (ferrocyanide) and sulfates/sulfides (Hatheway, 1997; Larsen, 1997; Srivastava, 1997; GZA, 1998; GRI, 1987). The wide variety of contaminants and the range in their physical and chemical properties makes the remediation of FMGP sites a challenge. The technology that works at one site may not work at another site. The base contaminant, coal tar, is composed of a complex and variable mixture of PAHs. The variability in coal tar composition is a function of the type of coal used and of the type of gasification process employed. Coal tar deposits generally consist of four fractions: solid or semi-solid, light non-aqueous phase liquids (LNAPL), dense non-aqueous phase liquids (DNAPL), and water-soluble hydrocarbons (Thrall, 1988). The solid or semi-solid portion tends to stay in place, the LNAPL migrates until it collects and floats on the groundwater surface, the DNAPL can migrate downward into the aquifer until it encounters a low-permeability layer and the water-soluble compounds dissolve into the groundwater (Thrall, 1988). Pools of coal tar collected at the bottom of an aquifer due to spill can act as a continuous source of groundwater contamination (Fischer et. al., 1999). The

presence of oils, which are LNAPLs, and tars, which are DNAPLs, creates a dual concern at MGP sites - migration of two groups of compounds at different depths, speeds, directions and requiring different groundwater treatment technologies.

The volume, characteristics, and toxicity of the wastes at contaminated sites depend on many factors such as the type of gas manufacturing process used, the raw materials and the feedstock used in the manufacturing process, and the former disposal practices for the by-products (Luthy et al., 1994; Larsen, 1997; GZA, 1998). Table 2.1 summarizes the numerous by-products or wastes produced from different gas manufacturing processes. Table 2.2 lists the chemical classes and common wastes/chemicals in each class encountered at FMGP sites (GRI, 1987). Table 2.3 summarizes the common physical and chemical properties of the several PAHs and BTEX compounds.

Table 2.1. Wastes or by-products from different gas manufacturing processes

By-product or Waste	Coal Carbonization	Carbureted Water Gas	Oil Gas
Coal Tar	X	X	-
Oil Tar	-	X	X
Lampblack	-	-	X
Tar/Oil/Water Emulsions	-	X	X
Tar Decanter Sludge	X	-	-
Ammonia Saturator Sludge	X	-	-
Acid/Caustic Hydrocarbon Treatment Sludges	X	-	-
Wastewater Treatment Sludges	X	X	X
Coke	X	-	-
Ash	X	X	X
Spent Oxide/Lime	X	X	X
Sulfur Scrubber Blow Downs	X	X	X
Ammonium Sulfate	X	-	-

The variety of possible inorganic and organic chemicals at FMGP sites and wide range of physical and chemical properties they exhibit makes the remediation

task a challenge. The other problems are that the owners of the sites may have changed several times in the past and the sites may have been used for multiple purposes. These sites had been used as city waste dumping stations, service stations and for residential purposes, causing commingling of different types of wastes. It is difficult to track the distribution of a variety of contaminants and their movement. The fate and transport of contaminants at FMGP sites is a subject of vast research activities. The following sections in this chapter describe the approaches used for site remediation and closure process, site characterization tools, computer models for fate and transport of contaminants and several case studies showing their successful implementation.

Table 2.2. Typical chemicals found at FMGP site (GRI, 1987)

Inorganics	Metals	Volatile Aromatics	Phenolics	PAHs
Ammonia	Aluminum	Benzene	Phenol	Acenaphthene
Cyanide	Antimony	Ethylbenzene	2-Methylphenol	Acenaphthylene
Nitrate	Arsenic	Toluene	4-Methylphenol	Anthracene
Sulfate	Barium	Xylenes	2,4-Dimethylphenol	Benzo(a)anthracene
Sulfide	Cadmium			Benzo(a)pyrene
Thiocyanates	Chromium			Benzo(b)fluoranthene
	Copper			Benzo(g,h,i)perylene
	Iron			Benzo(k)fluoranthene
	Lead			Chrysene
	Manganese			Dibenz(a,h)anthracene
	Mercury			Dibenzofuran
	Nickel			Fluoranthene
	Selenium			Fluorene
	Silver			Naphthalene
	Vanadium			Phenanthrene
	Zinc			Pyrene
				2-Methylnaphthalene

Table 2.3. Physical and chemical properties of BTEX and PAH compounds (Rogers et al., 2002; LaGrega et al., 1994)

Compound	Pure Solid Aqueous Solubility (μg/L)	Molecular Weight (g/mole)	Melting Temp. (^{0}C)	Vapor Pressure (Pa)	Henry's Law Constant (KPa m^3/mole)	n-Octanol Water Partition Coefficient (log K_{ow})	Organic Carbon Partition coefficient (log K_{oc})	Freundlich Parameters		
								pH	K (mg/kg)	1/n
Benzene	1.78E+7	78.12	5.5[1]	12.65E+3	5.5E-1	2.12	1.91	7	1	2.9
Toluene	5.15E-+5	92.15	-93[1]	3.77E+3	6.7E-1	2.73	2.47	5.6	26	0.44
Ethylbenzene	1.52E+5	106.18	-95[1]	1.26E+3	8.0E-1	3.15	3.04	7.3	53	0.79
Xylene	1.98E+5	106.18	-25[1]	8.77E+2	7.0E-1	3.26	2.38	7.3	85	0.19
Naphthalene	3.1E+4	128.18	81.0	1.04E+1	4.89E-2	3.37	3.11	NA	NA	NA
Acenaphthene	3.42E+3	154.21	95.0	2.9E-1	1.48E-2	4.00	3.65	5.3	190	0.36
Acenaphthylene	3.93E+3	152.2	93.0	8.9E-1	1.14E-3	3.70	3.4	5.3	115	0.37
Anthracene	4.5E+1	178.24	216.4	8.0E-4	7.30E-2	4.45	4.15	5.3	376	0.7
Fluorene	1.7E+3	166.22	116.0	8.0E-2	1.01E-2	4.18	3.86	5.3	330	0.28
Phenanthrene	1.0E+3	178.24	100.5	1.6E-2	3.98E-3	4.46	4.15	5.3	215	0.44
Fluoranthene	2.06E+2	202.26	108.8	1.2E-3	6.54E-4*	4.90	4.58	5.3	664	0.61
Pyrene	1.30E+2	202.26	150.4	6.0E-4	1.10E-3	4.88	4.58	NR	389	0.39
Chrysene	1.8	228.3	252.8	8.4E-5*	6.5E-5	5.61	5.3	NR	716	0.46
Benz(a)anthracene	5.7	228.3	160.7	2.8E-5	5.8E-4	5.60	6.14	NA	NA	NA
Benzo(b)fluoranthene	14	252.32	168.3	6.7E-5*	5.1E-5	6.06	5.74	NA	NA	NA
Benzo(k)fluoranthene	4.3	252.32	215.7	1.3E-8*	4.4E-5*	6.06	5.74	7.1	181	0.57
Benzo(a)pyrene	3.8	252.32	178.1	7.3E-7	3.4E-5*	6.06	6.74	7.1	34	0.44
Dinenz(a,h)anthracene	0.5	278.36	266.6	1.3E-8*	7.0E-6	6.80	6.52	7.1	69	0.75
Indeno(1,2,3-cd)pyrene	0.53	276.34	163.6	1.3E-8*	2.9E-5*	6.50	6.2	NA	NA	NA
Benzo(g,h,l)perylene	0.26	276.34	278.3	1.4E-8	2.7E-5*	6.51	6.2	7	11	0.37

NR - Not reported, NA - not available, * at 20 ^{0} C, others at 25^0 C

[1] - All in liquid state

2.3. Natural Attenuation

U.S. EPA (1997a) defines monitored natural attenuation as the reliance on natural attenuation processes (within the context of a carefully controlled and monitored site clean up approach) to achieve site specific remedial objectives within a time frame that is reasonable compared to that offered by other more active methods. The various in-situ physical, chemical and biological processes include biodegradation, dispersion, dilution, sorption, volatilization and chemical or biological stabilization, transformation or destruction of contaminants. The processes act without human intervention to reduce the mass, toxicity, mobility, volume or concentration of contaminants in soil and groundwater (Wiedemeier et al., 1999)

Natural attenuation offers various advantages in comparison to conventional engineered remediation technologies. It is a non-intrusive, less costly, no waste generating technique which may transform contaminants to innocuous by-products. It has certain limitations including longer monitoring time frame, changing hydrogeological and geochemical conditions and formation of intermediate compounds that may be more toxic than the original compounds (Wiedemeier et al., 1999).

Natural attenuation can be used in conjunction with, or as a follow-up to, several other active remedial measures. If used with engineered remedial technologies, the process is termed Monitored Enhanced Natural Attenuation (MENA). MENA is developed as a viable site remedial and closure approach by a research team at ISU/IDNR. Examples of engineered enhancements currently in use are removal and treatment of contaminated soils, recovery of dense non-aqueous phase liquids (DNAPLs) and use of air sparging/soil vapor extraction to rapidly reduce the overall mass of contamination and accelerate natural attenuation (Golchin et al., 2000).

2.4. Direct Push Technology

The advent of direct push technology in the last two decades has given a viable alternative to the conventional drilling methods for conducting subsurface

investigations. Direct push (DP) refers to a set of tools and sensors that are pushed or driven into the ground without removing soil cuttings to collect soil and groundwater samples and continuous information about subsurface properties such as stratigraphy and contaminant distribution (www.Geoprobe.com, 2001). DP probing rods can be advanced into the ground by using either high frequency percussion hammer system or hydraulic ram system using the weight of the truck as a reaction force (shown in Figure 2.1).

Expedited site characterization (ESC) relies on rapid collection of high quality data and its on-site analysis. DP technology serves the ESC requirement very efficiently and cost-effectively. Using DP technology, depth-discrete soil, soil gas and groundwater sampling can be done rapidly. In addition it can be used to install small temporary or permanent monitoring wells, piezometers, soil vapor extraction wells and air sparging injection points (EPA, 1997b).

In contrast to the conventional drilling methods, DP technology produces a minimal amount of waste, does not bring out the contaminated or other hazardous material, and can effectively grout and seal the surface to prevent vertical transport of contaminants down the penetrated hole while sampling soil and groundwater (Thornton et al., 1997, EPA, 1997b)

DP technology works effectively only in unconsolidated sediments, typically to depths less than 100 feet. DP compacts the soil due to advancement and retraction of the probe rods and thereby reduces the hydraulic conductivity of the soil at the point of their advancement. But the potential advantages of DP outweigh these small associated problems.

2.4.1. Soil sampling DP tools

There are two types of soil samplers: sealed and non-sealed. While sampling at a contaminated site, sealed samplers are preferred because they produce representative and depth discrete soil samples. Non-sealed samplers cannot be used below water table as the contaminated groundwater may enter the drive casing

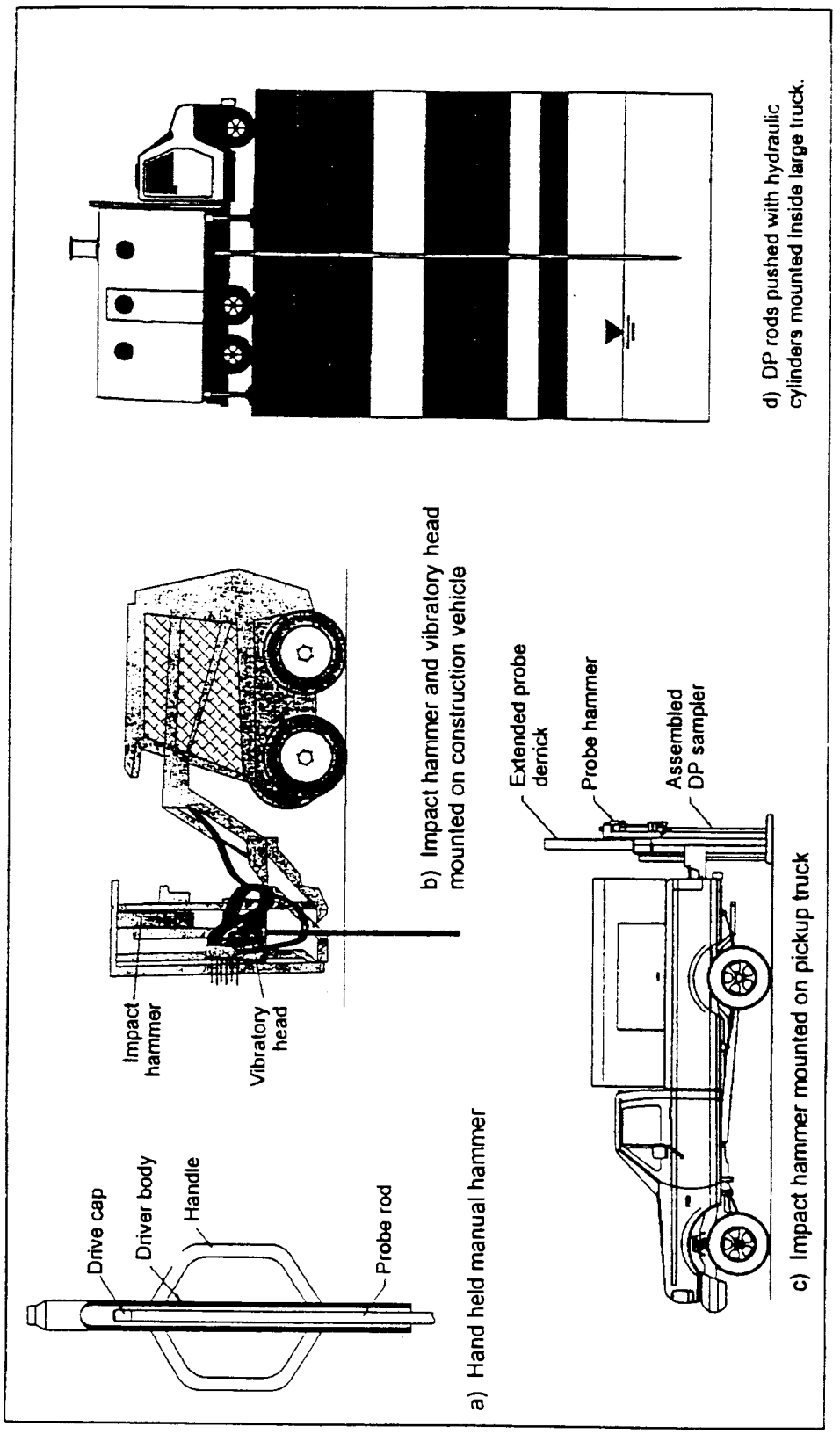

Figure 2.1. Equipment used to advance direct push rods (source: EPA, 1997b)

through the open bottom. Figure 2.2 explains the soil sampling procedure using sealed soil sampler.

2.4.2. Groundwater sampling DP tools

Like soil sampling tools, there are two types of groundwater sampling tools: exposed and sealed samplers. Groundwater samplers with DP technology can be used for one time sampling or can be left for an extended period of time (permanent or temporary monitoring well). Exposed ground water samplers can be used for multi-level sampling in a single probe but it has many disadvantages associated with it such as dragging down of NAPLs, contaminated soil and/or contaminated groundwater and clogging of exposed screen by silts and clays as it moves through fine layers. Sealed screen samplers are more appropriate for depth discrete groundwater sampling and can be used as either temporary or long term monitoring wells. The advantage of the sealed screen sampler is that the well screen is not exposed to soil while the tool is being pushed to the target depth. Therefore chances of plugging the screen and contamination of sample are highly reduced. Figure 2.3 shows the different types of groundwater samplers. The quantity of groundwater sampled depends on the hydraulic conductivity of formation. Water can be collected from the samplers by bailers, check valve pumps or peristaltic pumps.

DP methods can be used to install the permanent monitoring wells. Figure 2.4 exhibits the pre-packed screen monitoring well. Studies in literature show the ability of DP samplers to collect groundwater of quality equivalent to that by conventional monitoring wells (EPA, 2001; Smolley and Kappmeyer, 1991; Zemo et al., 1994). The issue that is most concerned with groundwater sampling is the stratification of contaminants and collection of representative samples from the contaminated site. Studies have shown that the concentrations of organic compounds may vary by several orders of magnitude over vertical distances of few centimeters (Cherry, 1990). Conventional monitoring wells are screened over many feet while high concentrations of contaminants may be limited only to a few inches,

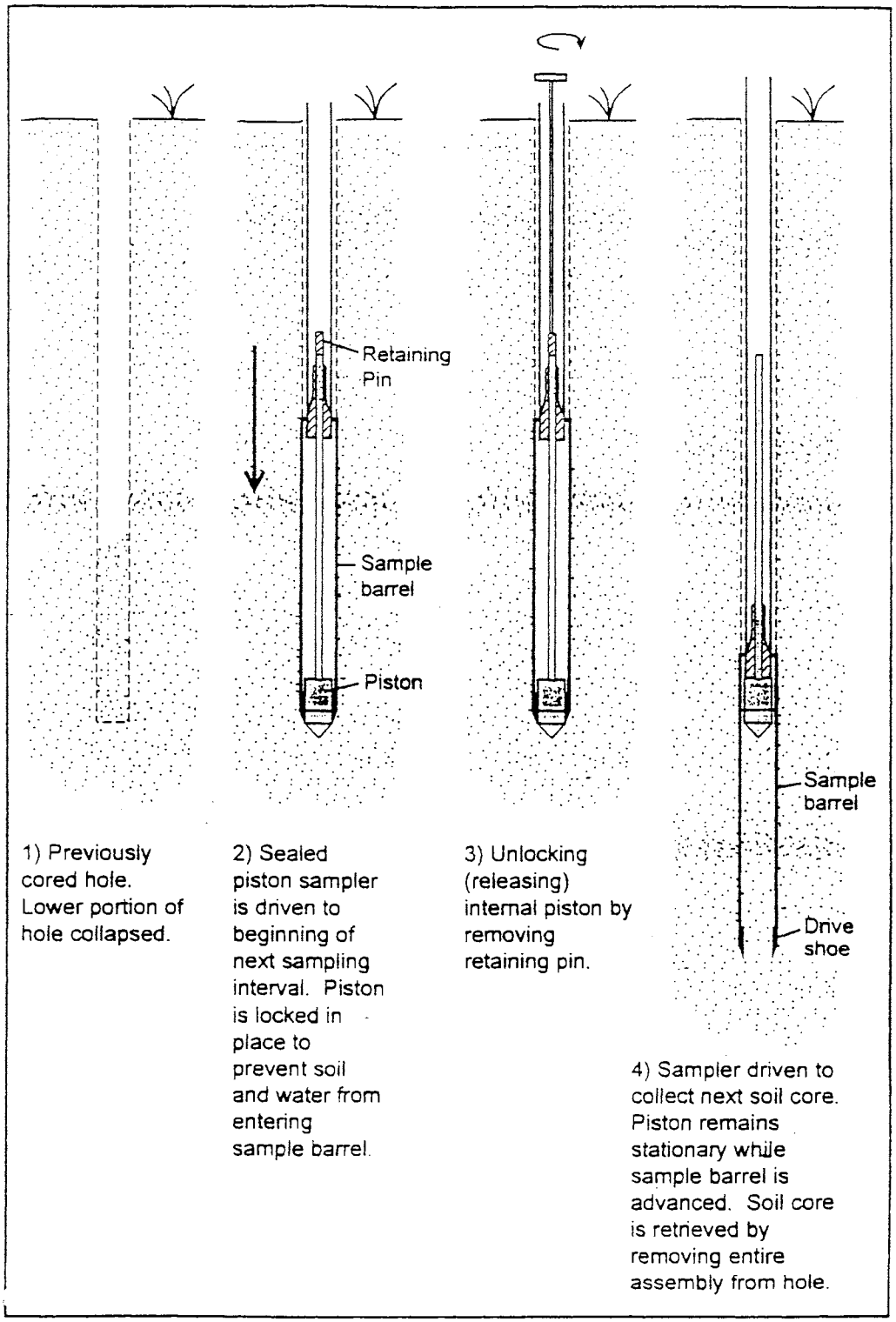

Figure 2.2. Soil sampling using the sealed direct push soil sampler (source: Geoprobe® Syestems, 2001)

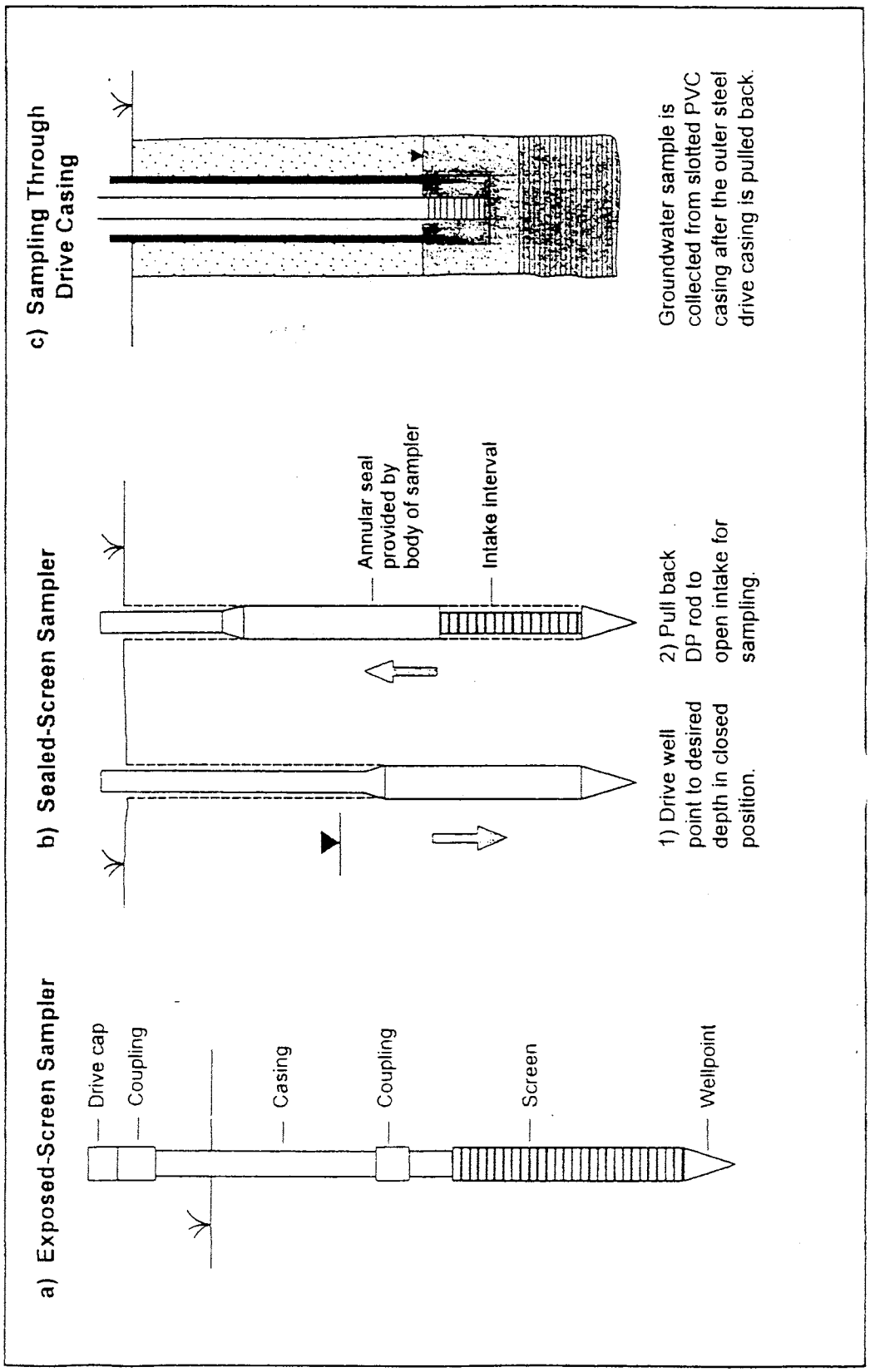

Figure 2.3. Types of direct push groundwater sampling tools (source: EPA, 1997b)

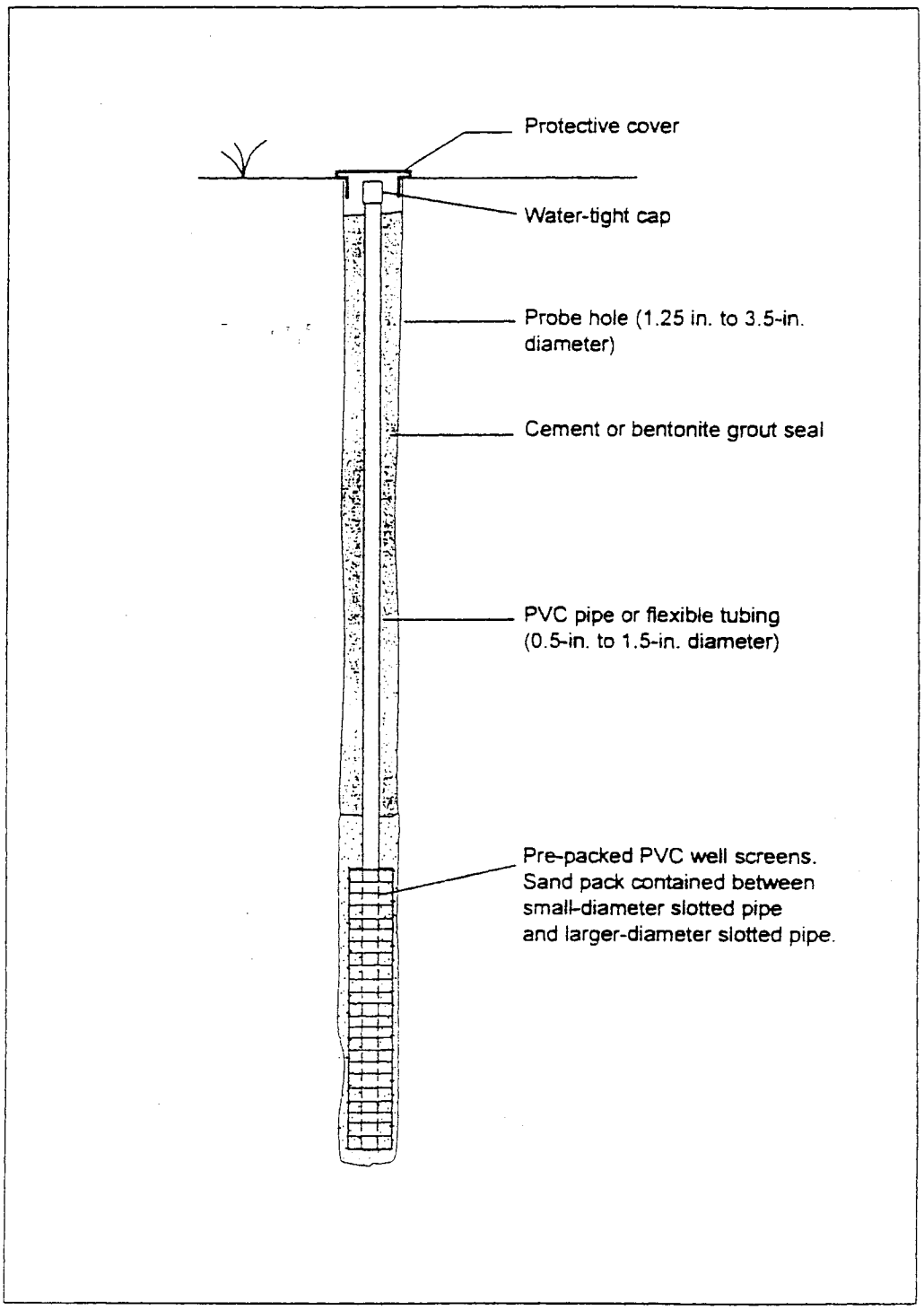

Figure 2.4. Pre-packed screen monitoring well (source: EPA, 1997b)

therefore resulting in a sample that represents an average for the entire screen length. DP wells can be used to avoid this problem by installing wells in a close nest at different depths and thereby collecting depth-discrete and representative samples for chemical analysis. The other advantage of DP pre-packed screen monitoring well is that they can be used in formations composed of silts. DPT wells are generally less costly and quick to install as they reach steady state conditions fast (because of their small diameters) in comparison to traditional 2-inch monitoring wells.

2.4.3. Hydraulic tests with DP equipment

Kansas Geological Survey (KGS) research group has demonstrated the use of DPT for determining the hydraulic conductivity of various soil units. Results of slug tests in DP pipe strings were in excellent match (within 4%) with those from conventional wells (Butler et al., 2002). Recent research has showed that the dual tube direct push method can be used for vertical profiling of hydraulic conductivity in unconsolidated formations (Butler et al., 2000), as shown in Figure 2.5. The figure shows that the nested rods are simultaneously advanced to the predetermined depths. The inner rods are then removed and the perforated screen is introduced into the formation for hydraulic conductivity testing. Once the testing is carried out, the screen is retrieved, the inner rods are reinserted and the system is advanced to the next depth. In comparison to conventional drilling methods, the DP procedures do not produce drill cuttings and the volume of development water is also less. Installation of DP probe rods is quick and easy and due to their small diameter water rapidly reaches steady state conditions. The speedy installation and ability to provide results closer to the conventional methods makes them a useful tool for ESC type approach. They can help in making in-field decisions to resolve the uncertainties in the hydrogeology between the observation wells at a site. Direct push installations can determine hydraulic conductivity for the unconsolidated formations by pumping, slug and pneumatic test methods. Figure 2.6 shows the use of DP equipment for pneumatic testing.

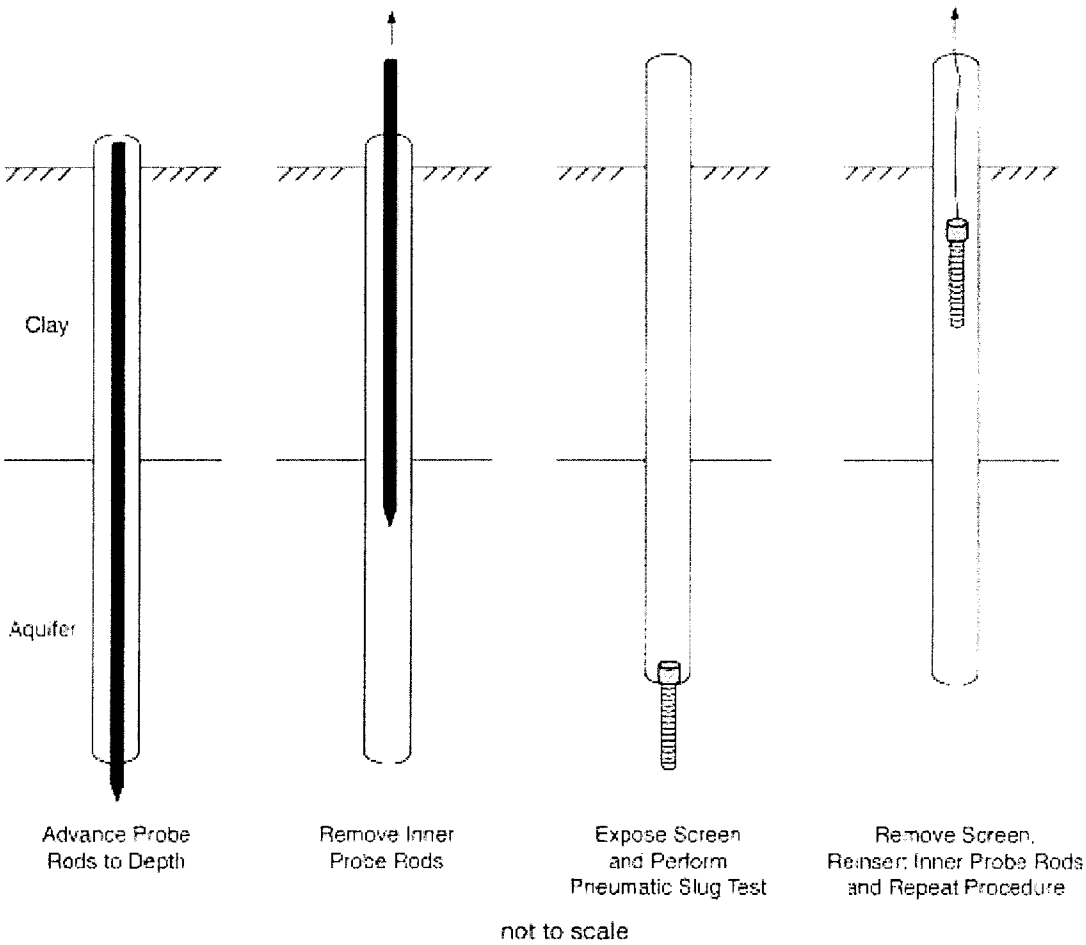

Figure 2.5. Schematic of profiling process (source: Butler et al., 2000)

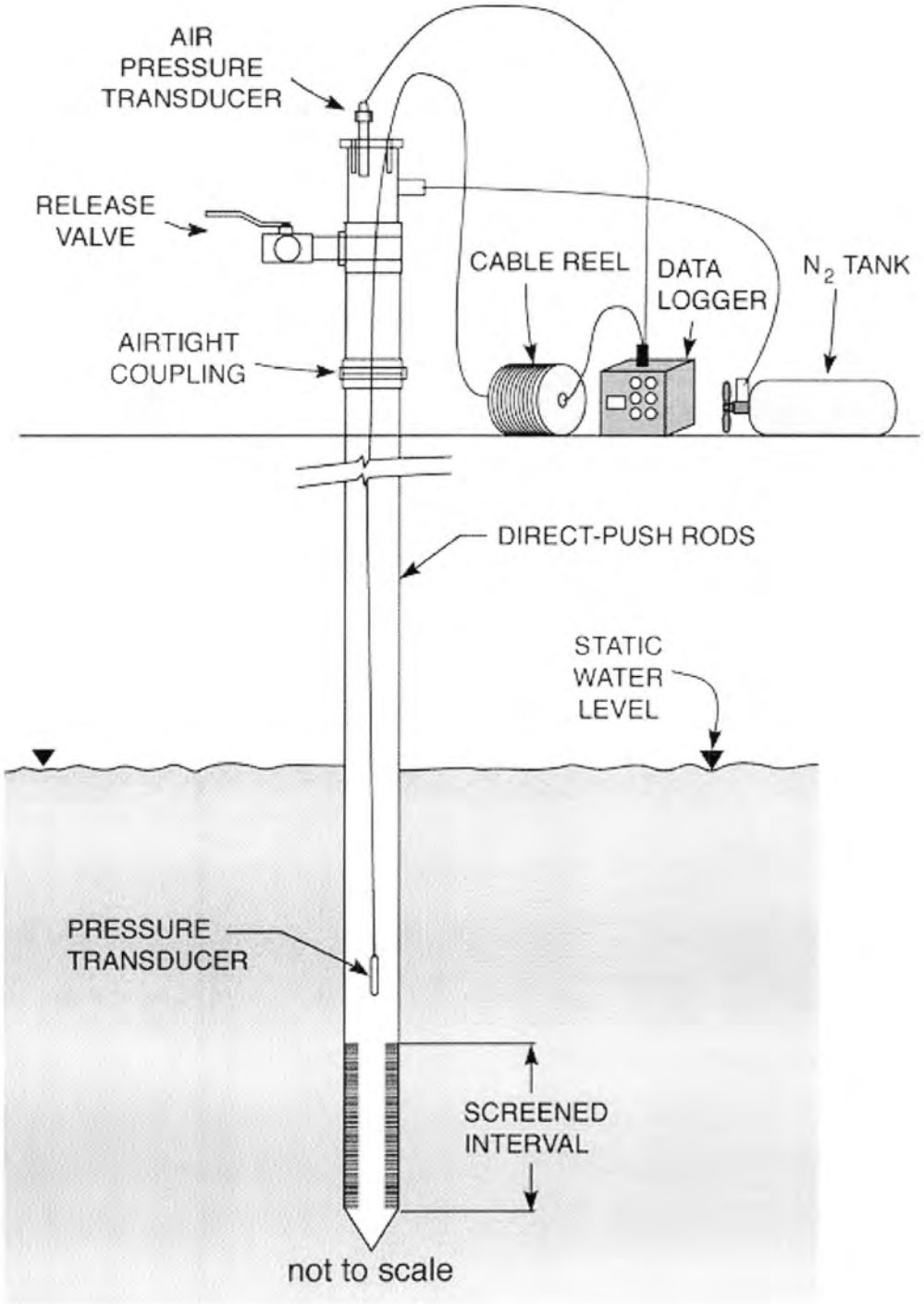

Figure 2.6. Schematic of the set up for the pneumatic initiation method (source: Butler et al., 2000)

Expected hydraulic conductivity of the formation governs the diameter of DP rods used for hydraulic conductivity testing. Small diameter rods (e.g., 0.016 m ID) should not be used for high permeability soils (greater than 70 m/day). Like any other method of hydraulic testing, well development is an issue for DP installed wells also. Though, use of a shielded screen can significantly reduce the amount of well development required for hydraulic conductivity testing.

2.4.4. Electrical conductivity sensor

Recently there has been a proliferation in the use of DP technology in conjunction with sensors to obtain subsurface information at an unprecedented level of detail without the need for permanent wells. The research work carried by KGS group at the Kansas River floodplain indicates that the EC sensor can be used for rapid delineation of stratigraphic units (Butler et al., 1999). Results show that the technique can map thin, laterally continuous layers very efficiently and accurately.

The Geoprobe soil conductivity sensor, shown in the Figure 2.7, identifies lithology and potential contamination by measuring the electrical conductivity of soil and hydro-geologic fluids. Soils vary in their electrical conductivity depending on particle size; for example, clays and silts generally have high conductivities, while sand and gravel exhibit low conductivities. Pore fluids and the amount of dissolved solids in these fluids also influence soil conductivity. The Geoprobe conductivity sensor uses an isolated array of sensing rings to measure the conductivity.

The principal components of the Geoprobe electrical conductivity system are:

- A Geoprobe hydraulic soil probing machine, which uses a combination of pushing and hammering to advance sampling rods
- Standard 3-foot long and 2.54-cm diameter hollow steel push rods
- A cable, threaded through the push rods to introduce the electric current
- The electrical conductivity sensor
- A data receiver connected to a personal computer to record the sensor's output.

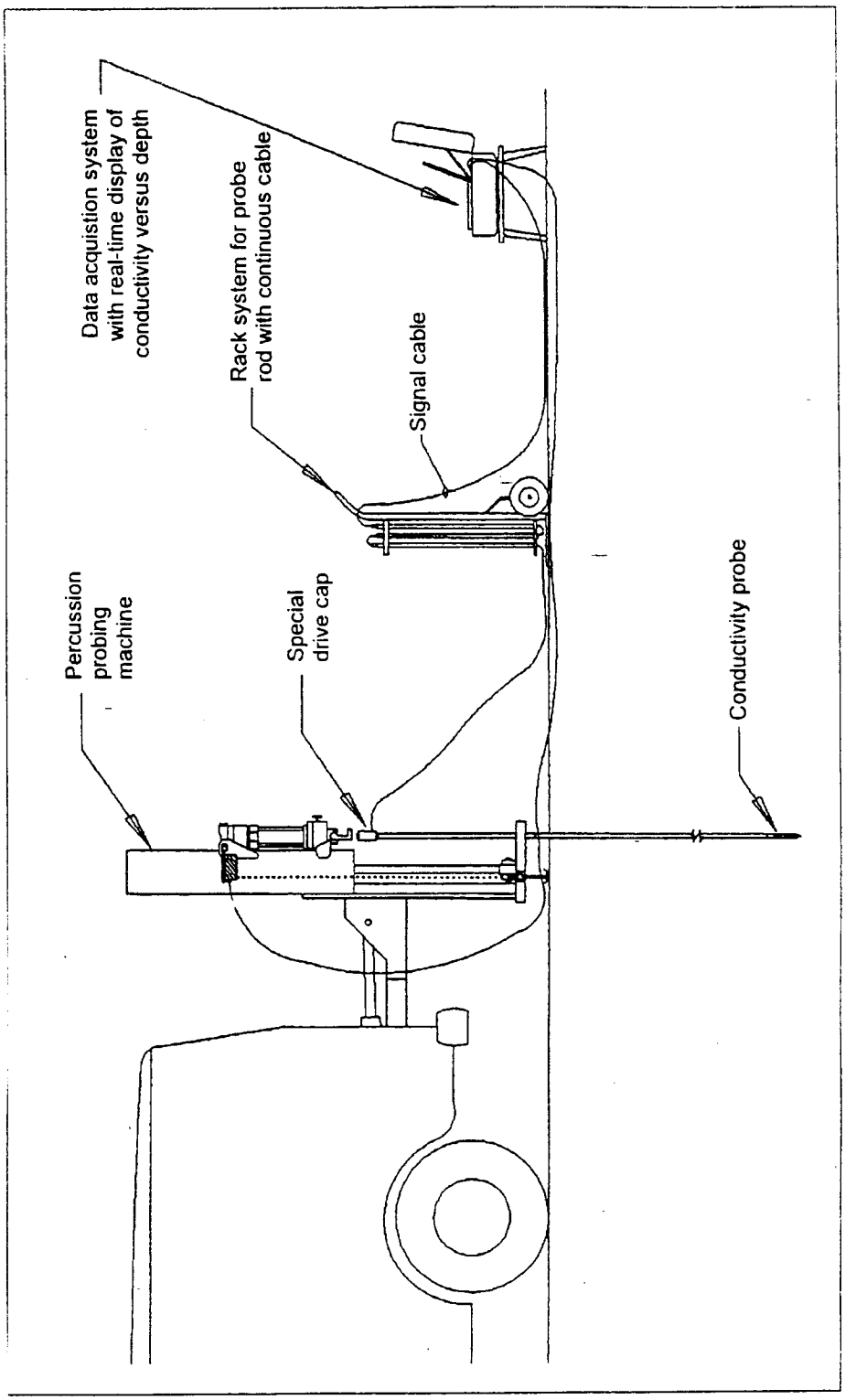

Figure 2.7. Small diameter direct push electrical conductivity probe (Source: Geoprobe® Systems, 2001)

The electrical conductivity sensor is limited by its applicability to soils (not rock) only and to soil lithology that can be penetrated by percussion type soil probing machines.

2.5. Modeling the Fate and Transport of Contaminants

State and federal agencies in the United States rely on risk-based corrective action (RBCA) and/or monitored natural attenuation (MNA) for clean up of contaminated sites (Brady et al., 1998). They need quantitative results of contaminant concentrations to determine the remediation strategy to be used at a site. There are several freely available computer models to simulate the migration and degradation of the contaminant plume. The models can be used to predict the time for the contaminant plume to reach a potential receptor, estimate contaminant concentration in a downgradient well, and estimate attenuation process and rates. Additionally, the model can be used as a guide for additional data collection to minimize the data gaps (Wiedemeier et al., 1995; Keeley et al., 2001).

Models for simulating groundwater flow and solute transport can be classified according to the mathematical technique used to solve the governing partial differential equations. The two common techniques are analytical and numerical. The type of model chosen for simulation depends on the amount of data available and type of solution expected. Analytical methods provide exact, closed form solution and are suited for sites with simple geology. Numerical methods provide approximate solutions and can model complex sites if requisite data is provided.

There are several models available for simulating fate and transport of dissolved contaminants in the subsurface. Three models were chosen for review - BIOPLUME III (version 1.0), BIOSCREEN and MODFLOW coupled with RT3D. These models are suitable for natural attenuation modeling.

2.5.1. BIOPLUME III (version 1.0)

BIOPLUME III (version 1.0) is a two-dimensional, finite difference model for simulating the natural attenuation of organic mass in ground water. BIOPLUME III

(version 1.0) is based on the U.S. Geologic Survey (USGS) Method of Characteristics Model dated July 1989 (Konikow and Bredehoeft, 1989). The model was developed for use with Air Force Technical Protocols for Implementing Intrinsic Bioremediation (Wiedemeier et al., 1995). It is integrated with Windows-based graphical platform.

The processes used for natural attenuation are advection, dispersion, sorption, ion exchange, and biodegradation. BIOPLUME III (version 1.0) simulates the biodegradation of organic contaminants using a number of aerobic and anaerobic electron acceptors: oxygen, nitrate, ferric, sulfate and carbon dioxide. The model can handle complex geological and hydro-geological site and various boundary conditions. The model supports first order decay, instantaneous reaction and Monod kinetics for simulating biodegradation reactions (Rifai et al., 1998).

BIOPLUME III (version 1.0) assumes negligible vertical variations in head and concentration, isotropic and homogeneous conditions with respect to the coefficients of longitudinal and transverse dispersivity, negligible molecular diffusion and no change in hydraulic conductivity and porosity with time. These simplifying assumptions also limit the use of the model at sites where there are significant vertical gradients in concentration and head and at places where an user may be interested in viewing the shape of contaminant plumes in three-dimensions. Also, the model simulates the hydrocarbon utilization as a lumped organic parameter. Therefore, if a single component is to be modeled then the amount of electron acceptor available to that component needs to be known. The stability and limitation in grid size in the program is also a problem as encountered by the research team at Iowa State University while using it for a FMGP waste site. The problem areas are discussed in detail in section A1 in Appendix A.

The BIOPLUME III (version 1.0) model is well documented and has been tested against other models (Rifai et al., 1998). BIOPLUME III (version 1.0) is the latest version of the BIOPLUME model. There are only few references available in literature on use of the BIOPLUME III (version 1.0) model for MNA including Miller (2001), Rifai et al., (2000), Rifai et al., (1998), and Newell et al., (1995). According

to Miller (2001), 'the versatility the model supports may make it a useful tool at MGP sites if the operational quirks can be reconciled'. Students in a contaminant modeling class at Dubuque University felt that 'models like BIOPLUME III (version 1.0) are ineffective, not because of the model or equations solved, but because of the lack of good characterization which could remove or quantify the uncertainty in the values of model input parameters' (http://nexus.chemistry.duq.edu/snes/esm/Course_Material/ESM552/Project/BIOPLUMEPRES/2BIOPLUME3/sld036.htm).

2.5.2. BIOSCREEN

BIOSCREEN is a three-dimensional analytical solute transport model based on the work of Domenico (1987). The program was developed by Groundwater Services, Inc., Houston, Texas for the Air Force Center for Environmental Excellence (AFCEE) Technology Transfer Division at Brooks Air Force Base (Newell et al., 1996). The program accounts for the effects of advective transport, three-dimensional dispersion, adsorption and first order or instantaneous decay in transport of contaminants. The model is designed to simulate biodegradation by both aerobic and anaerobic reactions using oxygen, nitrogen, iron, sulfate and carbon dioxide as electron acceptors.

BIOSCREEN works fine for simple groundwater flow condition but cannot be used for sites with pumping wells or other sources like recharge. Like BIOPLUME III (version 1.0), it assumes the aquifer to be isotropic and homogeneous and cannot model vertical flow gradient. The model calculates dispersivity from the assumed plume length (Gelhar et al., 1992) and assumes sorption to be linear and reversible. The model assumes a fully penetrating vertical plane source oriented perpendicular to groundwater flow, to simulate the release of organics into the moving water.

BIOSCREEN should be used at less complicated, lower-effort sites such as service stations (Newell et al., 1996). Some references on use of BIOSCREEN for modeling include Miller (2001), Wilson et al. (1999), Leuschner et al. (1997) and Newell et al. (1995).

2.5.3. MODFLOW/MODPATH/RT3D-GMS

Groundwater Modeling Software (GMS) is a sophisticated and comprehensive graphical user environment for performing groundwater modeling. GMS continues to be developed and enhanced by the Engineering Computer Graphics Laboratory at Brigham Young University, Provo, UT. It is a comprehensive package that provides tools for every phase of a groundwater simulation including site characterization, model development, post-processing, calibration and visualization. GMS supports several types of modules and information can be shared between different modules and data types. The entire GMS system consists of a graphical user interface (the GMS program) and several modules such as MODFLOW, MODPATH, MT3D, RT3D, etc. The input data for the modules are generated by GMS and saved to a set of files. These files are read by individual modules when launched from the GMS menu. The output from the modules can then be imported to GMS for post-processing. To model natural attenuation at a FMGP site, the modules used are MODFLOW, MODPATH and RT3D.

2.5.3.1. MODFLOW

MODFLOW is a three-dimensional (3-D) finite-difference ground-water flow model. It has a modular structure that allows it to be easily modified to adapt the code for a particular application. MODFLOW simulates steady and non-steady flow in an irregularly shaped flow system in which aquifer layers can be confined, unconfined, or a combination of confined and unconfined. Flow from external stresses such as flow to wells, aerial recharge, evapo-transpiration, flow to drains and flow through riverbeds can be simulated. The model can be used for heterogeneous and anisotropic aquifers with complex boundaries. Hydraulic conductivities or transmissivities for any layer may differ spatially and be anisotropic (restricted to having the principal direction aligned with the grid axes) and the storage coefficient may be heterogeneous. Boundaries with known head, known flux (recharge, evapo-transpiration, well and stream) and head dependent flux (river,

drain and general head) can be simulated. MODFLOW is currently the most reliable, verified and utilized groundwater flow model available (Kresic, 1997).

With GMS graphical user interface, data entry and visualization of results for MODFLOW are made easier. Using GMS, the user can select a single cell or a series of cells and then quickly define the hydro-geologic characteristics and/or boundary conditions using interactive dialog boxes. In addition, a spreadsheet dialog can be displayed, allowing the user to edit the values for each individual hydro-geologic characteristic for the entire model. Input data may be imported, or interpolated from a sparse set of scattered data points. Once the simulation is carried on MODFLOW, results can be exported to GMS and viewed on the graphical windows of GMS. It can display a defined groundwater model in either plan view or 3D oblique view, and can be rotated interactively. Cross-sections and fence diagrams may be cut anywhere in the model. Hidden surface removal, and color and light source shading can be used to generate highly photo-realistic rendered images. Contours, color fringes, and 3D plots can be used to display the variation of input data or computed results (GMS User's Manual, 1997).

2.5.3.2. MODPATH

MODPATH is a 3-D particle-tracking model that computes the path a particle takes in a steady state or transient flow field over a given period of time. MODPATH uses the hydraulic head and cell-by-cell flow terms computed by MODFLOW, in addition to the soil porosity, to compute the movement of each particle through the flow field. By specifying individual particle locations, MODPATH will compute the location of each particle at any instance in time. Both forward and backward tracking can be performed by MODPATH, making it ideal for well capture zone and wellhead protection studies.

2.5.3.3. Reactive Transport in 3-Dimensions (RT3D)

RT3D is a Fortran 90-based software code that solves coupled partial differential equations describing reactive-flow and transport of multiple mobile and/or immobile species in a 3-D saturated porous media. RT3D was developed from the

single-species transport code, MT3D (DoD_1.5 code) (Clement, 1997). RT3D uses the head distribution results of groundwater flow model MODFLOW.

The RT3D code was originally developed to support contaminant transport modeling efforts at natural attenuation demonstration sites (Clement et al., 1998; Clement et al., 1999). As a research tool, RT3D has been used to model several laboratory and pilot-scale active bioremediation experiments (Clement et al., 2000). Like BIOPLUME III (version 1.0) and BIOSCREEN, RT3D uses advection, dispersion, sorption and biodegradation as processes for natural attenuation. The advantage with RT3D is that it can accommodate multiple sorbed and aqueous phase species with any reaction framework that the user wishes to define. With a variety of pre-programmed reaction packages and the flexibility to insert user-specific kinetics, RT3D can simulate a multitude of scenarios. For example, natural attenuation processes can be evaluated or an active remediation can be simulated. Simulations could potentially be applied to scenarios involving contaminants such as heavy metals, explosives, petroleum hydrocarbons, and/or chlorinated solvents.

Use of MODFLOW/RT3D as a tool to simulate the fate and transport of contaminants to show natural attenuation as a viable remedial alternative for site remediation depends on the intricacy with which site characterization is carried out. The model demands extensive geological and hydrogeological data to give accurate modeling results.

Most of the references available in literature on RT3D are by Dr. Clement (Clement et al., 1998, Clement et al., 1999 and Clement et al., 2000). These papers describe the use of different pre-programmed reaction packages inbuilt with RT3D. No work related to FMGP site could be found in literature. There are several case histories to show the use of RT3D to model the reactive transport of chlorinated ethenes such as Harvey and Guiguer (2001), and Webber et al. (2001). Most of the papers concluded that RT3D is a very useful tool for modeling the contaminant plume in complex hydro-geological environments but the use of RT3D for natural attenuation simulations is limited because of the uncertainty in the biodegradation parameter estimates. Several studies demonstrate the importance of a well-planned

geological and hydro-geological site characterization and accurate source term definition for proper fate and transport modeling of contaminants (Boulding et al., 1993a; Landmeyer et al., 1998; Miller et al., 2001).

Table 2.4 gives a comparison of GMS, BIOSCREEN (version 4.0) and BIOPLUME III (version 1.0).

Table 2.4. Comparison of groundwater flow and contaminant transport models

Capabilities	BIOSCREEN (version 4.0)	BIOPLUME (version 1.0)	MODFLOW/ RT3D
3-D modeling	√		√
Model external source		√	√
Vertical flow gradient			√
Anisotropy & heterogeneity			√
Both linear & non linear sorption		√	√
User defined reaction kinetics			√
Particle Tracking			√
Stability	√		√
Geostatistics analysis			√
Vadose zone simulation			√
Solution	Analytical	Numerical (FDM[1], MOC[2])	Numerical (FDM, MOC, FED[3], TVD[4])

[1]FDM - Finite difference method, [2]MOC – Method of characteristic, [3]FED – Finite element method, [4]TVD – Total-variation diminishing

2.6. Published Work on MNA at FMGP Sites

MNA is a new remedial approach for FMGP sites to show site remediation. There are not many well-documented case histories in literature for FMGP sites primarily because of the difficulty in characterizing the source term at coal tar-contaminated sites. Also, the variety and range in physical and chemical properties of contaminants make it difficult to understand their fate and transport. However, MNA has been used extensively at underground storage tank (UST) and other

petroleum release sites (Tulis, 1997). Though not directly useful, case histories at UST sites will be reviewed as they explain the use of different fate and transport models. Many of the FMGP sites are commingled with petroleum products (Bockelmann et al., 2001; Zamfirescu et al., 2001;Landmeyer et al., 1998; Rogers et al., 2002). Case studies are reviewed in brief below:

Case Study 1. Assessment of Natural Attenuation of Aromatic Hydrocarbons in Groundwater near a Former Manufactured Gas Plant, South Carolina, USA

Landmeyer et al. (1998) assessed the natural attenuation of mono and polycyclic aromatic hydrocarbons in a shallow anaerobic groundwater near a FMGP site in Charleston, SC, USA. Adsorption isotherm experiments were run for naphthalene, toluene, and benzene using the method described by Schwarzenbach and Westall (1981) and microbial degradation rates were determined by quantifying the production of radiolabeled $^{14}CO_2$ over time from a known amount of uniformly labeled ^{14}C-napthalene, ^{14}C-toluene, and ^{14}C-benzene added to microcosm incubations of aquifer material. The first order biodegradation rates of toluene, benzene and naphthalene using aquifer sediments for aerobic and anaerobic environments were 0.84 d^{-1} and 0.002 d^{-1}, 0.03 d^{-1} and 0.00014 d^{-1}, 0.88 d^{-1} and 0.000046 d^{-1}, respectively. The laboratory adsorption coefficients were determined as 10 L/kg and 137 L/kg for toluene and naphthalene, respectively. The plumes of aromatic compounds were modeled using the numerical code SUTRA (Campbell et al., 1996). Numerical model simulations that incorporated field and laboratory measurements showed naphthalene, benzene and toluene transport using aerial or cross-sectional approaches. Predictive simulations indicated that the field degradation rates were closely related to anaerobic lab degradation rates.

Case Study 2. An Analytical Quantification of Mass Fluxes and Natural Attenuation Rate Constants at a Former Gasworks Site

Bockelmann et al. (2001) used a new approach to quantify natural attenuation rates at field scale. They calculated the total contaminant mass fluxes at the

pumping wells located at a distance of 140 and 280 m downstream of a contaminant source zone at a FMGP site contaminated with BTEX and PAH compounds. Pumping wells were installed in a group of four along two control planes perpendicular to the mean groundwater flow direction downstream of a suspected source zone and were operated in two consecutive campaigns with four active wells each to obtain complete coverage of aquifer width. Some of the changes in the geochemical environment between the wells, such as increase in dissolved iron flux and reduction in sulfate mass flux, indicate the presence of microbial degradation activity. Using mass fluxes for different compounds and average non-retarded groundwater travel time between two control planes, first-order natural attenuation rates were calculated. For BTEX and PAH compounds (naphthalene, acenaphthylene, acenaphtene, fluorene, anthracene, fluoranthene, and pyrene) the degradation rates ranged from 0.014 to 0.13 d^{-1} and 0.00037 to 0.031 d^{-1}, respectively.

Case Study 3. Occurrence and Attenuation of Specific Organic Compounds in a Groundwater Plume at a Former Gasworks Site

Work by Zamfirescu and Grathwohl (2001) at an FMGP site at Neckar Valley in Germany is not directly related to this research but adds a different perspective to MNA studies. The study showed that there are many other heterocyclic aromatic compounds apart from usual PAH and BTEX compounds present in the plume that need to be accounted for in the overall groundwater contamination. A special focus was given to the identification of recalcitrant compounds and attenuation rates were determined using point concentrations along the plume centerline for the compounds. First-order overall decay rate constants were measured for compounds exhibiting an exponential concentration decrease with distance along the plume centerline. Monoaromatic compounds (MAHs) were found to be degrading at the highest rate and the degradation rates decreased with increase in the number of carbon atoms in alkyl chains. Degradation rates for benzene and related MAHs

(methyl indene, acridine, methyl-quinolinol, methyl benzofuran) were in the range of 0.013 to 0.068 d^{-1}.

There are several case studies on MNA for sites other than FMGP sites. Some selected ones that are thought to be important for the discussion of different flow and transport models are presented:

Case Study 1. Natural Attenuation of BTEX Compounds: Model Development and Field Scale Application

Dr. Clement and his research group wrote this paper to show the usefulness of multi-species reactive transport model RT3D in modeling the transport of BTEX at a LNAPL-contaminated site (Clement et al., 1999).

Due to a lack of information on actual source zone, soil and groundwater sampling data for July-August 1993 was used to define the initial conditions for the model. The natural attenuation simulations were completed to simulate the plume fate after 365 days of transport, i.e., until July 1994. During site monitoring, the LNAPL plume was found to show different shapes at different time periods in a year. The total simulation time was therefore divided into three stress periods: 162,106, and 97 days and the LNAPL source was characterized in a variable shrink and spread pattern. The model was calibrated by varying the hydraulic conductivity values for flow pattern and biodegradation rates for contaminant transport. The first-order biodegradation rate constants, estimated by a calibrated RT3D model were 0.051, 0.031, 0.005, 0.004, and 0.002 day^{-1} for aerobic respiration, denitrification, Fe [III], sulfate reduction, and methanogenesis, respectively. Sensitivity analysis showed that the hydraulic conductivity, first order biodegradation rate constants and recharge, listed in the order of decreasing sensitivity, were the most critical parameters that control the total amount of BTEX mass present in the aquifer. Aquifer thickness and hydraulic conductivity were found to be the key parameters affecting the plume shape. Dispersivity, the next most sensitive parameter with respect to plume shape, had no effect on the total BTEX mass. Biodegradation was found to be more sensitive to anaerobic degradation than aerobic degradation.

Anaerobic processes were sensitive to changes in reaction rate constants, with sulfate reducing, Fe [III] reducing, methanogenesis and denitrification in decreasing order.

Case Study 2. Numerical Simulations of a Natural Attenuation Experiment with a Petroleum Hydrocarbon NAPL Source at the Columbus Air Force Base in Eastern Mississippi.

Widdowson and Brauner (2001) demonstrated the use of a multiple species transport code (SEAM3D) to simulate three-dimensional transport. They placed a known mass of NAPL as a source for BTEX, naphthalene, decane and bromide in the shallow aquifer. The concentration data for petroleum hydrocarbon compounds (PHCs), aqueous phase electron acceptors and reaction end products were measured using a three-dimensional, multilevel sampling network.

The model was designed to simulate the fate and transport of 11 constituents: one conservative tracer (bromide), five non-conservative PHCs (BTEX and naphthalene), two aqueous phase electron acceptors (dissolved oxygen and nitrate), one solid phase electron acceptor (Fe [III]) and two reaction end products (Fe [II] and CH_4). The mass balance files of SEAM3D gave the mass of each constituent remaining in a particular phase (i.e., NAPL, aqueous, or sorbed) and the mass of each substrate biodegraded under each terminal electron accepting process. Mass balance calculations based on a calibrated model after nine months of placing of NAPL source indicated that 49% of the aqueous phase BTEX and naphthalene mass was biodegraded, 13% was sorbed, and the remaining 38% was present in the aqueous phase. Mass balance calculations also showed that aerobic biodegradation accounted for 46% of the transformed PHC in aqueous phase, Fe [III] reduction for 28%, nitrate reduction for 21% and methanogenesis for 5%. Semi-quantitative sensitivity analysis showed the dependence of model results on NAPL release rate, initial Fe [III] concentration, dispersivity, hydrocarbon utilization rate and initial condition for the anaerobic microbial populations.

Case Study 3. Development of Groundwater Modeling for the Azraq Basin, Jordan

Abdulla et al. (2000) made a study on the existing threat to the groundwater resources in Azraq Basin, Jordan. There are around 500 wells operating in the basin. The excessive extraction of water from the wells poses a potential threat of decreasing the water table to an extent to cause intrusion of salt and hence, making ground water of no use to farming. To understand this, the three-dimensional groundwater flow model MODFLOW was applied to simulate water level changes in complex multi-aquifer systems of Azraq Basin.

The model was calibrated by adjusting hydraulic conductivity values during the sequential model runs and matching observed and simulated drawdown for steady state. For the transient case, calibration was done by adjusting specific yield and specific storage values. Results were matched for twelve stress periods between 1970 and 1992. The model was later validated against the head data for the period 1993-1997. Finally, several simulations were carried out with different pumping rates for the period of 1997-2025 to predict water table level and drawdown. The safe yield for the upper aquifer was determined to be about 25 million cubic meters yearly.

Case Study 4. Modeling natural attenuation of BTEX plume, Keesler Air Force Base, Mississippi, using BIOSCREEN.

Newell et al. (1996) used BIOSCREEN model to simulate natural attenuation of the BTEX plume at Keesler Air Force Base. Total simulation time was 6 years. Initial source mass, 2000 kg, was estimated from the GC/MS analysis of soil samples collected from both the vadose and saturated zones. An extensive groundwater sampling program was conducted by Groundwater Services, Inc. to get the representative background, maximum and minimum concentration of electron acceptors. The model was calibrated by varying the source concentration and dispersivity values. With longitudinal dispersivity as 32.5 ft and source concentration of BTEX in the center of source zone as 13.68 mg/L, the simulated plume matched the actual plume fairly well. Newell et al. found that the instantaneous model was

more accurate near the source, while the first order model was more accurate near the middle of plume. A mass balance study showed that 94% of the BTEX mass that left the source biodegraded in six years.

Case Study 5. Intrinsic Remediation Engineering Evaluation/Cost Analysis for Site ST-29, Patrick Air Force Base, Florida.

Site ST-29, Patrick Air Force Base, Florida is contaminated by a leaking 10,000 gallon UST and its product lines. An estimated 700 gallon of product (gasoline) was released in 1986. Potential receptors of this contamination are the Atlantic Ocean, lying 750 feet to the east, and the Banana River, which runs roughly north-south 2400 ft west of the site. Hydraulic conductivity in the aquifer region varies from 0.023 to 0.089 ft/min. Groundwater lies 4 to 5 ft below ground surface and flow is to the west with a hydraulic gradient ranging from 0.001 to 0.003 ft/ft.

Under an intense soil and groundwater sampling program, 29 locations were chosen for soil sampling and 48 for groundwater. Analysis of soil samples showed that soil BTEX contamination extends 220 ft downgradient of the source and was 90 ft wide at its greatest width. The highest concentration in soil was 1236 mg/kg for a soil sample taken 120 ft west-northwest of the suspected source. The majority of soil samples showed concentrations below detection limit. Thirty-eight out of 48 groundwater samples showed the presence of BTEX compounds. The BTEX plume was approximately 560 ft in length and 200 ft wide at its widest part, as defined by the 5 mg/L isopleth, with a maximum total BTEX concentration of 7304 μg/L. Geochemical data indicated the occurrence of biodegradation involving oxygen, iron and methane.

Rifai et al. (2000) used BIOPLUME III to model the fate and transport of the BTEX contamination at site. The site was modeled as an unconfined aquifer. Constant head boundaries were set at the upstream and downstream boundary of the modeling area. The upstream boundary corresponds to groundwater divide while the downstream boundary was the Banana River. The model was calibrated against the groundwater and soil data observed eight years after the leak occurred,

i.e., in 1994. Using the calibrated model as the base, steady-state predictive simulations were made. The 50-year prediction by the model showed that the plume would spread an additional 200 ft downgradient of the source from that observed in 1994.

2.7. Summary

Literature review on FMGP sites gives the current state-of-art on site characterization and site remediation techniques. DPT and MNA are among the best available alternatives for site characterization and remediation, respectively, but there are several outstanding issues and shortcomings related to use of DPT and MNA. Issues include:

- No protocols for the use of Geoprobe direct push technologies exist to allow adequate development of the geological and hydrogeological conceptual site models.
- A correlation between EC pushes results and soil types has not been fully developed.
- The performance of Geoprobe dual tube direct push equipment and pre-packed screen monitoring well has not been compared to conventional 2-inch monitoring well for determining hydraulic conductivity.
- No protocol for hydraulic conductivity testing using pneumatic method and their results in comparison to slug method.
- How statistically similar are the groundwater concentrations result obtained using pre-packed screen monitoring wells in comparison to conventional 2-inch monitoring wells needs to be determined.
- How to obtain the site specific input parameters for the groundwater flow and contaminant transport model such as dispersion, sorption constants, soil bulk density, porosity.
- Characterization of the source zone and source-loading rate.
- Which of the natural attenuation process: advection, dispersion, sorption, and biodegradation are more dominant at a FMGP site.

This study shall deal with the issues mentioned above. Review of the literature on MNA shows that most of the studies were done in controlled environments where the contaminant concentration and location is known and boundary conditions are known and controlled (Widdowson and Brauner, 2001; Clement et al., 1999). In addition, most of them dealt with fuel derived contamination only and very little is known about the sites where complex mixtures of contaminants are observed. The few case histories available on FMGP sites have not used flow and transport models to predict the fate of contaminants. It is interesting to note that despite being a 3-D reactive transport model there is no single case study on the use of RT3D for modeling the transport of contaminants at a FMGP site. This may be due to the extensive site-specific geological and hydrogeological data required by the model. This study shall use DPT as a tool to characterize the site and resolve the issues discussed above and then use the best available groundwater flow/transport model to determine the fate of contaminants at a FMGP site in Cherokee, Iowa.

Based on the case studies reviewed above and the other studies (not discussed here) a list of overall attenuation rate constants for different contaminants is presented in Table 2.5. Table 2.6 summarizes the list of biodegradation rate constants.

Table 2.5. Overall attenuation rate constants

Contaminant	**Overall Attenuation Rate Constant (day^{-1})**	**Reference**
Benzene	0.13	Bockelmann et al. (2001)
	0.042-0.084 (anaerobic)	Wiedemeier et al. (1995)
	0.042-0.203	MacIntyre et al. (1994)
Toluene	0.031	Bockelmann et al. (2001)
	0.07 – 0.133	Wiedemeier et al. (1995)
Ethylbenzene	0.07-0.217 (anaerobic)	Wiedemeier et al. (1995)
	0.051	Bockelmann et al. (2001)
Xylenes	0.029-0.038	Bockelmann et al. (2001)
	0.203-0.301	Wiedemeier et al. (1995)

Table 2.5. Overall attenuation rate constants (continued)

Contaminant	Overall Attenuation Rate Constant (day^{-1})	Reference
	0.161-0.273	Stauffer et al. (1994)
	0.063-0.203	MacIntyre et al. (1993)
Total BTEX	0.07	Chapelle (1994)
	0.07-0.14	Wilson et al. (1994)
	0.05-0.084	Wiedemeier et al. (1995)
Naphthalene	0.029	Bockelmann et al. (2001)
Fluoranthene	0.0037	Bockelmann et al. (2001)
	1.30	MacIntyre et al. (1993)
Pyrene	0.031	Bockelmann et al. (2001)
Flourene	0.012	Bockelmann et al. (2001)
Anthracene	0.018	Bockelmann et al. (2001)

Table 2.6. List of biodegradation rate constants

Contaminant	Decay Rate Constants (day^{-1})	Reference
Benzene	0.03 (aerobic)	Landmeyer et al. (1998)
	0.00014 (anaerobic)	Landmeyer et al. (1998)
	0.005 (aerobic)	Wang et al. (1998)
	0.003-0.013 (aerobic)	McAllister and Chiang.
	0.007-0.012 (anaerobic)	MacIntyre et al. (1993)
Toluene	0.84 (aerobic)	Landmeyer et al. (1998)
	0.002 (anaerobic)	Landmeyer et al. (1998)
Xylene	0.01-0.02 (aerobic)	MacIntyre et al. (1993)
	0.019 (anaerobic)	Stauffer et al. (1994)
Total BTEX	0.051 (aerobic)	Clement et al. (1999)
	0.002-0.031 (anaerobic)	Clement et al. (1999)
	0.0024-0.067 (anaerobic)	Wilson et al. (1993)
	0.001-0.01	Buscheck et al. (1993)
Naphthalene	0.88 (aerobic)	Landmeyer et al. (1998)
	0.000046 (anaerobic)	Landmeyer et al. (1998)

2.8. References

Abdulla, F.A., Khatib, M.A., and Ghazzawi, Z.D., 2000. Development of Groundwater Modeling for the Azraq Basin, Jordan. Environmental Geology, 40 (1-2): 11-18.

Ackerman, J., Jonathan L. F., and Roache. W. J. (year not known). Environmental & Economic Fusion: The Brownfields Revitalization Process. Vanasse Hangen Brustlin, Inc., Watertown, MA.

Bockelmann, A., Ptak, T., and Teutsch, G., 2001. An Analytical Quantification of Mass Fluxes and Natural Attenuation Rate Constants at a Former Gas works Site. Journal of Contaminant Hydrology 53(2001): 429-453.

Brady, P.V., Brady, M.V., and Borns, D.J., 1998. Natural Attenuation-CERCLA, RBCA's, and the Future of Environment Remediation. Lewis Publishers, Boco Raton, FL.

Butler, J.J., Healey, J.M., Zheng, L., McCall, W., and Schulmeister, M.K., 1999. Hydrostratigraphic Charcterization of Unconsolidated Alluvium Deposits With Direct Push Technology. 1999 Annual Meeting of the Geological Society of America, Denver, CO.

Butler, J.J., Healey, J.M., McCall, W., Lanier, A., Sellwood, S.M., and Garnett, E.J., 2000. A Dual Tube Direct-Push Method for Vertical Profiling of Hydraulic Conductivity in Unconsolidated Formations. Geological Society of America, 2000 Annual Meeting, Abstracts with Program, 32 (7): A522.

Butler, J.J., Healey, J.M., McCall, W., Loheide, S.P., and Garnett, E., 2002, Hydraulic Tests with Direct-Push Equipment. Ground Water, 40(1): 25-36.

Buscheck, T.E., O'Reilly, K.T., Nelson, S.N., 1993. Evaluation of Intrinsic Bioremediation at Field Sites. Proceedings, Petroleum Hydrocarbons and Organic Chemicals in Groundwater: Prevention, Detection, and Restoration. National Groundwater Association/API, Houston, TX, 367-381.

Campbell, B.G., Petkewich, M.D., Landmeyer, J.E., and Chapelle, F.H., 1996. Geology, Hydrogeology and Potential of Intrinsic Bioremediation at a National Park Service Dockside II Site and adjacent areas, Charleston, South Carolina, 1993-94. U.S. Geological Survey Water Resources Investigations Report 96-4170, Columbia SC.

Chapelle, F.H., 1994. Assessing the Efficiency of Intrinsic Bioremediation. EPA/540/R-94/515. United States Environmental Protection Agency. Washington, DC.

Cherry, J.A., 1990. Groundwater Monitoring: Some Current Deficiencies and Alternative Approaches. Hazardous Waste Site Investigations: Toward Better Decisions. B.A. Berven & R.B. Gammage (ed.). Lewis Publishers. Proceedings, 10th ORNL Life Sciences Symposium, May 21-24, Gatlinburg, TN.

Clement, T.P., 1997. RT3D - A Modular Computer Code for Simulating Reactive Multi-Species Transport in 3-Dimensional Groundwater Aquifers. PNNL-11720. Pacific Northwest National Laboratory, Richland, Washington, DC.

Clement, T.P., Sun, Y., Hooker, B.S., and Petersen, J.N., 1998. Modeling Multi-species Reactive Transport in Ground Water. Ground Water Monitoring & Remediation, 18(2): 79-92.

Clement, P., Lu, G., Zheng, C., and Weidemeier, T.H., 1999. Natural Attenuation of BTEX Compounds: Model Development and Field-Scale Application. Ground Water, 30(5): 707-717.

Clement, T.P., Johnson, C.D., Sun, Y., Klecka, G.M., and Bartlett, C., 2000. Modeling Natural Attenuation of Chlorinated Ethene Compounds: Model Development and Field-Scale Application at the Dover Site. Journal of Contaminant Hydrology 42: 113-140.

Domenico, P.A., 1987. An Analytical Model for Multidimensional Transport of a Decaying Contaminant Species. Journal of Hydrology. 91: 49-58.

Edison Electric Institute, 1984. Handbook on Manufactured Gas Plant Sites, ERT Project Number P-D215, Utility Solid Waste Activities Group Superfund Committee, Washington DC.

EPA, 1997a. Use of Monitored Natural Attenuation at Superfund, RCRA Corrective Action, and Underground Storage Tank Sites, OSWER Directive Number: 9200.4-17. United States Environmental Protection Agency, Office of Solid Waste and Emergency Response, Washington DC.

EPA, 1997b. Chapter 5: Direct Push Technology from Expedited Site Assessment for Underground Storage Tank Sites: A Guide for Regulator, EPA/510/B-97/001. United States Environmental Protection Agency, the Office of Underground Storage Tanks, Washington, DC.

EPA, 1997c. Natural Attenuation of PCP and Naphthalene at Popile Inc. Superfund Site. < http://www.epa.gov/earth1r6/6sf/popilweb/html/modeling.html>. (Date accessed: May 6, 2002).

EPA, 2001. Performance Comparison: Direct Push Wells versus Drilled Wells. Technical Report TR-2120-ENV, Naval Facilities Engineering Command, Washington, DC.

Fischer, C.L.J., Schmitter, R.D., O' Neil, E., 1999. Manufactured Gas Plants: The Environment Legacy. <http://www.hsrc.org/hsrc/html/tosc/sswtosc/mgp.html - introduction>. Publication of Hazardous Substance Research Center, Atlanta, GA. (Date accessed: March 29,2002).

Gelhar, L.W., Welty, C., and Rehfeldt, K.R., 1992. A Critical Review of Data on Field Scale Dispersion in Aquifers. Water Resources Research. 28(7): 1955-1974.

Geoprobe Systems, 2001. Direct Push Technology. http://www.geoprobe.com/faq/faqdesc.htm#whatisdp, Salina KS. (Date accessed: April 25, 2002).

GMS User's Manual, 1997. Boss International, Inc., and Brigham Young University, Engineering Computer Graphics Laboratory, Provo, UT.

Golchin, J., Stenback, G.A., Kjartanson, B.H., and Ong, S.K., 2000. A Streamlined Process for Contaminated Site Closure. Proceedings, 13th Annual International Symposium on Site Remediation Technologies and Environmental Management Practices in the Utility Industry, December 4-7, Lake Buena Vista (Orlando), FL.

GRI (Gas Research Institute), 1987. Management of Manufactured Gas Plant Sites. Vol. I-IV, Report GRI-87/0260.1, Gas Research Institute, Chicago, IL.

GZA GeoEnvironmental, Inc. (1998). Former Manufactured Gas Plants. <http://www.gzea.com/gasplants/gasplants.asp>. Report on Environmental Remediation, Norwood, MA. (Date accessed: March 29, 2002).

Harvey, D.J.M., and Guihuer, N., 2001. Determining Practical Input for Reactive Transport Modeling: A Case Study. Proceedings of MODFLOW '2001, Golden, CO.

Hatheway, A.W., 1997. Manufactured Gas Plants: Yesterday's Pride, Today's Liability. Civil Engineering, ASCE, 67(11), 38-41.

Johnson, C.D., Skeen, R.S., Leigh, D.P., Clement, T.P., and Sun, Y., 1998. Modeling Natural Attenuation of Chlorinated Ethenes at a Navy Site Using the RT3D code, Proceedings of WESTEC 98 conference, October 3-7th, Water Environmental Federation, Orlando, FL.

Keeley, A.A., Keeley, J.W., Russell, H.H., Sewell, G.W., 2001. Monitored Natural Attenuation of Contaminants in the Subsurface: Applications. Ground Water Monitoring and Remediation 136(2): 136-143.

Konikow, L. F. and J. D. Bredehoeft, 1989. Computer Model of Two-Dimensional Solute Transport and Dispersion in Ground Water, Techniques of Water Resources Investigation of the United States Geological Survey, Book 7, USGS, Reston, VA.

Kresic, N., 1997. Quantitative Solutions in Hydrogeology and Groundwater Modeling. CRC Lewis Publishers, Boca Raton, FL.

LaGrega, M.D., Buckingham, P.L., and Evans, J.C., 1994. Hazardous Waste Management. McGraw Hill, Inc., New York.

Landmeyer, J.E., Chapelle, F.H., Petkewick, M.D., and Bradley, P.M., 1998. Assessment of Natural Attenuation of Aromatic Hydrocarbons in Groundwater Near a Former Manufactured Gas Plant, South California, USA. Environment Geology 34 (4): 279-292.

Larsen, B. R., 1997. Remediating MGP Brownfields. <http://www. Pollutionengineering.com>. Online report from *Pollution Engineering.* (Date accessed: May 7, 2002).

Leuschner, A.P., Westray, M.S., Ankles, D.V, and Bradbury, L.C., 1997. Investigation of Natural Attenuation for Management of Groundwater at MGP Sites. Proceedings, 10th Annual IGT Symposium on Gas, Oil and Environmental Biotechnology and Site Remediation Technologies, Dec. 8-10. IGT, Orlando, FL.

Luthy, R.G., Dzombak, D. A., Peters, C.A., Roy, S.B., Ramaswamy, A., Nakles, D.V., and Nott, B.R., 1994. Remediating Tar-Contaminated Soils at Manufacturing Gas Plant Sites. Environmental Science and Technology, 28 (6): 266-276.

Macintyre, W.G., Stauffer, T.B., Antworth, C.P., Boggs, M., 1993. Degradation Kinetics of Aromatic Organic Solutes Introduced into a Heterogeneous Aquifer. Water Resources Research. 29(12): 4045-4051.

McAllister, P.M. and Chiang, C.Y., 1994. A Practical Approach to Evaluating Natural Attenuation of Contaminants in Groundwater. Groundwater Monitoring Review 18(2): 161-173.

Miller, R.N., 2001. Assessment of Natural Attenuation at Two Manufactured Gas Plant Sites in Iowa. Master's Thesis, Iowa State University, Ames, IA.

Murarka, I. P., 1995. Site Management Trends and Research Directories in the United States of America. Land Contamination & Reclamation, 3(4).

Newell, C.J., McLeod, R.K., and Gonzales, J.R., 1996. BIOSCREEN Natural Attenuation Decision Support System User's Manual, Version 1.3, EPA/600/R-96/087, Robert S. Kerr Environmental Research Center, Ada, OK.

Newell, C.J., Winters, J.W., Rifai, H.S., Miller, R.N., Gonzales, J., and Wiedemeier, T.H., 1995. Modeling Intrinsic Bioremediation with Multiple Electron Acceptors: Result from Seven Sites. Proceedings, National Groundwater Association Petroleum Hydrocarbons and Organic Chemicals in Groundwater Conference, Houston, TX, Nov., 33-48.

Rifai, H.S., Charles, P.E., Newell, C.J., Gonzales, J.R., and Wilson, J.T., 2000. Modeling Natural Attenuation of Fuels with BIOPLUME III. Journal of Environmental Engineering, 126(5): 428-438.

Rifai, H.S., Newell, C.J., Gonzales, J.R., Dendrou, S., Dendrou, B., Kennedy, L., and Wilson, J.T., 1998. BIOPLUME III Natural Attenuation Decision Support System User's Manual Version 1.0 OSWER EPA/600/R-98/010. U.S. Environmental Protection Agency, Washington, D.C.

Rogers, S.W., Ong, S.K., Kjartanson, B.H., Golchin, J., and Stenback, G.A., 2002. Natural Attenuation of PAH-Contaminated Sites: A Review. ASCE Hazardous Waste Management Practice Periodical (accepted).

Shwarzenbach, R.P. and Westall, J., 1981. Transport of Nonpolar Organic Compounds from Surface Water to Groundwater- Laboratory Sorption Studies. Environmental Science Technology 15:11-18.

Smolley, M. and Kappmeyer, J.C., 1991. Cone Pentrometer Tests and Hydropunch Sampling: A Screening Technique for Plume Definition. Ground Water Monitoring Review, 11(3): 101-106.

Srivastava, V.J., 1997. MGP Site Remediation Strategies and a Review of Available Technologies and IGT's Innovative Approaches. Proceedings, 20th World Gas Conference, Copenhagen, IGU, Copenhagen, Denmark.

Stauffer, T.B., Antworth, C.P., Boggs, M., and Macintyre, W.G., 1994. A Natural Gradient Tracer Experiment in a Heterogeneous Aquifer with Measured In situ Biodegradation Rates: A Case for Natural Attenuation. EPA/540/R-94/515. United States Environmental Protection Agency, Washington, DC.

Thornton, D., Ita, S., and Larsen, K., 1997. Broader Use of Innovative Ground Water Access Technologies. Superfund XVIII Conference Proceedings, Vol. 2., United States Environmental Protection Agency, Washington, DC.

Thrall, A., 1988. Health Risks as a Coal Tar Disposal Site. EPRI Journal, 7-8: 53-55.

Tulis, D.S., 1998. Issues Associated with Natural Attenuation, http://www.epa.gov/OUST/rbdm/issues.htm., U.S. Environmental Protection Agency Office of Underground Storage Tanks, Washington, DC. (Date accessed: April 5, 2002).

Wang, X., Ngo, T.X., Zhou, Y., and Nonner, J.C., 1998. Modeling and Remediation of Groundwater Contamination at the Engelse Werk Wellfield. Groundwater Monitoring and Remediation, Summer: 114-124.

Webber, P.A., Anderson, P.F., Travis, B.J., and Noffsinger, D.C., 2001. Modeling of Biosparging and Natural Attenuation of Chlorinated Ethenes at SRS. In Situ and On-Site Bioremediation: Vol. 10. Sixth International In-Situ and On-Ste Bioremediation Symposium, San Diego, June 4-7, Battelle Press, Columbus, OH.

Widdowson, M.A., and Brauner, J.S., 2001. Numerical Simulation of a Natural Attenuation Experiment with a Petroleum Hydrocarbon NAPL Source. Ground Water 39 (6): 939-951.

Wiedemeier, T.H., Rifai, H.S., Newell, C.J., and Wilson, J.T., 1999. Natural Attenuation of Fuels and Chlorinated Solvents in the Subsurface. John Wiley & Sons, Inc, New York.

Wiedemeier, T.H., Wilson, J.T., Kampbell, D.H., Miller, R.N., and Hansen, J.E., 1995. Technical Protocol for Implementing Intrinsic Remediation with Long-Term Montoring for Natural Attenuation of Fuel Contamination Dissolved in Groundwater. Air Force Center for Environmental Excellence, Technology, Transfer Division, San Antonio, TX.

Wilson, B.H., Hai, S, Jong, S.C., and James, V., 1999. Use of BIOSCREEN to Evaluate Natural Attenuation of MTBE, in Natural Attenuation of Chlorinated Solvents, Petroleum Hydrocarbons and Other Organic Compounds, Volume1, Alleman, B.C., and Andrea, L. (eds). Proceedings, Fifth International In Situ and On-Site Bioremediation Symposium, San Diego, California, April 19-22, 1999, Battelle Press, Columbus, Ohio, 115-120.

Wilson, J.T., Kampbell, D.H., and Armstrong, J., 1993. Natural Bioreclamation of Alkylbenzene (BTEX) from a Gasoline Spill in Methanogenic Groundwater. In

Hydrocarbon Bioremediation, Hinchee, R., Allenman, B.C., Hopel, R.E., and Miller, R.N. (eds.). Lewis Publishers, Boca Ralton, FL, 201-218.

Wilson, J. T., Pfeffer, M.F., Weaver, J.W., Kampbell, D.H., Wiedemeier, T.H., Hansen, J.E., Miller, R.N., Kerr, R.S., 1994. Intrinsic Bioremediation of JP-4 Jet Fuel. Symposium on Intrinsic Bioremediation of Ground Water, Denver, CO, Aug1st-Sept 1st, EPA/600/R-94-162. Office of Research and Development, United States Environmental Protection Agency, Washington, DC.

Zamfirescu, D., and Grathwohl, P., 2001. Occurrence and Attenuation of Specific Compounds in the Groundwater Plume at Former Gasworks Site. Journal of Contaminant Hydrology, 53: 407-427.

Zemo, D.A., Pierce, Y.G., and Galinatti, J.D., 1994. Cone Penetrometer Testing and Discrete-Depth Groundwater Sampling Techniques: A Cost Effective Method of Site Characterization in a Multiple-Aquifer Setting. Groundwater Monitoring and Remediation, 14(4): 176-182.

CHAPTER 3 DEVELOPMENT OF SITE CHARACTERIZATION AND GROUNDWATER MONITORING PROTOCOLS AT THE FMGP SITE IN CHEROKEE, IOWA

A paper to be submitted to the Journal of Groundwater Monitoring and Remediation

Rahul Biyani[1], Bruce Kjartanson[2], Say Kee Ong[2], Greg Stenback[3]

Abstract

An expedited site characterization (ECS) like approach was used at the former manufactured gas plant (FMGP) site at Cherokee, Iowa. ESC stresses the use of cost effective, minimally or non-invasive technologies like Direct Push Technology (DPT) for site characterization. Protocols were developed and implemented for the use of Geoprobe direct push (DP) percussion probe technology. The objectives of this study were to use electrical conductivity probes to define the stratigraphy of the site, conduct groundwater and soil sampling to define the contaminant plume shape and size, use DP dual tube equipment to estimate the hydraulic conductivities at the site, and to install and compare pre-packed screen monitoring wells with conventional 2-inch monitoring wells for groundwater monitoring.

The Geoprobe electrical conductivity sensor defined the geology of the site and gave a good match with earlier borehole log data results. Hydraulic conductivities measured by slug testing pre-existing monitoring wells, installed pre-packed monitoring wells and dual-tube direct push equipment varied from 0.0000092 cm/sec in loess to 0.46 cm/sec in alluvium. Faster installation, low cost and similar hydraulic conductivity results (same order of magnitude) make DPT method more efficient than conventional 2-inch monitoring wells for estimation of hydraulic

[1] Graduate Student, Department of Civil & Construction Engineering, Iowa State University, Ames, IA.
[2] Associate Professor, Department of Civil & Construction Engineering, Iowa State University, Ames, IA.
[3] Associate Scientist, Department of Civil & Construction Engineering, Iowa State University, Ames, IA.

conductivity at the site. Results of electrical conductivity indicated the variations in the thicknesses of different geologic layers – fill, loess, and alluvium and the depth to a till, at the site. A region with reduced aquifer thickness (2-4 ft) was termed a pinch zone and was found to extend across the central portion of the site (east - west). Low hydraulic conductivity values (approximately 0.00002 cm/sec) estimated at three Geoprobe dual tube push locations in the pinch zone also indicated a grading of the sandy alluvium with fine silts. Geo-technical index tests on soil samples from the pinch zone confirmed the low hydraulic conductivity values. Organic carbon content values measured in several soil samples obtained from site varied from 0.2% to 3.9%. A non-parametric test (Friedman's test) conducted on the geochemical and contaminant concentration data obtained from the groundwater sampled at MW6 (a conventional 2-inch well) and surrounding pre-packed screen monitoring wells 6A, 6B and 6C indicated no significant difference in the results from the two types of well. A non-parametric Sign test used for statistical comparison of the geochemical and contaminant concentration data obtained from MW6 individually with each of the surrounding pre-packed screen monitoring wells, 6A, 6B and 6C found no significant difference in the results.

The contaminant plume originating from the primary contaminant source was restricted by the pinch zone. Contaminant concentration data from groundwater sampling also indicated the presence of a probable secondary BTEX source in the pinch zone. The shape of the contaminant plumes along with water level heads measured at six newly installed pre-packed screen monitoring wells and 11 existing monitoring wells indicated the groundwater flow in the S-SE direction, towards the Little Sioux River located on the south of the site. Estimated overall first-order attenuation rates for BTEX and four PAH compounds (phenanthrene, naphthalene, acenaphthene and acenaphthylene) were from 0.0058 d^{-1} to 0.011 d^{-1} and 0.013 d^{-1} to 0.022 d^{-1}, respectively. Biodegradation rates for BTEX and PAHs estimated by the Buscheck and Alcantar (1995) method varied from 0.00019 d^{-1} to 0.0023 d^{-1} and 0.00003 d^{-1} to 0.0003 d^{-1}, respectively.

3.1. Introduction

Application of a natural attenuation remedial approach such as monitored enhanced natural attenuation (MENA) requires a thorough site characterization. The Expedited Site Characterization (ESC) like approach used at Cherokee FMGP site, Iowa, emphasized the use of minimally intrusive technologies to optimize sampling locations and to minimize the installation of monitoring wells. In-field decisions and dynamic work plans, characteristic of ESC, streamline the site characterization work and allow sites to be characterized quickly, accurately, and at considerably lower costs than with traditional methods.

In the last decade, direct push technology (DPT) has evolved as a major alternative to conventional drilling approaches for environmental site investigations (Butler et al., 2001). DPT methods can install both permanent and temporary monitoring wells, provide depth-discrete and continuous soil, groundwater and soil gas samples for geological characterization, chemical analysis, and qualitative to semi-quantitative information about the distribution of the subsurface contaminants. On-board sensors may also be deployed with the DPT systems for both stratigraphic logging and chemical detection on site (EPA, 1997). Once the geology and hydrogeology of the contaminant migration pathways have been sufficiently defined, the updated site geological and hydrogeological model can be used for groundwater flow and contaminant transport modeling.

Some locations where DPT has been used successfully include Kansas Geological Survey (GEMS) research site in Kansas (Butler et al., 2002), FMGP site at Marshalltown, Iowa (Bevolo et al., 1996), Savannah River Site, South Carolina (Kjartanson et al., 1997), Pease Air Force Base, New Hampshire (Johnson Company Inc., 1996), Pine Street Barge Canal Superfund site, Bulington, Vermont (EPA 2000) and Naval Base Ventura County, Port Hueneme, California (EPA, 2001). EPA (2001) compared the performances of direct push installed monitoring wells and hollow stem auger-drilled monitoring wells at a Naval Base site in California and concluded that "no significant differences in performances were observed and, within experimental error, the performance was comparable". Butler

et al. (2002) used the DPT for hydraulic conductivity estimation at the research site in Kansas and found that results from direct push installations were in very good (within 4%) agreement with those from conventional wells. Butler et al. (1999), demonstrated the level of hydrostratigraphic detail that can be obtained by coupling DP technology with electrical conductivity logging in an unconsolidated alluvial unit at two of their research sites in Kansas. The electrical conductivity results were in agreement with information obtained from well bore geophysics, soil core samples, hydraulic tests, and water-level data. However it may be difficult to distinguish electrical conductivity log responses produced by lithologic variations from those produced by variations in water chemistry (Mack, 1993). Because of the potential advantages of DPT over conventional methods (Thornton et al., 1997), DPT was used for site characterization at the FMGP site at Cherokee, Iowa.

The objective of this paper is to present the protocols developed for use of direct push technology for site characterization and optimized groundwater monitoring and their implementation at the Cherokee, Iowa FMGP site. Direct push technology was used at the site to obtain stratigraphic information and for soil and groundwater sampling, hydraulic conductivity testing, installation and testing of pre-packed monitoring wells. The study includes mapping the contaminant plumes and estimating the contaminant attenuation rates.

3.2. Site Description

The FMGP site is located in Cherokee, in the northwestern portion of Iowa (see in Figure 3.1). A carburetted water gas plant operated at the site from 1905 to 1936, (Black and Veatch, 1994). The Little Sioux River bounds the site at approximately 600 feet to the south. The site has a typical continental climate with an average of 28 inches of annual precipitation and an average seasonal snowfall of 32 inches (USDA, 1989).

Prior site investigations were carried out at the site between 1991 and 1997. Locations of soil and groundwater samples collected and monitoring wells installed during this period are shown in Figure 3.2. Eleven monitoring wells (MW) were

installed to monitor the groundwater plume. As part of the remedial investigation/feasibility study, 25 soil borings and several rounds of groundwater sampling were conducted in 1993-94. A direct push investigation was carried in November 1997 whereby, 29 groundwater and 3 soil samples were collected (Black & Veatch, 1998b). Slug tests were performed in MW's 1, 2, 3, 5 and 7 during the preliminary site investigation in January 1992, December 1993 and June 1994. Hydraulic conductivity was measured in the alluvium (well graded, medium to coarse grained sand) unit at all the monitoring wells and resulted in an average value of 0.05 cm/sec. MW4 and MW6 could not be tested during the preliminary site investigation due to adverse weather conditions (Black & Veatch, 1994). Hydraulic conductivity was also tested in MW's 8 to 11, which were installed in March 1998. Hydraulic conductivity values in MW's 8 to 11 were higher than that found in other wells during preliminary site investigation (average value of 4.2 cm/sec). Particularly at MW11, the hydraulic conductivity was (15.7 cm/sec) three orders of magnitude higher than at the other monitoring wells.

In July and August 1997, the first interim remedial action was conducted at the site by removing heavily contaminated soil and three below-grade structures containing coal tar. The depth of soil removal was approximately 8 feet below ground level and corresponded to the depth of gasholder and tar cistern base (Black & Veatch, 1998b). Since March 1998, geochemical parameters have been monitored quarterly or semi-annually to assess the attenuation of PAH and BTEX compounds. All the samples were collected using a flow-through cell and low flow well purging methods.

The historical data for groundwater level measurements and hydraulic conductivity are presented in Tables B1 and B2 in Appendix B.

3.3. Site Investigation

Phase I of the site characterization for this work at Cherokee, Iowa began in August 2001 under a flexible work plan. As per work plan, the geology and the hydrogeology of site was investigated. A Geoprobe direct push electrical

conductivity sensor was used to develop stratigraphic profiles at selected push locations. Soil and groundwater samples were collected, followed by installation of pre-packed monitoring wells, well development and hydraulic conductivity testing. Lastly, all Geoprobe push locations, pre-existing monitoring wells and two new benchmarks marked along the river (one upgradient and one down gradient) were surveyed. Surveying was performed relative to MW3, MW8 and MW11 and matched the surveying results of site investigations performed in 1991-1997. Table C1 in Appendix C presents the raw surveying data.

3.3.1. Electrical conductivity probe

The Geoprobe soil conductivity sensor can be used to identify lithology by measuring the electrical conductivity of bulk soil and pore fluids (Direct Image® Electrical Conductivity (EC) System, Geoprobe Systems, Kansas City).

Electrical conductivity (EC) pushes were performed at 24 locations (shown in Figure 3.3) during the August 2001 site sampling event. The probing locations were selected where either the soil stratigraphy was unknown/unclear or where the contaminant plume was most likely to be present as per earlier site investigations results. Groundwater flow was in the south-south-east direction on the basis of previous studies. Pushes were made along a transect perpendicular to the groundwater flow direction to cover the lateral extent of plume. The probes were pushed to the till layer, which was evident by a sharp increase in the electrical conductivity values.

The protocol developed for using Geoprobe electrical conductivity sensor to infer information about soil strata was:

- All the push locations were identified in a work plan before going to the field. Depending on the access to the push location on site and field personnel's judgement, changes may be made in the push locations. During the August 2001 site sampling event, changes in two EC push locations, EC20 & EC25, were made due to the presence of subsurface obstructions.

- The EC sensor was calibrated against the borehole log data from existing monitoring wells. In the August 2001 site-sampling event, two calibration pushes, EC2 & EC3 were conducted close to MW6 & MW8, respectively. Thicknesses and depths of different soil zones such as fill, loess and alluvium resulting from EC logs were compared with MW borehole logs.
- Results should be verified by repeating the probing at a minimum of two locations. Second probing should be conducted within 5 to 10 feet from the first probing.
- After every push, all the rods were cleaned with detergent to avoid cross-contamination.
- Pushes were not allowed to go deeper than the top of the till layer at the Cherokee site to minimize the risk of creatinga conduit for contaminant spreading below the till.
- Results were downloaded from data logger on a 1.44-MB disk in a spreadsheet format.

3.3.2. Soil and groundwater sampling

Soil and groundwater samples were collected as part of the MENA studies to demonstrate the change in contaminant mass and concentration with time. The method used for sampling soil and groundwater can have a significant impact on their true representation to the site.

Protocol for groundwater sampling

Applying standard water sampling protocols may alleviate the effects of water column disturbance due to remedial activities such as source removal, well installation, and water sampling, on the quality of ground water. During the August 2001 sampling event, ground water samples were collected at 26 push locations, 11 existing monitoring wells and 6 newly installed pre-packed monitoring wells. Locations for groundwater sampling are shown in Figure 3.4. Locations for groundwater pushes were chosen closer to the EC pushes and in the areas where

the plume was assumed to be migrating on the basis of earlier site investigations. GPW 14 provides the background concentrations for different contaminants in the aqueous phase. The soil stratigraphy based on the EC logs helped in determining the depths for groundwater sampling. Samples were collected both from the upper and lower portion of the aquifer for the analysis of PAH, BTEX and geochemical constituents. Field-filtered groundwater samples were analyzed on site to evaluate the three-dimensional geochemical environment at Cherokee, FMGP site and to aid in selecting suitable soil sample locations. On-site analysis of geochemical/biodegradation indicators such as nitrate, nitrite, sulfate, sulfide, ammonia, nitrogen, ferrous iron, total dissolved iron, and manganese was carried out at several locations where sufficient water flow rate was available. A flow-through cell was used at selected locations to measure dissolved oxygen, redox potential, and electrical conductivity of the groundwater. Groundwater samples were sent to TestAmerica Laboratory for PAH, BTEX and geochemical analyses. PAH and BTEX were analyzed using EPA method and SW 8310 and SW 8021 respectively. Results from laboratory testing of aqueous phase concentration of contaminants and geochemical parameters in conjunction with the geochemical environment predicted from on-site measurement were used to define the plume shape for different BTEX and PAH compounds.

Groundwater samples at Cherokee, Iowa were collected according to the procedures listed in Alliant Energy quality assurance project plan (QAPP) (Black & Veatch, 2001).

The groundwater sampling plan as per QAPP was:

- Each well or direct push drive, for groundwater sampling, should first be purged to remove stagnant water. Low flow purging techniques were preferred as they cause fewer disturbances to the well-aquifer system. The purging rate, as specified in the QAPP, was not allowed to exceed 0.25 gallon per minute and a volume of at least three times the submerged volume of the casing was purged in all the wells. During the August 2001 site sampling event, ground water samples

were collected from the midpoint of the screen using a peristaltic pump and disposable plastic tubing.

- Purged fluids were collected in a 55-gallon drum, later disposed as per the requirements of publicly–owned treatment works.
- The field parameters such as temperature, specific conductance, pH, dissolved oxygen, oxidation-reduction potential and turbidity of the water purged from the well were monitored for stability according to the criteria in Table 3.1. During the August 2001 site sampling event, all the parameters were monitored, except pH, at all locations producing adequate flow of water (greater than 2 L/min) using the flow-through cell. The flow-through cell was cleaned with distilled water after every sampling event.
- Groundwater samples were first collected in bottles using 0.45-micrometer disposable filters to reduce the turbidity by filtering contaminated soil particles and globules of NAPL and then sent to Test America Laboratory for PAH, BTEX and geochemical analysis. If additional water was left then it was used for on-site analysis of geochemical environment in the mobile laboratory and for measuring field parameters using the flow-through cell. While collecting groundwater, no air bubbles were allowed to enter bottles or the flow-through cell.
- Ground water samples were properly stored in ice and were sent within 24 hours to the analytical laboratory for analysis.

Protocols for soil sampling

Soil at the site was sampled for chemical analysis of contaminants, organic carbon content and geotechnical index tests. Results from earlier groundwater sampling and the geochemistry testing carried out on-site aided in locating the soil sampling locations. Sample locations were selected in the area where the plume was most likely to propagate or places where high concentrations of contaminants were found in the past. Depths of soil samples were governed by the soil stratigraphy. Locations of soil sampling in August 2001 are shown in Figure 3.5.

Locations SS1A and SS2, upgradient to the source area, were chosen to give background concentrations for the contaminants.

Soil was sampled at twelve locations from 8-10 feet below ground surface to the till surface in the form of 1.75-inch diameter by 4-foot long continuous soil cores using a Geoprobe soil sampling device. Soil cores were capped tightly, sealed with electrical tape and preserved on ice. Soil samples were taken to Iowa State University's Soil Tilth Laboratory where they were kept in a refrigerator at 4 ^{0}C. The amounts of contaminants present in the soils were determined by direct extraction method. The method involves extracting 2 g of contaminated soil and 5 ml with acetone in a 10-ml glass tube with Teflon-lined screw cap was used. The contents in tube were vigorously shaken with a wrist action shaker (Model 75, Burrell Scientific, Pittsburg, PA) for 24 hours and then the tubes were put in centrifuge for 40 minutes at 3000 rpm to separate the solvents from the soil. A 5 μL aliquot of the supernatant was taken from the tubes and analyzed with a gas chromatograph (Model HP5890A, Hewlett-Packard, Palo Alto, CA) for PAHs. The injection temperature was set at 240^0 C and the detector temperature at 320^0 C. The initial oven temperature was set at 50^0 C and then raised at 8^0 C/min to a final temperature of 300^0 C for 5 min. Peaks of different analytes were identified. The individual amounts were calculated by comparing the peak area for different analytes against their individual calibration curves. The calibration curve for each compound is a plot of the area under the curve versus concentration, formed by running known concentrations of individual compound through the gas chromatograph. The dry mass of soil was determined by decanting the supernatant in tube and drying the soil in oven at 105^0 C for 24 hours (Lee, 2000). The final concentration of analytes in soil was given in terms of weight of contaminant per gram of dry soil.

3.3.3. Pre-packed screen monitoring wells

As a part of the process of developing a standard optimized groundwater monitoring program and protocols for natural attenuation monitoring that contribute to site closure, six new 1.4-inch outer diameter Geoprobe pre-packed screen

monitoring wells (GMW) were installed at three locations at the Cherokee FMGP site. Locations of new pre-packed monitoring wells are shown in Figure 3.6.

Pre-packed screen monitoring wells were installed at Cherokee FMGP site with three objectives. First, to compare their use with conventional monitoring wells. To meet this objective, three pre-packed screen monitoring wells, GMW 6A, 6B, and 6C were installed around a pre-existing well MW6. Both GMW 6A and GMW 6B have 3-foot long screens placed next to the upper and lower portions of MW6, respectively. GMW 6C has a 10–foot long screen placed adjacent to the 10-foot MW6 screen. Results of PAH, BTEX and geochemical concentrations from MW6 and newly installed pre-packed screen wells were compared. Second, the pre-packed screen monitoring wells were used to fill in data gaps in ground water elevations between monitoring wells and to define the ground water gradients across the site. GMW 12 was installed primarily to better define the hydraulic head field and groundwater flow. Third, the pre-packed screen monitoring wells were installed to develop protocols for the installation and use of pre-packed screen monitoring wells for future use at other FMGP sites.

Locations of the new wells were selected on the basis of contaminant and geochemistry data from earlier sampling events and to fill in the hydraulic head data gaps. The contaminant plume for most of the contaminants from the earlier site sampling events showed the plume to be extending from the source around MW5 to somewhere between MW6 and MW9. Two pre-packed screen monitoring wells, GMW 13A & 13B were installed in between MW6 and MW9 primarily for plume monitoring.

New pre-packed screen monitoring wells were developed prior to hydraulic head measurements. Well development was done as per QAPP. The purpose of well development is to reduce the turbidity, effect of disturbance to ground water and well installation, and to remove any water introduced into the formation during drilling and well installation. All the newly installed monitoring wells were left for more than 12 hours before development. Wells were developed by pumping approximately three or more well volumes of water.

3.3.4. Hydraulic conductivity measurements

Hydraulic conductivity was determined at twelve locations during August 2001 site sampling event. Locations are shown in Figure 3.7. The twelve locations include two of the earlier installed monitoring wells, 5 new pre-packed screen monitoring wells and 5 Geoprobe dual tube push locations. Locations for Geoprobe dual tube push were selected to fill the hydraulic conductivity data gap between the existing and new pre-packed screen monitoring wells. In all previous site sampling events, hydraulic conductivity was determined in the alluvium unit only. In the August 2001 site sampling event, hydraulic conductivity values were determined in the fine loess unit at three of the Geoprobe dual tube push locations. The pneumatic method for hydraulic conductivity was planned for all the locations in the alluvium unit. But due to inadequate air supply to produce sufficient drawdown, the conventional slug test method was used instead. The pneumatic method was run at location HC5 between MW10 and MW11. In both of these wells, high hydraulic conductivity was determined in earlier sampling events. HC5 was also slug tested. MW10 was re-slug tested to verify the unusually high hydraulic conductivity value observed during the previous site investigation in the aquifer near the Little Sioux River. The Location of HC5 for hydraulic conductivity testing using pneumatic method was also chosen primarily for the same reason.

The protocol developed for hydraulic conductivity testing procedure using slug method was:

<u>Steps before starting slug test</u>

- Push rods and screen were cleaned to remove any sort of blockage.
- Transducer and data logger were calibrated according to the manufacturer's instructions.
- Hydraulic conductivity should not be conducted until all nearby soil and groundwater sampling activity is completed.

Steps for conducting slug test with the two-foot long Geoprobe groundwater screen

- The dual tube probe rods were advanced to the desired depth. Distilled water was added to fill in the space between the outer and inner rods to prevent heaving.
- Inner rods were removed completely and the outer rods were retracted by approximately 2 feet. The 2-foot screen was lowered to the bottom of the outer rods and screen was properly set into the bottom opening of the outer rod (shown in Figure 2.5).
- The well development was performed as per QAPP (Black & Veatch, 1999, pages 15-17).
- The pressure transducer was submerged using the cable in the water column inside the outer rod. A data logger was attached to the pressure transducer cable above ground. The transducer was kept a foot or two above the top of the well screen, if sufficient water was present to do this.
- The water level was allowed to stabilize (variation not more than +/- 0.05 inches in data logger reading).
- Distilled water was added into the rod. About ¼ to ½ gallon was sufficient for testing at the Cherokee site. The water head above the transducer was recorded in the data logger at all times. Readings were measured until the water head becomes constant with time (no changes in four consecutive water head readings with time).

  Data was downloaded into a hand-held computer at site.

Steps for conducting the slug test with the Geoprobe pre-packed screen monitoring well

- Pre-packed screen monitoring wells were installed and developed as per QAPP.
- Last three steps in the preceding section, 'Steps for conducting the test with the two-foot long Geoprobe groundwater screen' were performed.

  Protocol for the pneumatic method is presented in section D1 in Appendix D.

3.4. Laboratory Testing

3.4.1 Geotechnical index testing

Grain-size analysis

Unified Soil Classification System (USCS) was used for the classification of soil samples obtained from the Cherokee site. The USCS classifies the soils on the basis of simple index properties such as grain-size distribution and Atterberg limits (Das, 1998).

Grain size distribution

Soil samples collected from all the locations during soil sampling event were tested for the type and amount of PAH's present, using gas chromatograph. Six locations, out of thirteen, were found to be contaminant free. Depending on the level of contamination and the amount of soil available, soil samples from four locations were chosen for grain-size distribution. Samples tested for grain size analysis were collected from the alluvium. ASTM D-2487 was used as a procedure for conducting the analysis.

Atterberg limit tests

The moisture content at which soil changes from semisolid to plastic is called plastic limit and from plastic to liquid is the liquid limit (Das, 1998). Casagrande's liquid limit device and the procedure illustrated in ASTM D 4318-84 were used for determining liquid limit and plastic limit of the soil samples collected from four locations.

Correlation of grain-size distribution and hydraulic conductivity

The hydraulic conductivity of sandy sediments can be inferred from the grain size distribution by the Hazen method. The method is applicable to sands where the effective grain size (D_{10}) is between approximately 0.1 and 3 mm (Fetter, 1991). The Hazen formula is:

$$K = C(D_{10})^2 \qquad \text{(Eq. 3.1)}$$

where K = Hydraulic conductivity (L/T)

C = A coefficient based on sand type and size.

Porosity and bulk density

Porosity and bulk density were estimated for soil samples at six locations on site. For determining porosity and bulk density, a small cylindrical soil sample was cut from approximately 2-ft long soil core samples. Diameter and height of the samples were measured using vernier calliper at several locations along the circumference of the soil core and the average value computed. Samples were dried and weighed for dry soil weight. Three assumptions were made for estimation of porosity and bulk density 1) there was no disturbance to the soil structure by cutting the soil sample, 2) all the samples were completely saturated, and 3) specific gravity for loess was 2.65 and for alluvium was 2.75.

3.4.2. Organic carbon testing

Organic carbon testing was done at the Soil and Plant Analysis Lab at Iowa State University. Instead of using conventional methods such as Walkley-Black method, loss of weight on ignition (LOI), or colorimetric determination of organic matter, separate tests for total and inorganic carbon content were done. Organic carbon content was later found by taking the difference between the total and inorganic carbon content. The reason behind this was to avoid using any correlation factor from the literature to convert organic mass to organic carbon. Another reason for using this procedure was that if the inorganic carbon content in the soil was found to be less than 2% then it would be safe to assume the total carbon in the soil was approximately equal to the organic carbon content.

Dry combustion analysis using a LECO CHN-2000 (LECO Corporation, St. Joseph, MI) was used for total organic carbon content and the modified pressure calcimeter (Model 280E Setra Systems, Inc., Boxborough, MA) method was used for inorganic carbon content. Seventeen soil samples were taken from seven locations at the Cherokee FMGP site. Figure 3.5 shows the locations for soil samples used

for organic carbon content testing. The seventeen samples consist of six samples from the loess unit and the rest from the alluvial unit. Results of the dry combustion test for some of the samples in the loess unit reflected high total carbon content than normally expected indicating high inorganic carbon content in the soil. Inorganic carbon testing using a pressure calcimeter showed that the percent $CaCO_3$/gm of soil was as high as 57% at location SS10. Also, at several places the inorganic carbon content exceeded total carbon content, which indicated that the inorganic content measured using pressure calcimeter was too high in the soil to be recovered completely by dry combustion method for total carbon content. The LECO machine was set at 950^0 C; and at that temperature all of the organic carbon will burn but the inorganic carbon will not. An acid test was conducted to verify the high inorganic carbon content in the soil. A 3.25 N HCL solution was poured in the vessel containing small amounts of soil sample and instantaneous bubbles of CO_2 were evolved indicating high inorganic carbon content in the soil.

The presence of high inorganic carbon content puts the results of the organic carbon content testing into question and therefore conventional Walkley Black method was used for estimating the organic carbon content. The Walkley Black method gives the total organic matter in the soil. Organic carbon content can then be estimated by multiplying the organic matter content by a factor of 0.58 (Nathan and Combs, 1998).

Organic carbon content values were used to estimate the retardation factor for different compounds at different depths. Retardation factor is given by:

$$R = 1 + \frac{K_d * \rho}{n} \qquad \text{(Eq. 3.2)}$$

where ρ = Soil bulk density (M/L^3),

n = Porosity

K_d = Partition coefficient for a compound (L^3/M).

3.5. Results

3.5.1. Conceptual geological site model using electrical conductivity probe

The electrical conductivity (EC) probe was first correlated with borehole geologic log data obtained from monitoring well locations during previous site investigations. Two such calibration pushes were conducted close to MW6 (EC2) and MW8 (EC3). The thickness of the different soil layers indicated by EC pushes at EC2 and EC3 matched fairly well with that from the borehole log data of MW6 and MW8, as shown in Figures 3.8a & 3.8b. The small variation in the results of EC pushes from boring log data may be attributed to the lack of a distinct boundary separating the soil zones such as loess and alluvium. Most of the time they grade into one another, indicating the natural variability of the alluvial depositional environment.

The geology at the site, as predicted from electrical conductivity probing results and borehole logs, consists of four layers. The top most layer is silty fill, overlying wind blown loess followed by sandy alluvium and low permeability till. The thickness of the different layers varies across the site. The fill varies between 2-10 feet thick across the site. Loess is present across the site except near the Beech Street and north of it. Its thickness increases downgradient of the source area. Directly underlying the fine loess layer is a sandy alluvium of variable thickness. Near GMW 13A & 13B, EC10 and EC11, the loess almost pinches out the underlying alluvium layer. Alluvium thickness varies from 2 feet in the pinch zone to approximately 30 feet upgradient of the source area. The till underlying the alluvium south of Beech Street has an irregular surface and slopes down to the Little Sioux River (Figures 3.10-3.14). It is expected that DNAPL, if present, may migrate to the top of the till and flow downgradient along the till surface or pool in local depressions in the till surface. EC data from the 24 push locations along with the earlier soil boring data were used to produce the cross-sections across the site (transects shown in Figure 3.9) and contours of the top of each soil layer. Figures 3.10-3.14 show the thicknesses of each layer on the cross-sections. Figure 3.15 shows the contours for alluvium thickness and the pinch zone in plan view.

At two of the locations, EC20 and EC25, rods could not be pushed to the top of the till layer due to the subsurface obstructions. Other pushes EC20A and EC25A were performed approximately 5 feet to the west of EC20 and approximately 10 feet to the east of EC25, respectively. On comparing the logs for EC20 and EC20A and EC25 and EC25A in Figure 3.16, a high level of repeatability in the results was observed.

A correlation was made between the EC values and soil type using the data from August 2001 EC investigation and ESC data from a FMGP site at Marshalltown, Iowa (Bevolo et al., 1996). Table 3.2 and Figure 3.17 show the EC values and corresponding soil types. As seen in Table 3.2, the range of EC values for closely similar soil types overlap. Therefore it may be difficult to obtain more than a general characterization of the soil type on the basis of the correlation. But EC technique can assist in distinguishing sand, silt and clay layers. Generally it is the upper limit of the EC value for a particular soil type, which helps in the identification of the graded soil.

3.5.2. Organic carbon content

Organic carbon content results varied from 0.29 to 3.9% in loess and 0.2 to 2.6% in alluvium (see Table 3.3). Organic carbon content was generally found to be lower for deeper samples. High organic carbon content suggests high sorptive nature of the soil. Results from SS10 and SS12, both in the pinch zone, showed high organic carbon content. SS6, which is just downgradient of source area, also showed high organic carbon content.

3.5.3. Hydraulic conductivity measurements

Results of hydraulic conductivity testing during August 2001 site sampling event are presented in Table 3.4. Hydraulic conductivity values were calculated by the Hvorslev (Case B) graphical method (using, Superslug version 3.1, Starpoint Software, Inc., Cincinnati, Ohio). The well development and agitated water column caused by well installation may have affected the initial readings of hydraulic

conductivity tests. Therefore, later readings of the test, which may be more representative of in situ conditions, were used for the calculations.

In general the hydraulic conductivity at the site varied from 0.0000092 cm/sec to 0.00003 cm/sec in loess and 0.000032 cm/sec to 0.46 cm/sec in alluvium. Hydraulic conductivity values in the aquifer were particularly low in the pinch zone. Three Geoprobe dual probe pushes conducted in the pinch zone resulted in a very low average hydraulic conductivity value of 0.000025 cm/sec. Hydraulic conductivity estimated at the newly five-foot distance apart installed pre-packed screen monitoring wells, GMW 13A & 13B, differed approximately by a factor of 8, which indicates the noticeable changes in the geology between the close by monitoring wells.

Hydraulic conductivity results from MW6 could not be measured for direct comparison with surrounding pre-packed monitoring wells due to artesian conditions. But the hydraulic conductivity measured at GMW 12 was in close match to that at near-by pre-existing MW9 (see Table 3.4 and Table B2). Hydraulic conductivities of re-slugged MW10 and Geoprobe dual push location HC5 matched the high hydraulic conductivity values estimated earlier in MW10 and MW11.

3.5.4. Grain size analysis

Results of grain size analysis are presented in Table 3.5. Out of the four samples used for analysis, SS10 and SS12 were from the loess overlying the pinch zone. All the four samples showed high sand and silt content percentages. Sand content was generally more than silt content at all locations except SS12. In SS10, sand content was only slightly higher than silt indicating grading of loess into alluvium in the pinch zone. The liquid limit results for one run at SS10 were unexpectedly high. This might be due to the presence of organic content in the sample. There was not enough quantity of soil from the same depth to re-run the test for confirmation. HC5, which is very close to river, showed approximately 97% sand content and was a non-plastic soil, which is very common for outwash soils.

Figures D1, D2, D3 and D4 showing the grain-size distribution at SS2, HC5, SS10 and SS12, respectively, are presented in Appendix D.

The grain-size analysis was used to estimate the hydraulic conductivity using the Hazen correlation for sandy aquifer and to verify hydraulic conductivity results obtained on site. Table 3.6 gives the hydraulic conductivities estimated from the effective grain size using Hazen's formula at four soil sampling locations and the hydraulic conductivity values based on slug tests in near-by monitoring wells. The values for hydraulic conductivity compared fairly well.

Table 3.7 summarizes the estimated porosity and bulk density values of various soil samples collected. The average porosity for alluvium is 30% and for loess is 50%. The average bulk density for alluvium is 1.9 g/cm^3 and for loess is 1.3 g/cm^3.

3.5.5. Soil and groundwater sampling

Soils and groundwater samples collected during August 2001 site sampling event at Cherokee FMGP site were used to identify the soil properties, shape and size of contaminant plume, source location, geochemical environment and overall attenuation and biodegradation rates with distance at the site. Results of the chemical analysis of geochemistry, contaminants and field parameters such as temperature, dissolved oxygen, redox potential and electrical conductivity are presented in Tables D1, D2 and D3 in Appendix D. To study the changes in contaminant concentrations with depth, the aquifer was divided into two equal halves - the upper and lower half of the aquifer. Figures 3.18 - 3.29 show the iso-concentration lines for the August 2001 groundwater sampling for compounds: benzene, ethylbenzene, phenanthrene, acenaphthene, nitrate and sulfate in the upper and lower halves of the aquifer. Plots for other constituents are presented in Figures D5 - D16 in Appendix D. These plots indicate the extent of the contaminant plumes in the aquifer. Most of the contaminant plumes, except for benzene, ethylbenzene and xylene, appear to extend southward from the source. Detection of benzene, ethylbenzene and xylene near GPW 13A and GPW 13B show the

probable presence of a second source. The BTEX plumes appear to be a superposition of two plumes emanating from two contaminant sources at the site.

Aqueous PAH and BTEX concentration data around MW5 shows high concentrations in groundwater probes at GPW 20, GPW 21, GPW 24 and for some compounds in GPW 22 and GPW 23. The extent of the primary source to the west of MW5 is not known. For fate and transport modeling, the source is assumed to be between GPW 23 in the west and MW5 in the east at the site. GPW 20 and GPW 24 are assumed to be the north and south bound of the contaminant source area. Contaminant sources might also be present to the east of MW5 but due to inaccessibility of several private properties, this was not verified. A second probable source around GPW 13A and GPW 13B would not be used for fate and transport modeling as there was no historical data about its presence.

Concentration data for most of the PAH and BTEX compounds showed large differences in values in the groundwater samples taken from the upper and lower halves of the aquifer at the same push locations (see Figure 3.18 - 3.29 & D5 – D16). This indicates the possible need for multilevel groundwater sampling in the future at the site. There may be various reasons for the variation in concentrations with depth including the variation in organic carbon content with depth or the heterogeneous nature of the source materials. Organic carbon percentages for the site are presented in Table 3.3. At most of the places with high organic carbon content, low aqueous concentrations for contaminants were seen. It was interesting to note that the groundwater probes and MW's, down-gradient of the primary source (around MW5), showed higher concentrations for many of the compounds than the wells or groundwater probes in the source region. For most of the PAHs, MW3 showed higher or almost equal concentration in the upper half of the aquifer in comparison to the MW5, and GPW 24 (Figure 3.22, 3.24, D9, and D11). Similarly GPW 21, a groundwater probe down gradient of MW5 and GPW 24, showed the highest concentration for benzene in the upper half of the aquifer at the site (Figure 3.18)

The plots of geochemistry supported the natural attenuation process occurring at site. Sulfate, nitrate, and dissolved oxygen concentrations in the contaminant plume zone showed decrease in concentrations from the background values. Nitrate concentration dropped from 10 mg/L (background concentration) measured in groundwater probe GPW 14 to 2.4 mg/L at MW5 and 2.8 mg/L at GPW 13A. High concentration of nitrite at both areas showed that denitrification could be occurring at the site. Similarly high concentration of sulfide concentration near MW13A &13B indicated that sulfate reduction condition might be present at the site. Increase in the total iron concentration from background value of 0.18 mg/L to 1.6 mg/L at MW5 indicated that Fe [III] reduction was also present at the site. Methanogenic conditions were not strong at the site, as methane concentrations in the groundwater were found to be below 0.04 mg/L at all locations on the site.

Results of gas chromatography on soil samples showed high concentrations for all the PAHs at SS 3, SS 4 and in loess unit at SS 9 (the GC analysis was conducted by Shane Rogers). High concentrations of PAHs found at SS 3 and SS 4, closer to GPW 23 and GPW 20 supports the extent of source zone in the west of MW5.

3.5.6. Pre-packed screen monitoring wells

Pre-packed screen monitoring wells were installed at three locations in conjunction with earlier installed wells to determine the hydraulic heads, define the groundwater flow direction at the site and to fill the data gaps in geochemistry and contaminant concentration between existing monitoring wells. Results of contaminant concentration and geochemistry from pre-packed monitoring wells were also compared with a previously installed 2-inch diameter monitoring well.

Water levels measured in all the MW's are presented in Table B1 in Appendix B. Figure 3.30 shows the potentiometric surface map, generated using the average hydraulic head data in the monitoring wells. Groundwater direction is not uniform as presented in Figure 3.30. However, for biodegradation and overall decay rate estimation, the groundwater flow direction may be assumed to be in the same

direction in which most of the contaminant plumes appear to be extending at the site, i.e., S-SE direction or A - A' in Figure 3.30.

Hydraulic heads in the wells near the source area were nearly constant with time where hydraulic gradient was as low as 0.0003 ft/ft. In contrast, across the pinch zone, the hydraulic gradient was approximately 0.1 ft/ft. All the new pre-packed screen monitoring wells were slug tested for hydraulic conductivity, except GMW 6C. GMW 6C was a flowing artesian well. Low hydraulic conductivity was found for GMW 6A and GMW 6B and no water or very slow recovery of water was encountered in the upper half of the aquifer in nearby Geoprobe groundwater sample push locations, GPW 6 and GPW 7. This shows that the aquifer around MW 6 is confined by a very low hydraulic conductivity unit. Two new pre-packed screen monitoring wells (GMW 13A & 13B), installed at a distance of 5 feet above the pinch zone, showed a 2.38 foot difference in hydraulic head. However, hydraulic conductivity estimated in the fine unit showed lower value at GMW 13B than GMW 13A by an approximate factor of 8.

PAHs, BTEX and geochemicals concentration in MW 6 compares well with newly installed GMW's 6A, 6B and 6C except for 2- methylnaphthalene, total iron and total nitrogen (Table 3.8). It is interesting to note that even though both GMW 6C and MW6 showed artesian condition, have the same screen length in the aquifer zone, and were installed adjacent to each other (approximately 6-feet apart), the concentrations of total iron and total nitrogen in GMW 6C were about two to three times higher than the concentration in MW6. The difference in concentrations could be either due to sampling variability or the concentrations of geochemical parameters varied in an unknown fashion with distance near the well. Geochemical and contaminant concentration data obtained at each of the pre-packed screen monitoring wells 6A, 6B and 6C was compared individually and in overall with the data obtained at MW6 using non-parametric tests, Sign and Friedman respectively (software XLSTAT version 5.1, Addinsoft, Paris, France). Comparison results indicated no significant differences at 95 % confidence level (α = 0.05) in the two

types of monitoring wells (Table 3.8). Friedman's and Sign's test decision are presented in section D2 in Appendix D.

3.6. Overall Attenuation and Biodegradation Rates

Overall attenuation rates and biodegradation rates for BTEX and four PAH compounds, phenanthrene, naphthalene, acenaphthene, and acenaphthylene, were estimated by assuming that the contaminant plumes were stable at the site. Overall attenuation rates were estimated by plotting the natural log of the measured concentrations for the compounds against distances along the assumed flow path. A regression equation for concentration versus distance (for 1-D flow with no transverse dispersion) is given by Kemblowski et al. (1987) as:

$$C_{(X)} = C_0 e^{-\left(k\frac{x}{v_x}\right)} \qquad \text{(Eq. 3.3)}$$

where C_O = Concentration in upgradient well in M/L^3

v_x = Linear groundwater velocity (L/T)

k = First order overall attenuation rate constant (T^{-1})

x = Distance between upgradient and downgradient well (L)

C_x = Concentration in downgradient well at distance x from upgradient well (M/L^3)

Flow paths for the contaminants were derived from their plume shapes. Overall attenuation rates of contaminants were estimated along two possible flow paths, A - A' and B - B' (presented in Figure 3.31). Flow path A - A' is through GPW20, MW3, GPW3, GPW8, and MW7. Flow path B - B' is through MW5, GPW24, GPW4, and GPW9. Concentrations at MW3, MW5, and MW7 were obtained by averaging the concentrations obtained since 1991 at the site. For groundwater probe wells, the August 2001 data was used. MW5 and GPW20 were taken as the upgradient wells along the two flow paths. Trends with distance for BTEX and PAH compounds along flow path A – A' and B – B' are shown in Figures 3.32.a,b - 3.33.a,b. For the target analytes, the slope between any two adjacent locations along the flow path was calculated from Figures 3.32.a,b – 3.33.a,b and

multiplied by the average seepage velocity between them to get the overall attenuation rate constant. Overall attenuation rate constant for a target analyte at the site was obtained by averaging the attenuation rate constants estimated between all the adjacent locations along the flow path for the analyte. Table 3.9 shows the calculation for the seepage velocities and the overall attenuation rates at the site. Average overall attenuation rates for BTEX varied from 0.0058 – 0.011 d^{-1} and for PAHs from 0.013 – 0.022 d^{-1}.

The method of Buscheck and Alcantar (1995) was used to estimate the biological attenuation rate constants for a steady-state plume using the overall attenuation rate constants and the estimated retardation factor and longitudinal dispersivity. The Buscheck and Alcantar equation for estimating the first order biodegradation rate constants is given by:

$$\lambda = \frac{v_c}{4\alpha_x}\left[\left(1+2\alpha_x\left(\frac{k}{v_x}\right)\right)^2 - 1\right] \qquad \text{(Eq.3.4)}$$

where λ = First order biodegradation rate constant (T^{-1})

v_c = Retarded contaminant velocity along the flow path (L/T)

k = Overall attenuation rate constant (T^{-1})

α_x = Longitudinal dispersivity (L)

v_x = Linear groundwater velocity (L/T)

Like the overall attenuation rate constants, the biodegradation rates were also estimated between all the adjacent push locations along the flow path and then the average was taken to estimate the biodegradation rate for each contaminant at the site. The results are given in Table 3.10 along with estimated retardation and dispersivity values. The biodegradation rates varied from 0.00019 – 0.0022 d^{-1} for BTEX compounds and from 0.00003 – 0.0003 d^{-1} for PAHs. Table 3.11 compares the estimated overall attenuation rates and biodegradation rates with published results. The rates estimated for the Cherokee site were found to be lower than the published range.

Miller (2001) estimated the overall attenuation and biodegradation rate constants at Cherokee, FMGP site by assuming a flow path between MW5 and MW6. Miller (2001) used the concentrations obtained till 1998 at the site for BTEX, phenanthrene, and naphthalene. To compare the results, rate constants were estimated by assuming a flow path between MW5 and MW6 (C – C' in Figure 3.31) and using the average concentrations obtained at both wells since their installation in 1993. The comparison of overall and biodegradation rate constants between Miller (2001) and this study are presented in Table 3.12. Table 3.12 shows that the estimated overall attenuation rate constants were nearly the same for both studies but estimated biodegradation rates were significantly lower in this study than Miller (2001). There are two reasons for the difference: 1) Miller (2001) used the distance between MW5 and MW9 to estimate dispersivity while in this study the phenanthrene plume length was used to estimate dispersivity and 2) Miller (2001) used the estimated literature values for the retardation factors while in this study actual organic carbon contents obtained at the site were used to estimate retardation factors.

An attempt was made to assess plume stability with respect to time at MW3, MW5 and MW6. Data from the earlier groundwater sampling events and August 2001 event were used to produce trends in the concentration (shown in Figures 3.34 – 3.36). But due to the high variability in the concentrations with time no significant trend was made. However, the plots show that some contaminant concentrations have decreased from the high values seen in 1993-1994 for the eight target analytes at all three MW's.

3.7. Summary

Protocols were developed and strategically applied at Cherokee FMGP site for the use of direct push technology to characterize geology, hydrogeology and geochemical environment at the site. Both electrical conductivity and hydraulic conductivity results indicated the thinning of the aquifer unit in south of Beech Street. Hydraulic conductivity at the site varied from 0.0000092 cm/sec to 0.00003 cm/sec

in the loess and 0.000032 cm/sec to 0.46 cm/sec in the alluvium. The hydraulic conductivity in the pinch zone was found to be as low as 0.000025 cm/sec. Hydraulic conductivity value measured at a newly installed pre-packed screen monitoring well, GMW 12, was almost the same as that of near-by pre-existing MW9 (see Table 3.4 & Table B2). Hydraulic conductivity of Geoprobe dual push location HC5 matched the high hydraulic conductivities estimated earlier in the nearby pre-existing MW10 and MW11. Hydraulic conductivity results indicate that the pre-packed screen monitoring wells and Geoprobe dual tube direct-pushes might be a less expensive alternative for hydraulic conductivity testing than conventional 2-inch monitoring well. Estimates of hydraulic conductivity by Hazen's correlation were found to be similar to the measured hydraulic conductivity in the pinch zone at the site. Groundwater concentrations measured using new pre-packed screen monitoring wells gave statistically similar concentrations as that of 2-inch monitoring well. Due to ease in installation and lower cost, the pre-packed monitoring wells may be an efficient method for monitored natural attenuation application.

Results of the groundwater sampling indicated that the pinch zone restricted the contaminant plume. Most of the contaminants except for benzene, ethylbenzene and xylene were found to extend in S-SE direction from the source area in the same direction as for the groundwater flow. Presence of benzene, ethylbenzene and xylene (aqueous) concentrations near GPW 13A and GMW 13B showed the possible presence of a second source. Large differences in the concentrations were observed in the groundwater samples taken from the upper and lower halves of the alluvium. However, the depth of the contaminant source was not clear from August 2001 groundwater sampling data as compounds didn't show consistent high or low concentrations in either upper or lower halves of the aquifer. Overall attenuation and biodegradation rates for BTEX were estimated to vary from 0.0058 d^{-1} - 0.011 d^{-1} and 0.0002 d^{-1} - 0.0022 d^{-1}, respectively, and 0.013 d^{-1} - 0.022 d^{-1} and 0.00003 d^{-1} - 0.00029 d^{-1}, respectively, for PAHs (naphthalene, phenanthrene, acenaphthylene, and acenaphthene). Overall attenuation and biodegradation rates obtained at the Cherokee site were found to be lower than published values for these contaminants.

3.8. Recommendations for future sampling programs

There are some data gaps in phase I activity that need to be filled in the phase II site characterization activity. The direction and extent of the pinch in the alluvium is not clearly known. More EC pushes between MW6 and MW8, in the vicinity of the gas tanks at the site, and in between the existing EC pushes down gradient of MW6 should help identifying the extent of the pinch. EC locations for phase II are presented in Figure E1 in Appendix E. The flow direction of groundwater has a certain level of uncertainty. Data showed large differences in hydraulic heads, 12.9 ft and 10.2 ft between MW6 and MW8, and MW6 and GMW13A, respectively. There is a need to install new pre-packed screen monitoring wells in this vicinity in phase II to help to determine the groundwater flow pattern (presented in Figure E2 in Appendix E). The source zone for contaminants is not well defined. Soil and groundwater sampling to the west and south of the assumed source area will reduce the uncertainty. High PAH concentrations found in GPW19 and GPW22 indicate the possible existence of source to the west of Fourth Street. More soil and groundwater probes should be conducted downgradient of MW5 as high concentrations were found for BTEX in GPW21 and GPW24. Locations for soil and groundwater sampling south and west of MW5 to be conducted in phase II are presented in Figures E3 – E4 in Appendix E.

The second potential source of contamination found near GPW 13A & B needs to be characterized. It may be a gasoline spill because of the low PAH concentrations found near GPW 13A & B. Groundwater samples shall also be collected from pre-packed monitoring wells to be installed in phase II of site investigations. Groundwater should be sampled every three to four months from both 2-inch and pre-packed monitoring wells for MNA study at this site. Additional hydraulic conductivity tests need to be conducted at the locations presented in Figure E5 in Appendix E. Hydraulic conductivity test locations are based on data gaps found under existing test locations. The new pre-packed monitoring wells to be installed during phase II need to be tested for hydraulic conductivity.

Table 3.1. Groundwater stabilization criteria for flow-through cell

Parameter	Criteria
pH	3 consecutive measurements within 0.2 units
Conductivity	3 consecutive measurements within 0.02 mS/cm
Turbidity	3 consecutive measurements within 4 NTUs and ≤ 10 NTUs
ORP/E_h	± 30 mV (3 consecutive measurements within 60 mV)
Temperature	± 0.5°C (3 consecutive measurements within 1°C)
Dissolved Oxygen	± 0.2 mg/L (3 consecutive measurements within 0.4 mg/L)

Table 3.2. EC values for different soil types

Soil Type	EC Value (mS/m)	Average Particle Size (mm)
Gravel	<40	>2.00
Sandy Gravel	40-50	>1.75
Sand	40-60	1-2
Silty Gravel	60-80	1-0.006
Silty Sand	60-90	1-0.005
Silt	80-110	0.006-0.002
Silty Clay	80-180	0.006-0.0005
Clay	140-200	<0.002

Table 3.3. Average organic carbon content (%) in soil at different depths

Soil Sample	Depth (ft) (bgs)	Layer Type	Total C by Dry Combustion (%)	Average Total C (%)	$CaCO_3$ by Pressure Calcimeter (%)	Inorganic Carbon (%)	Org. Carbon by Walkley - Black Method (%)	Average Organic C (%)
SS 2	4-8	loess	2.30 2.97	2.63	24.5	2.9	0.29 0.29	0.29
SS 2	18-20	alluvium	2.95 2.63	2.79	21.7	2.6	0.2 0.3	0.25
SS 2	24-26	alluvium	2.60 3.41	3.00	35.5	4.3	0.2 0.2	0.2
SS 5	12-14	alluvium	0.62 0.61	0.62	0.4	0.05	0.8 0.8	0.8
SS 5	16-18.5	alluvium	1.77 1.40	1.59	15.3	1.8	0.3 0.3	0.3
SS 6	6-8	loess	5.55 5.56	5.56	20.5	2.5	2.97 3.14	3.05
SS 6	12-14	alluvium	4.46 4.39	4.42	11.6	1.4	2.6 2.6	2.6
SS 6	16-18	alluvium	2.62 2.86	2.74	35.4	4.2	0.4 0.3	0.35
SS 8	8-10	loess	1.29 1.03	1.16	48.1	5.8	0.3 0.3	0.3
SS 8	10-12	loess	2.25 2.51	2.38	21.5	2.6	0.2 0.2	0.2
SS 8	16-18.5	alluvium	2.43 1.99	2.21	25.6	3.1	0.1 0.2	0.15
SS 10	12-13.5	loess	5.26 5.52	5.39	23.3	2.8	2.6 2.6	2.6
SS 10	16-18	loess	8.76 8.73	8.75	57.1	6.8	2.9 2.9	2.9
SS 12	8-10	loess	0.74 0.76	0.75	2.9	0.3	0.8 0.6	0.7
SS 12	16-18.5	loess	5.04 5.63	5.34	18.9	2.3	3.8 4	3.9
HC 5	12-16	loess	4.27 4.16	4.21	40.1	4.8	0.3 0.4	0.35
HC 5	22-26	alluvium	3.72 3.07	3.40	38.9	4.7	0.3 0.3	0.3

Table 3.4. Hydraulic conductivity measurements during August 2001 sampling event at Cherokee FMGP site, Iowa

Location	Date of Testing	Method	Soil Type	Elevation (ft)	Water Level at Location (bgs) (ft)	Screen Range (bgs) (ft)	Screen Length (ft)	Shape Factor (m)	Hydraulic Conductivity	
									B&V[1] (cm/sec)	Superslug[2] (cm/sec)
HC 1A	08/12/2001	rising	alluvium	1182.71	11.5	21-22	1	0.8	4.00E-05	4.08E-05
HC 2	08/12/2001	rising	alluvium/till	1175.2	7	24-25	1	0.8	3.20E-05	3.208E-05
HC 3	08/12/2001	falling	loess	1175.49	4.5	21-22	1	0.8	1.68E-05	1.577E-05
HC 4	08/12/2001	falling	loess	1175.64	4.65	21-22	1	0.8	2.55E-05	8.44E-05
HC 5	08/09/2001	rising	alluvium	1172.97	14.5	14-15	1	0.8	1.48E+01	NC
HC 5	08/10/2001	falling	alluvium	1172.97	14.5	14-15	1	0.8	4.58E-01	7.31E-02
MW 4	08/14/2001	falling	alluvium	1188.73	12.37	20.5-30	9.8	7.54	6.11E-02	NC
MW 10	08/13/2001	falling	alluvium/till	1172.48	14.84	36.2-41	4.8	5.23	4.78E-01	1.30E-01
GPMW6A	08/13/2001	rising	alluvium	1176.34	NR	11-14	3	1.6	9.03E-04	8.90E-04
GPMW6B	08/13/2001	rising	alluvium/till	1176.29	NR	18-21	3	1.6	3.31E-04	3.27E-04
GPMW12	08/13/2001	rising	alluvium	1172.71	15	32-35	3	1.6	1.24E-02	1.24E-02
GPMW13A	08/13/2001	rising	loess	1174.7	8.8	15-18	3	1.6	7.72E-05	3.89E-05
GPMW13B	08/13/2001	rising	loess	1174.53	11.1	24-27	3	1.6	9.29E-06	8.43E-06

NR - Not reported

NC - Data is not correct

[1] - Estimated by Black & Veatch, Inc.

[2] - Estimated by using Superslug Software

Table 3.5. Grain size distribution for some of the soil samples collected during August 2001 sampling event at Cherokee FMGP site, Iowa

SS2		**HC5**		**SS10**		**SS12**	
Depth = 18-22 bgs		Depth = 16-20 bgs		Depth = 14-20 bgs		Depth = 16-24 bgs	
Fraction (%)		Fraction (%)		Fraction (%)		Fraction (%)	
gravel	12.08	gravel	0.20	gravel	4.00	gravel	0.5
sand	52.92	sand	96.57	sand	46.68	sand	28.1
silt	19.50	silt	3.07	silt	45.72	silt	66.4
clay	15.50	clay	0.16	clay	3.60	clay	5.0
Classification		Classification		Classification		Classification	
SC-SM		**SP**		**SM**		**CL-ML**	
Silty Clayey sand		Poorly graded sand		Silty sand		Silty Clayey Sand	

Table 3.6. Estimated hydraulic conductivity by Hazen's formula and actual measured values in nearly wells at Cherokee FMGP site, Iowa

Location	D_{10} (mm)	Estimated K (cm/sec)	Closest MW	Measured K (cm/sec)
HC 5	2.8E-01	6.3E-02	MW 10	1.3E-01
SS 10	9.0E-03	3.2E-05	HC 2	3.2E-05
SS 12	7.5E-03	2.3E-05	HC 3	1.6E-05

Table 3.7. Porosity and bulk density measured in soil samples from August 2001 sampling event at Cherokee FMGP site, Iowa

Location	Depth (bgs) (ft)	Expected Layer	Porosity (%)	Bulk Density (g/cm^3)
SS IA	11	alluvium	22.49	2.054
	19	alluvium	28.85	1.886
SS 2	13.5	alluvium	26.22	1.955
	22	alluvium	32.68	1.694
	25.5	alluvium	17.25	2.192
SS 6	7.5	loess	44.26	1.5
	13	alluvium/loess	53.11	1.265
	17	alluvium	32.5	1.43
SS 8	9	alluvium/loess	40.58	1.604
	13	alluvium	22.35	2.058
SS 10	14	loess	50.72	1.33
	17.5	loess	59.92	1.08
SS 12	11.5	loess	51.62	1.306
	14	loess	53.47	1.256
	22	alluvium/loess	52.5	1.282

Table 3.8. Comparison of the data obtained by MW6 & GPMW 6A, 6B & 6C

Analyte	GPMW6A (µg/L)	GPMW6B (µg/L)	GPMW6C (µg/L)	MW6 (µg/L)
BTEX				
Benzene	1	1.1	1.5	1
Toluene	1	1	1	1
Ethylbenzene	1	1	1	1
Xylenes	3	6.7	3.2	3
PAH				
1-Methylnaphthalene	1.9	13.7	10.1	9
2-Methylnaphthalene	1.9	0.19	0.19	0.19
Acenaphthene	64	18.2	6.97	6.59
Acenaphthylene	17.3	16.7	12.7	15
Anthracene	0.1	0.1	0.1	0.1
Benzo(a)anthracene	0.1	0.1	0.1	0.1
Benzo(a)pyrene	0.1	0.1	0.1	0.1
Benzo(b)fluoranthene	0.1	0.1	0.1	0.1
Benzo(g,h,i)perylene	0.1	0.1	0.1	0.1
Benzo(k)fluoranthene	0.1	0.1	0.1	0.1
Chrysene	0.1	0.1	0.1	0.1
Dibenz(a,h)anthracene	0.1	0.1	0.1	0.1
Fluoranthene	0.1	0.1	0.1	0.1
Fluorene	0.19	0.19	0.19	0.19
Naphthalene	1	3.67	1.76	3.18
Indeno(1,2,3-cd)pyrene	0.1	0.1	0.1	0.1
Phenanthrene	0.86	0.1	0.33	0.3
Pyrene	0.19	0.19	0.19	0.19
GEOCHEM				
Ammonia Nitrogen	200	200	200	200
Total Iron	130	160	1350	405
Magnesium	31900	38700	38700	34000
Total Nitrogen	1300	1000	3300	1450
Orthophosphate	100	100	100	100
Sulfate	140000	130000	150000	155000
STATISTICS				
Sign's Test				
at α = 0.025, n=28, P =	0.377	0.113	0.033	
Result	Statistically similar results as MW6			
Friedman's Test				
at α = 0.05, n=28, P =	0.542			
Result	Statistically similar results as MW6			

Table 3.9. Estimated overall natural attenuation rate constants for target analytes at Cherokee FMGP site, Iowa

Along Flow Path A-A' *								
Analytes	GPW20-MW3		MW3-GPW3		GPW3-GPW8		GPW8-MW7	
	Slope (ft^{-1})	Attenuation Rate (d^{-1})	Slope (ft^{-1})	Attenuation Rate (d^{-1})	Slope (ft^{-1})	Attenuation Rate (d^{-1})	Slope (ft^{-1})	Attenuation Rate (d^{-1})
Benzene	-0.0067	0.003	PS	-	-0.016	0.0187	-0.0062	0.014
Toluene	-0.0161	0.0073	-0.0074	0.0086	PS	-	-0.0111	0.026
Ethylbenzene	-0.0118	0.0054	-0.0183	0.021	PS	-	-0.0044	0.01
Xylenes	-0.0094	0.0043	-0.0035	0.0041	-0.0011	0.0013	-0.0078	0.018
Phenanthrene	PS	-	-0.0082	0.0096	-0.0324	0.038	PS	-
Naphthalene	-0.0107	0.0048	-0.0377	0.044	PS	-	-0.0274	0.064
Acenapthene	PS	-	-0.01	0.012	-0.029	0.034	-0.0038	0.0089
Acenaphthylene	PS	-	-0.0104	0.012	-0.0332	0.039	PS	-
Field Parameters								
k (ft/day)	170		5		5		10	
Hydraulic gradient (ft/ft)	0.0008		0.07		0.07		0.07	
Porosity	0.3		0.3		0.3		0.3	
Seepage velocity (ft/day)	0.453		1.167		1.167		2.333	

PS - Positive slope (indicates increase in concentration with distance from source along the flow path)

* - See Figure 3.31

Table 3.9. Estimated overall natural attenuation rate constants for target analytes at Cherokee, Iowa (continued)

Along Flow Path B-B' *							Overall Average Attenuation Rate (d^{-1})**
Analytes	MW5-GPW24		GPW24-GPW4		GPW4-GPW9		
	Slope (ft^{-1})	Attenuation rate (d^{-1})	Slope (ft^{-1})	Attenuation rate (d^{-1})	Slope (ft^{-1})	Attenuation rate (d^{-1})	
Benzene	-0.006	0.0027	PS	-	-0.0166	0.011	0.001 ± 0.007
Toluene	-0.03	0.014	-0.0112	0.006	-0.0079	0.0053	0.011 ± 0.008
Ethylbenzene	PS	-	-0.0134	0.0071	-0.007	0.0047	0.010 ± 0.007
Xylenes	-0.0022	0.001	-0.0071	0.0038	-0.0121	0.008	0.006 ± 0.006
Phenanthrene	-0.0065	0.003	-0.0083	0.0044	-0.0249	0.017	0.014 ± 0.014
Naphthalene	-0.0019	0.00086	-0.0291	0.016	-0.0067	0.0045	0.022 ± 0.026
Acenapthene	-0.0096	0.0044	-0.0048	0.0026	-0.022	0.0015	0.013 ± 0.011
Acenaphthylene	-0.016	0.0073	-0.0082	0.0044	-0.0257	0.017	0.016 ± 0.014
Field Parameters							
k (ft/day)	170		20		2		
Hydraulic gradient (ft/ft)	0.0008		0.008		0.1		
Porosity	0.3		0.3		0.3		
Seepage velocity (ft/day)	0.453		0.533		0.667		

PS - Positive slope (indicates increase in concentration with distance from source along the flow path)

* - See Figure 3.31

** - Calculated by taking average of rates along both flow path A - A' and B - B'

Table 3.10. Estimated biodegradation rate constants at Cherokee FMGP site, Iowa

Analytes	Overall Attenuation Rate (d^{-1})	Retardation Factor*	Dispersivity (ft)**	Biodegradation Rate (d^{-1})***
Benzene	1.00E-02	6	25	2.18E-03
Toluene	1.12E-02	19	25	8.05E-04
Ethylbenzene	9.82E-03	67	25	1.94E-04
Xylenes	5.84E-03	14.6	25	4.80E-04
Phenantherene	1.43E-02	79.1	25	2.94E-04
Naphthalene	2.23E-02	273.5	25	1.42E-04
Acenapthene	1.27E-02	152	25	1.25E-04
Acenaphthylene	1.25E-02	853	25	3.05E-05

* - Retardation factor was calculated assuming linear sorption

** - Dispersivity was taken as 10% of phenanthrene plume size

*** - Biodegradation rates were calculated using Buscheck & Alcantar equation

Table 3.11. Comparison of estimated overall and biodegradation decay rate constants at Cherokee FMGP site, Iowa with published values

Compound	Estimated Overall Attenuation Rates (d^{-1})	Published Overall Attenuation Range (d^{-1})*	Estimated Biodegradation Rates (d^{-1})	Published Biodegradation Range (d^{-1})**
Benzene	1.0E-02	4.0E-02 - 2.0E-01	2.2E-03	1.4E-04 - 3.0E-02
Toluene	1.1E-02	7.0E-02 - 1.3E-01	8.0E-04	2.0E-03 - 8.4E-01
Ethylbenzene	1.0E-02	7.0E-02 – 2.2E-01	2.0E-04	NA
Xylenes	6.0E-03	2.9E-02 – 3.0E-01	5.0E-04	0.01-0.2
Naphthalene	1.4E-02	0.029	3.0E-04	4.6E-05 - 8.8E-01
Phenanthrene	2.2E-02	NA	1.4E-04	NA
Acenaphthene	1.3E-02	NA	1.2E-04	NA
Acenaphthylene	1-2E-02	NA	3.0E-05	NA

NA - Not available
* - See Table 2.5 for reference
** - See Table 2.6 for reference

Table 3.12. Comparison of estimated overall and biodegradation decay rate constants at Cherokee FMGP site, Iowa against Miller (2000) results

Compound	Estimated Overall Attenuation Rates (d^{-1})	Miller's Overall Attenuation Rates (d^{-1})*	Estimated Biodegradation Rates (d^{-1})	Miller's Biodegradation Rates (d^{-1})*
Benzene	0.007	0.008	0.0015	0.0063
Toluene	0.013	0.012	0.001	0.0017
Ethylbenzene	0.012	0.013	0.0003	0.006
Xylenes	0.01	0.011	0.001	0.0053
Naphthalene	0.014	0.015	0.00008	0.0019
Phenanthrene	0.0076	0.008	0.00013	0.0001

* - Rates were estimated for the compounds assuming flow path between MW5 and MW6.

Figure 3.1. Plan view of the Cherokee FMGP site, Iowa

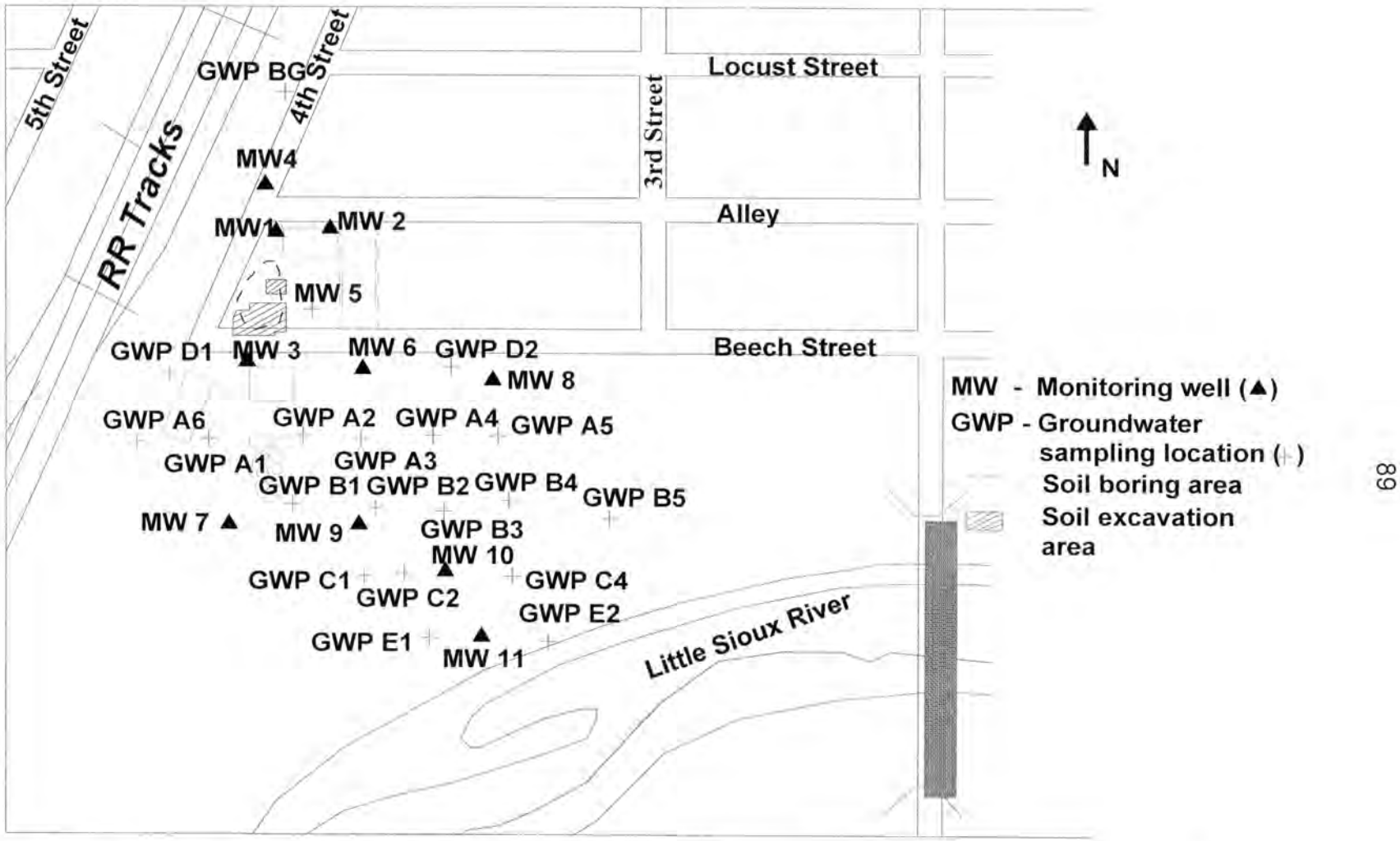

Figure 3.2. Sketch showing monitoring wells, soil excavation zone, some soil and groundwater sampling locations at Cherokee FMGP site, Iowa prior to 1999
(Not all historic soil sample locations are shown here)

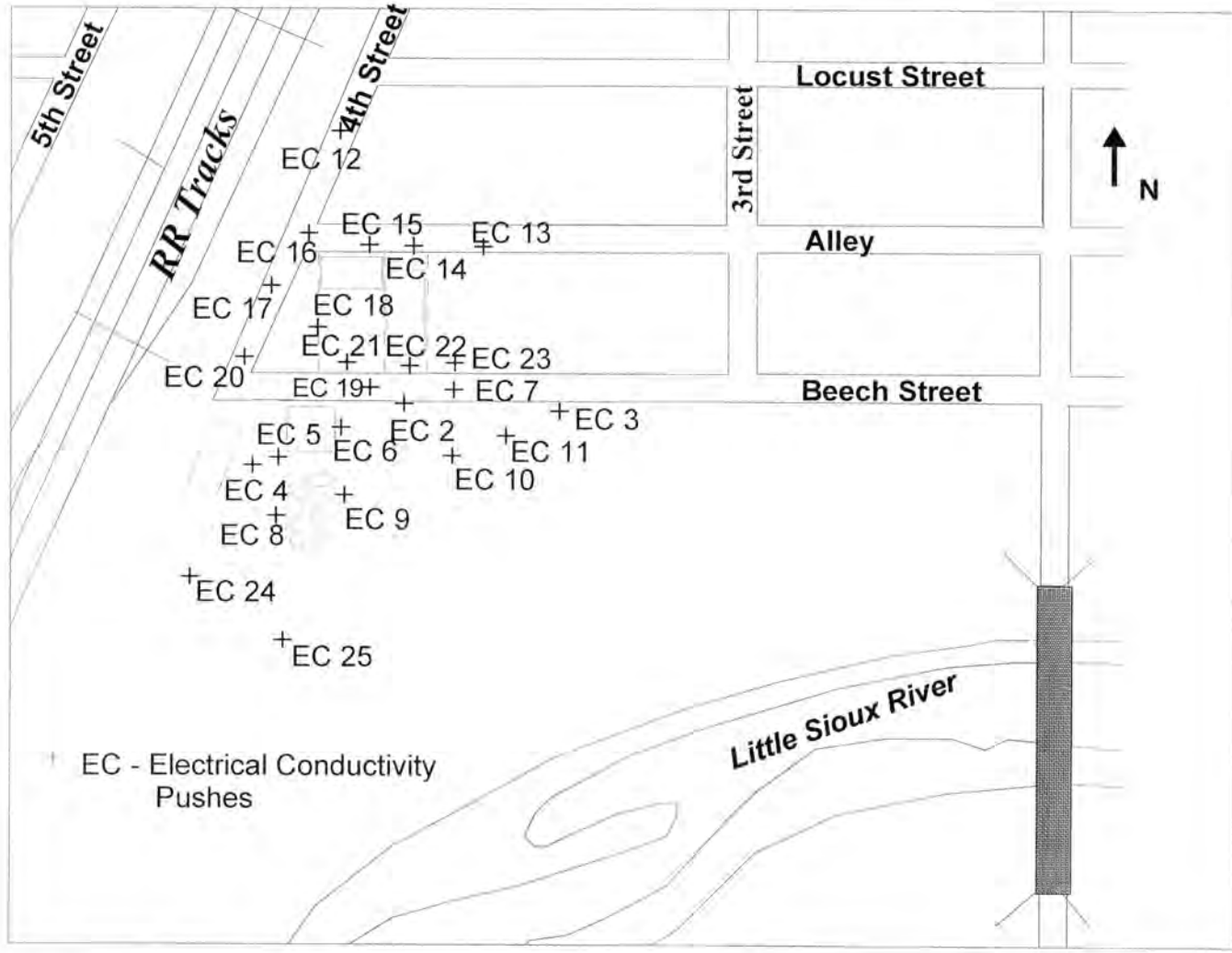

Figure 3.3. Electrical conductivity push locations at Cherokee FMGP site, Iowa (conducted in August 2001)

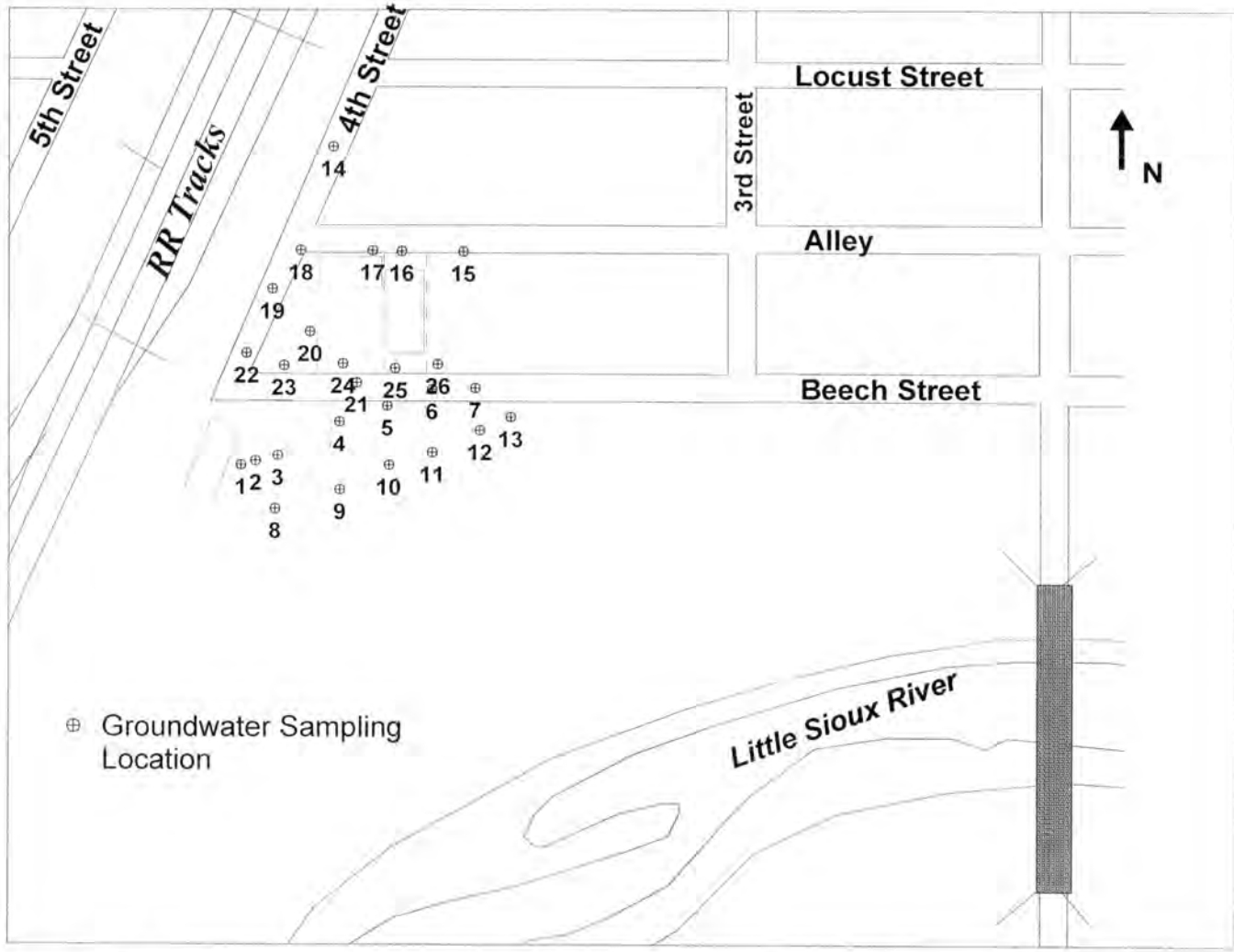

Figure 3.4. Groundwater sampling locations at Cherokee FMGP site, Iowa (conducted in August 2001)

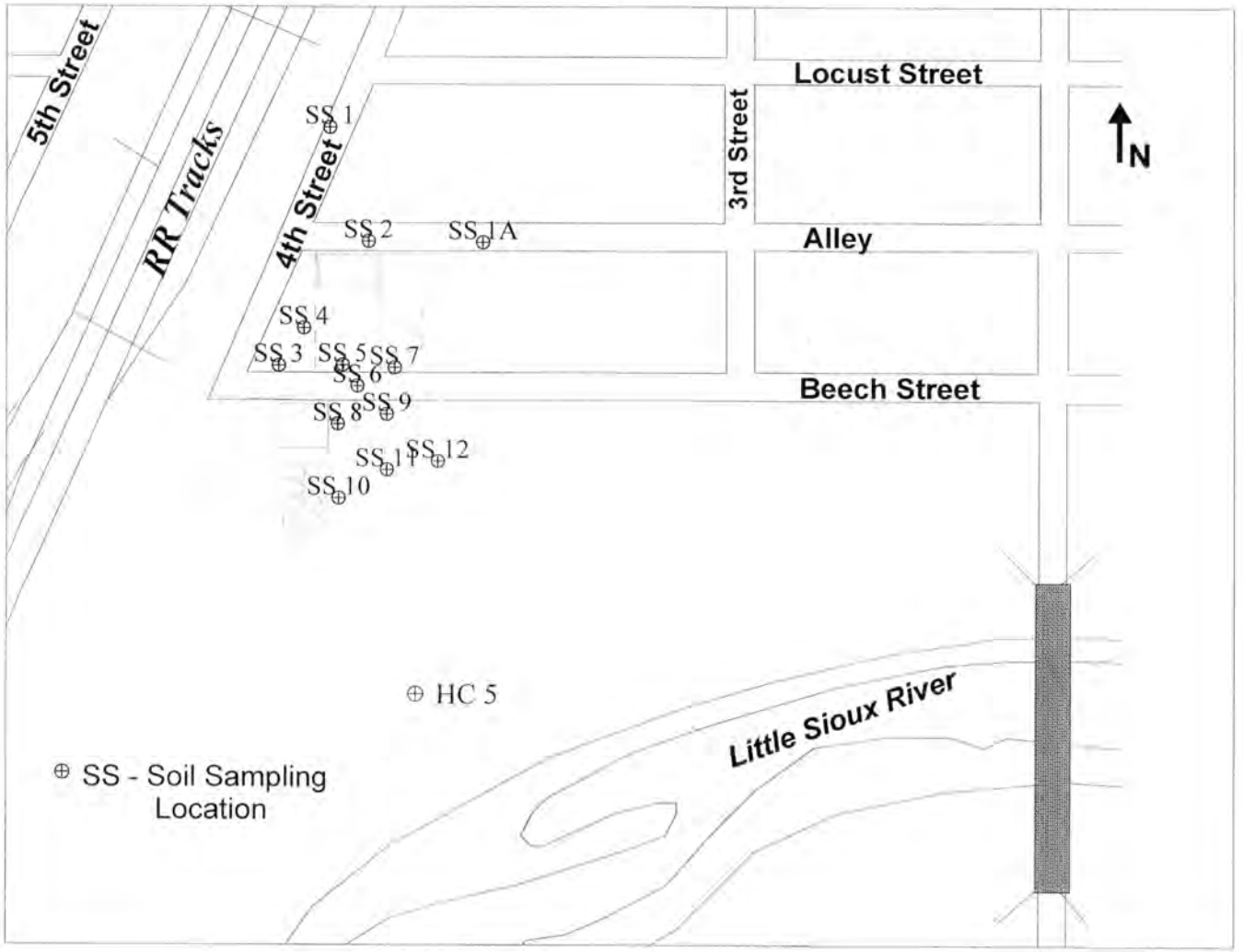

Figure 3.5. Soil sampling locations at Cherokee FMGP site, Iowa (conducted in August 2001)

Figure 3.6. Pre-packed screen monitoring well locations at Cherokee FMGP site, Iowa (installed in August 2001)

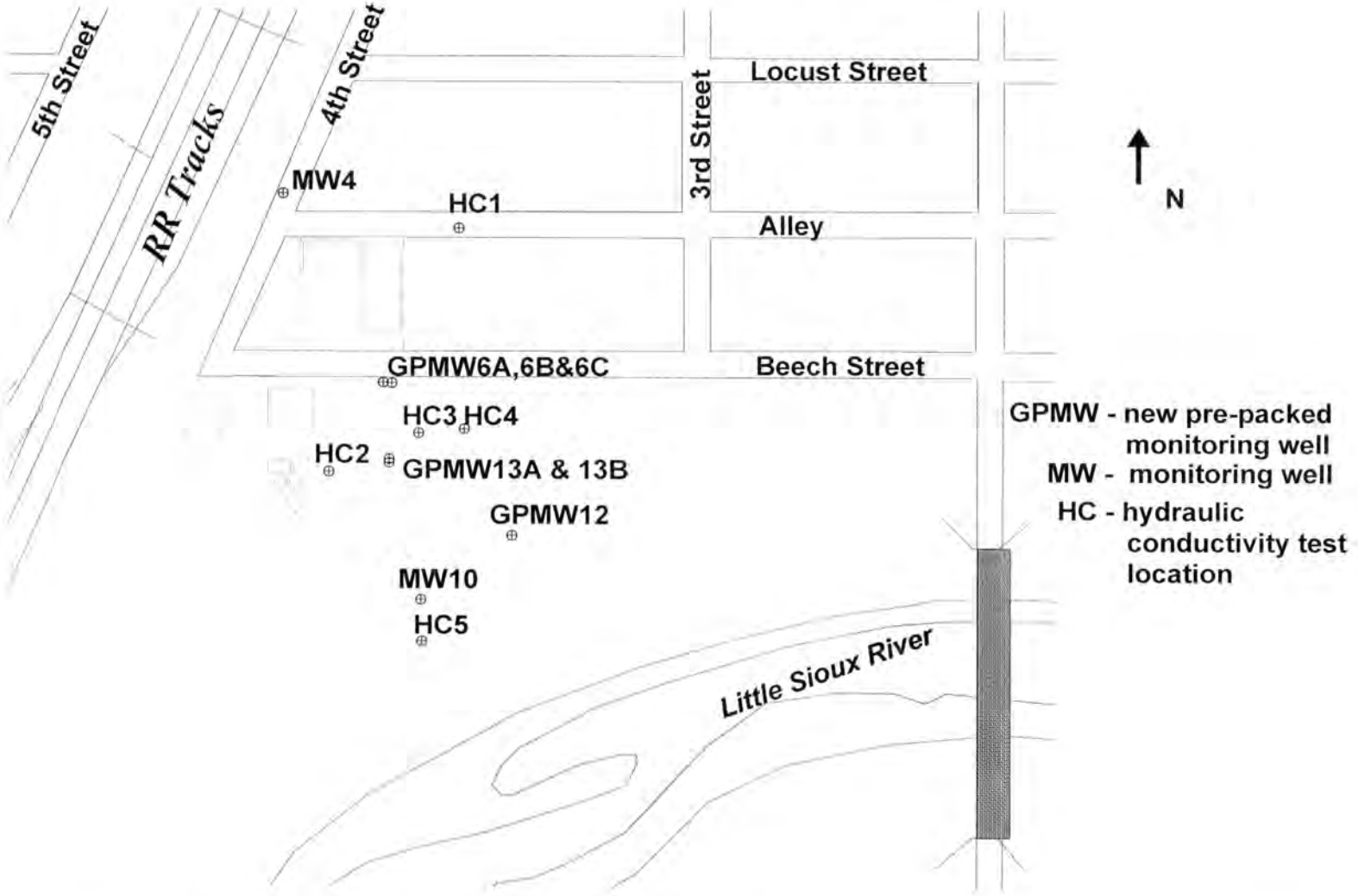

Figure 3.7. Hydraulic conductivity test locations at Cherokee FMGP site, Iowa (conducted in August 2001)

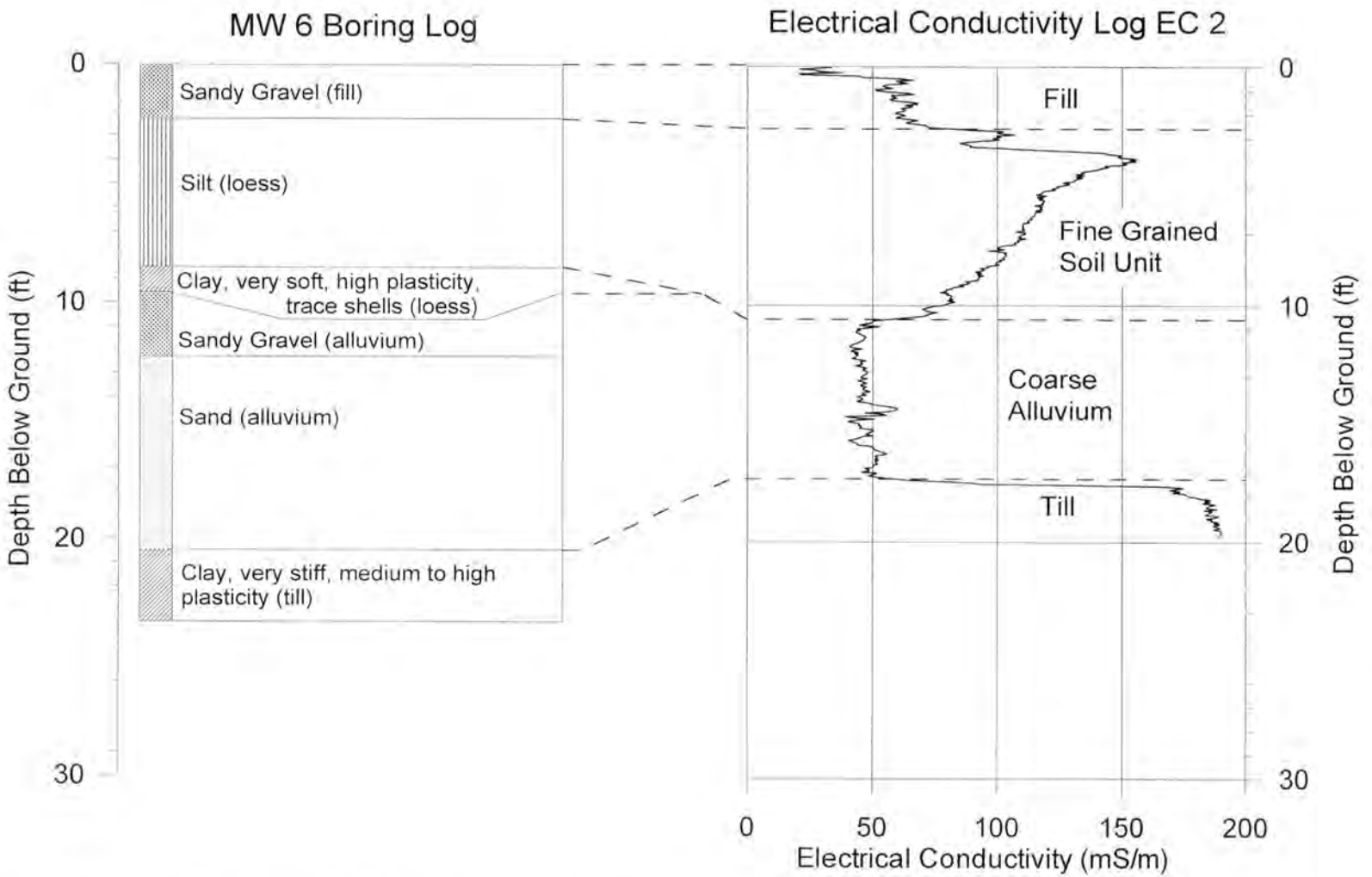

Figure 3.8a. Comparison of electrical conductivity log at EC2 and soil boring log for MW6 at Cherokee FMGP site, Iowa

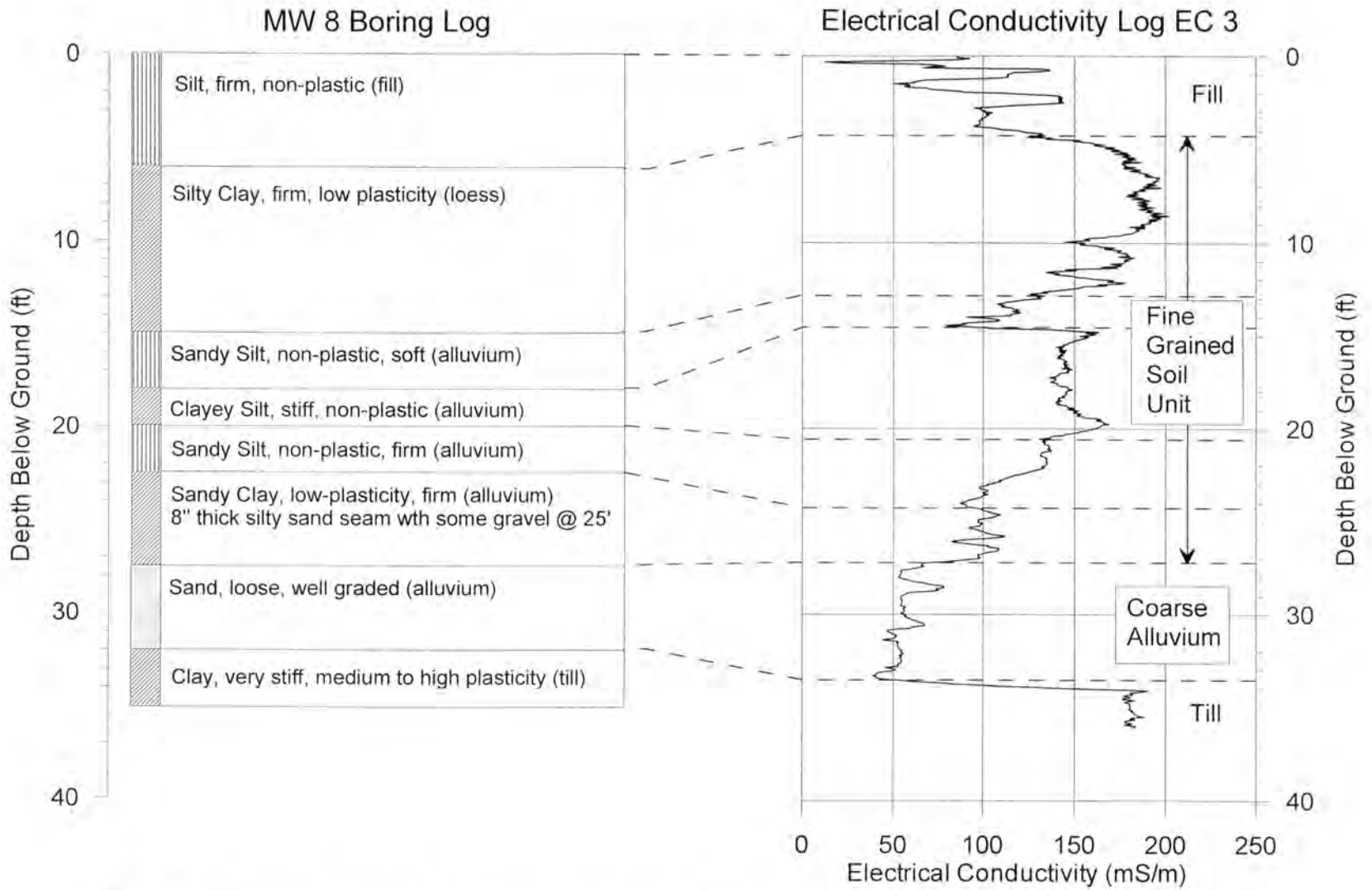

Figure 3.8b. Comparison of electrical conductivity log, EC3, and soil boring log for MW8 at Cherokee FMGP site, Iowa

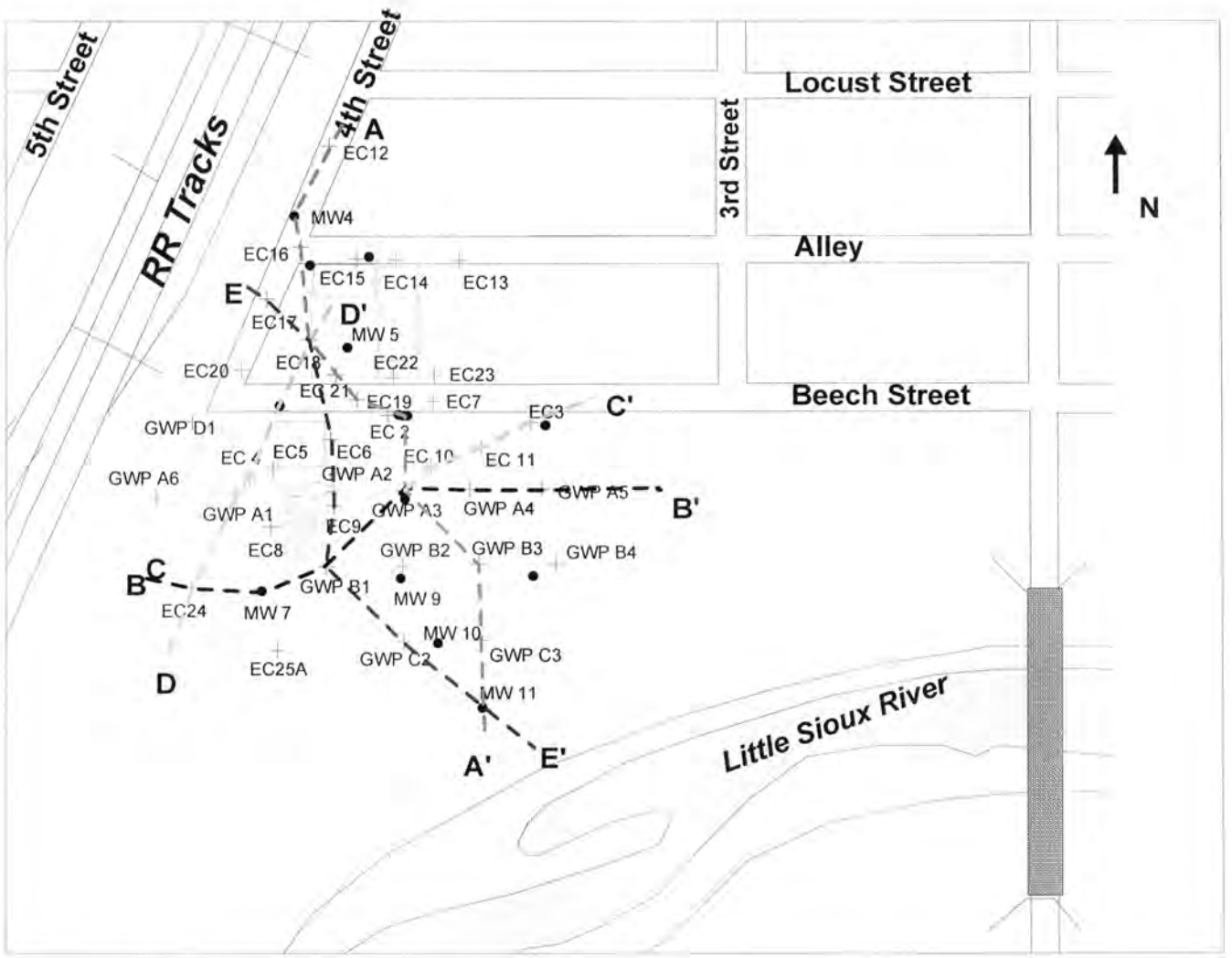

Figure 3.9. Transects across the Cherokee FMGP site, Iowa

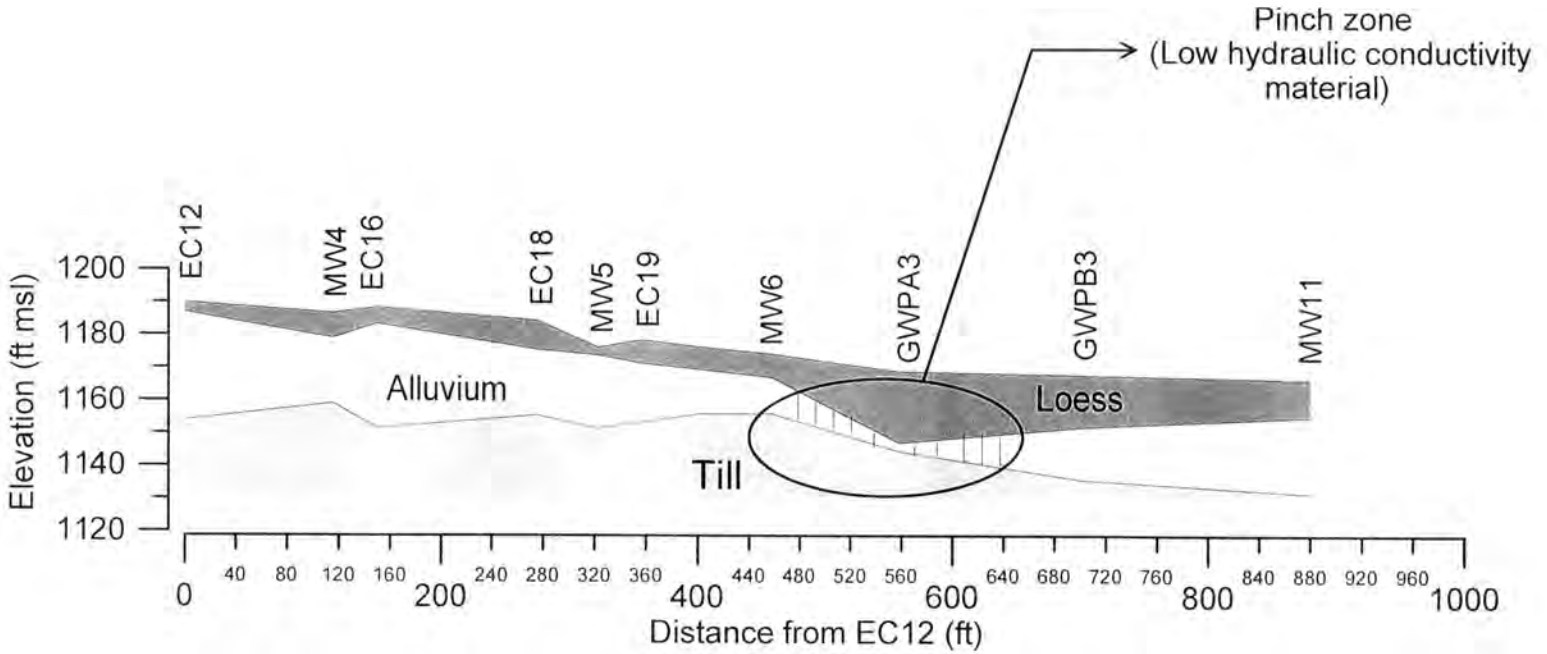

Figure 3.10. Transect A-A' at Cherokee FMGP site, Iowa

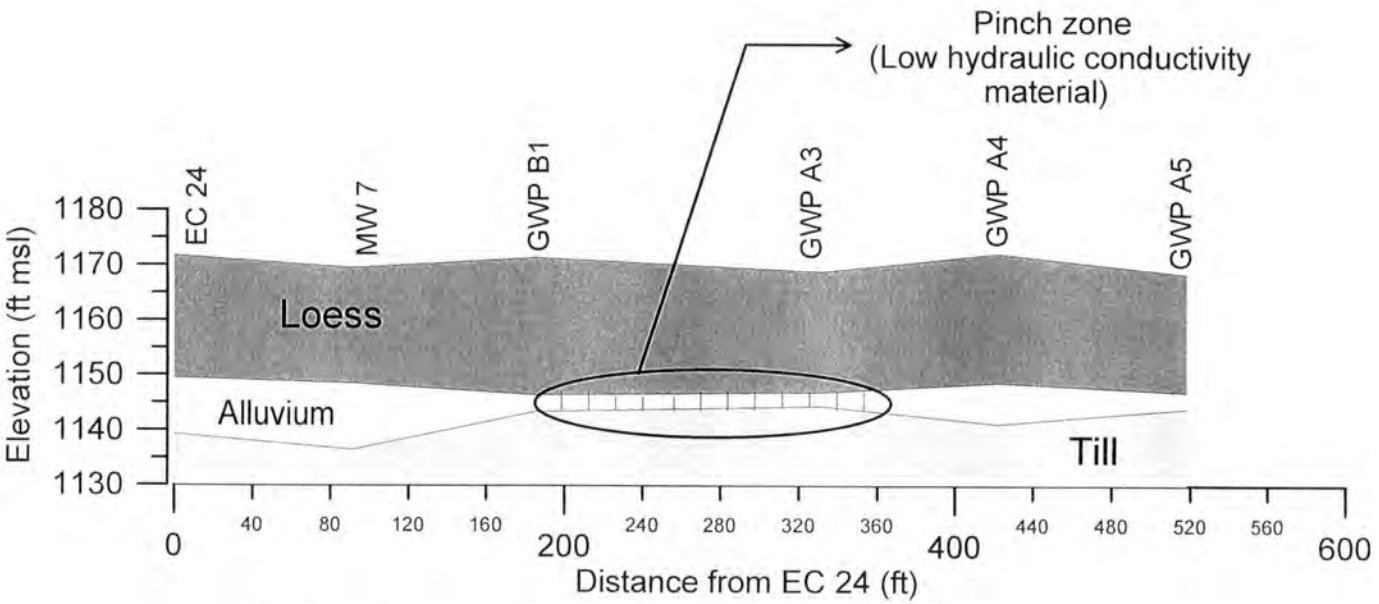

Figure 3.11. Transect B-B' at Cherokee FMGP site, Iowa

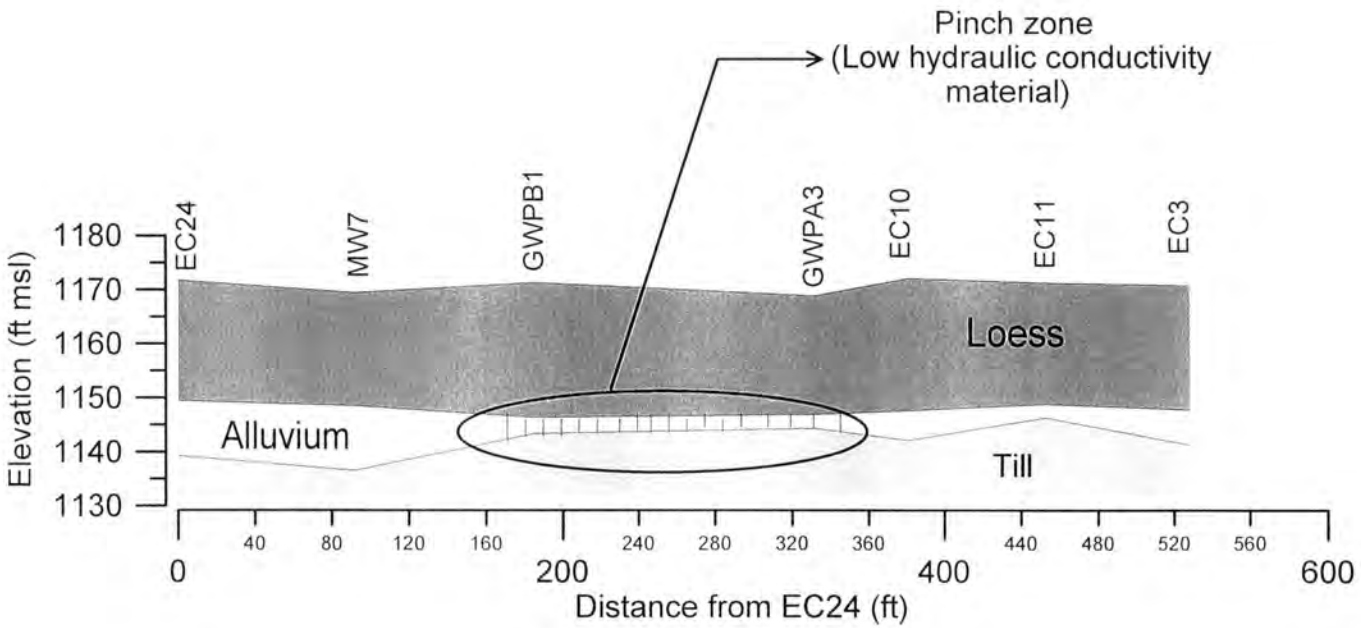

Figure 3.12. Transect C-C' at Cherokee FMGP site, Iowa

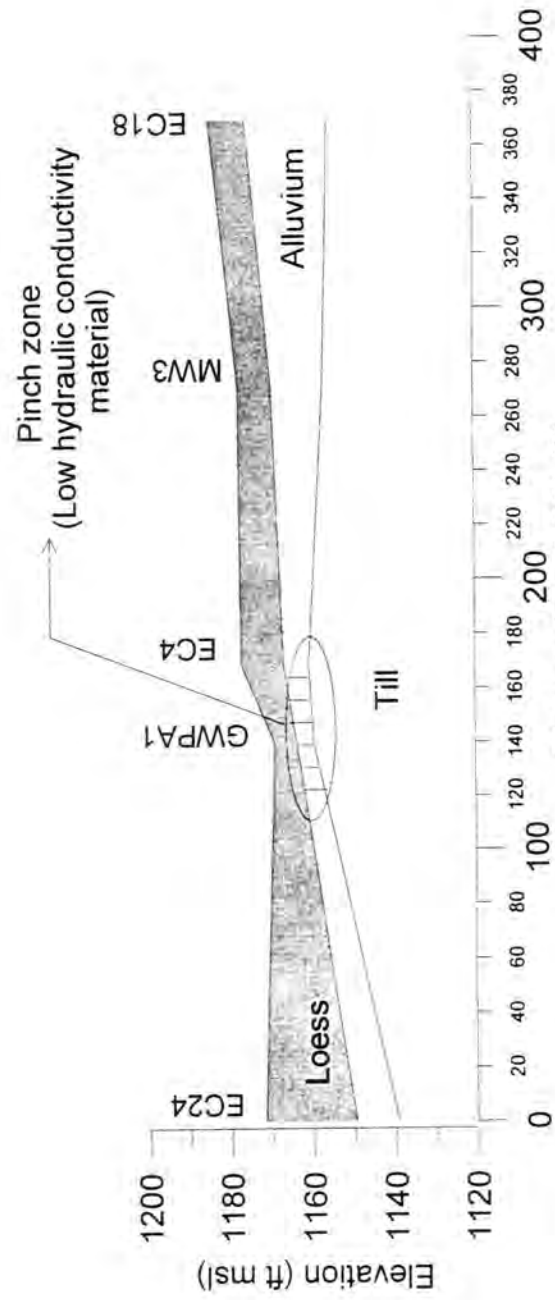

Figure 3.13. Transect D-D' at FMGP site at Cherokee FMGP site, Iowa

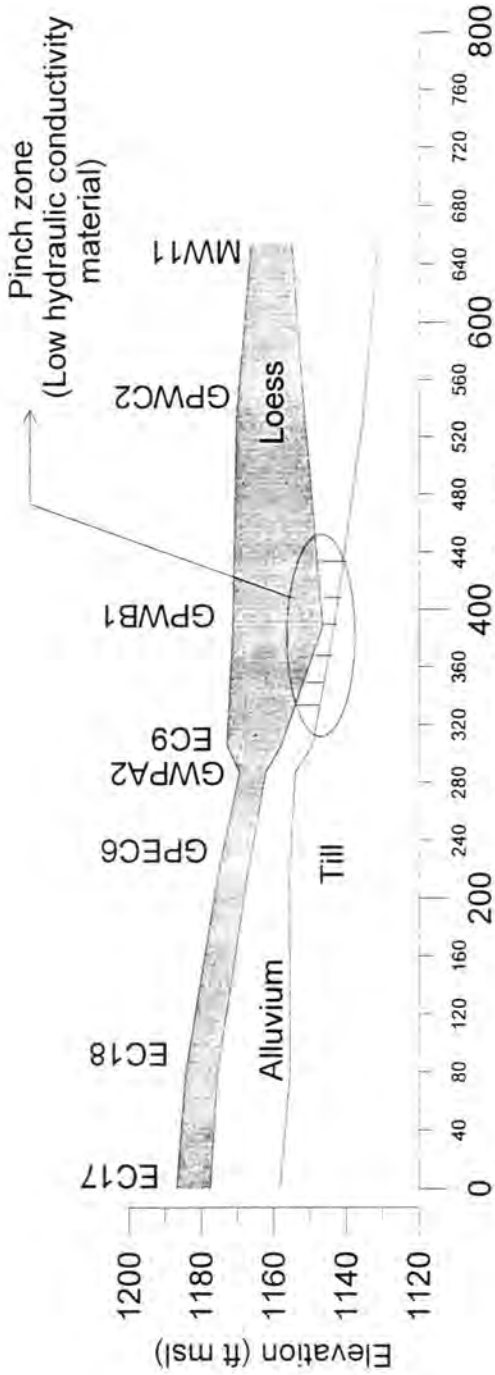

Figure 3.14. Transect E-E' at FMGP site at Cherokee FMGP site, Iowa

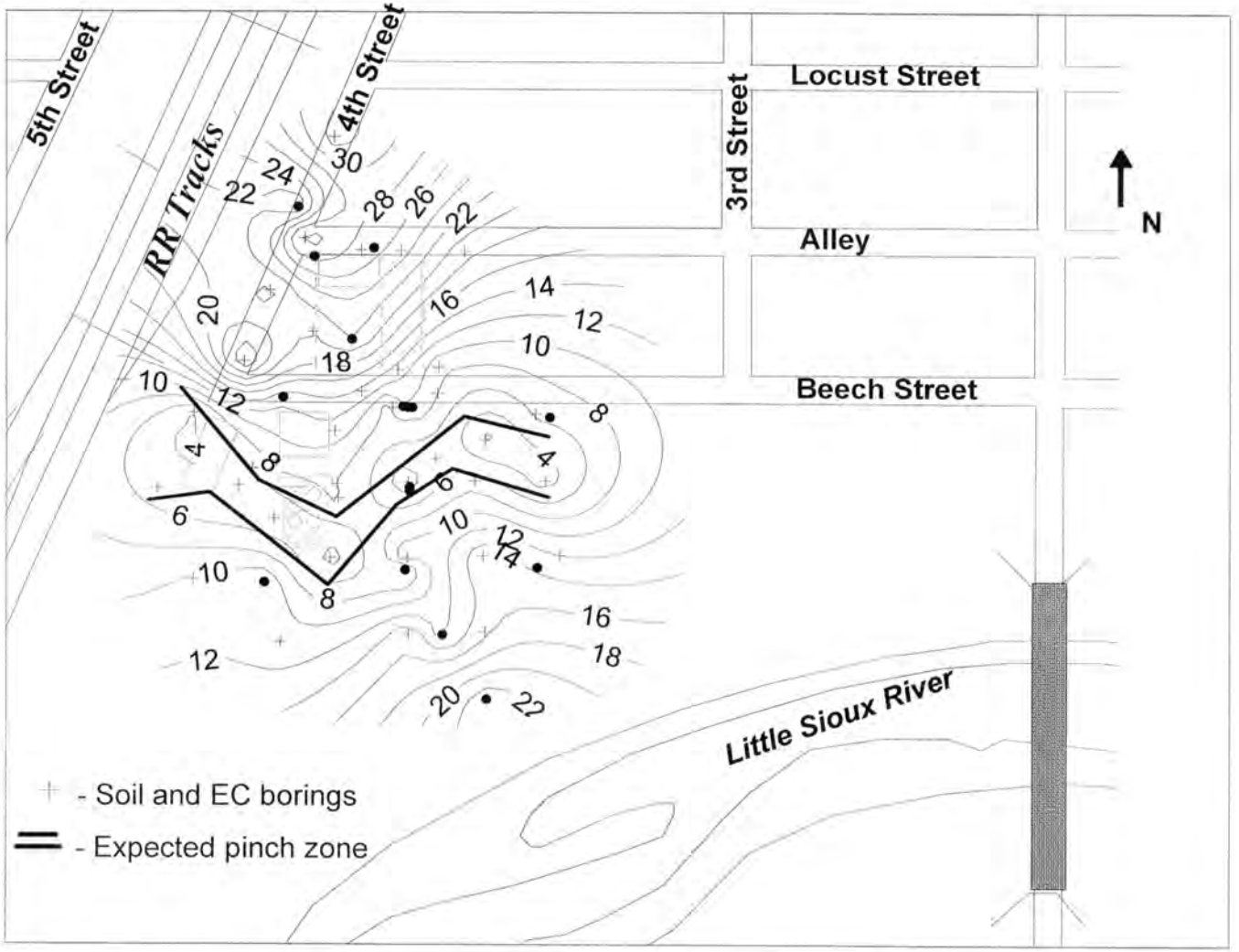

Figure 3.15. Contours of alluvium thickness and observed pinch zone in alluvium (thickness less than 3-foot) at Cherokee FMGP site, Iowa

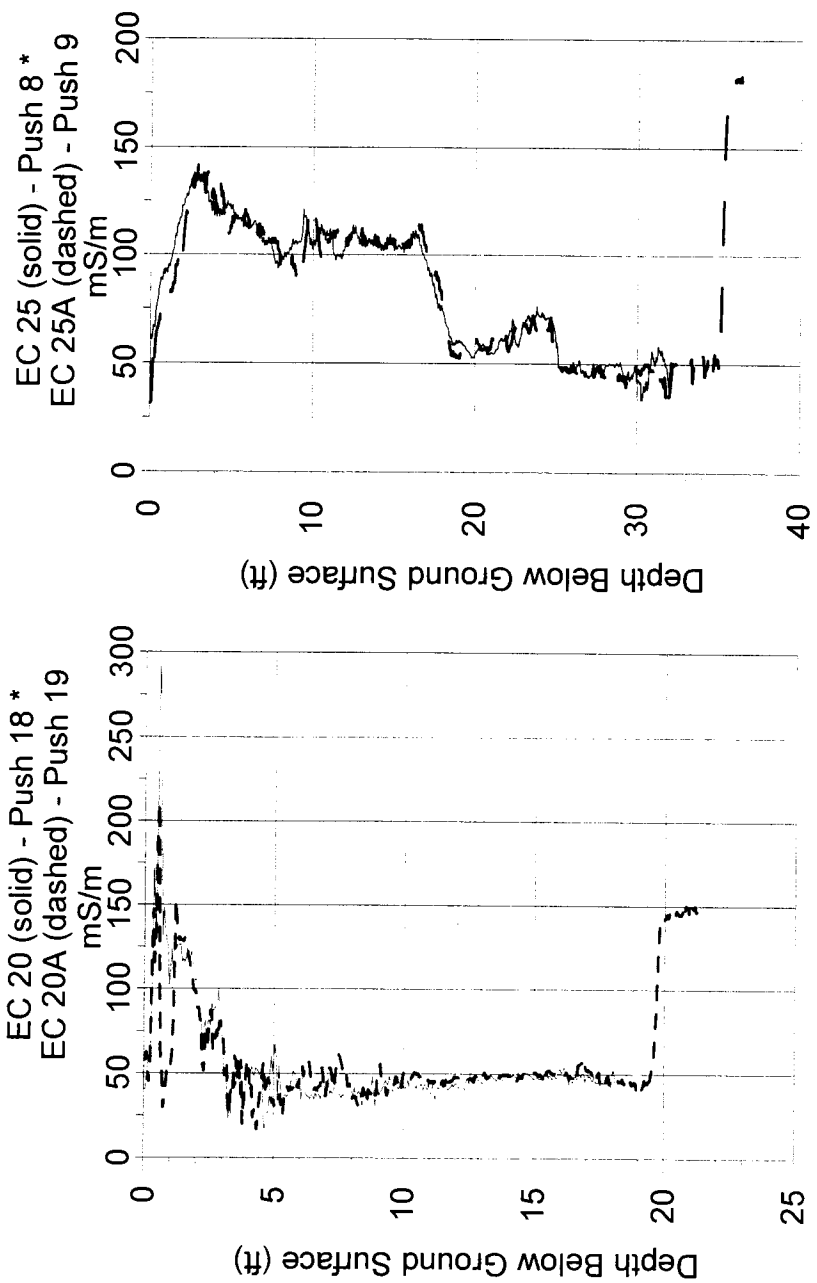

Figure 3.16. Geoprobe electrical conductivity data showing a high level of repeatability
* These pushes hit a subsurface obstruction at 17 feet for EC20 and at 32 feet for EC25 and could not be driven deeper.

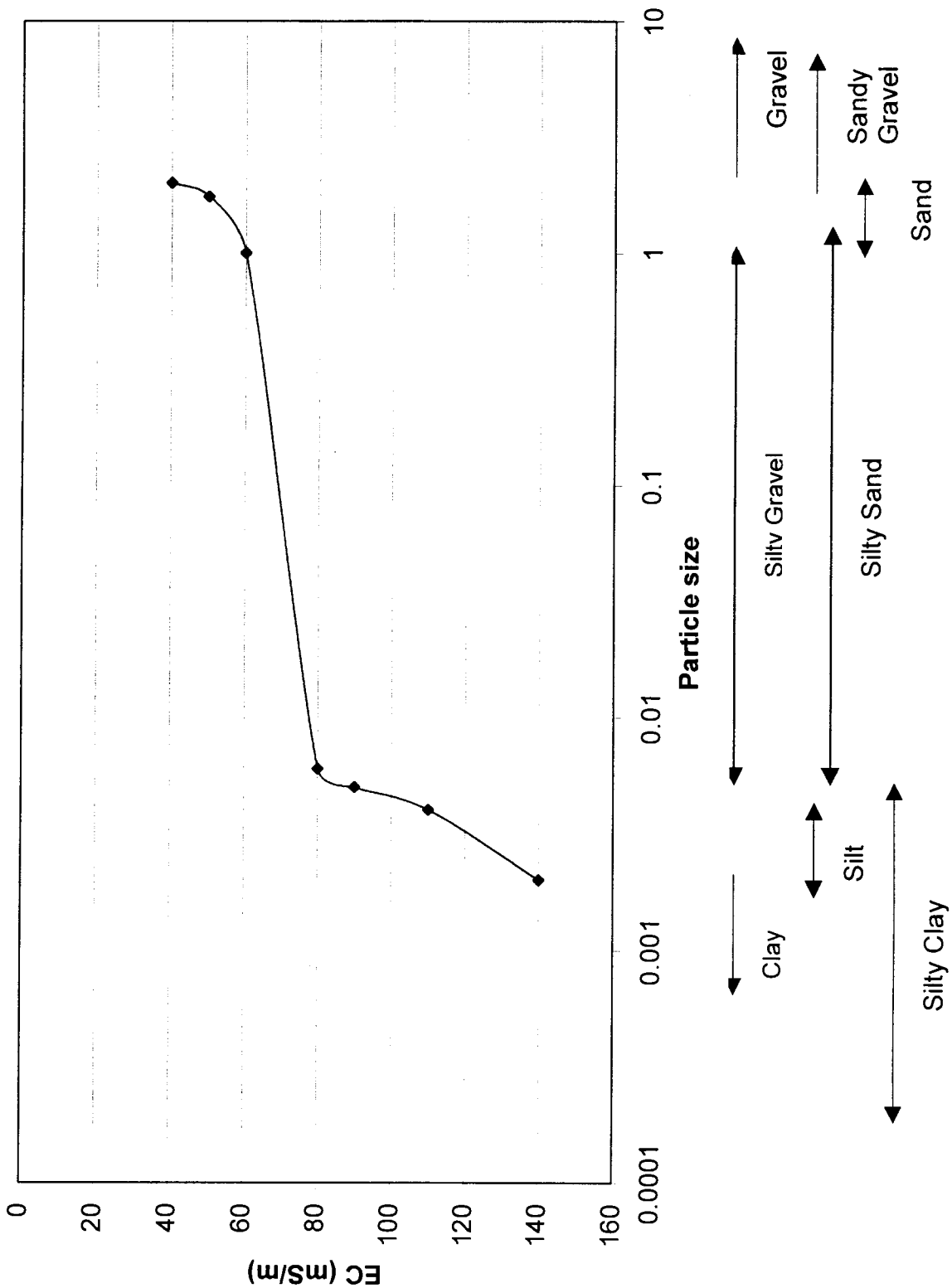

Figure 3.17. Association of electrical conductivity values with soil types

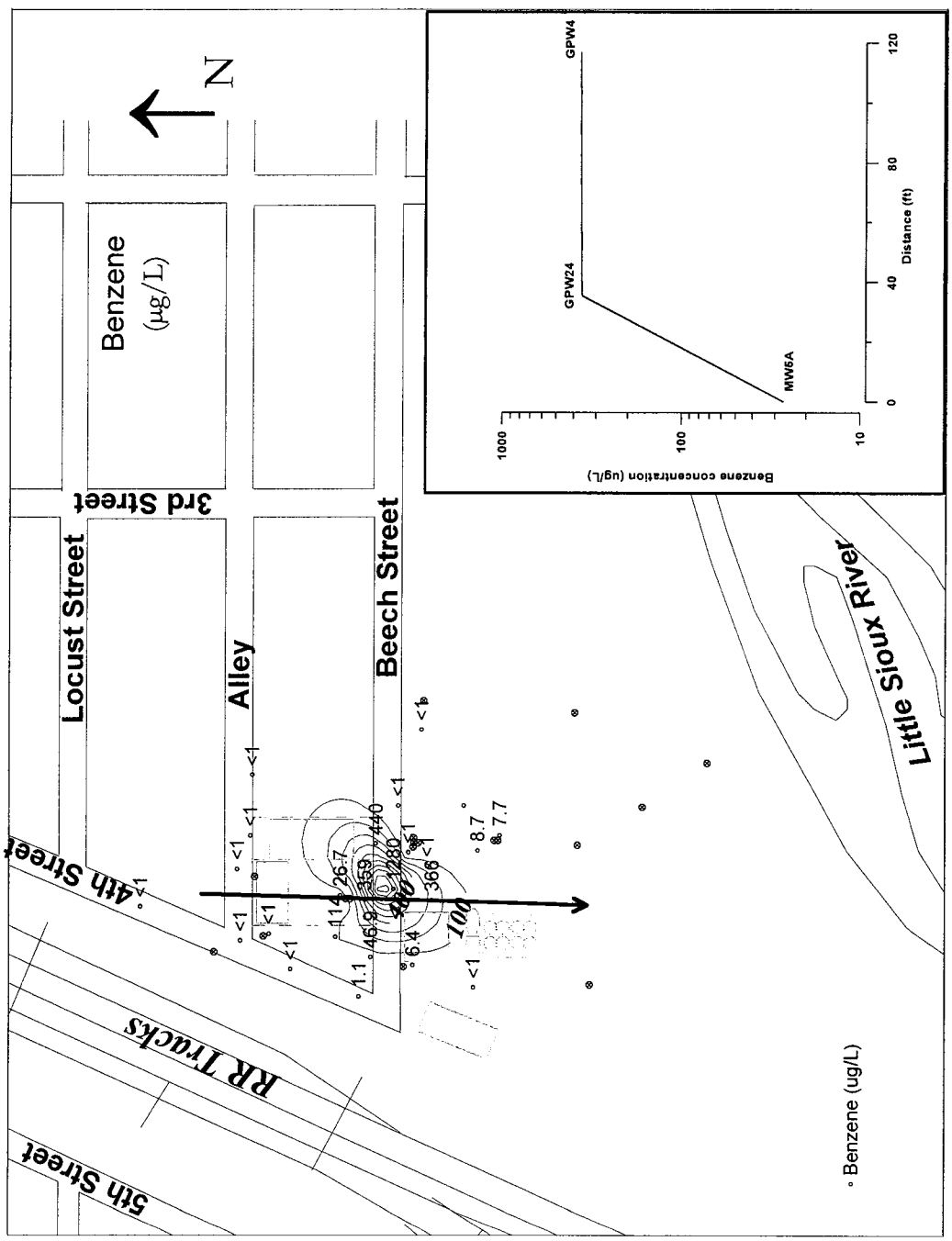

Figure 3.18. Contours of benzene concentration in the upper half of the aquifer (August 2001 data)

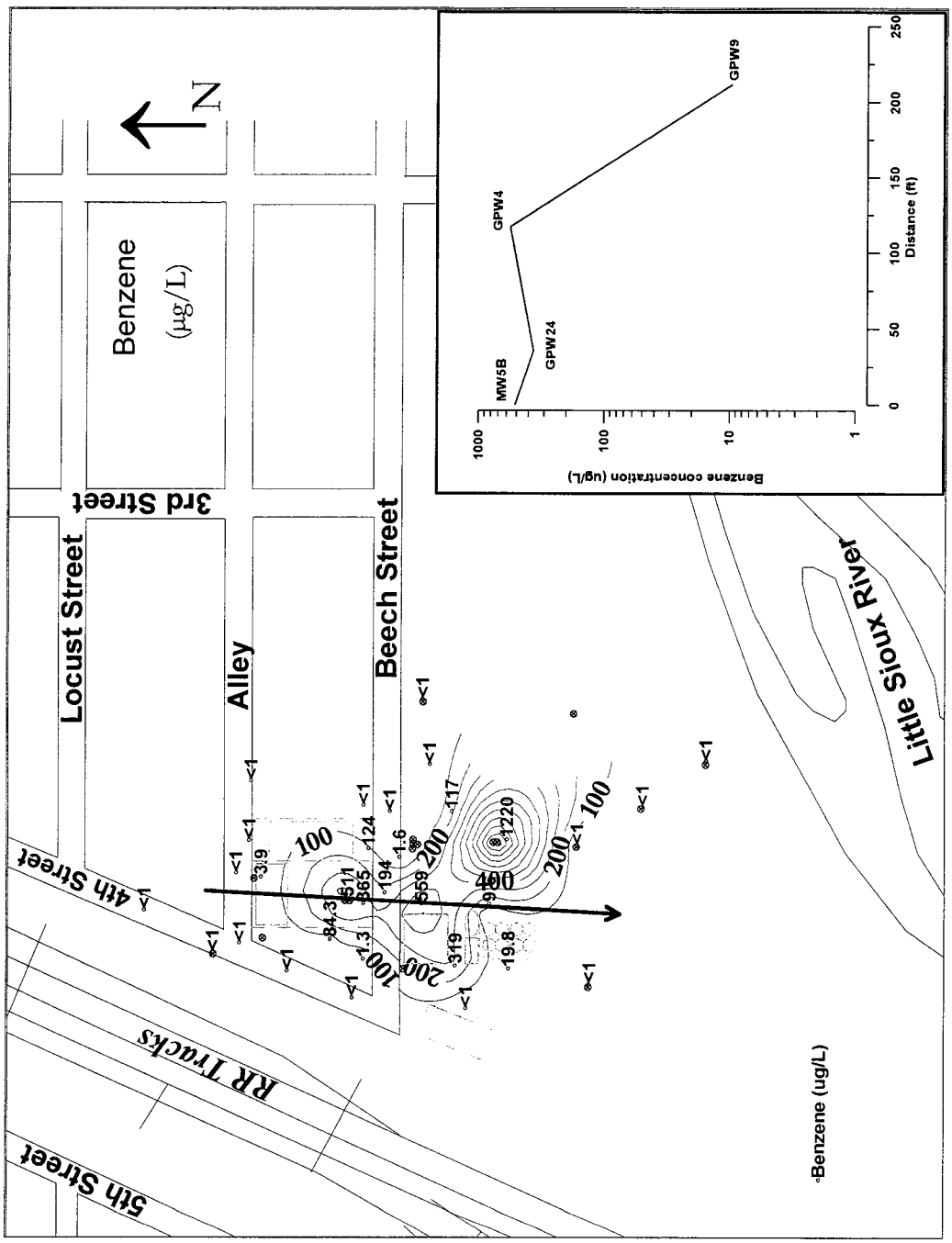

Figure 3.19. Contours of benzene concentration in the lower half of the aquifer (August 2001 data)

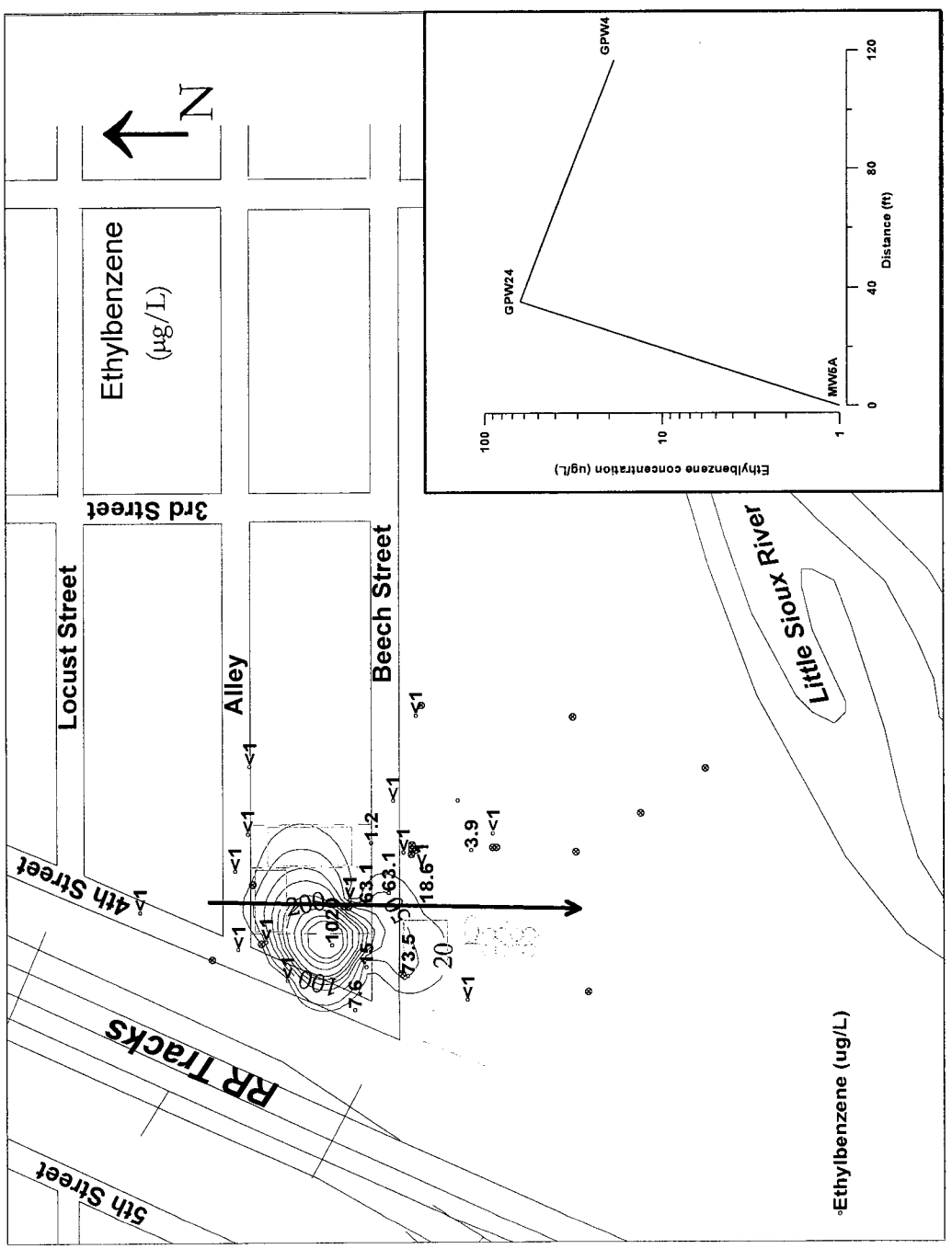

Figure 3.20. Contours of ethylbenzene concentration in the upper half of the aquifer (August 2001 data)

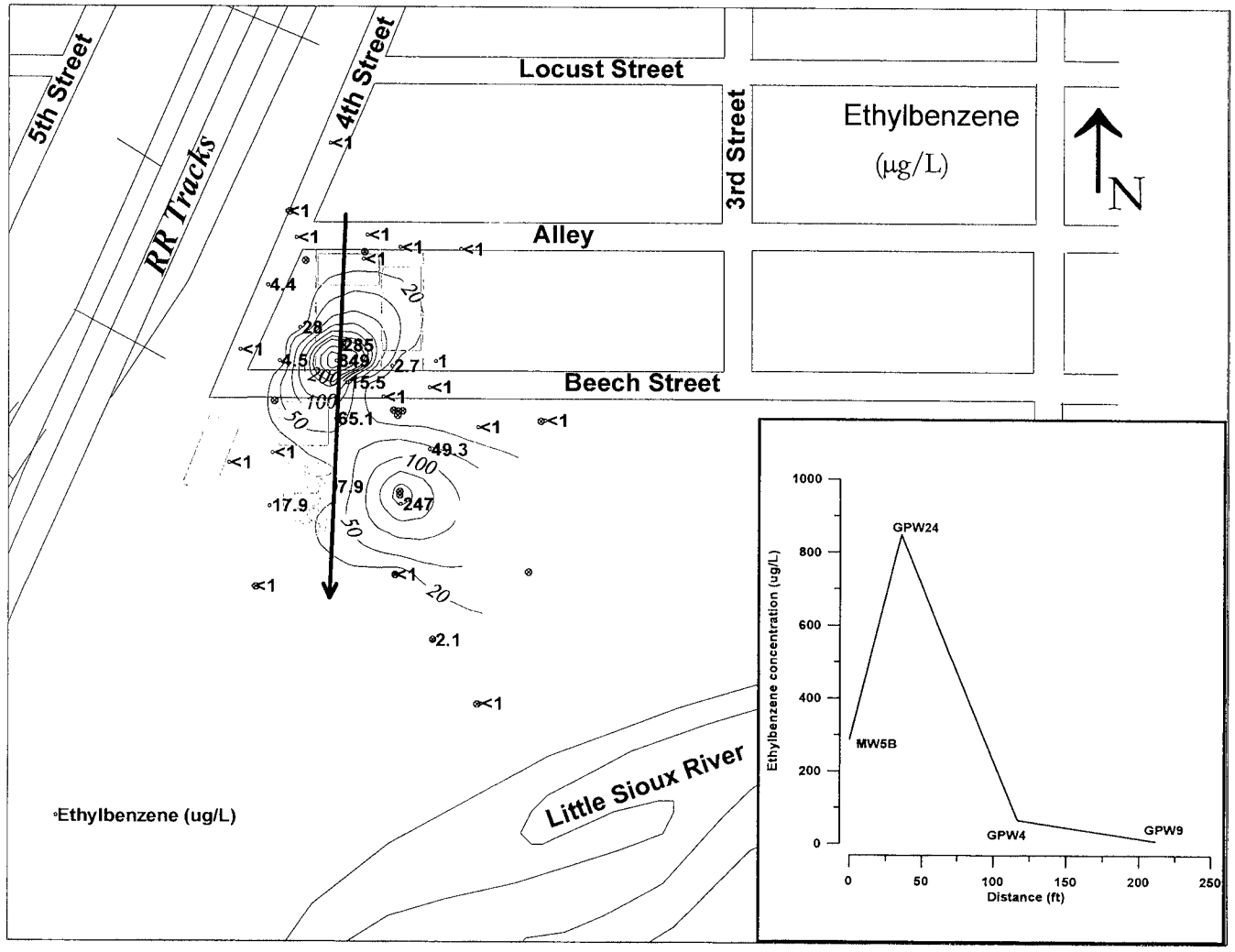

Figure 3.21. Contours of ethylbenzene concentration in the lower half of the aquifer (August 2001 data)

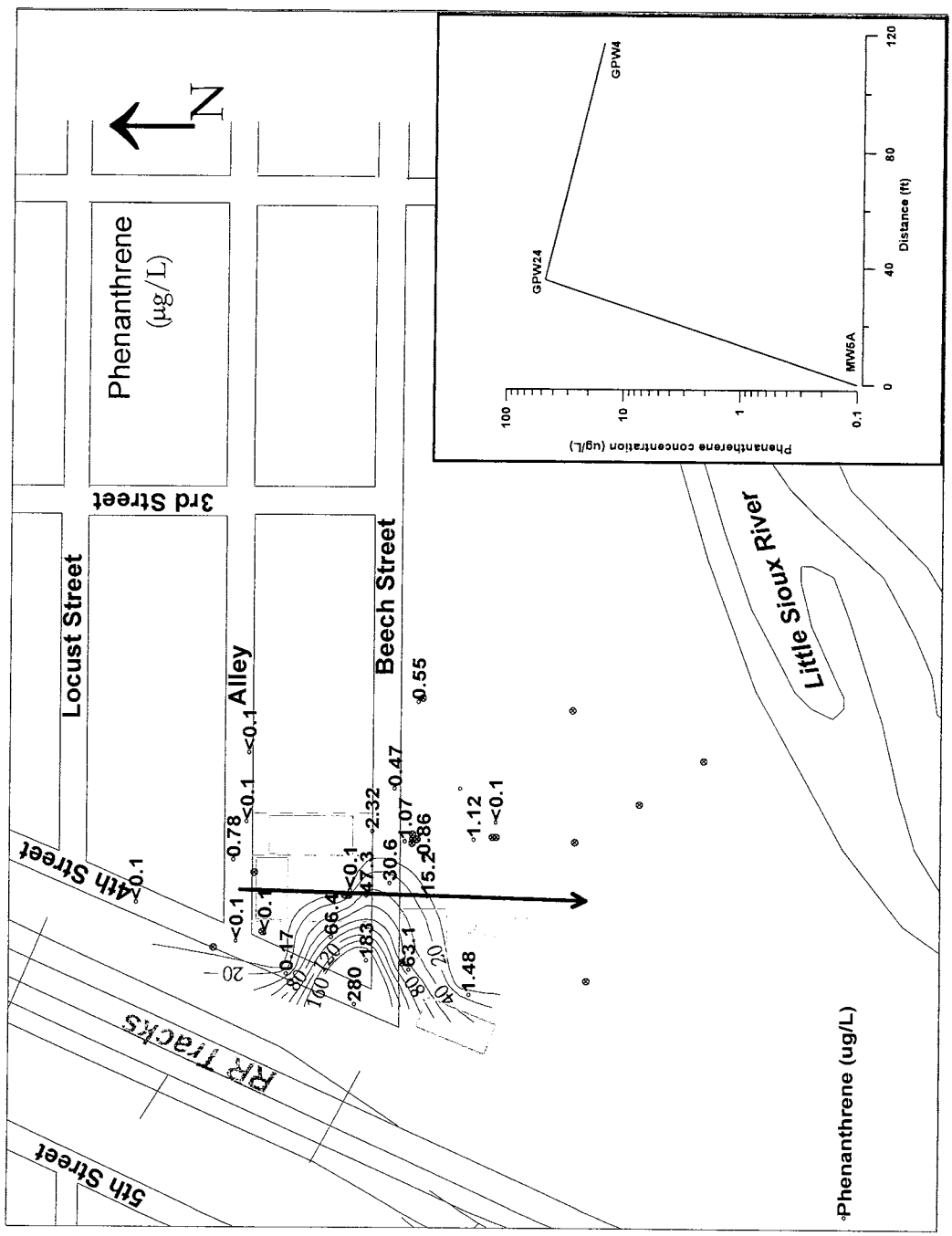

Figure 3.22. Contours of phenanthrene concentration in the upper half of the aquifer (August 2001 data)

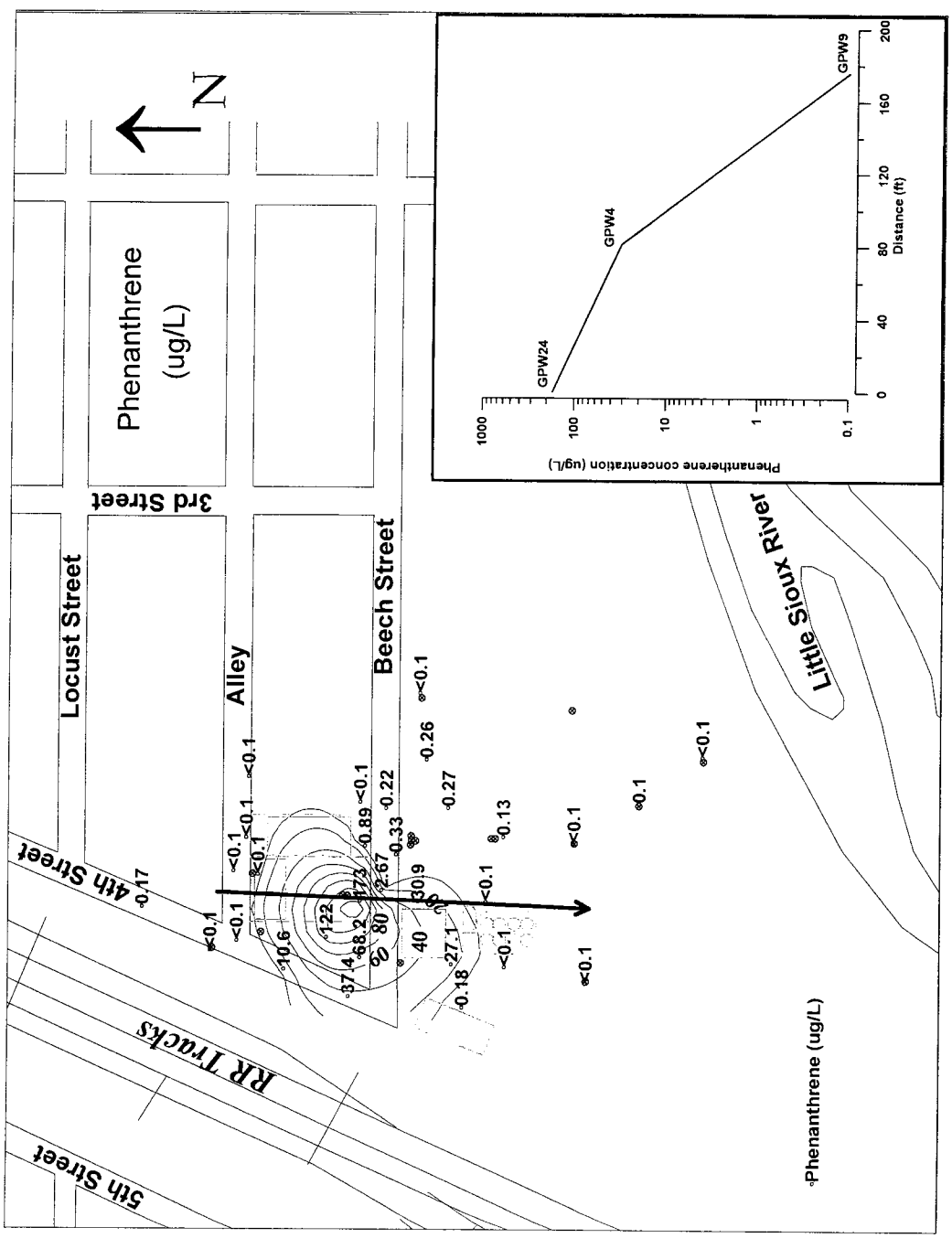

Figure 3.23. Contours of phenanthrene concentration in the lower half of aquifer (August 2001data)

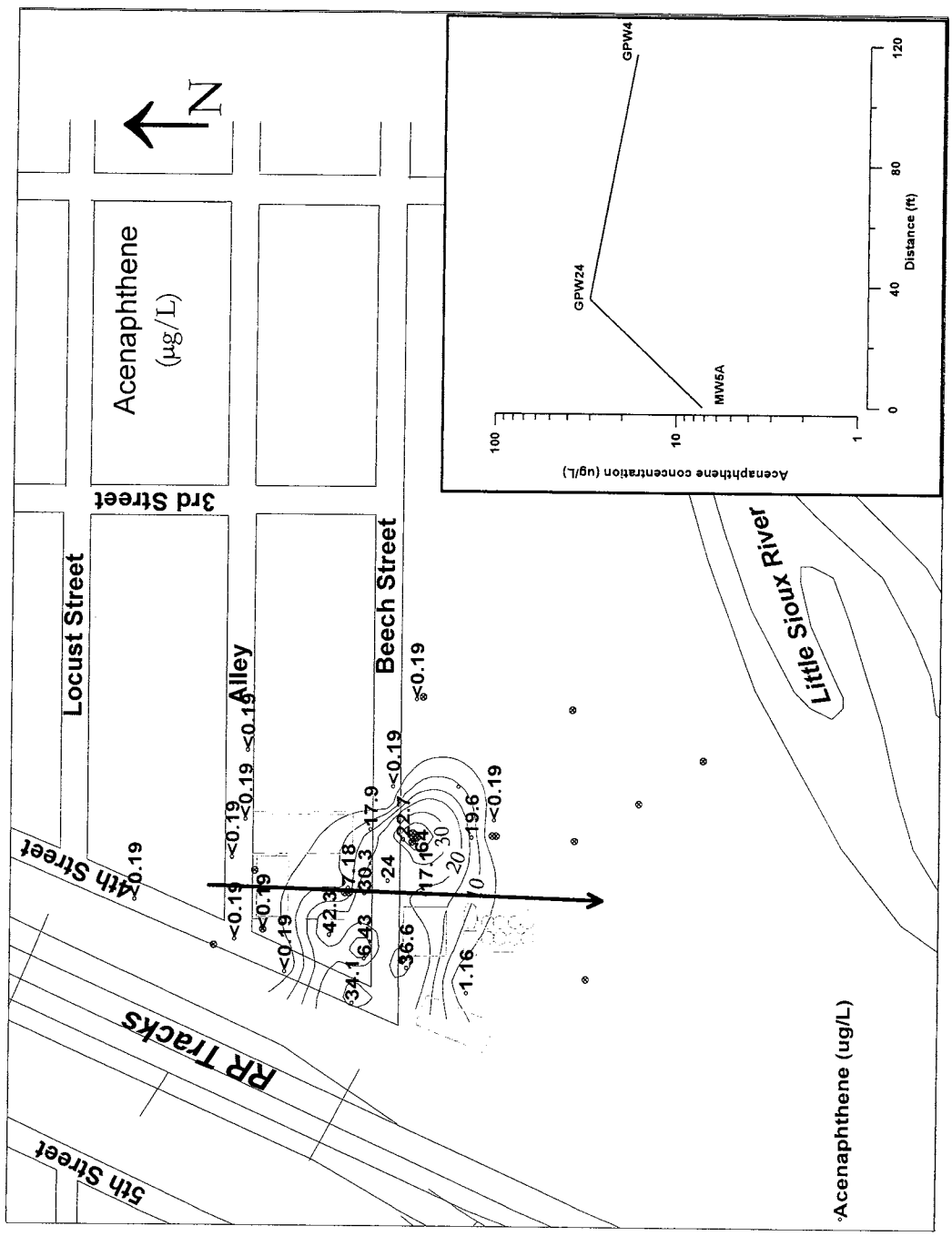

Figure 3.24. Contours of acenaphthene concentration in the upper half of the aquifer (August 2001 data)

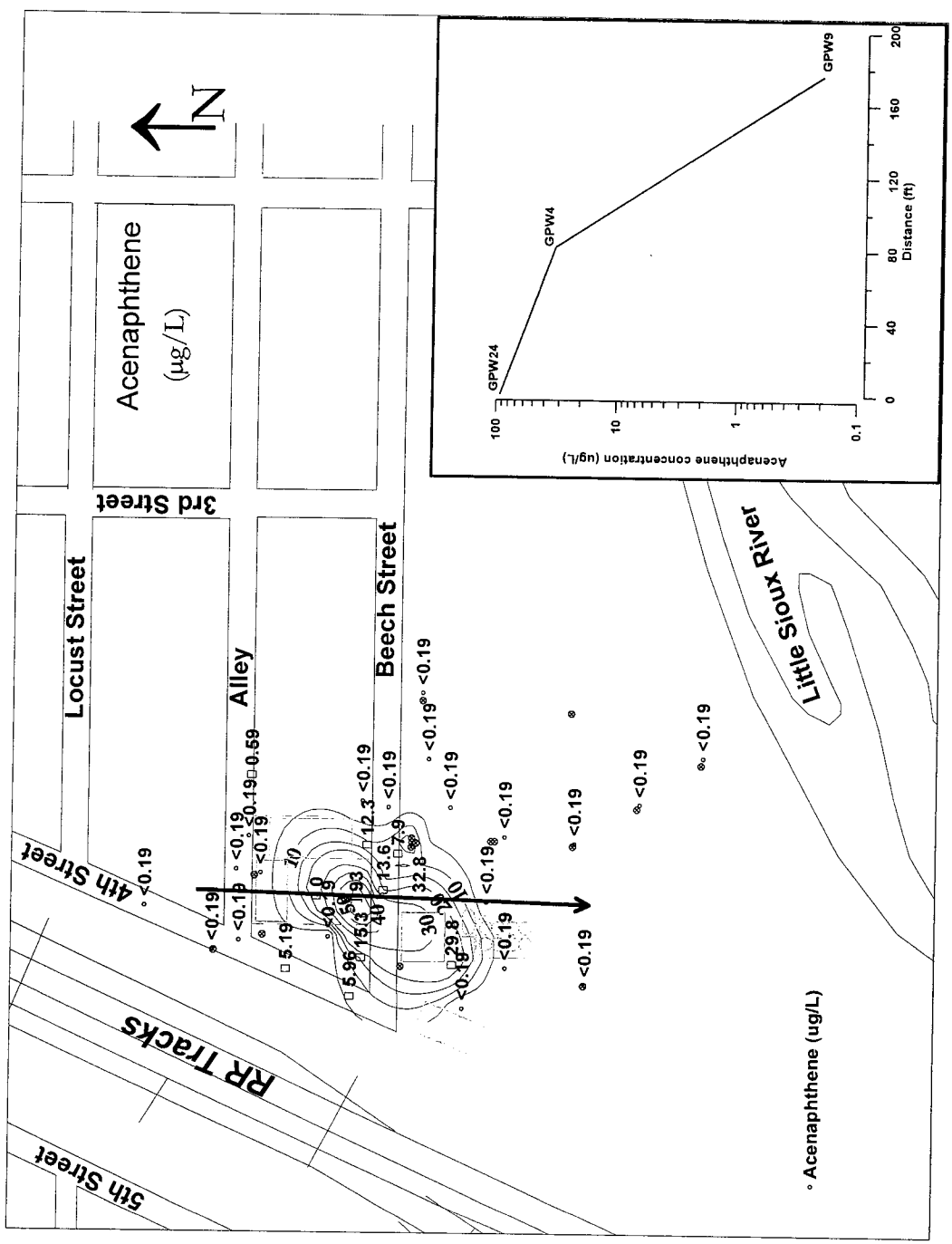

Figure 3.25. Contours of acenaphthene concentration in the lower half of the aquifer (August 2001 data)

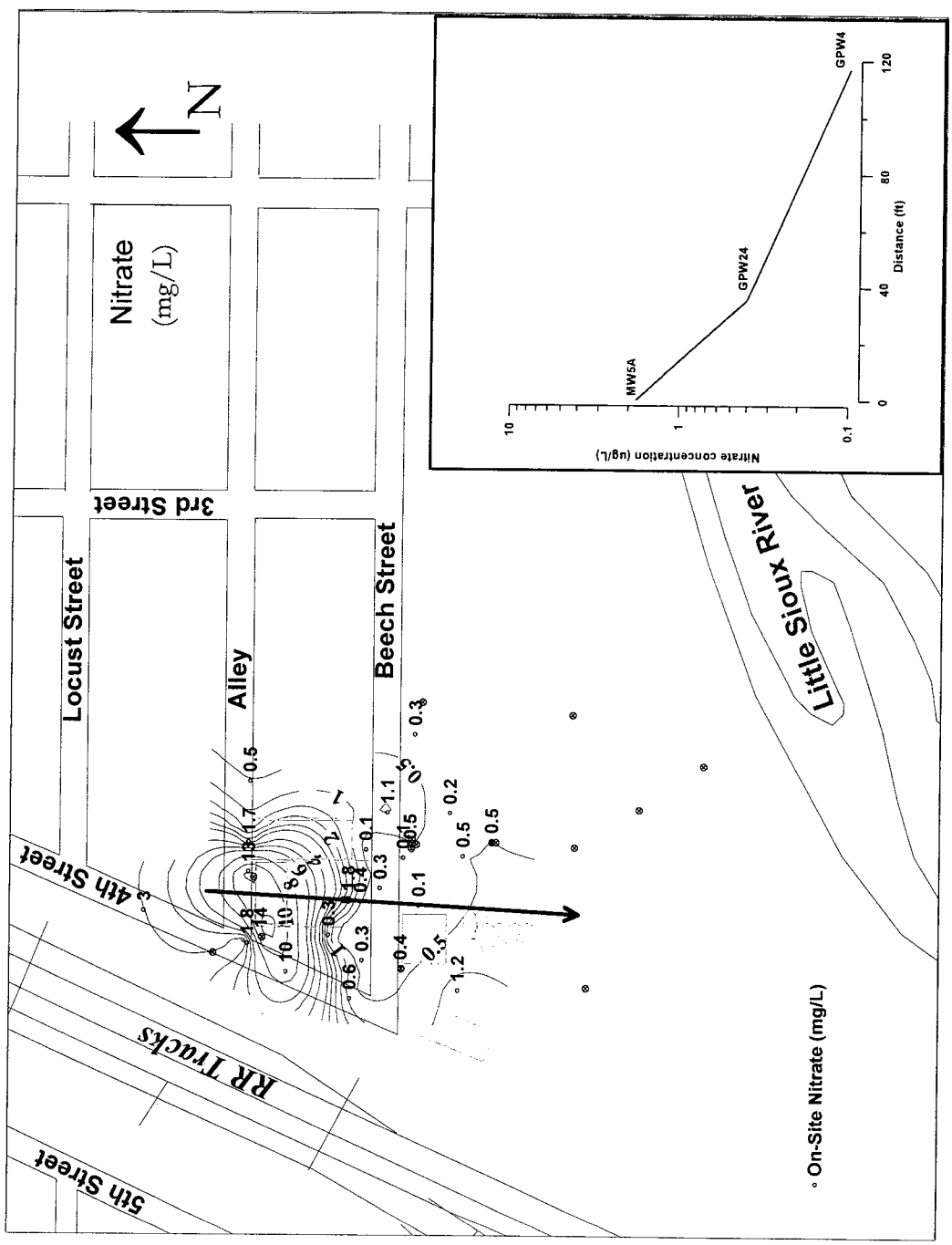

Figure 3.26. Contours of nitrate concentration in the upper half of the aquifer (August 2001 data)

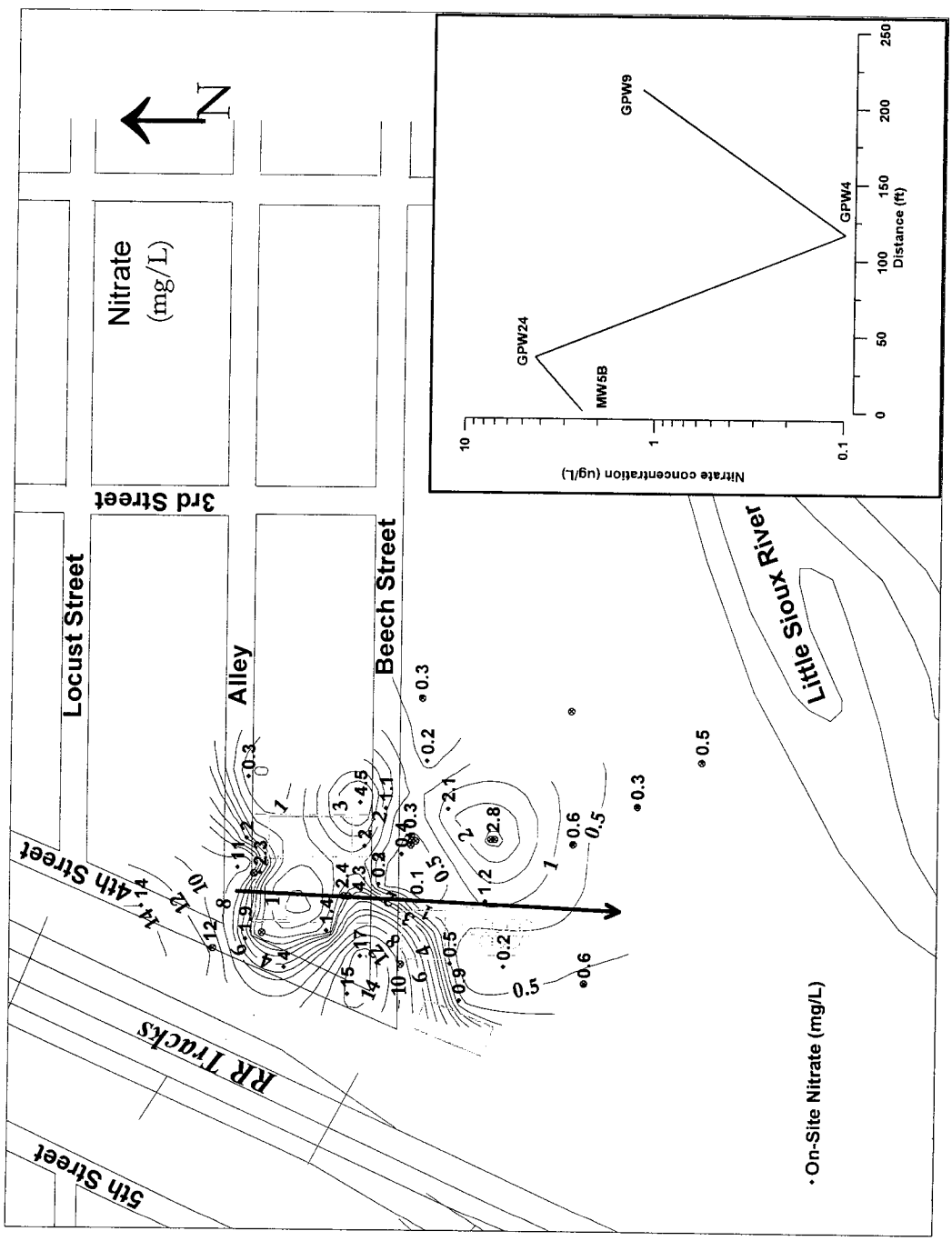

Figure 3.27. Contours of nitrate concentration in the lower half of the aquifer (August 2001 data)

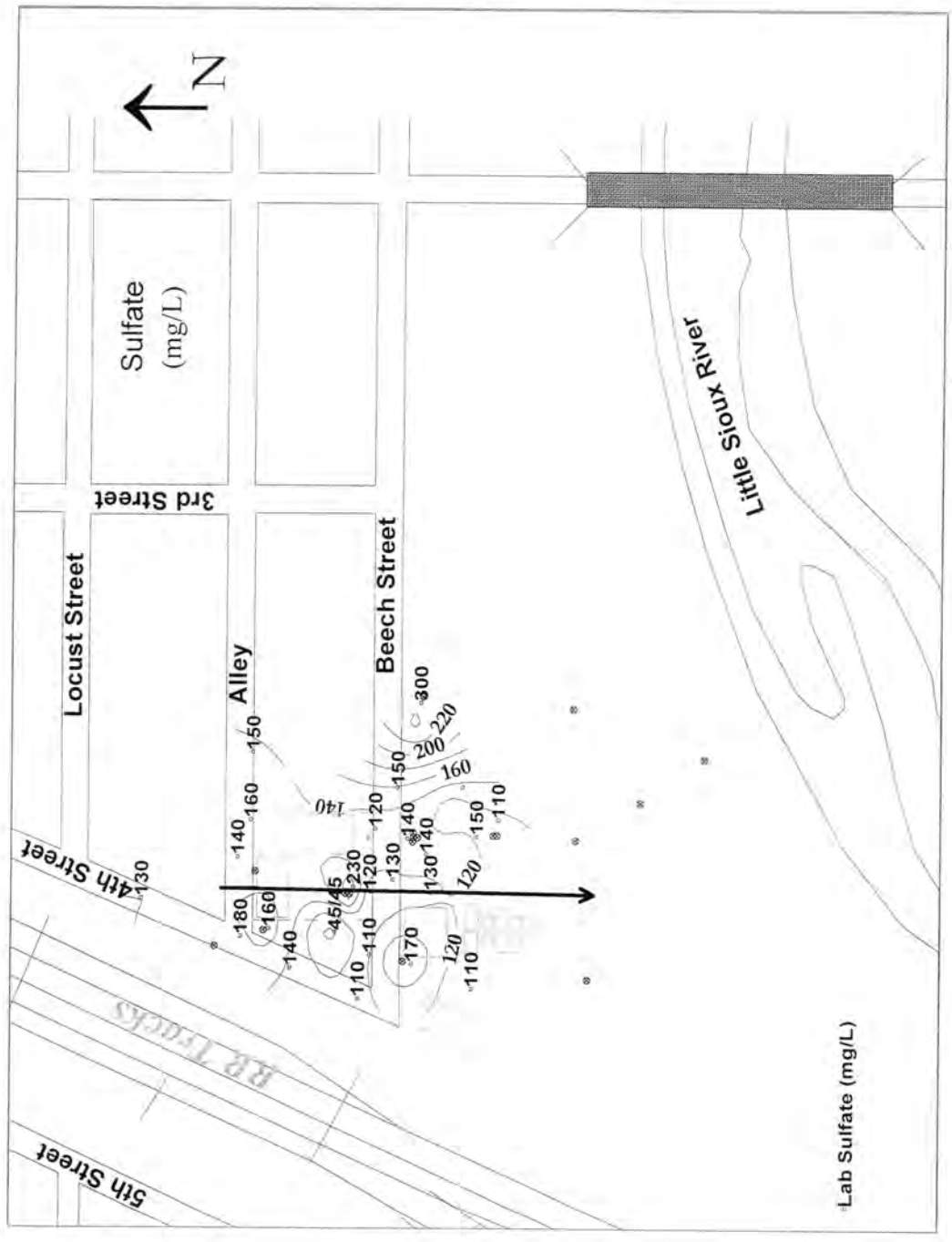

Figure 3.28. Contours of sulfate concentration in lthe upper half of the aquifer (August 2001 data)

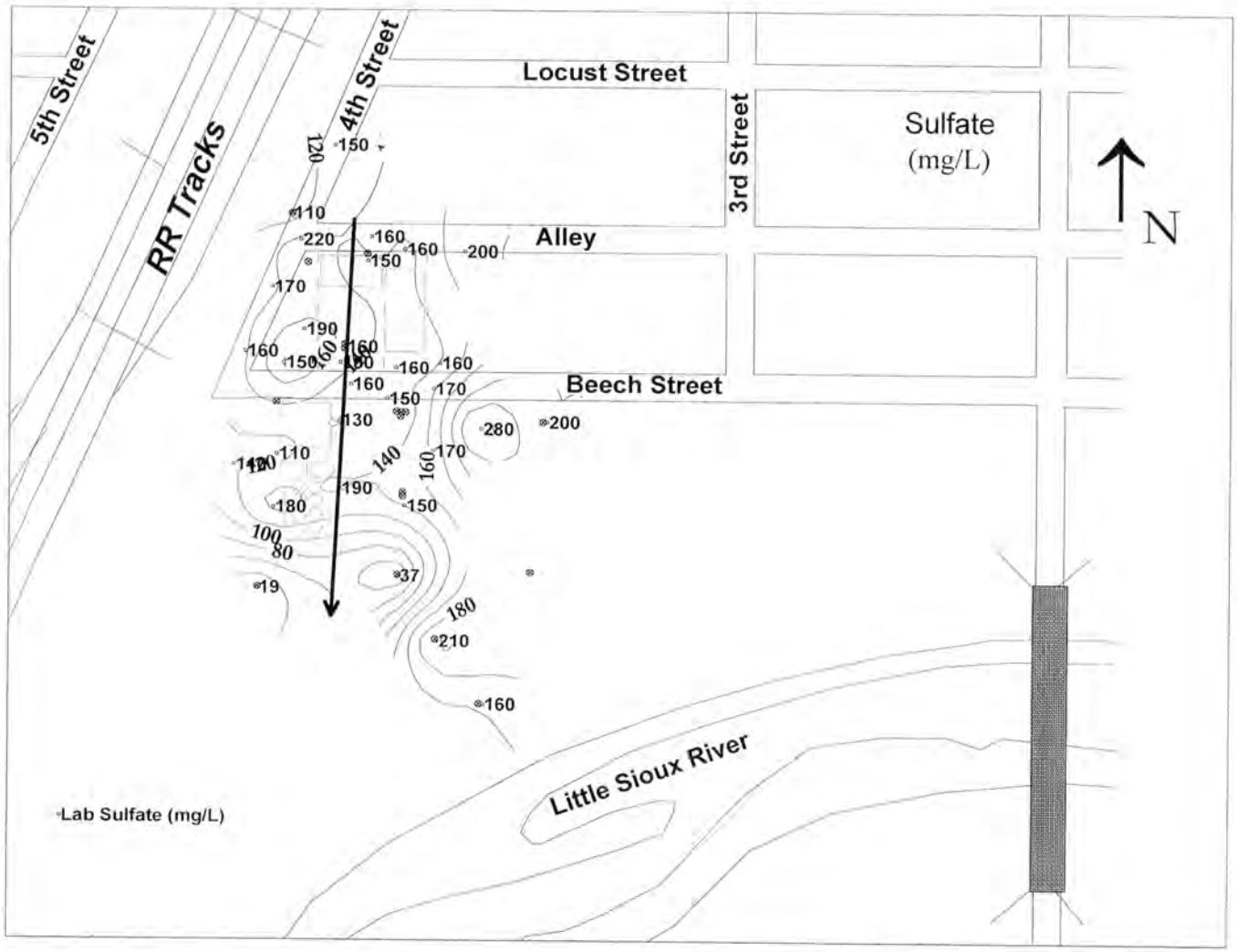

Figure 3.29. Contours of sulfate concentration in the lower half of the aquifer (August 2001 data)

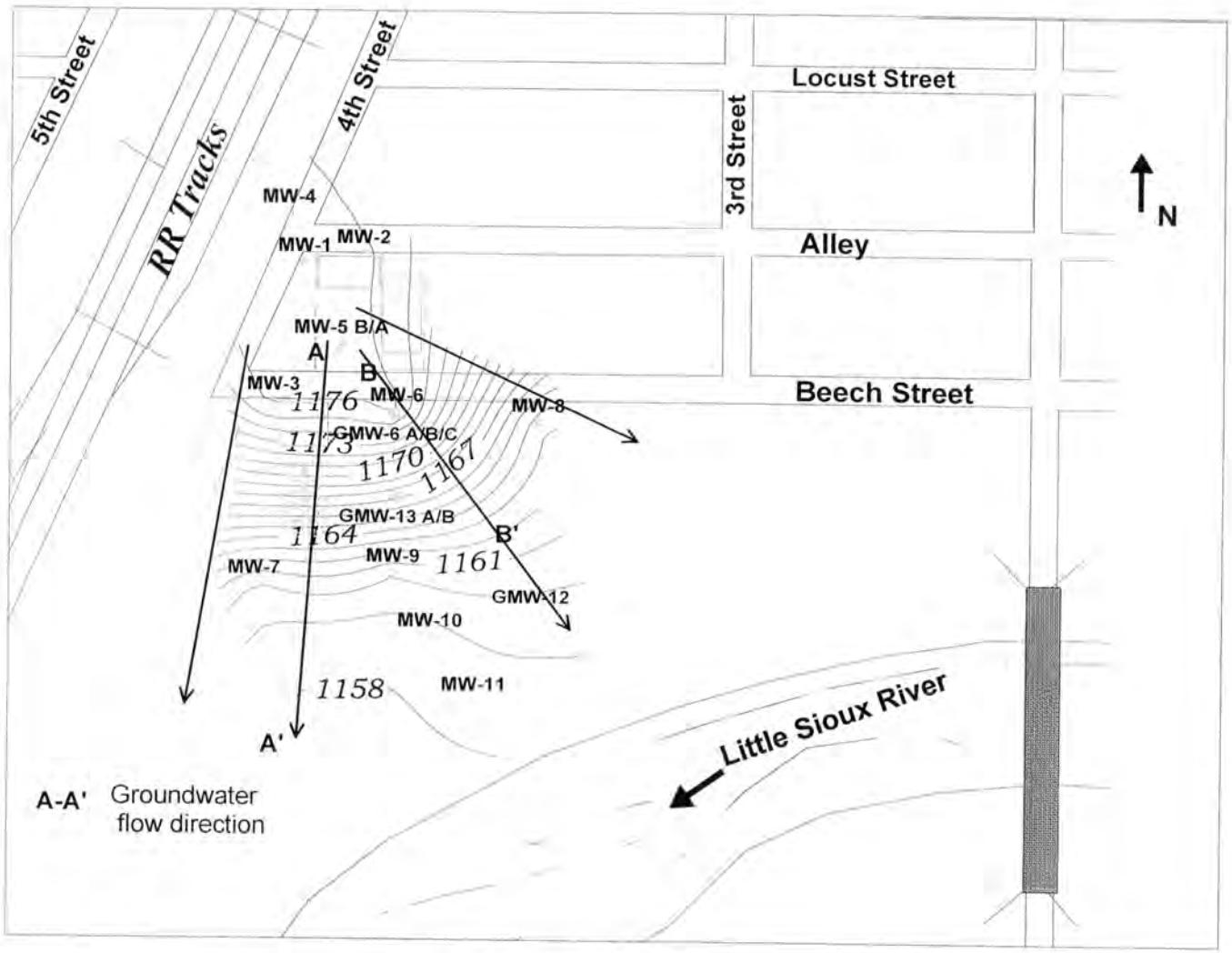

Figure 3.30. Estimated ground water flow directions using hydraulic heads at MW's at Cherokee FMGP site, Iowa. Flow direction A-A' used for degradation rate estimation

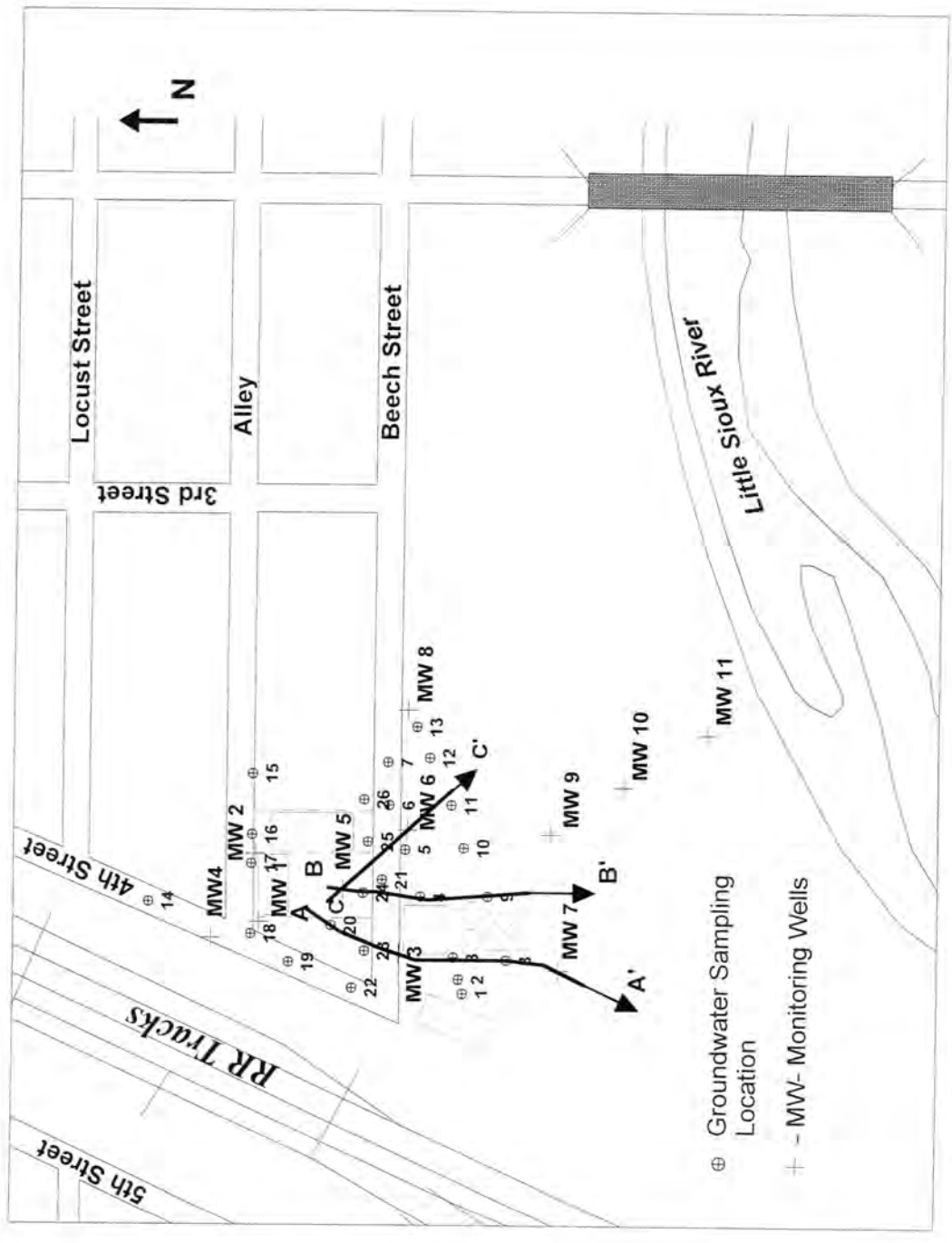

Figure 3.31. Flow path A-A', B-B', and C-C' at Cherokee FMGP site, Iowa

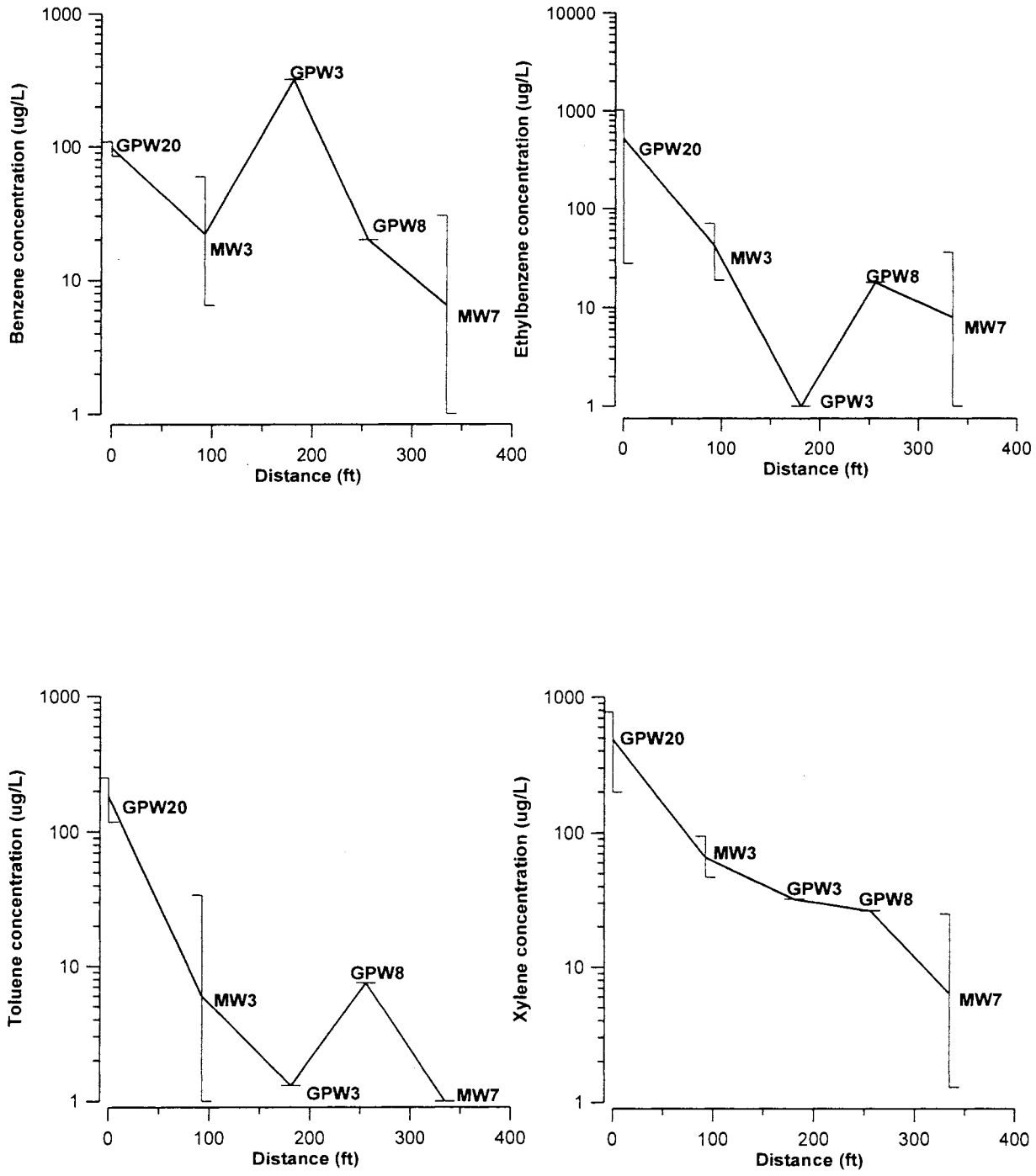

Figure 3.32.a. Average concentration of BTEX compounds along the flow path A-A' and variation in concentration of BTEX compounds at groundwater sampling locations

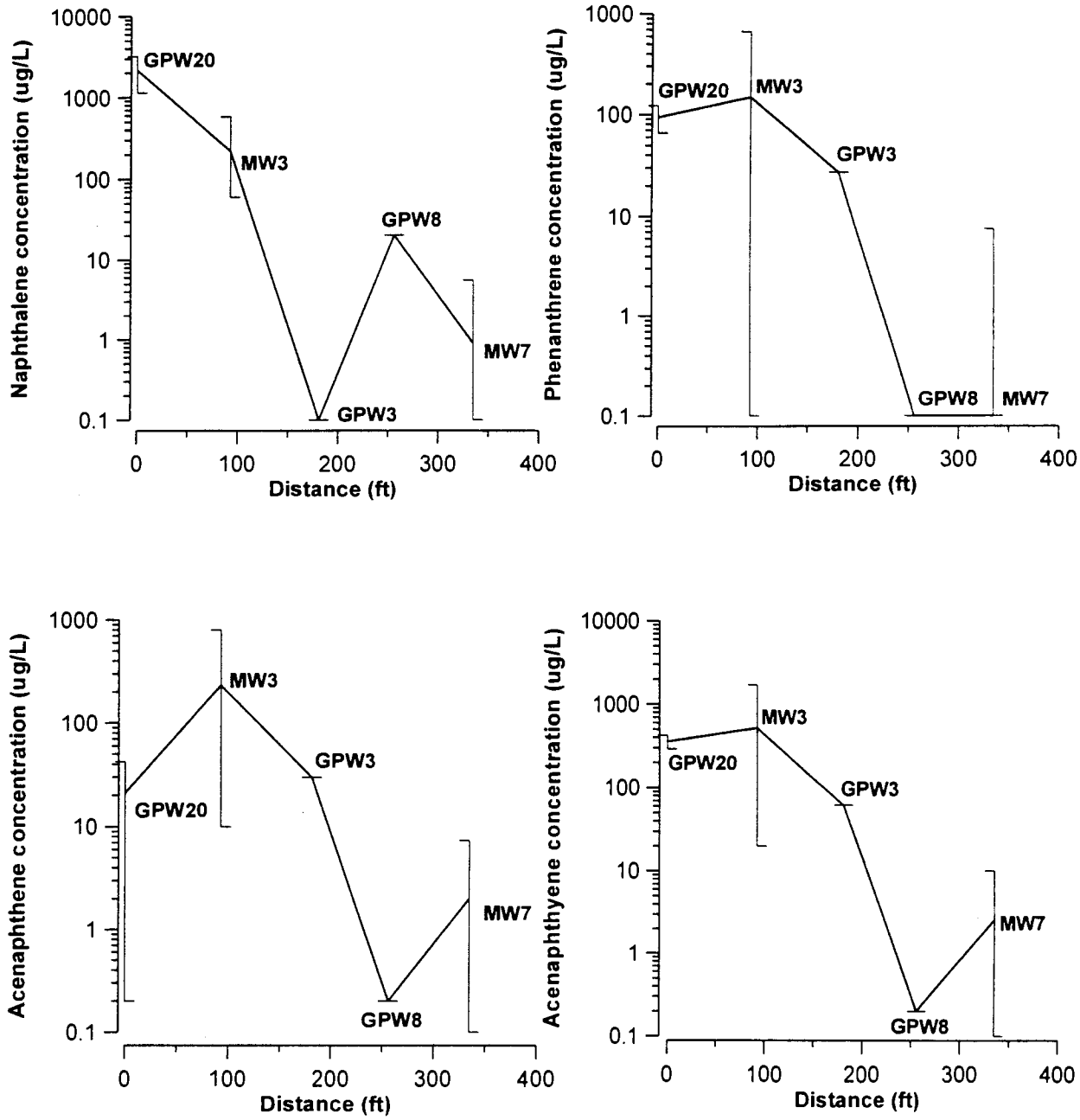

Figure 3.32.b. Average concentration of PAH (naphthalene, phenanthrene, acenaphthene, acenaphthylene) compounds along the flow path A-A' and variation in concentration of PAH compounds at groundwater sampling locations

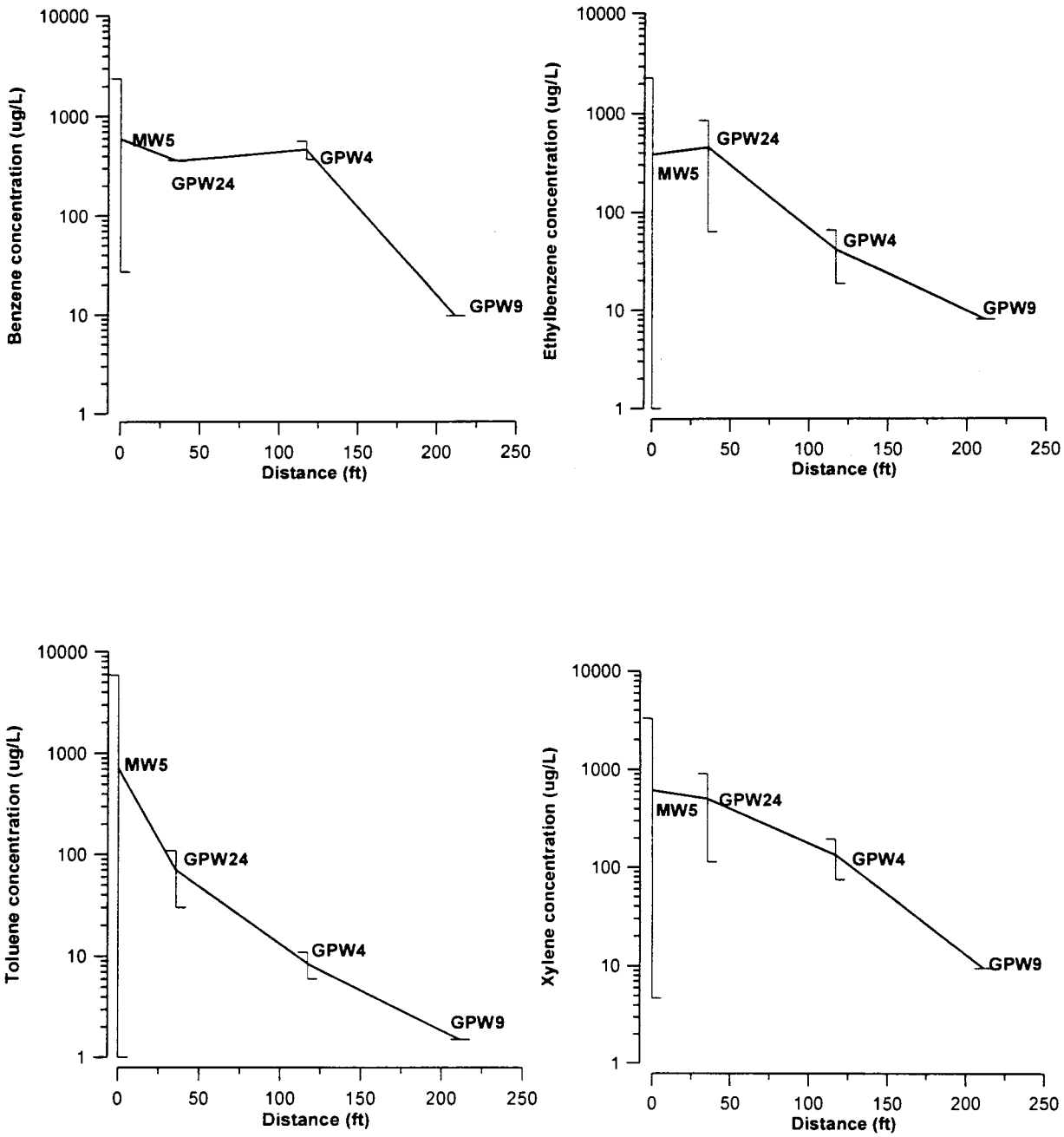

Figure 3.33.a. Average concentration of BTEX compounds along the flow path B-B' and variation in concentration of BTEX compounds at groundwater sampling locations

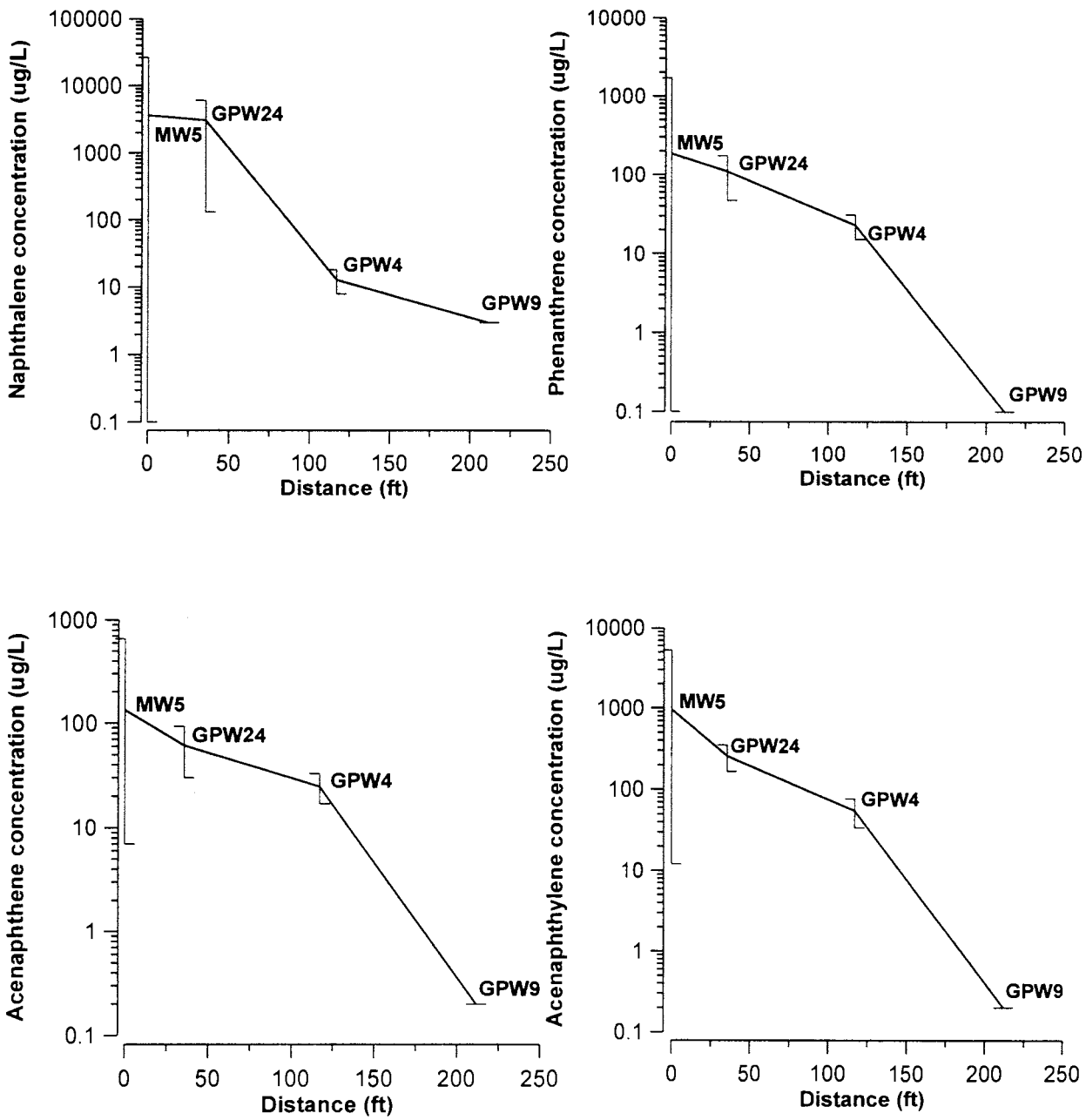

Figure 3.33.b Average concentration of PAH (naphthalene, phenanthrene, acenaphthene, acenaphthylene) compounds along the flow path B-B' and variation in concentration of PAH compounds at groundwater sampling locations

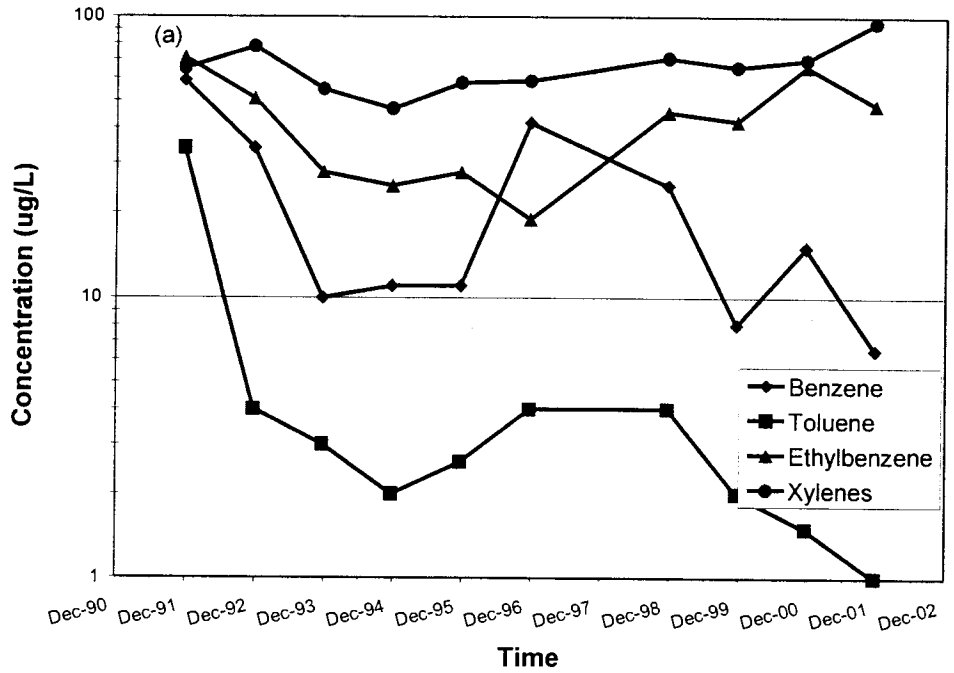

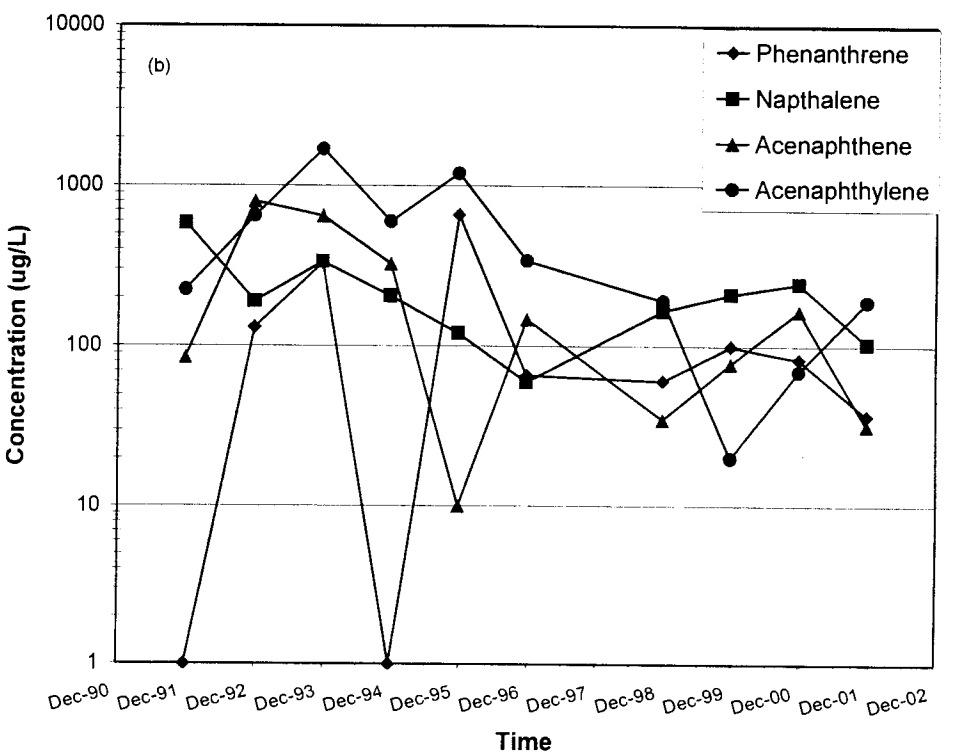

Figure 3.34 (a) & (b). Variation in BTEX and PAH concentrations with time at MW3

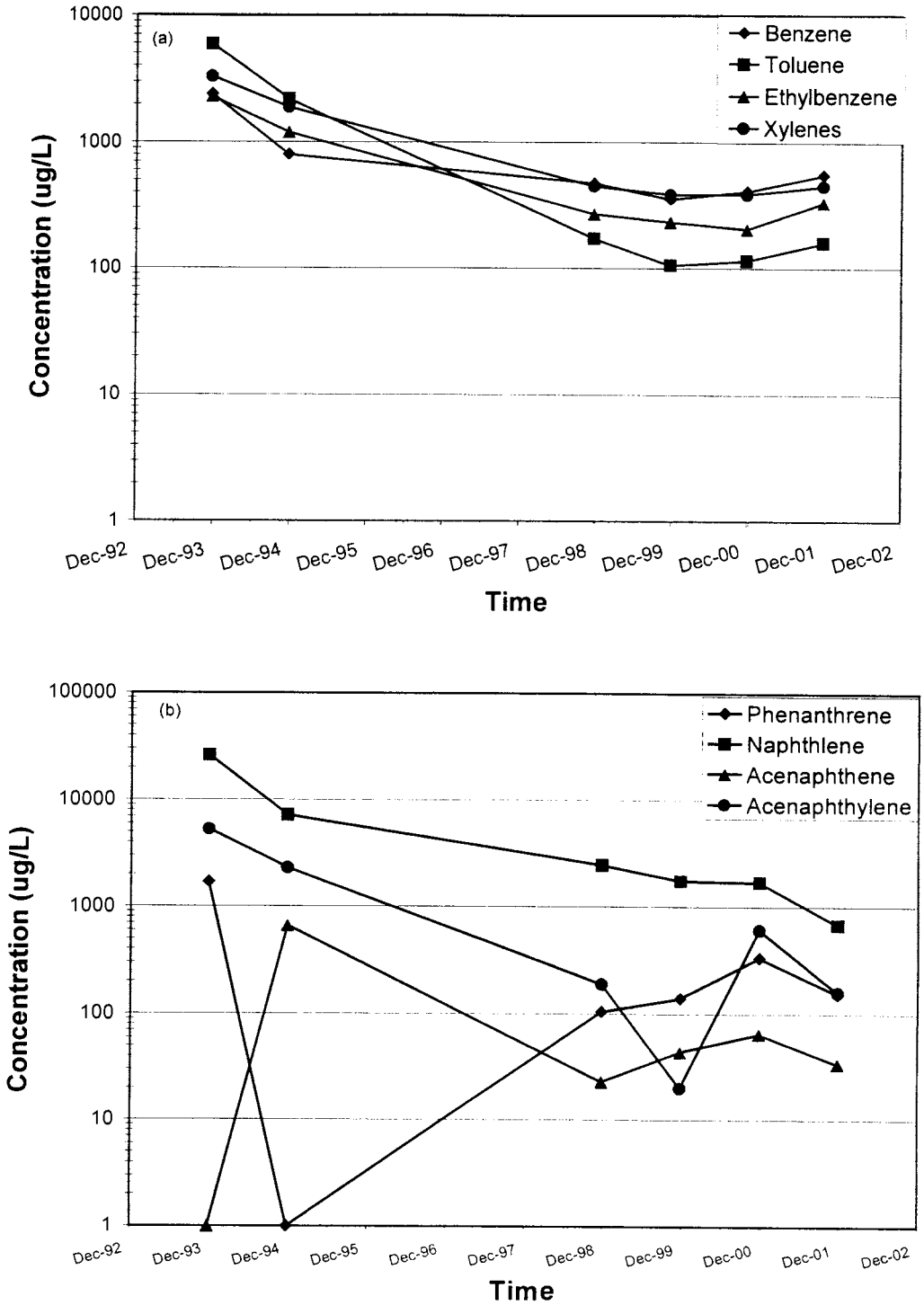

Figure3.35 (a) & (b). Variation in BTEX and PAH concentrations with time at MW5B

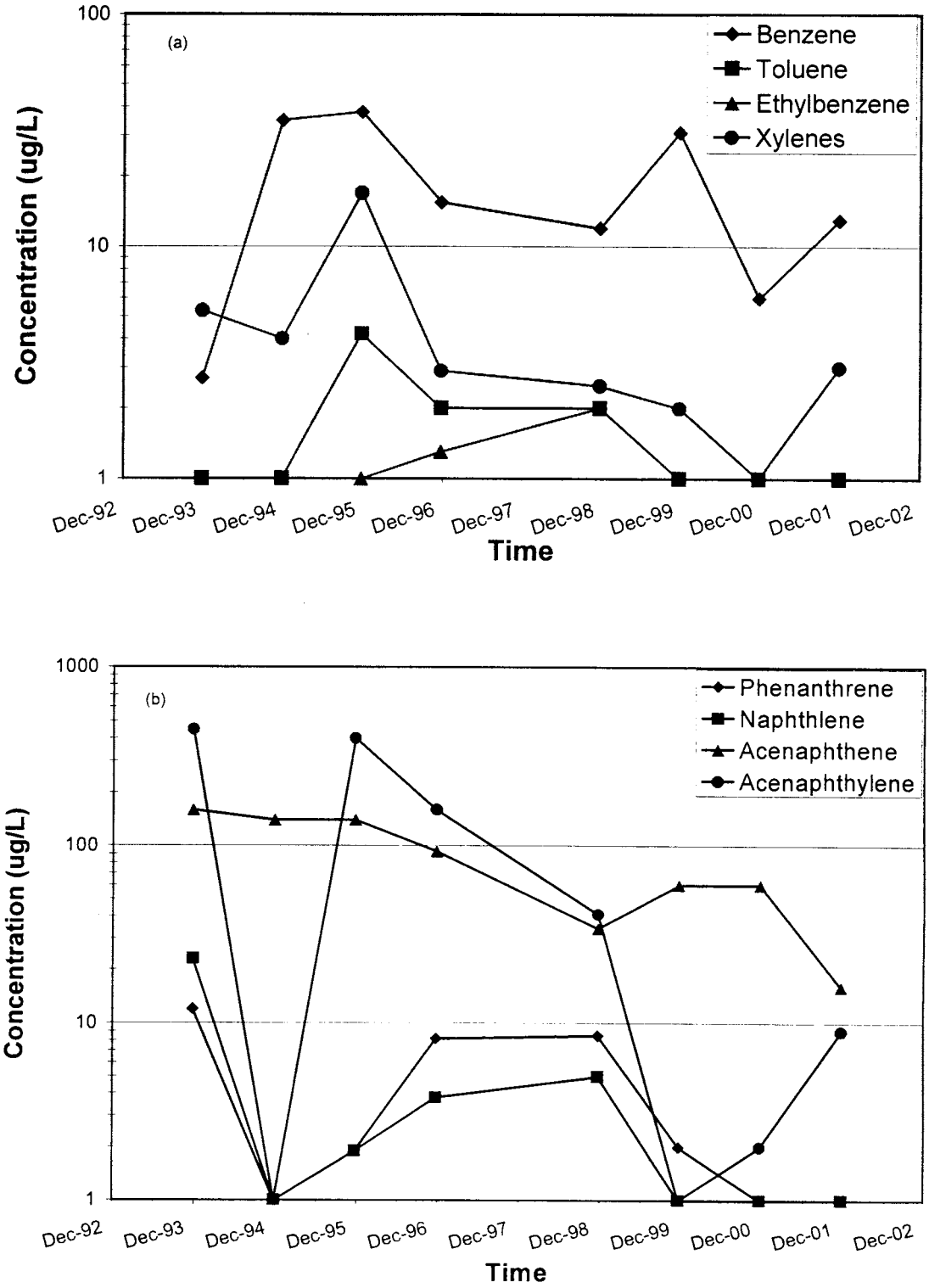

Figure 3.36 (a) & (b). Variation in BTEX and PAH concentrations with time at MW6

3.9. References

Addinsoft SARL, Software XLSTATM version 5.1 http://www.xlstat.com/indexus.html, Paris, France. (Date accessed: May 22, 2002)

Bevolo, A.J., Kjartanson, B.H., and Wonder, J.D., 1996. Ames Expedited Site Characterization Demonstration at the Former Manufacturing Gas Plant Site, Marshalltown, Iowa, IS-5121/UC-630. Ames Laboratory, Ames, Iowa.

Black & Veatch, 1994. Remedial Investigation/Feasibility Study Report Cherokee, Iowa. (Dated August 1994). Kansas City, Missouri.

Black & Veatch, 1998b. Interim Remedial Action Report for Soil and Source Material. (Dated 4/27/1998). Kansas City. Missouri.

Black & Veatch, 1999. Former Manufactured Gas Plant Program Quality Assurance Project Plan. (Dated May 1999). Kansas City, Missouri.

Black & Veatch, 2001. Phase I Site Investigation Report. (Dated August 2001). Kansas City, Missouri.

Buscheck, T.E. and Alcantar, C.M., 1995. Regression Techniques and Analytical Solutions to Demonstrate Intrinsic Bioremediation, in Proceedings of the 1995 Battelle International Conference on In-Situ and On Site Bioremediation, April 1995.

Butler, J.J., Healey, J.M., Zheng, L., McCall, W., and Schulmeister, M.K., 1999. Hydrostratigraphic Charcterization of Unconsolidated Alluvium Deposits With Direct Push Technology. Presented in 1999 Annual Meeting of the Geological Society of America, Denver, Colorado.

Butler, J.J., Healey, J.M., Schulmeister, M.K., and Zheng, L., 2001. A Field Assessment of Direct Push Technology for Site Characterization Investigations (abstract), Proceedings of18th Annual Water and the Future of

Kansas Conference, Center of Agricultural Resources and the Environment and Kansas Water Resources Research Institute, Manhattan, Kansas.

Butler, J.J., Healey, J.M., McCall, W., Loheide, S.P., and Garnett, E., 2002, Hydraulic Tests with Direct-Push Equipment. Ground water, 40(1): 25-36.

Das, B.M., 1994. Principles of Geotechnical Engineering (3rd ed). PWS Publishing Boston, MA.

EPA, 1997. Chapter 5: Direct Push Technology from Expedited Site Assessment for Underground Storage Tank Sites: A Guide for Regulator, EPA 510-B-97-00, Office of Underground Storage Tanks, United States Environmental Protection Agency, Washington, DC.

EPA, 2000. Evaluation Report on the Pine Street Barge Canal Coordinating Council, Burlington, VT. http://www.epa.gov/superfund/tools/cag/resource/r1/pineeval.pdf, United States Environmental Protection Agency Region 1, Office of Regional Administrator, Boston, MA. (Date accessed: April 5, 2002).

EPA, 2001. Performance Comparison: Direct Push Wells versus Drilled Wells. Technical Report TR-2120-ENV, Naval Facilities Engineering Command, Washington, DC.

Fetter, C.W., 1993. Contaminant Hydrogeology. Macmillan Publishing Company, NewYork.

Johnson Company Inc, http://www.johnsonco.com/direct_push_technology.htm, Vermont, USA. (Date accessed: April 7, 2002)

Kemblowski, M.W., Salanitro, J.P., Deeley, G.M., Stanley, C.C., 1987. Fate and Transport of Residual Hydrocarbon in Groundwater – a case study. Proceedings, Petroleum Hydrocarbons and Organic Chemicals in

Groundwater: Prevention, Detection and Restoration. National Water Well Association/API, Houston, TX. 207-231.

Kjartanson, B.H., Starke, T.P., and Purdy, C.B., 1997. Expedited Site Characterization Training Coursebook, Version 1. LA-UR-97-527, USDOE EM-13, Office of Training and Education, USDOE, Los Alamos, NM.

Lee, P.H., 2000. Use of Solvents for PAHs Extraction and Enhancement of the PAHs Bioremediation in Coal-Tar Contaminated Soils. Ph.D. Thesis. Iowa State University.

Mack, T.J., 1993. Detection of Contaminant Plumes by Borehole Geophysical Logging. Ground Water Monitoring and Remediation, 13(1).

Nathan, M.V. and Combs, S.M., 1998. Chapter 12 of Recommended Chemical Soil Test Procedures for the North Central Region. North Central Regional Research Publication no. 221(revised).

Starpoint Software Inc., Software Superslug version 3.1 http://www.pointstar.com/Aquifer/SuperSlug.htm, Cincinnati, Ohio, USA. (Date accessed: Feb 15, 2002)

Thornton, D., Ita, S., and Larsen, K., 1997. Broader Use of Innovative Ground Water Access Technologies. In: Superfund XVIII Conference Proceedings, Vol. 2. United States Environmental Protection Agency, Washington, DC.

USDA 1989. U.S. Department of Agriculture (USDA), Soil Conservation Service, Soil Survey of Cherokee County, Iowa, July 1989.

CHAPTER 4 MODELING GROUNDWATER FLOW AND FATE AND TRANSPORT OF CONTAMINANTS AT CHEROKEE FMGP SITE, IOWA

A paper to be submitted to the Journal of Groundwater Monitoring and Remediation

Rahul Biyani[1], Bruce Kjartanson[2], Say Kee Ong[2], Greg Stenback[3]

Abstract

Modeling of groundwater flow and transport of contaminants at the former manufactured gas plant (FMGP) site in Cherokee, Iowa was conducted. The Little Sioux River approximately 600-ft downgradient of the site is a potential receptor of contaminants leaching and migrating from the source area. To assess the vulnerability of the river to the contaminants, a fate and transport model contaminants was constructed using MODFLOW/RT3D. The site was modeled with a three-layer hydro-geologic stratigraphy. Groundwater was calibrated against the observed hydraulic heads by varying the hydraulic conductivity values using MODFLOW. Calibrated hydraulic conductivity ranged from 0.25 to 400 ft/day (8.7E-05 – 1.4E-01 cm/sec) and was similar to the measured values on site. In the pinch zone low hydraulic conductivity of 0.25 ft/day (8.7 E-05 cm/sec) was used to match the high hydraulic gradient of 0.1 ft/ft. MODPATH results showed that the particle movement emerging from the source area was in the south-southeast direction. RT3D was run with limited site concentration data and incomplete characterization of the source. Calibration of RT3D was conducted by minimizing the root mean square (RMS) errors between the simulated and observed concentrations of the contaminants. Except for toluene, none of the other BTEX compounds matched the simulated and observed concentrations at the site due to the possible presence of a

[1] Graduate Student, Department of Civil & Construction Engineering, Iowa State University, Ames, IA
[2] Associate Professor, Department of Civil & Construction Engineering, Iowa State University, Ames, IA
[3] Associate Scientist, Department of Civil & Construction Engineering, Iowa State University, Ames, IA

secondary source. Transport modeling for phenanthrene with an extended source to the west indicated the possibility of more soil contamination to the west of the GWP20. The first-order biodegradation rates for toluene and phenanthrene (with extended source), estimated on the basis of model calibration were 0.03 d^{-1} and 0.006 d^{-1}, respectively. The results of sensitivity analysis showed that the first-order biodegradation rate was the most sensitive input parameter for both toluene and phenanthrene.

4.1. Introduction

During the past decade, MNA technique has become one of the widely accepted choices among regulators and site owners for the clean up of contaminated sites (Keeley et al., 2001). Acceptance of MNA at a contaminated site requires evidence of it's capability to achieve site-specific remediation objectives within a time frame that is reasonable compared to other alternatives at a site (EPA, 1997). A groundwater solute fate and transport model is a useful method to evaluate the effectiveness of natural attenuation in cleaning the contaminated site (Wiedemeier et al., 1999). Fate and transport models can predict the amount of time required to reduce the contaminant concentrations below environmentally acceptable concentrations in groundwater and the impact of contamination migrating from the contaminated site to a distant receptor. Anderson and Woessner (1992) developed a modeling protocol to provide evidence to demonstrate natural attenuation as a cleanup alternative at a contaminated site. Their protocol includes formulation of a conceptual site model (defining hydrogeologic features, flow system, sources and sinks of water and contaminants), calibration of the site model, verification of the calibrated model, and prediction of the fate of contaminants using the calibrated model.

Several researchers have demonstrated the usefulness of numerical models to study the fate and transport of a single or multi-species in multi-dimensions (Konikow and Brehehoeft, 1978; Zheng, 1990; Clement el at., 1997; Landmeyer et al., 1998; Clement el al., 1999; Abdulla et al., 2000; Widdowson et al., 2001). There

are several analytical and numerical computer models available for modeling groundwater flow and fate and transport of contaminants. Some models include both flow and transport, while others are either flow models or transport models alone. Some common models in use include BIOPLUME III, BIOSCREEN, MODFLOW, RT3D, MT3D, and SEAM 3D. Each of the models has various limitations in their applicability and accuracy (Bredehoeft et al., 1993, Miller, 2000).

Both BIOPLUME III and BIOSCREEN models are intended largely for simulating transport and biodegradation of petroleum compounds. According to Miller (2001) and Zhang et al. (2001), both BIOPLUME III and BIOSCREEN are good for contaminated sites with simple geologic and hydrogeologic features. In both models, depth-averaged two-dimensional transport is assumed, bacterial growth is neglected and only hydrocarbon kinetics are considered in a heterogeneous and isotropic aquifer (Clement et al., 1998). But in the field most of the plumes are 3-D in nature and usually large variations in contaminant concentrations with depth are seen (Wiedemeier et al., 1995). For instance, at FMGP site in Cherokee, Iowa, multi-level groundwater sampling showed concentration variations to be as high as 1000 μg/L for both BTEX and PAHs. Also, to assume subsurface geology to be homogeneous and isotropic could lead to wrong results. It is essential to produce a site-representative 3-D geological model before modeling the groundwater flow (Keeley et al., 2001). Miller (2001) used BIOPLUME III to model the FMGP site at Cherokee, Iowa and concluded that use of BIOPLUME III to model the complex aquifer geometry at the site may not be appropriate.

RT3D coupled with MODFLOW can model the groundwater flow and fate and transport of multiple mobile and/or immobile species in 3-D in a heterogeneous and anisotropic aquifer with complex boundaries (GMS User's Manual, 1997; Clement et al, 1997). In addition, it handles microbial metabolism and its transport kinetics (Clement et al., 1998). Apart from being a 3-D model, RT3D has several other advantages over BIOPLUMEIII, such as BIOPLUME III has only one transport solver: method of characteristics while RT3D has finite difference and total-variation

diminishing (TVD) solvers in addition to the method of characteristics, and BIOPLUME III can simulate only two types of multi-species reactions, instantaneous and sequential electron donor-acceptor reactions, while RT3D, in addition to these two, can simulate rate limited sorption reaction, double Monod model and user definable reactions (Zhang et al., 2001). RT3D/MODFLOW models provided with Groundwater Modeling System (GMS) software package (a graphical interface for pre and post-processing, model calibration and visualization) were used to model the fate and transport of contaminants at the Cherokee FMGP site, Iowa.

The scope of this chapter is to (1) develop a conceptual model for the FMGP site in Cherokee, Iowa; (2) simulate groundwater flow using a 3-D finite difference MODFLOW model and calibrate it against the hydraulic heads observed in the monitoring wells at the site; (3) use the particle tracking model, MODPATH, to track the movement of particles emanating from the source zone in 3-D under the effect of advection alone; (4) simulate the fate and transport of BTEX and four PAH compounds, phenanthrene, naphthalene, acenaphthene, and acenaphthylene, using the RT3D model; (5) estimate the biodegradation rate constants for the same compounds; (6) assess the relative sensitivity of model input parameters with respect to matching of simulated concentration results in groundwater to the observed concentrations.

4.2. Study Area

The FMGP site at Cherokee, Iowa is located in the south end of the city at the intersection of West Beech and 4th Streets (Figure 4.1). The site is surrounded by the Illinois Central Gulf Railroad to the west and northwest, residential areas to the north and northeast, and the Little Sioux River at approximately 600 feet to the southeast. Cherokee has typical continental climate with 28 inches of annual precipitation and an average seasonal snowfall of 32 inches (USDA, 1989). A carburetted water gas plant operated at the site from 1905 to 1936 (Black and Veatch, 1994). Soil contaminated with coal tar was first observed at the site in 1984 while sewer lines were being installed along the north side of Beech Street.

Preliminary investigation began in 1986 at the site followed by preliminary site assessment in 1991.

4.3. Site Geology and Hydrogeology

The Cherokee FMGP site is located to the west of the Little Sioux River floodplain. The valley deposits associated with the Little Sioux River are characterized by distinct alluvial terraces, underlain by sand and gravel. The geology at the site, as predicted from electrical conductivity probing results during August 2001 site characterization activity and pre-existing borehole logs, may be divided into four layers. The top most layer is silty fill, overlying loess followed by sandy alluvial and low permeability till. The thickness of the different layers varies across the site. Pinching of the alluvium layer by the overlying loess layer at the middle of the site is a prominent feature of the geology at the site. The estimated pinch zone (thickness less than 3 feet) runs across the site in the alluvium layer and has a more silty and clayey texture than the alluvium layer with a very low hydraulic conductivity approximately 0.072 ft/day (2.5E-05 cm/sec) (see Figure 4.1). The alluvium layer is approximately 30 feet thick in the north of the FMGP site and narrows to as low as 3 feet in the pinch zone. The thickness increases to approximately 25 feet near the Little Sioux River. In contrast to the alluvium layer, the overlying fine loess is almost absent in the areas north of the FMGP site but its thickness increases to 25 feet over the pinch zone. Figures 3.10-3.14 show the geology at the site along several cross-sections.

There are 18 monitoring wells at the site to monitor the groundwater flow (see Figure 4.2). The hydraulic heads at the site were between 9 - 15 feet below ground surface, both upgradient of the MW5 and downgradient of MW6. Between MW5 and MW6, the hydraulic heads were between 0 - 5 feet below ground surface with MW6 showing artesian condition. Hydraulic heads were nearly the same (within 0.2 feet) in the MW6 and upgradient wells and remain nearly constant with time. There was an average drop of 13.39 ft in hydraulic head between MW6 and MW9 and 12.9 ft between MW6 and MW8 in the south and the east of the site, respectively. This

drop in the water level is thought to be caused by the pinch running across the site in the alluvium layer. Rainfall had a very little to no effect on the water elevations in the monitoring wells upgradient of MW6 but the wells downgradient of MW6 showed a maximum of 6 feet of variation in water elevations over ten year period of time. The rise in water elevations in the downgradient wells could be attributed to rise in surrounding Little Sioux river water level during the rainfall.

Hydraulic conductivity at the site measured by slug testing in pre-existing monitoring wells, pre-packed screen monitoring wells and Geoprobe dual probe direct push equipment varied from 0.0265 ft/day (9.2E-06 cm/sec) to 0.092 ft/day (3.2E-05 cm/sec) in the loess and 0.092 ft/day (3.2E-05 cm/sec) to 1.3 E+03 ft/day (0.46 cm/sec) in the alluvium. Hydraulic conductivity values were as low as 0.072 ft/day (2.5E-05 cm/sec) in the pinch zone.

4.4. Conceptual Site Model

The conceptual model for modeling the FMGP site at Cherokee, Iowa consists of three hydrogeological layers (see Figure 4.3). Figure 4.3 also presents a cross section of the geology at the site. The first layer represents the fine loess unit consisting of poorly graded silt and clay size particles. The second and third layers represent the upper and lower halves of the alluvium layer (aquifer). The alluvium layer was divided into two layers of equal thicknesses to study the variation in contaminant concentration with depth. Underlying the alluvium layer is an impermeable till layer, which acts to restrict vertical migration of water and contaminants.

A finite difference grid of 40 rows and 40 columns was used to model the site. The width of the cell along the rows (Δx) was 18.43 ft and along the columns (Δy) was 20.63 ft. Total area of the model grid was 14 acres. The conceptual model grid is presented in Figure 4.4. The model grid was oriented perpendicular to the flow of water in the river.

4.5. Groundwater modeling

The groundwater flow at Cherokee site was modeled using MODFLOW. Due to rainfall, the down-gradient monitoring wells, MW7 – MW13, often show a higher water level by approximately 6 foot (maximum) in the month of June -July than the water levels taken during other months in the year. However, the average of all the groundwater level readings taken in a year had remained nearly constant for all of the monitoring wells at the site since the beginning of site investigations (see Table B1). In this study, the average measured groundwater levels (1991-2001) were used as inputs for the model.

MODFLOW utilizes a numerical solution for the equation governing groundwater flow:

$$\frac{\partial}{\partial x}\left(K_{xx}\frac{\partial h}{\partial x}\right)+\frac{\partial}{\partial y}\left(K_{YY}\frac{\partial h}{\partial y}\right)+\frac{\partial}{\partial z}\left(K_{zz}\frac{\partial h}{\partial z}\right)-W=S_s\frac{\partial h}{\partial t} \qquad \text{(Eq 4.1)}$$

where K_{XX}, K_{YY}, K_{ZZ} = Hydraulic conductivity along x, y and z directions (Lt^{-1})
h = Hydraulic head (L)
W = Volumetric flux per unit volume (sources/sinks of water) (t^{-1})
S_s = Specific storage (L^{-1})
t = Time (t)

4.5.1. Input parameters

Groundwater modeling requires hydraulic conductivities, recharge, starting heads and top and bottom elevations of layers as input parameters. Due to the complex subsurface geology and hydrogeology observed, it would be inappropriate to give constant hydraulic conductivities for the aquifer at Cherokee, Iowa. Hydraulic conductivity values in both of the aquifer layers were varied from 170 ft/day (0.06 cm/sec) in the areas upgradient of MW6 to 0.12 ft/day (0.00004 cm/sec) in the pinch zone to 400 ft/day (0.14 cm/sec) in the areas downgradient of MW10. Change in hydraulic conductivity was made gradual from one model cell to another. In loess, the uppermost model layer, a constant value of 0.1 ft/day (0.000032 cm/sec) was assigned. The output of the MODFLOW, presented in section F1 in Appendix F, gives the listing of input parameters for each cell.

The elevation data for the layers was obtained from the results of Geoprobe electrical conductivity probing carried out during the phase I site characterization activity and borehole logs at pre-existing monitoring well locations. Top elevations of various layers at Geoprobe electrical conductivity push and soil boring locations are presented in Table F1 in Appendix F. Layer elevations were imported into the model and interpolated throughout the model domain.

Since average measured hydraulic head data for a year was used to define the boundary conditions, putting recharge as a separate source for water would be superfluous. However an attempt was made to model the groundwater using recharge. Since rainfall had negligible effect on the water levels in the MW's upgradient of MW6 and that the slope was approximately 4% between MW1 & MW6, no recharge was applied for this area. A recharge rate of 0.0025 ft/day (7.2 cm/sec) was used in the cells downgradient of MW6. Table 4.1 presents the input parameters for the groundwater flow model.

4.5.2. Boundary and initial conditions for groundwater model

Boundaries for the model were identified by drawing the contours of potentiometric surface using the average hydraulic head at the site. Hydraulic heads in MW1 to MW6 were almost constant and equal. Therefore a specific head boundary was used initially along the north and part of the west boundary (northwest edge) of the model grid. The hydraulic heads were varied from 1176.0 ft to 1176.33 ft along the northwest specific head boundary and from 1176.33 ft to 1176.35 ft along the north specific head boundary of the model grid. These constant head values were obtained by interpolation of hydraulic heads from the nearby monitoring wells. Specific hydraulic head boundary was also defined along the Little Sioux River in the south. The head was varied from 1158.1 ft to 1158.0 ft along the direction of river flow from east to west in the model domain. The east boundary and the remaining portion of west boundary were assigned as no flow boundaries. Hydraulic heads in the monitoring wells were imported into the GMS and interpolated to give the starting heads.

4.5.3. Calibration

The flow model was calibrated by varying the hydraulic conductivity values to match the observed hydraulic heads in the MW's at the site. The calibrated hydraulic conductivities in both aquifer layers varied from 170 ft/day (6.0E-02 cm/sec) upgradient of MW6 to 0.25 ft/day (8.8E-05 cm/sec) in the pinch zone to 400 ft/day (1.4E-01 cm/sec) downgradient of MW10. The pinch zone in the aquifer, which appeared to be running in the west – east direction in Figure 3.15 was extended more toward the northeast direction to account for the decrease in hydraulic head between MW6 and MW8. The calibrated groundwater model is presented in Figure 4.5. The calibrated hydraulic conductivity values for the model with recharge as a separate source of water varied from 0.001 ft/day (3.0E-06 cm/sec) to 400 ft/day (1.4E-01 cm/sec). Hydraulic conductivity values were lowered to maintain the same hydraulic heads at the monitoring wells. The calibrated groundwater flow model is presented in Figure F1 in Appendix F. Tables 4.2 and F2 present comparisons between the average measured and simulated hydraulic head distribution for models without and with recharge as separate source of water, respectively. The root mean square errors between observed and calibrated hydraulic head values for groundwater model without and with recharge were 0.63 ft and 0.54 ft, respectively. Even though the RMS values for groundwater model with recharge condition was less, the hydraulic conductivity for the test locations had to be reduced by two orders of magnitude from that measured at the site. This may invalidate the "with recharge" model.

Several difficulties were encountered during the calibration exercise. The loess layer at the site was dry in the area upgradient of MW5 (shown in Figure 4.3). Therefore assigning specific hydraulic head boundary for all the three layers along the northern boundary, as stated earlier, was giving an error in running MODFLOW. The problem was circumvented by assigning specific hydraulic head boundaries only along the aquifer layers, i.e., layers 2 and 3 and making the boundary for loess a no-flow boundary. The other difficulty encountered while varying the hydraulic conductivity values was to match the drop of 13.9 feet in hydraulic head between

MW6 and MW9. Hydraulic conductivity values were altered on a cell-by-cell basis and the model was run to simulate hydraulic heads. Also, between MW8 and MW6 an average drop of 12.9 feet in hydraulic head was observed even though the hydraulic conductivities at both places were almost the same. It was probable that the pinch zone, which is causing the drop in hydraulic head between MW6 and MW9, may be continuous between MW6 and MW8. The thickness of the different layers were not available for most of the portion of the model domain near the Little Sioux River in the south and in the private property areas north of the site. For these areas, artificial elevations for each layer were generated by interpolation using the elevations for the nearest electrical conductivity pushes.

Since the groundwater flow direction could not be estimated exactly using data from the site characterization activity in August 2001 (see section 3.5.6), the assumption of no flow boundaries along the east and west boundary of the model grid may or may not be correct. To test the assumption that no flow boundaries was not affecting the groundwater modeling results, a run was made by assuming all the boundaries as constant head boundaries. The resulting groundwater flow pattern, presented in Figure 4.6 with all boundaries as constant head, showed no difference from the run with no flow boundaries along the east and west boundary of the model grid.

4.6. Fate and transport modeling

Soil and groundwater samples extracted during phase I of the site investigation showed contamination in the form of tar, poly and monocyclic aromatic hydrocarbons. The actual extent of the source of contamination is not known nor is full extent of the concentration of contaminants at the source. Figures 3.18 – 3.29 and D5 - D16 present iso-concentration lines for eight target analytes (BTEX and four PAHs: naphthalene, phenanthrene, acenaphthene and acenaphthylene). Benzene, ethylbenzene and xylene showed high concentrations at GPMW 13 in comparison to surrounding groundwater sampling locations, suggesting the presence of a secondary source. For PAHs, high concentrations were found in

GPW19 and GPW22 and in soil sampling locations SS3 and SS4, indicating that the source zone may extend further to the east. RT3D was used to model the fate and transport of the eight target analytes.

The general macroscopic equation describing the fate and transport of aqueous phase species is written as:

$$R_{Ck}\frac{\partial(C_k)}{\partial t}=\frac{\partial}{\partial X_i}\left(D_{ij}\frac{\partial(C_k)}{\partial X_j}\right)-\frac{\partial(v_i C_k)}{\partial X_i}+\frac{q_s}{\varphi}C_{sk}+r_{Ck} \qquad \text{(Eq. 4.2)}$$

where, k = 1,2....m

m = The total number of aqueous species

C_k = The aqueous phase concentration of k^{th} species (ML^{-3})

R_c = Retardation factor

D_{ij} = The hydrodynamic dispersion tensor

v = The pore velocity (LT^{-1})

φ = Porosity

q_s = Volumetric flux of water per unit volume of aquifer representing sources and sinks (T^{-1})

r_{Ck} = Reaction rate ($ML^{-3}T^{-1}$)

4.6.1. Boundary and initial conditions for fate and transport modeling

A no mass flux condition was applied at the west and east boundary of the model domain. Specified concentrations at the north and the northwest boundary and specified mass flux at the south boundary were applied. The concentrations of electron acceptors and contaminants were assumed to have no seasonal variation and were assigned at the upstream boundary as the measured background values. Constant contaminant concentrations were assumed as point sources in the cells corresponding to MW5, GPW20 and GPW24. Concentrations in the cells between the three measured concentrations were interpolated accordingly.

4.6.2. Input parameters and methodology

RT3D requires longitudinal and transverse dispersivity, sorption constants, biodegradation rate constants, upgradient electron acceptors concentrations, soil bulk density, groundwater flow modeling result, source location and source concentration as input parameters. The longitudinal dispersivity estimated on the

basis of the phenanthrene plume size (Gelhar et al., 1992), was estimated to be 25 feet in the alluvium layer and 10 feet in the loess layer. This estimated longitudinal dispersivity was used for all the other analytes. Organic carbon content was measured for the soil samples collected during the site investigation in August 2001. Linear sorption constants were estimated for different compounds at different depths using the average organic carbon content and values of K_{ow} and K_{oc} (taken from LaGrega et al. (1994)). Linear sorption constants and corresponding retardation factors are presented in Tables F3 and F4, respectively, in Appendix F. Using the Freundlich parameters for the target analytes from Lagrega et al. (1994), it was found that the concentrations encountered on site for the target analytes lie along the linear portion of the curve and hence the linear sorption assumption was valid. To simplify modeling, a constant sorption coefficient for each layer was assigned (see Table 4.3 for data). The source for fate and transport modeling was assumed to be between MW5 in the west, GWP20 in the east and north, and GPW24 in the south of the site. Constant source terms equal to the average aqueous concentrations for the target analytes obtained during groundwater sampling from 1993 - 2001 were assumed for MW5A and 5B in the upper and lower halves of the aquifer, respectively. In addition constant source terms were assumed for GPW20 and GPW24 using the August 2001 target analytes concentrations for the upper and lower halves of the aquifer. The constant source terms were assumed to be point sources at the cells corresponding to the MW and groundwater push locations. For the cells between the source term cells corresponding to the MW and groundwater push locations, constant source terms were assumed by interpolating the concentrations. Electron acceptor concentrations obtained from groundwater sampling location GPW12 (see Figure 3.4) were used as background concentrations. The average soil bulk density used in the model was measured from several soil samples collected during the August 2001 sampling event (see Table 3.7). Input parameters for the transport model are presented in Table 4.3.

The methodology used for fate and transport modeling of contaminants was to run the RT3D model (using a predefined reaction package: BTEX degradation

with multiple electron acceptor) with best-estimated input field parameters and a constant source for 65 years. The model was calibrated for each target analyte against the observed aqueous concentrations on-site during August 2001 site sampling event by varying four input parameters: biodegradation rate constants, sorption constant, dispersivity, and ratio of transverse to longitudinal dispersivity to obtain the least root mean square (RMS) error between the simulated and observed concentrations for each target analyte. The contaminant plume was assumed to be in a steady state condition. Therefore the rate of contaminant influx from source should be equal to its overall attenuation rate.

Since it would be difficult to partition the electron acceptor (oxygen, nitrogen, ferrous iron, sulfate, and methane) concentrations according to the target analytes, an overall first order biodegradation constant was estimated for a target analyte by assuming that all the electron acceptors were used by the target analyte. For a given simulation, one input parameter was varied while the others were kept constant. The value of parameter for which the least RMS error was found was assigned as an estimated value of that parameter for the analyte. Similarly other input parameters were varied and the iterative exercise was continued till the least RMS error value was achieved for an analyte.

4.6.3. Particle tracking

MODPATH model was used to track the particles released from the assumed source zone under the effect of advection alone. MODPATH uses the hydraulic head and cell-by-cell flow terms computed by MODFLOW, in addition to the soil porosity, to compute the movement of particles through the flow field. Estimated soil porosity for soil samples used for the modeling were obtained during August 2001 and are presented in Table 3.7. Particles were generated in the cells in layer 2 and 3, between GWP22 and MW5. Result of MODPATH in layer 2 for steady state case is presented in Figure 4.7. Layer 3 being same in all hydraulic properties as layer 2 shows the same result. Results of MODPATH indicate that with the groundwater flow obtained by MODFLOW and the assumed source area, the flow of

contaminants would be in the south-southeast direction. This is contrary to the south-southwest flow of contaminants observed by assuming the shape and direction of plume found at the site (see section 3.5.6).

4.6.4. Flow and transport modeling results

Toluene was calibrated first to estimate the field longitudinal and transverse dispersivity values and biodegradation rate of toluene. To evaluate the effects of sorption and biodegradation in controlling the plume sizes at the site, runs were simulated first for 15 years with advection and dispersion only and then adding sorption and biodegradation in consecutive runs. Results are presented in Figures 4.8 - 4.10. With dispersion and advection only the contaminant was found to migrate to the river in the south of the site. The plume size was much shorter when sorption and biodegradation were added as the processes of natural attenuation. On comparing plume sizes in Figures 4.8 - 4.10 with iso-concentration lines formed using August 2001 toluene data (see Figures D5 – D6), it is evident that biodegradation and sorption may be important natural attenuation processes controlling the size of the plume at the site.

Table 4.4 shows the iterative runs made by varying the input parameters and RMS error calculation to calibrate the toluene plume against the 2001 site observed concentrations. The estimated dispersivity, ratio of longitudinal to transverse dispersivity, sorption constant for aquifer layers, and biodegradation rate for a least RMS error of 3.75×10^{-9} g/ml were 25 ft, 0.3, 30 ml/g, and 0.03 d^{-1}, respectively. Figures 4.11 – 4.12 present the simulated toluene plume in the lower and upper halves of the aquifer. Using the RT3D model for other BTEX compounds, RMS errors higher than that for toluene were obtained. This may be due to higher concentrations, potential secondary source at site around GPW 13A & B. The location and the concentration of both main and the potential secondary source needs to be further characterized before running a reactive transport model on BTEX compounds other than toluene.

In case of PAHs, high PAH concentrations were observed in GWP19 and GWP22 indicating that the source area for PAH compounds might extend to the west of the assumed source area. Simulations were run for phenanthrene by assuming that the PAH source area extended beyond the BTEX source to GWP22 in the west. The dispersivity was kept the same as that for toluene and the input parameters for sorption and degradation were varied. Table 4.5 presents the iterative runs made for phenanthrene. The sorption and biodegradation constants that gave the least RMS error of 9.31×10^{-9} g/ml were15 ml/g and 0.006 d^{-1}, respectively. Figures 4.13 – 4.14 present the simulated phenanthrene plume in the lower and upper halves of the aquifer. Simulations were conduced for other target analytes but the results did not match the actual site data due to incomplete information on the source area. The modeling exercise will be continued using concentration results from phase II site investigation. Groundwater pushes and new pre-packed monitoring wells to be installed in phase II should provide more information on the extent of the source.

The sorption coefficient for toluene was found to be an order of magnitude higher and for phenanthrene, an order of magnitude lower than the average value obtained from the organic carbon content in field. Biodegradation rates lie in the published range of values for the respective compounds but are higher than the rates estimated by the Buscheck and Alcantar (B & A) method (see Chapter 3 & Table 3.11). The difference are probably due to R values, velocity used with the B & A equation versus the numerical method, the fact that B & A assume 1-D flow but the numerical method is 3-D, the fact that the B & A biodegradation rate constant is estimated from only some of the data while that of the RT3D is based on all the data and the fact that the plume is probably not at steady state as assumed in B & A equation.

4.6.5. Sensitivity analysis

A sensitivity analysis was conducted to evaluate the effect of input parameters on the resulting plume size. The sensitivity of a model dependent

variable to a model input parameter is the partial derivative of the dependent variable with respect to that input parameter (McElwee, 1982). Several model dependent variables can be used in sensitivity analysis. In the past, researchers have used the longitudinal length of the contaminant plume or total mass of contaminant within a particular concentration value contour as the variable. Zheng and Bennett (1995) recommended RMS error as a single sensitivity coefficient, which is indicative of the sensitivity of a group of observation wells to a model input parameter for calibration criterion. The sensitivity coefficient is given by:

$$X = \frac{\partial y}{\partial a_k} = \frac{\partial S}{\partial a_k} \cong \frac{(S(a_k + \Delta a_k) - S(a_k))/S(a_k)}{\Delta a_k / a_k} \qquad \text{(Eq. 4.3)}$$

Where X = Sensitivity coefficient

y = Model dependent variable

a_k = Model input parameter

S = Root mean square error of measured versus modeled concentration

Sensitivity analysis was conducted by keeping the runs with least RMS error as a base case and estimating the sensitivity coefficients for toluene and phenanthrene for the runs shown in Tables 4.4 and 4.5. Sensitivity analysis was taken by averaging the value obtained for all the runs. Table 4.6 summarizes the results of the sensitivity analysis. As shown in the Table 4.6, the RMS errors for both toluene and phenanthrene were most sensitive to first-order biodegradation rate. High sensitivity to biodegradation rate indicates the need to understand microbial metabolism in fate and transport simulations for the site.

4.7. Conclusion

Groundwater flow modeling, particle tracking, and transport of two contaminants: toluene and phenanthrene, for natural attenuation purposes were evaluated at Cherokee FMGP site using MODFLOW, MODPATH, and RT3D. Results of groundwater flow modeling indicated the need for further site characterization to define the true extent and hydraulic conductivity of the pinch

zone. The reason for the large drop of 12.9-ft in the hydraulic head between MW6 and MW8 is still elusive. To account for the hydraulic head drop, it was assumed that the pinch in the aquifer is running between the two monitoring wells. The calibrated hydraulic heads matched fairly well with the observed heads at the site (RMS error = 0.63 ft). Use of no flow boundary along the east and west boundaries of the model domain was verified by changing them to constant head boundaries and no change in the simulated hydraulic heads was observed at the MW locations. MODPATH was used to track the particles emerging from the source area and moving under the hydraulic heads generated by MODFLOW. MODPATH results for a steadystate condition showed the movement of particles to be in the south-southeast direction. Since most of the contaminants were residing in the region where the water was at almost constant head due to the pinch, it was possible that the plumes were expanding in transverse direction along the pinch shape due to dispersion, and advection was having minimal effect on movement.

Due to insufficient information on the source area and contaminant concentrations, high RMS errors were found between simulated concentrations using RT3D and observed concentrations at site. High concentrations around GWP13A and 13B (a possible secondary source) and in some of immediate downgradient groundwater push locations indicate the need for more monitoring wells and groundwater pushes to better define the extent of source area. Simulations were run for toluene and phenanthrene. The calibration was done by varying four input parameters: dispersivity, ratio of transverse to longitudinal dispersivity, sorption constants, and biodegradation rate constants and obtaining the least RMS error between the simulated and observed concentrations. Runs with the least RMS error for toluene and phenanthrene indicated the first-order biodegradation rate to be 0.03 and 0.006 d^{-1}, respectively. Biodegradation rates were higher than the rates calculated using analytical solutions but lie in the published ranges for the two compounds. Results of sensitivity analysis showed that the biodegradation rate was the most critical input parameter in controlling the simulated concentrations and RMS error.

Table 4.1. List of input parameters for groundwater flow modeling*

Parameter	Value
Discretization in:	
x-direction (Δx)	18.43 ft
y-direction (Δy)	20.63 ft
Extent of model in:	
x-direction	740 ft
y-direction	825 ft
Hydraulic conductivity	
Layer1 - Loess	0.15 ft/day (held constant)
Layer2 – Upper half of alluvium	0.12 – 400 ft/day
Layer3 – Lower half of alluvium	0.12 – 400 ft/day

* For recharge option – recharge was 0.0025 ft/day

Table 4.2. Comparison of simulated and observed hydraulic heads

Monitoring Well Location	Simulated Head (ft)	Observed Head (ft)	Difference (ft)	Square of Difference
MW1	1176.3	1176.28	0.02	0.0004
MW2	1176.3	1176.29	0.01	0.0001
MW3	1176.2	1176.33	-0.13	00.017
MW4	1176.33	1176.27	0.06	0.0036
MW5B	1176.27	1176.22	0.05	0.0025
MW6	1176.02	1176.13	-0.11	0.012
MW7	1159.7	1159.73	-0.03	0.0009
MW8	1165.2	1163.21	-1.99	3.96
MW9	1159.6	1160.35	-0.75	0.56
MW10	1158.12	1158.53	-0.41	0.17
MW11	1158.07	1158.53	-0.46	0.21
MW12	1158.25	1157.7	0.55	0.3
MW13B	1165.9	1165.9	0	0
			Total square of difference=	5.24
			Root mean square of difference=	0.63

Table 4.3. List of input and final parameters for transport modeling of contaminants

Parameter	Input Value	Final Value
Porosity		
Layer1	0.5	0.5
Layer2	0.3	0.3
Layer3	0.3	0.3
Soil bulk density		
Layer1	1.3 g/ml	1.3g/ml
Layer2	1.9 g/ml	1.9g/ml
Layer3	1.9 g/ml	1.9g/ml
Sorption constant		
Toluene		
Layer1	5.0 ml/g[a]	5.0 ml/g
Layer2	3.0 ml/g[b]	100ml/g
Layer3	3.0 ml/g[c]	100ml/g
Phenanthrene		
Layer1	240 ml/g[a]	240 ml/g
Layer2	150 ml/g[b]	15 ml/g
Layer3	150 ml/g[c]	15 ml/g
Dispersivity		
Layer1	10	10
Layer2	25	25
Layer3	25	25
Ratio of longitudinal to transverse dispersivity	0.2	0.3
Background concentrations (µg/L)[d]	Held constant	
Toluene & Phenanthrene	0	
Oxygen	4000	
Nitrate	15000	
Ferrour iron	90	
Sulfate	150000	
Methane	0	
Saturation constants	1	
Inhibition constants	1	
Source location*		
Toluene	MW5A, MW5B, GWP20, GPW24	
Phenanthrene	MW5A, MW5B, GWP20, GPW24, GWP23, GWP24	

* For cells lying in between the source locations, concentrations were interpolated
[a] Average of two values (in loess) (see Table F3)
[b] Average of ten values (in upper half of the aquifer) (see Table F3)
[c] Average of five values (in lower half of the aquifer) (see Table F3)
[d] Average of concentrations at GWP12 and MW4

Table 4.4. Calibration runs for toluene using RT3D as transport model

Run	Dispersivity (ft)	Ratio*	Sorption constant (L/µg)		Decay rate (d^{-1})	RMS error**	Comment
			Layer 2	Layer 3			
Set 1 with best estimated field result for input parameter							
1.1	25	0.2	3.00E-08	3.00E-08	0.01	24.48	
1.2	25	0.2	3.00E-08	3.00E-08	0.03	6.03	
1.3	25	0.2	3.00E-08	3.00E-08	0.05	4.34	Min. error
1.4	25	0.2	3.00E-08	3.00E-08	0.06	4.68	
1.5	25	0.2	3.00E-08	3.00E-08	0.07	5.43	
Set 2 with min. error run in set 1 as input parameter							
2.1	25	0.2	1.50E-08	1.50E-08	0.05	6.28	
2.2	25	0.2	3.00E-08	3.00E-08	0.05	4.34	
2.3	25	0.2	6.00E-08	6.00E-08	0.05	4.28	
2.4	25	0.2	1.00E-07	1.00E-07	0.05	4.24	Min. error
2.5	25	0.2	5.00E-07	5.00E-07	0.05	4.84	
Set 3 with min. error run in set 2 as input parameter							
3.1	25	0.2	1.00E-07	1.00E-07	0.05	4.24	
3.2	25	0.2	1.00E-07	1.00E-07	0.04	4.22	
3.3	25	0.2	1.00E-07	1.00E-07	0.03	4.08	Min. error
3.4	25	0.2	1.00E-07	1.00E-07	0.02	8.07	
Set 4 with min. error run in set 3 as input parameter							
4.1	25	0.2	3.00E-08	3.00E-08	0.03	6.03	
4.2	25	0.2	1.00E-07	1.00E-07	0.03	4.08	Min. error
4.3	25	0.2	1.50E-07	1.50E-07	0.03	7.84	
Set 5 with min. error run in set 4 as input parameter							
5.1	25	0.2	1.00E-07	1.00E-07	0.03	4.08	
5.2	25	0.3	1.00E-07	1.00E-07	0.03	3.75	Min. error
5.3	25	0.4	1.00E-07	1.00E-07	0.03	3.87	
Set 6 with min. error run in set 5 as input parameter							
6.1	25	0.3	2.00E-07	2.00E-07	0.03	4.4	
6.2	25	0.3	1.00E-07	1.00E-07	0.03	3.75	Min. error
6.3	25	0.3	5.00E-08	5.00E-08	0.03	3.84	
Set 7 with min. error run in set 6 as input parameter							
7.1	25	0.3	1.00E-07	1.00E-07	0.02	5.7	
7.2	25	0.3	1.00E-07	1.00E-07	0.03	3.75	Min. error
7.3	25	0.3	1.00E-07	1.00E-07	0.04	4.27	
Set 8 with min. error run in set 7 as input parameter							
8.1	20	0.3	1.00E-07	1.00E-07	0.03	4.01	
8.2	25	0.3	1.00E-07	1.00E-07	0.03	3.75	**Min error (final result)**
8.3	30	0.3	1.00E-07	1.00E-07	0.03	3.76	
8.4	35	0.3	1.00E-07	1.00E-07	0.03	4.1	

* Ratio of transverse to longitudinal dispersivity

** Root mean square error calculated between measured and simulated concentrations at MW's and GWP's

Table 4.5. Calibration runs for phenanthrene using RT3D as transport model

Run	Dispersivity (ft)	Ratio*	Sorption constant (µg/l)		Decay rate (d^{-1})	RMS error**	Comment
			Layer 2	Layer 3			
Set 1 with dispersivity from toluene result and others as best field obtained parameter							
1.1	25	0.3	1.5E-07	1.5E-07	0.03	24.62	
1.2	25	0.3	1.5E-08	1.5E-08	0.03	20.54	
1.3	25	0.3	1.5E-08	1.5E-08	0.01	18.24	Min. error
1.4	25	0.3	1.5E-08	1.5E-08	0.005	21.23	
Set 2 with source is extended to the west							
2.1	25	0.3	1.50E-08	1.50E-08	0.01	11.01	
2.2	25	0.3	1.50E-08	1.50E-08	0.008	10.59	
2.3	25	0.3	1.50E-08	1.50E-08	0.007	9.87	
2.4	25	0.3	1.50E-08	1.50E-08	0.006	9.31	Min. error
2.5	25	0.3	1.50E-08	1.50E-08	0.005	9.84	
Set 3 with min. error run in set 2 as input parameter							
3.1	25	0.3	1.50E-07	1.50E-07	0.06	10.2	
3.2	25	0.3	1.50E-08	1.50E-08	0.06	9.31	Min. error (final result)
3.3	25	0.3	1.50E-09	1.50E-09	0.06	9.48	

* Ratio of transverse to longitudinal dispersivity

** Root mean square error calculated between measured and simulated concentrations at MW's and GWP's

Table 4.6. Results of parameter sensitivity analysis for toluene and phenanthrene

Parameter	Avg. Sensitivity Coefficient	
	Toluene	Phenanthrene
Biodegradation rate (d^{-1})	0.99	0.35
Sorption constant (µg/L)	0.125	0.015
Dispersivity	0.244	0.244*

* Dispersivity was kept constant as that of toluene.

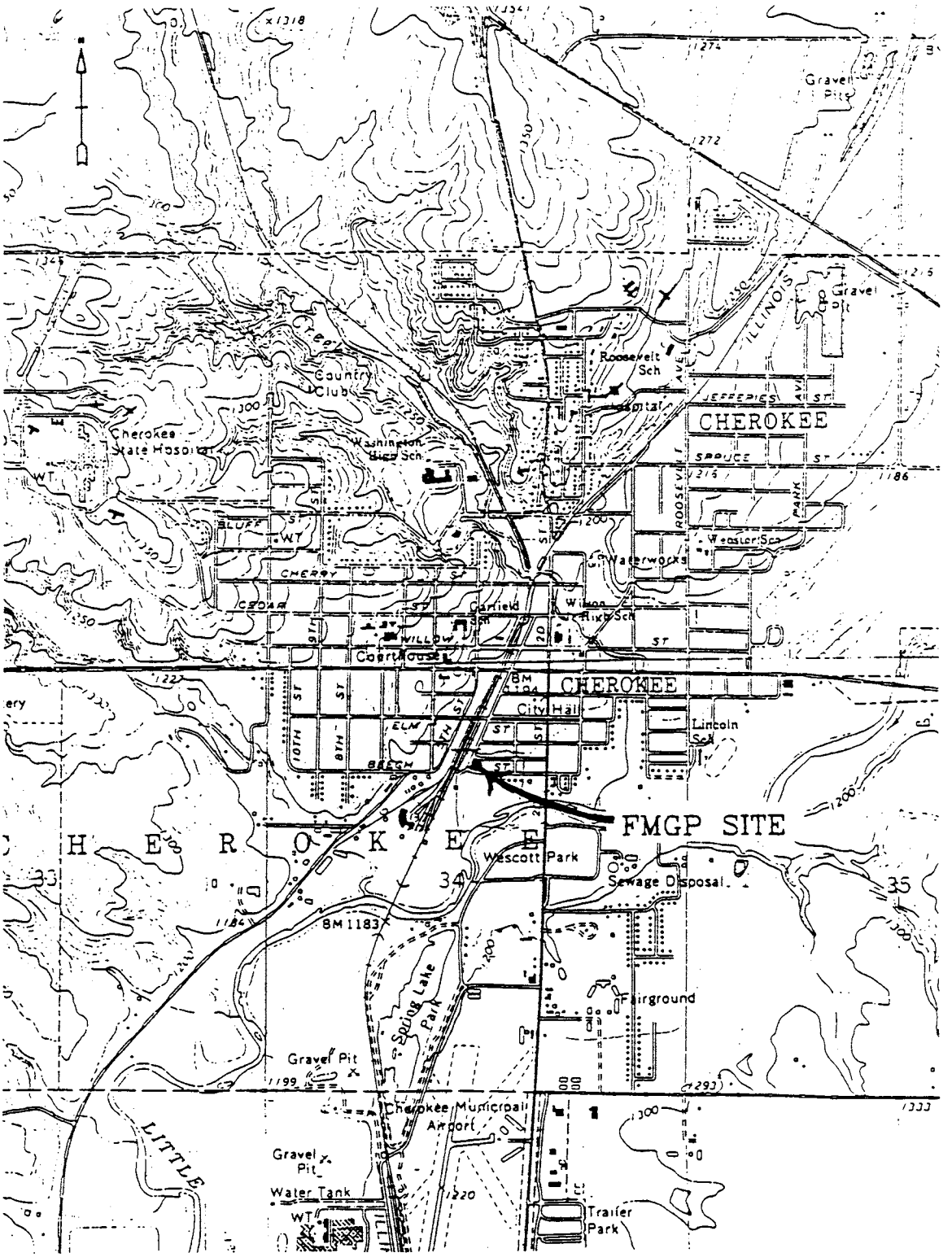

Figure 4.1. Cherokee FMGP site location map

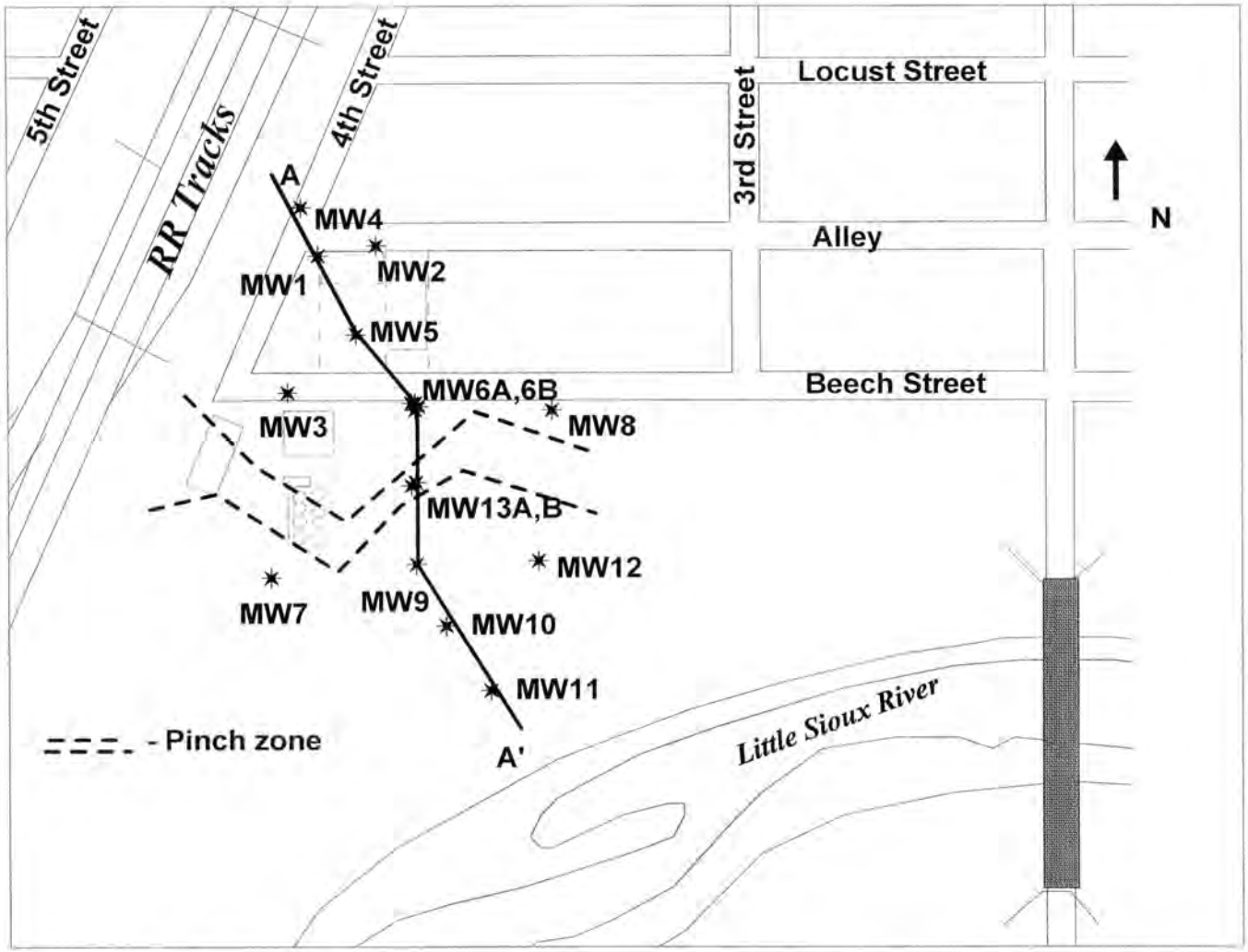

Figure 4.2. Monitoring wells locations and a cross-section at Cherokee FMGP site, Iowa. Pinch zone defined as thickness of less than 3 feet

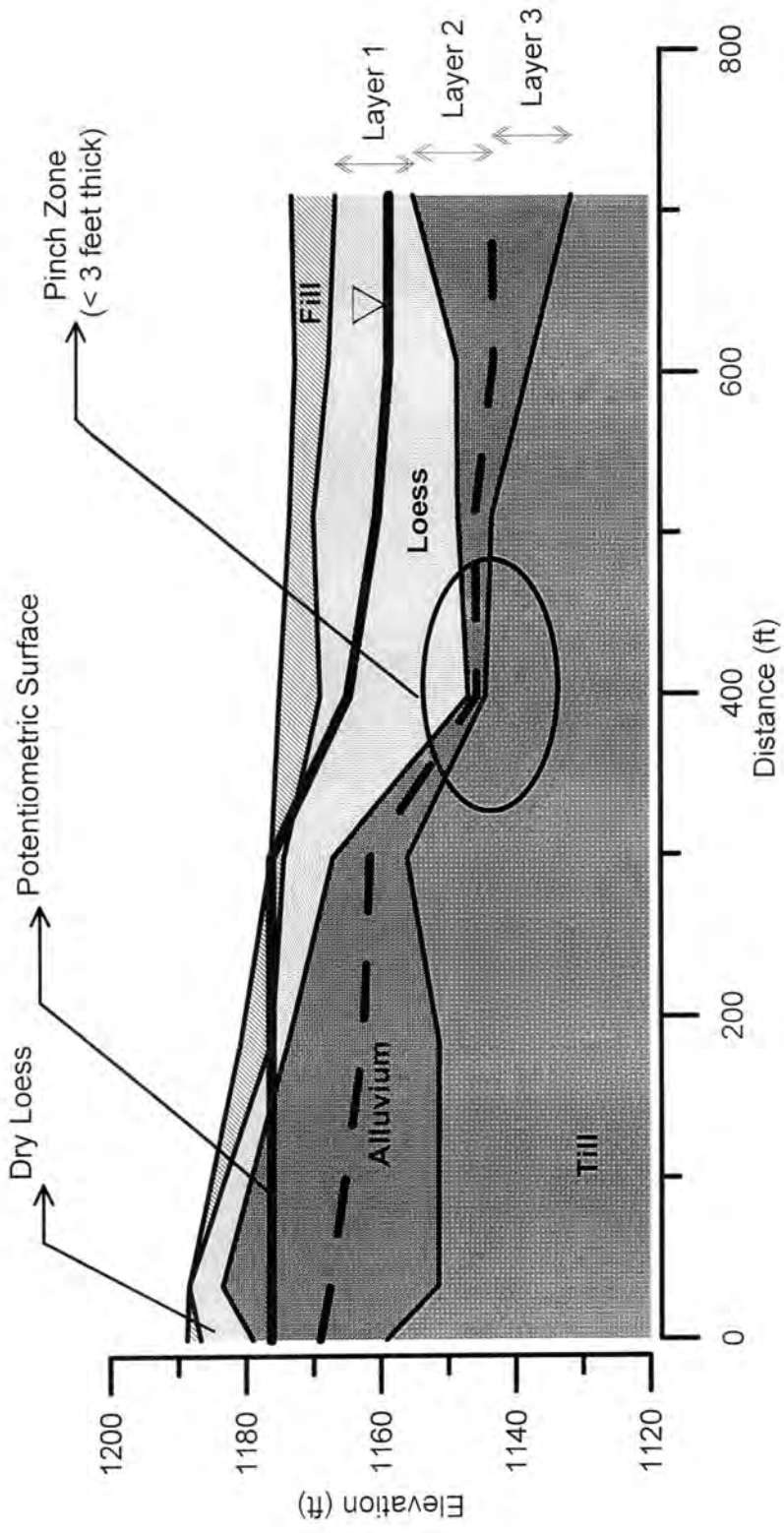

Figure 4.3. Geology at Cherokee FMGP site, Iowa along the transect A-A' and layers used for the modeling efforts (Layer 2 and 3 are of equal depth, dividing the alluvium layer into upper and lower halves)

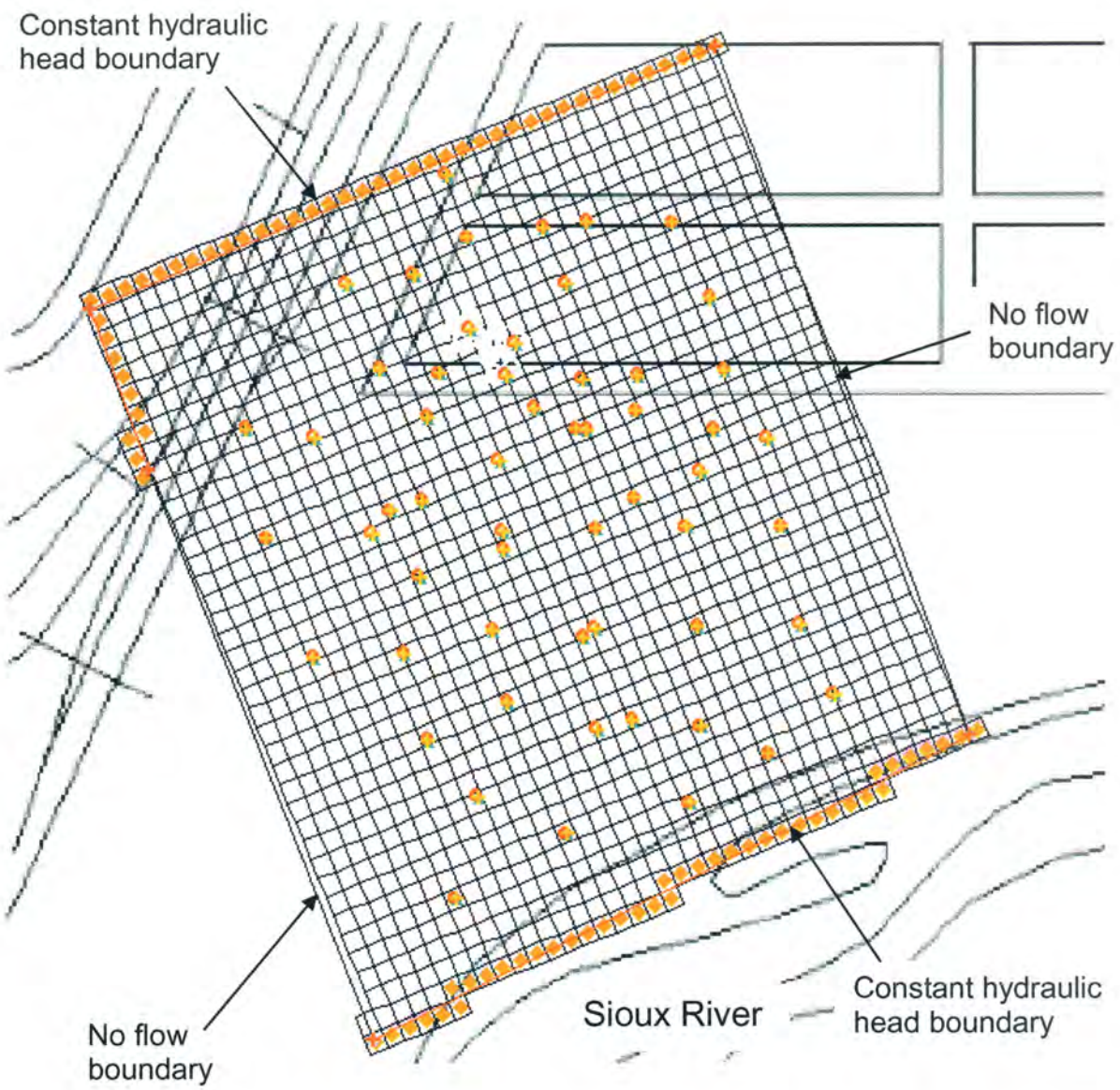

Figure 4.4. Conceptual site model for Cherokee FMGP site, Iowa

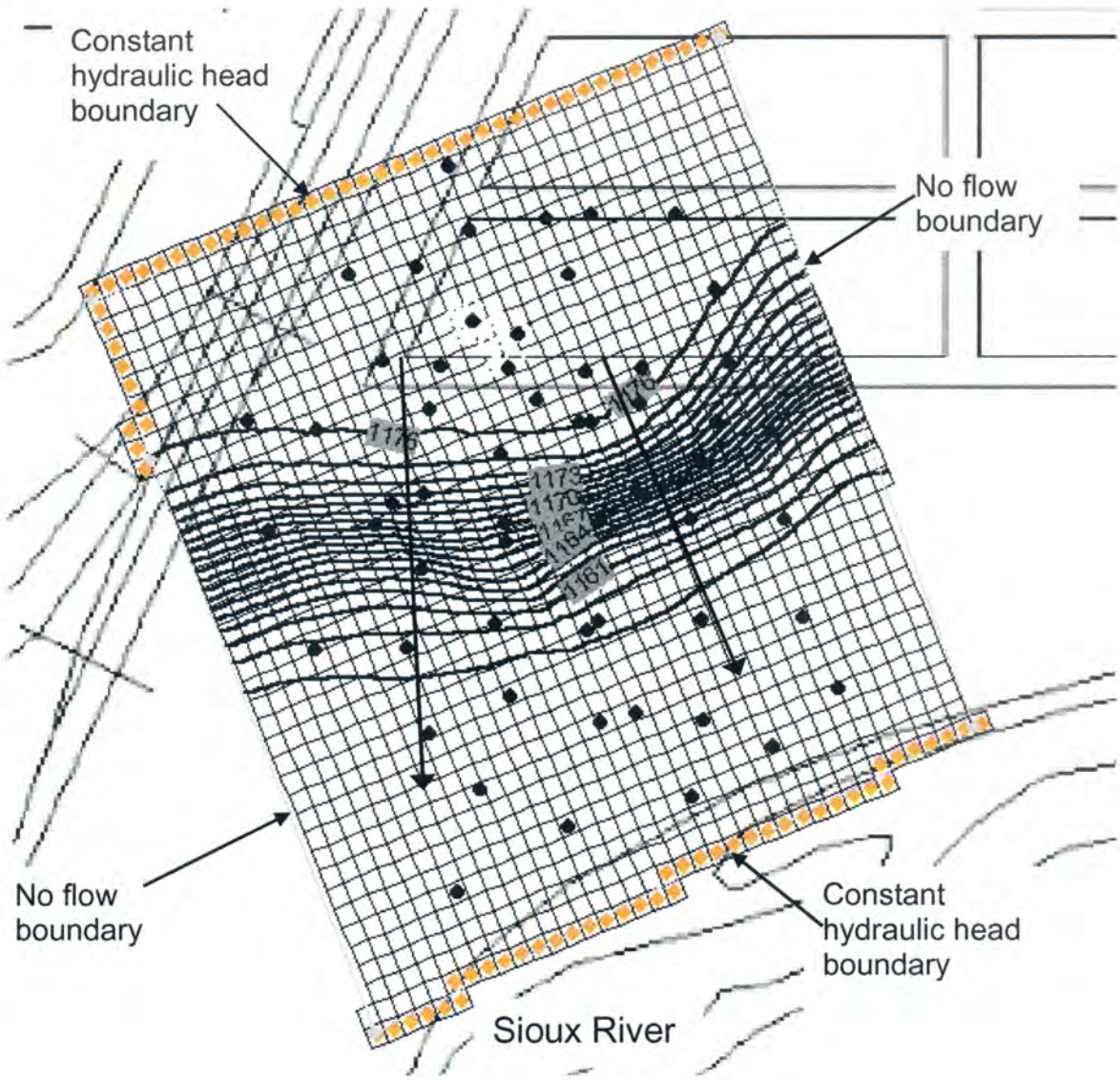

Figure 4.5. Hydraulic heads as simulated by MODFLOW using August 2001 and previous hydraulic head data for Cherokee FMGP site, Iowa

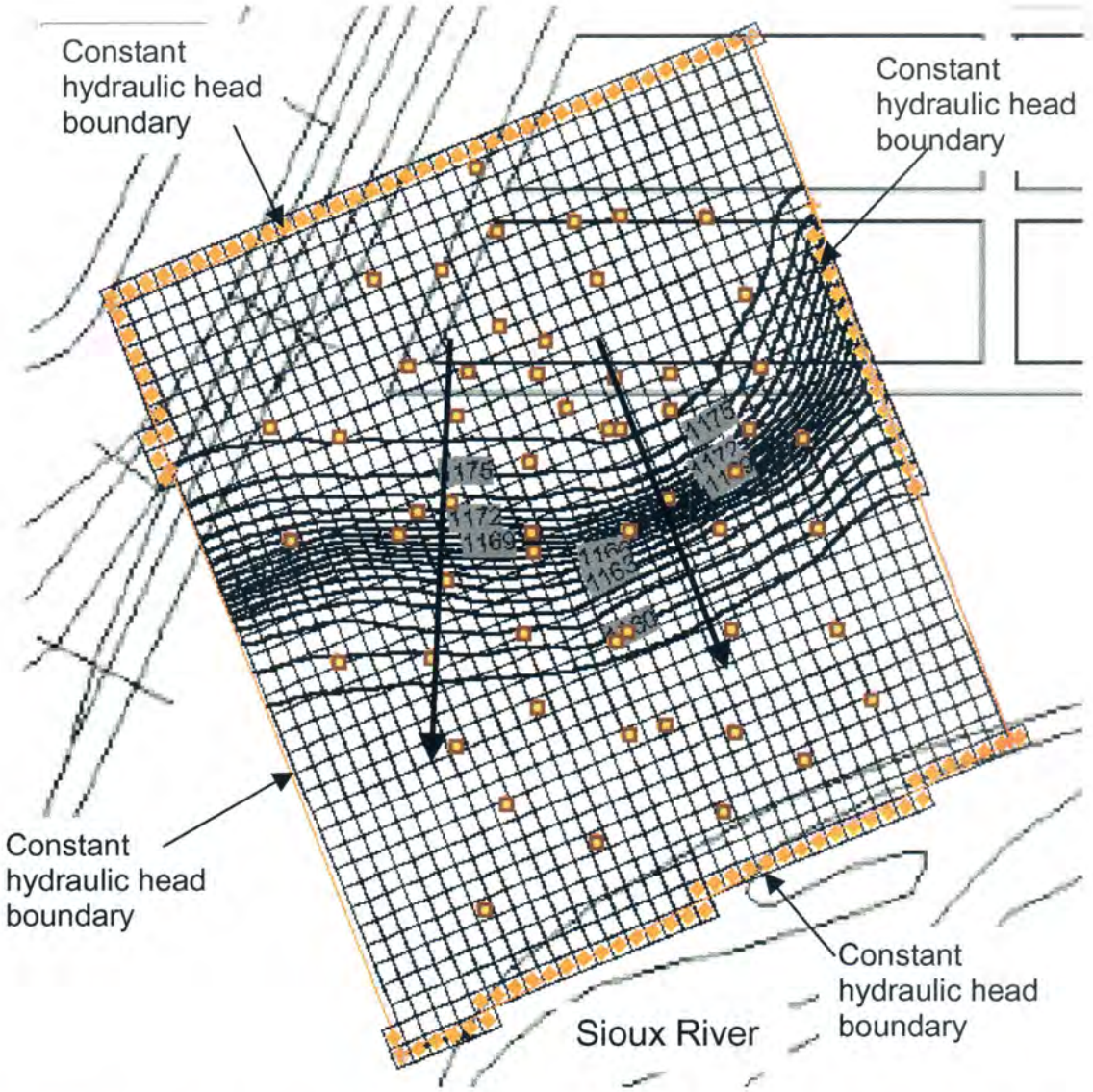

Figure 4.6. Hydraulic heads as simulated by MODFLOW with all boundaries as constant head boundaries

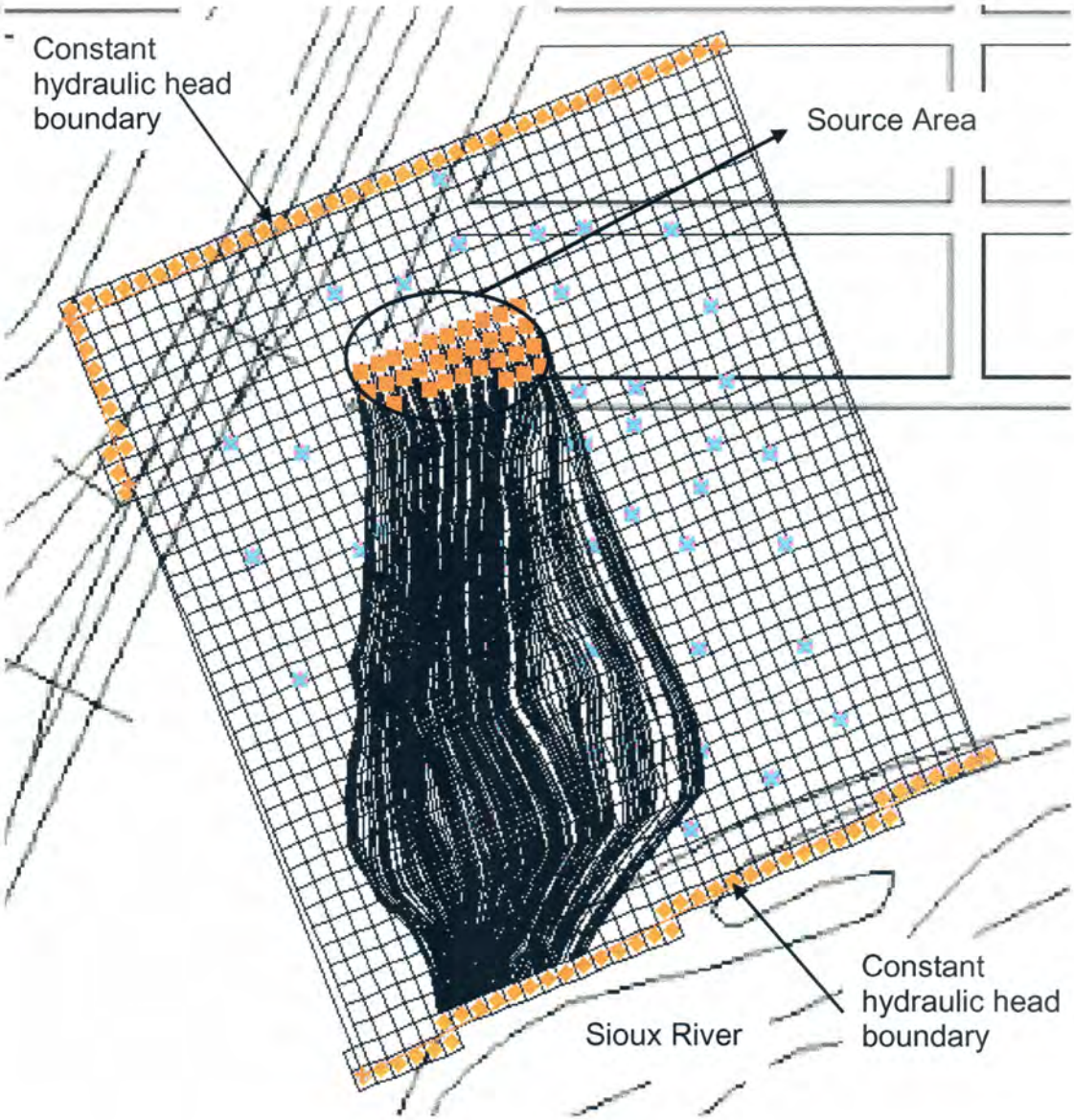

Figure 4.7. Results of tracking of particles releasing from source area by MODPATH under steady state condition

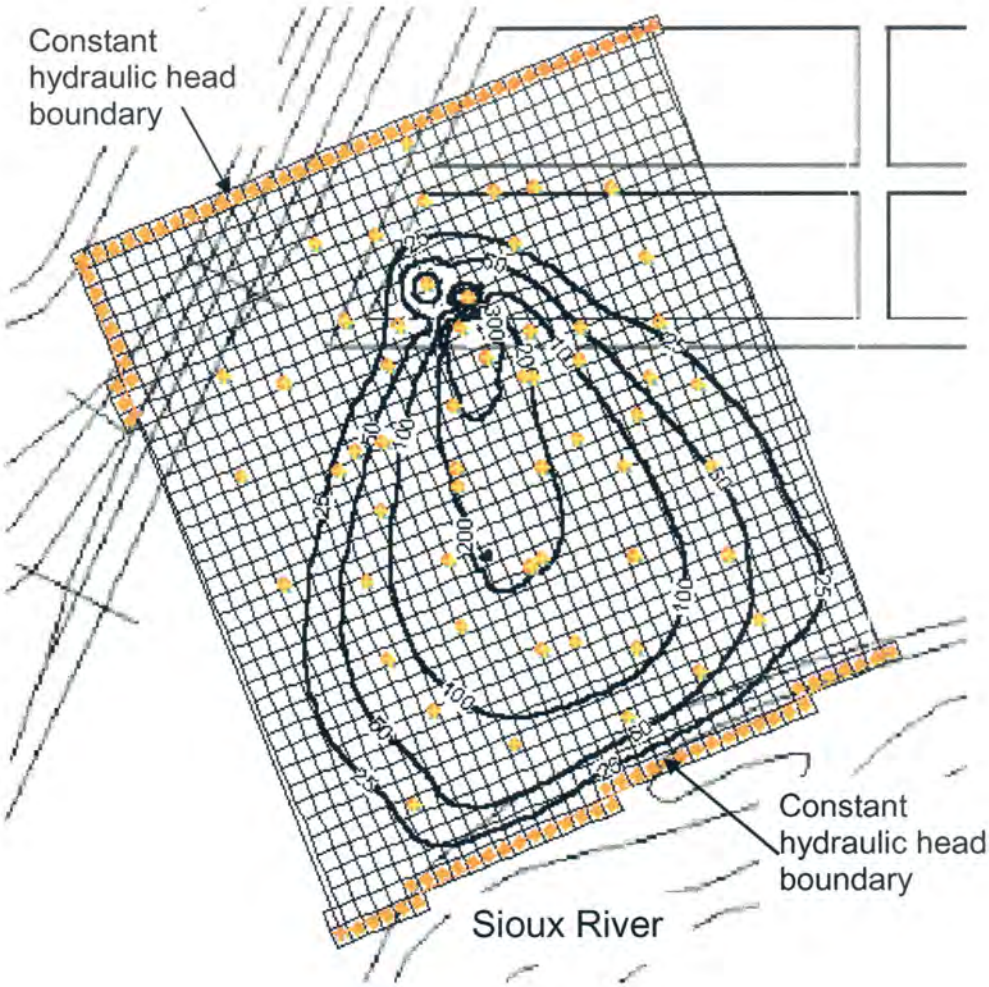

Figure 4.8. Simulated toluene plume in 15 years with advection and dispersion only as natural attenuation processes

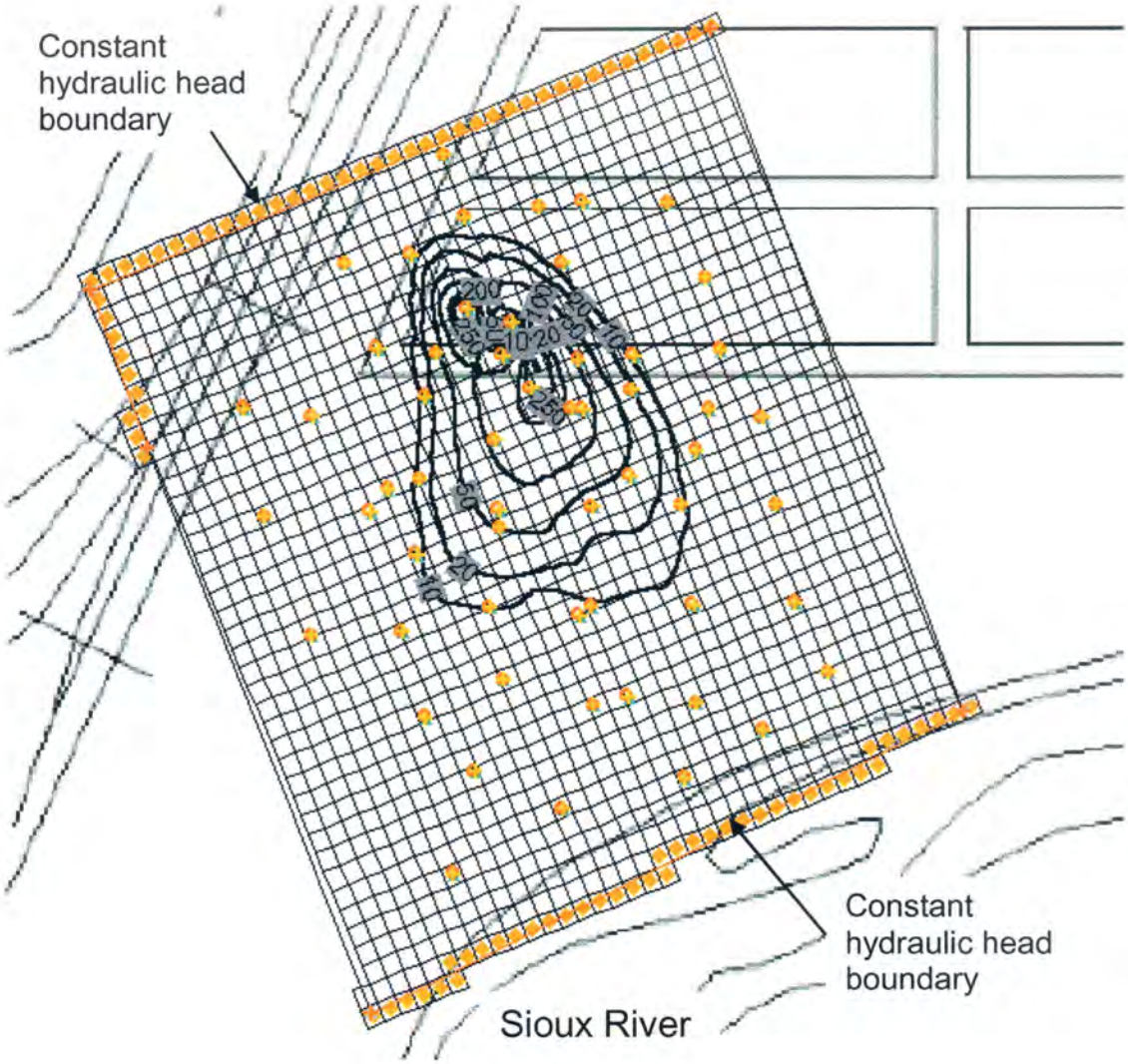

Figure 4.9. Simulated toluene plume with advection, dispersion and sorption as natural attenuation processes

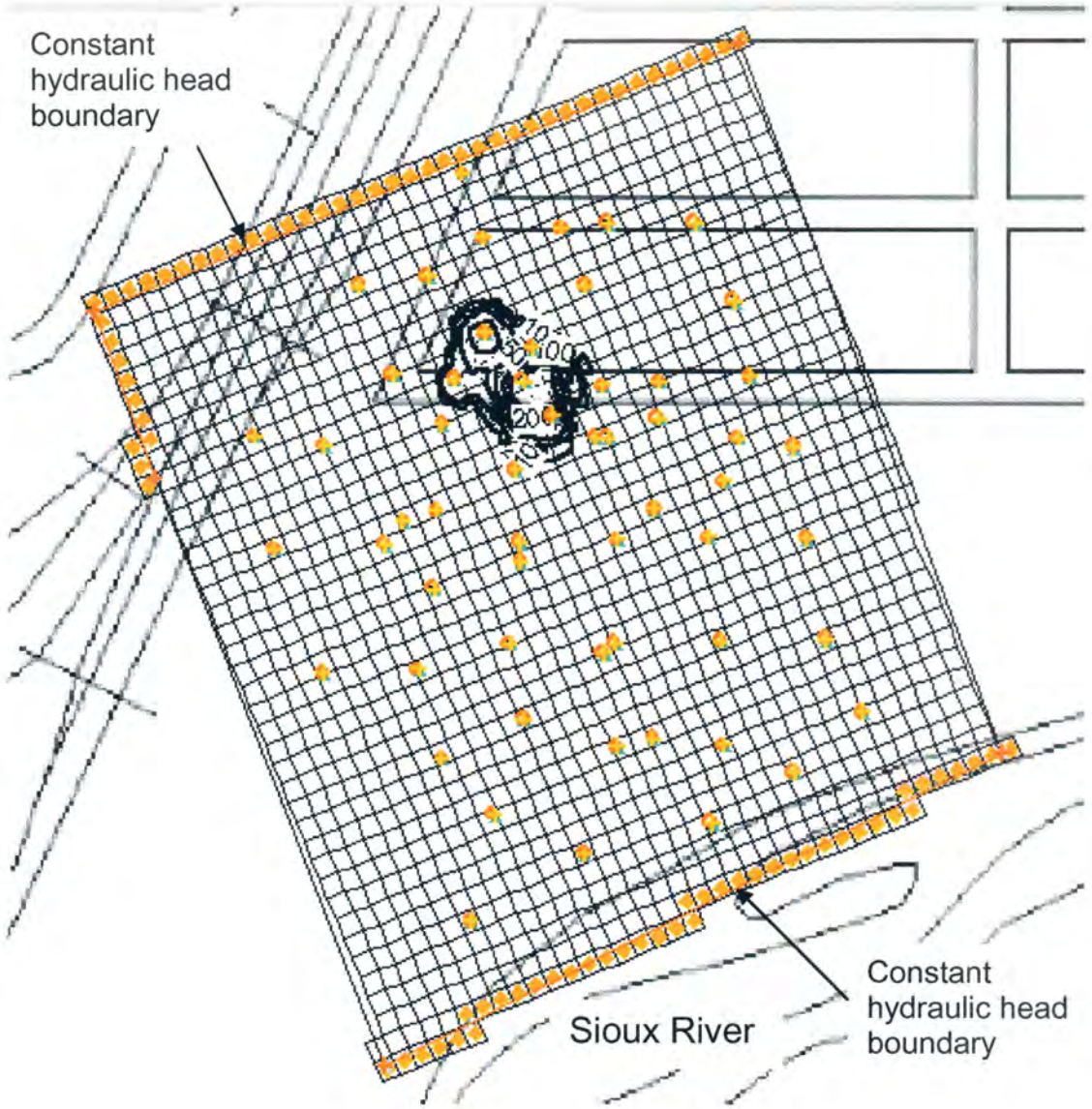

Figure 4.10. Simulated toluene plume with advection, dispersion, sorption and biodegradation as natural attenuation process

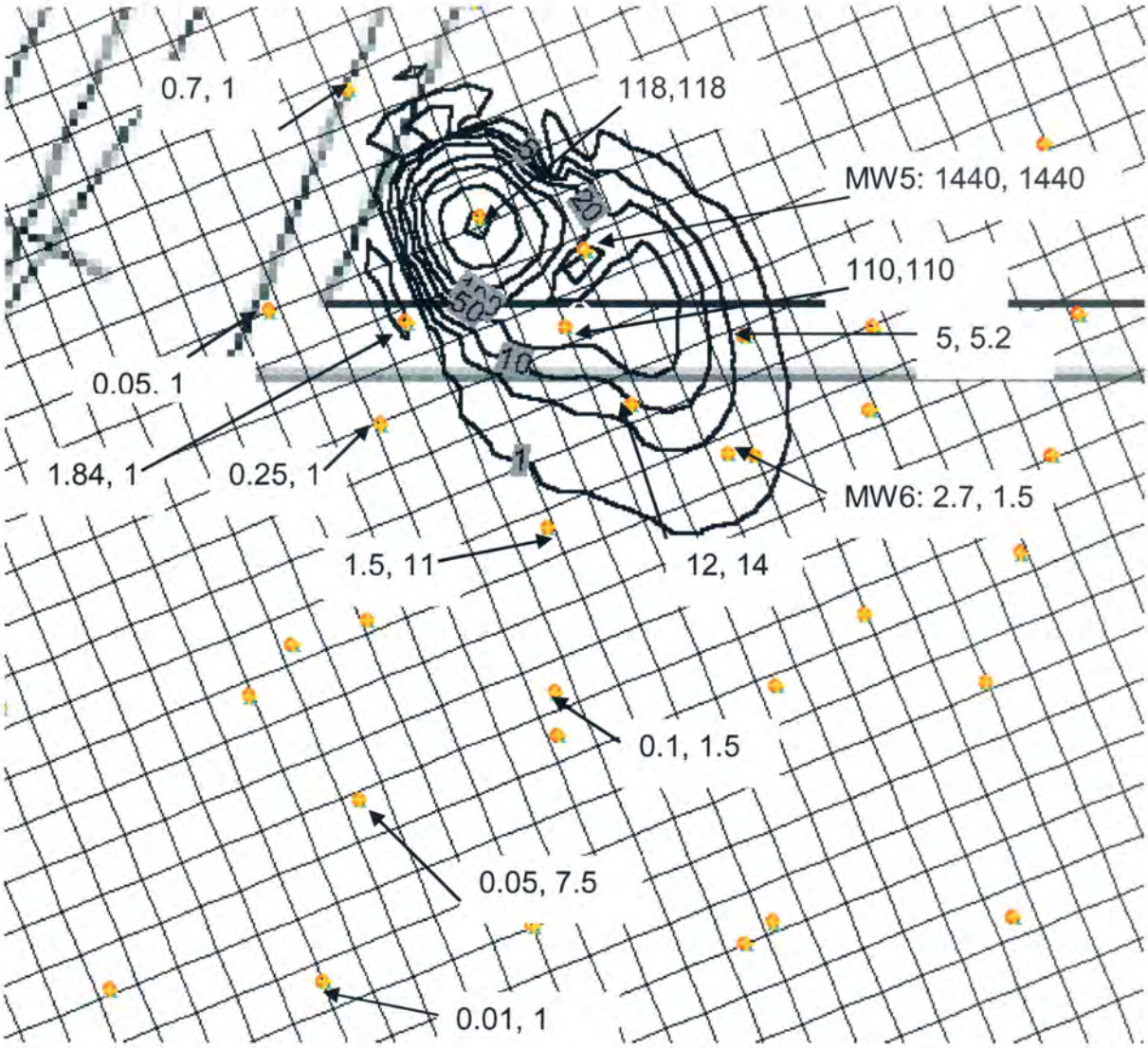

Figure 4.11. Toluene concentrations (simulated and observed) at MW's and groundwater pushes after 65 years in the lower half of the aquifer

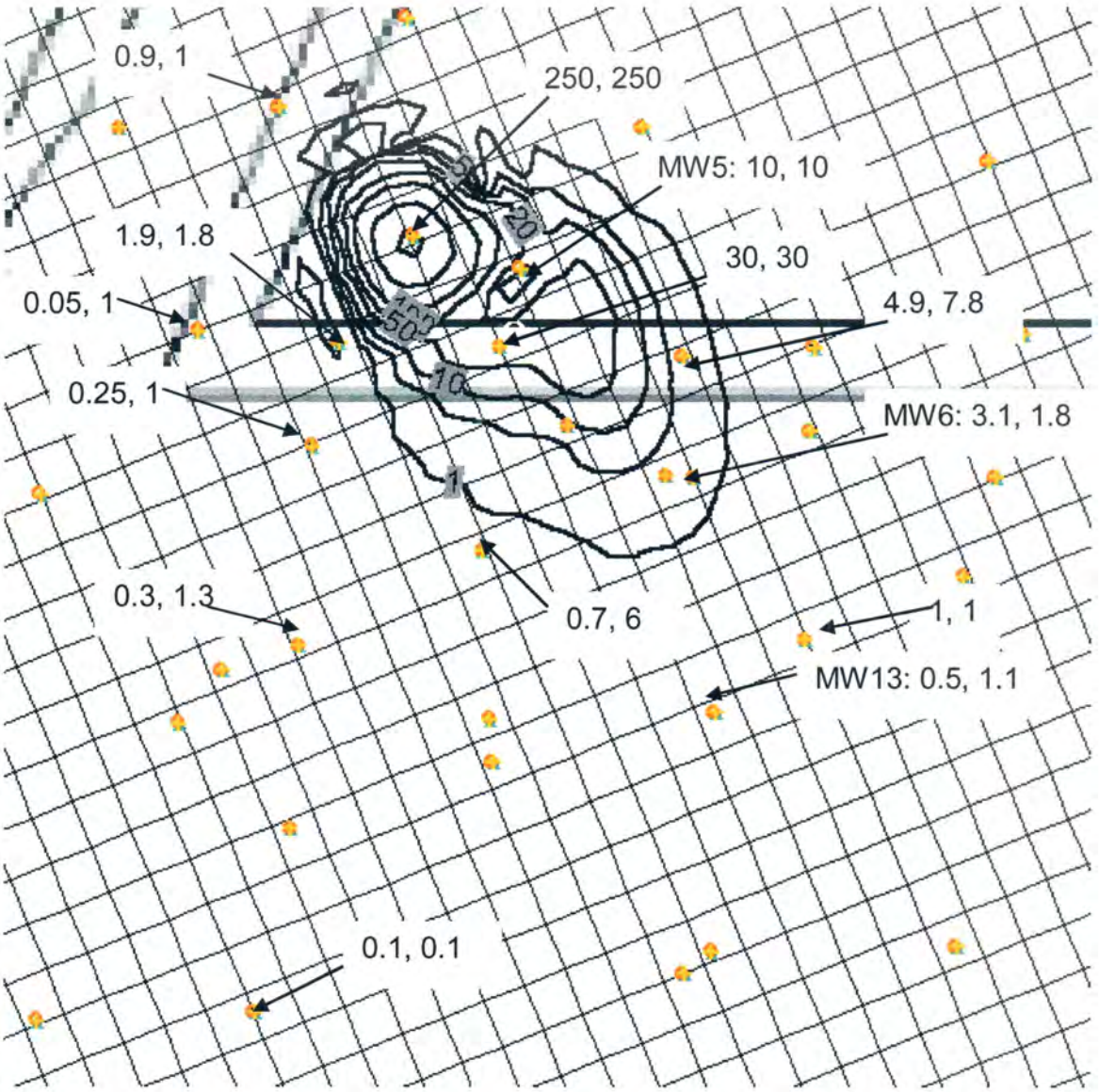

Figure 4.12. Toluene concentrations (Simulated and observed) at MW's and groundwater pushes after 65 years in the upper half of the aquifer

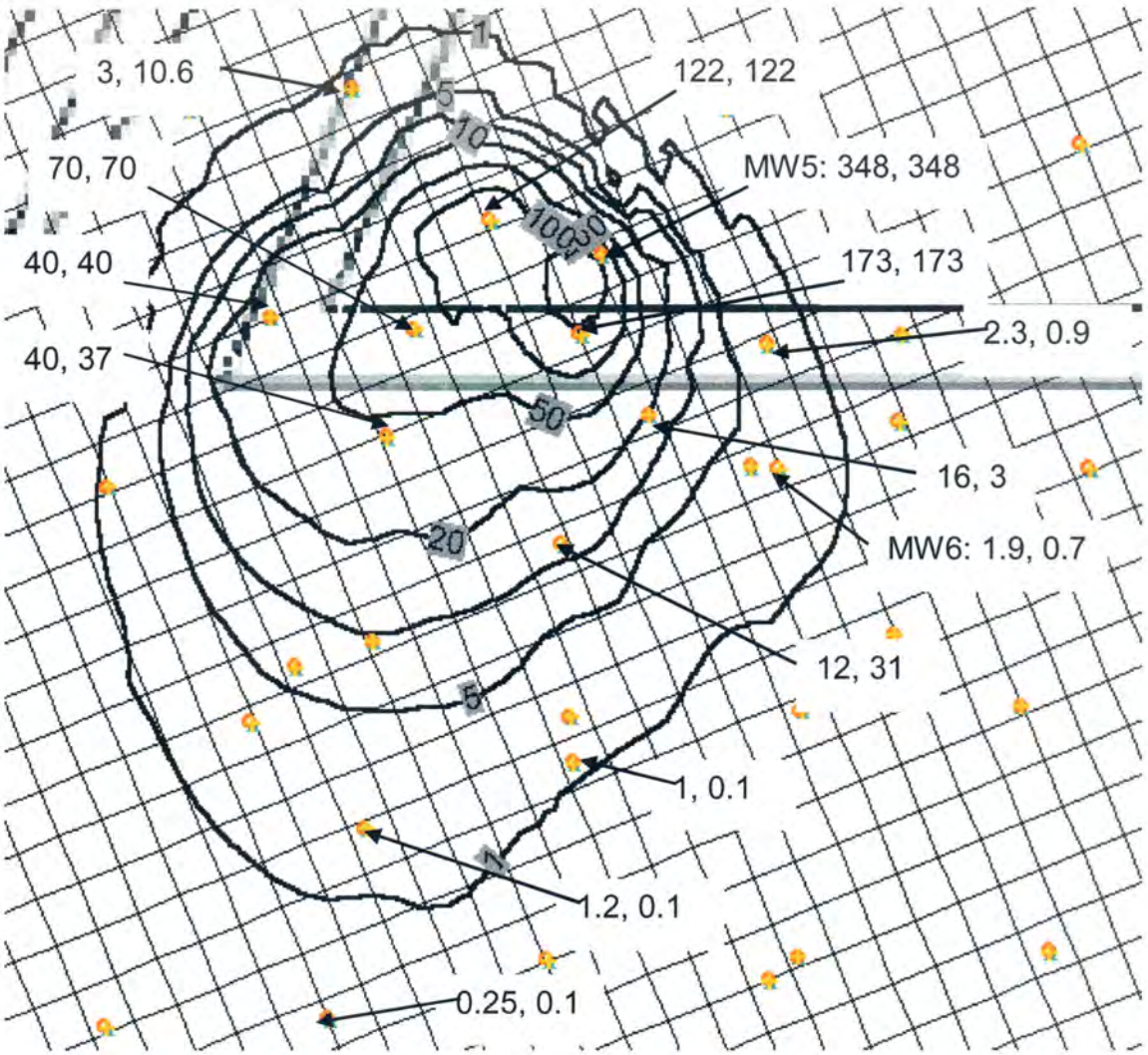

Figure 4.13. Phenanthrene concentrations (simulated and observed) at MW's and groundwater pushes after 65 years in the lower half of the aquifer

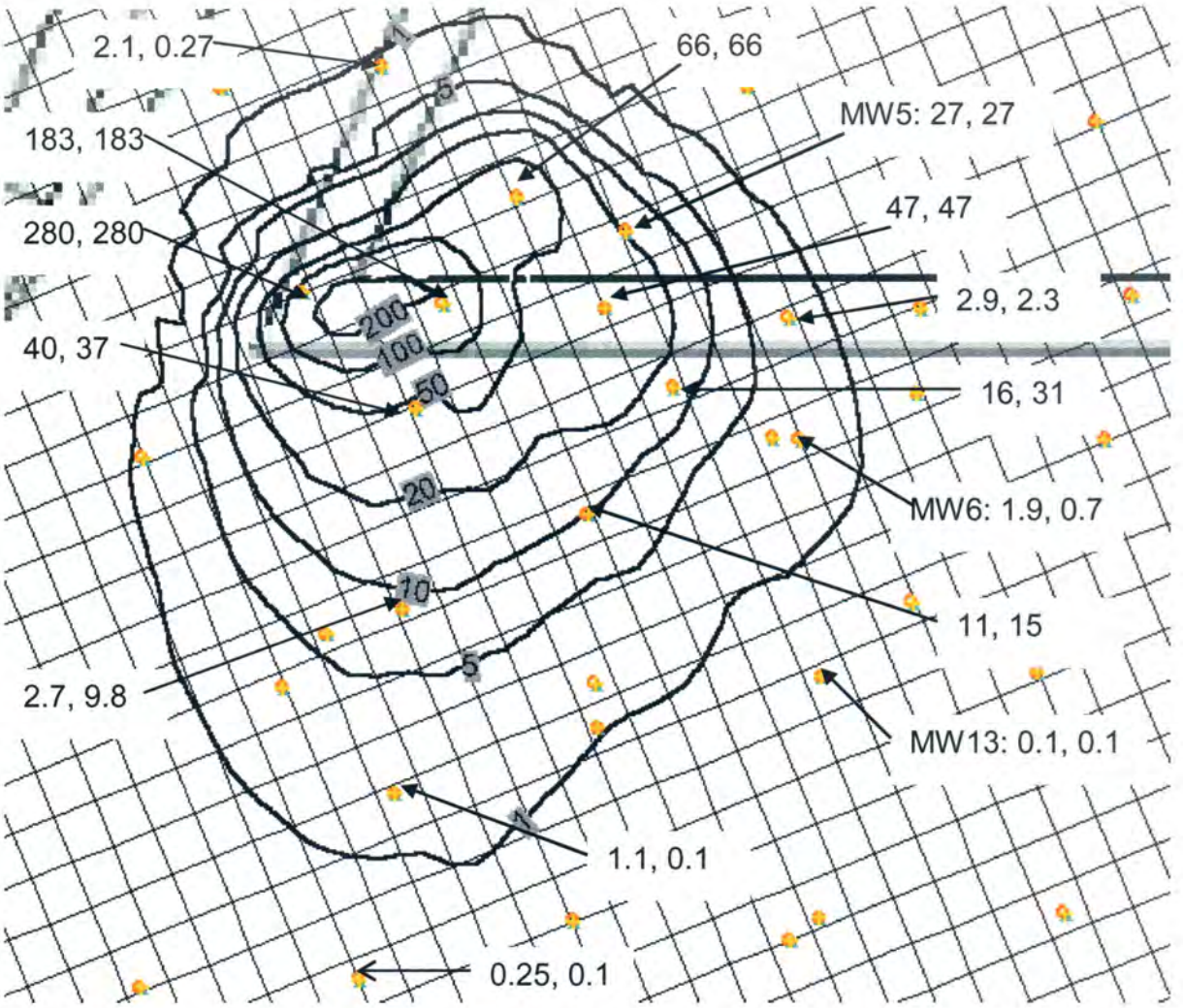

Figure 4.14. Phenanthrene concentrations (simulated and observed) at MW's and groundwater pushes after 65 years in the upper half of the aquifer

4.8. References

Abdulla, F.A., Khatib, M.A., and Ghazzawi, Z.D., 2000. Development of Groundwater Modeling for the Azraq Basin, Jordan. Environmental Geology, 40 (1-2): 11-18.

Black & Veatch, 1994. Remedial Investigation/Feasibility Study Report Cherokee, Iowa. (Dated August 1994). Kansas City, Missouri.

Bredehoeft, J.D., Konikow, L.F., 1993. Groundwater Models: Validate or Invalidate. Groundwater 31(2):1978-1979.

Clement, T.P., 1997. RT3D - A Modular Computer Code for Simulating Reactive Multi-Species Transport in 3-Dimensional Groundwater Aquifers. PNNL-11720. Pacific Northwest National Laboratory, Richland, Washington, DC.

Clement, T.P., Sun, Y., Hooker, B.S., and Petersen, J.N., 1998. Modeling Multi-Species Reactive Transport in Ground Water. Ground Water Monitoring & Remediation, 18(2): 79-92.

Clement, P., Lu, G., Zheng, C., and Weidemeier, T.H., 1999. Natural Attenuation of BTEX Compounds: Model Development and Field-Scale Application. Ground Water, 30(5): 707-717.

EPA, 1997. Use of Monitored Natural Attenuation at Superfund, RCRA Corrective Action, and Underground Storage Tank Sites, OSWER Directive Number: 9200.4-17. United States Environmental Protection Agency, Office of Solid Waste and Emergency Response, Washington DC.

Gelhar, L.W., Welty, C., and Rehfeldt, K.R., 1992. A Critical Review of Data on Field Scale Dispersion in Aquifers. Water Resources Research. 28(7): 1955-1974.

GMS User's Manual, 1997. Boss International, Inc., and Brigham Young University. Engineering Computer Graphics Laboratory, Provo, UT.

Keeley, A.A., Keeley, J.W., Russell, H.H., Sewell, G.W., 2001. Monitored Natural Attenuation of Contaminants in the Subsurface: Applications. Ground Water Monitoring and Remediation 136(2): 136-143.

Konikow, L.F., Bredehoeft, J.D., 1978. Computer Model of Two – Dimensional Solute Transport and Dispersion in Groundwater, TWRI USGS Report I-19.15/5. USGS, Reston, VA.

Landmeyer, J.E., Chapelle, F.H., Petkewick, M.D., and Bradley, P.M., 1998. Assessment of Natural Attenuation of Aromatic Hydrocarbons in Groundwater near a Former Manufactured Gas Plant, South California, USA. Environmental Geology, 34 (4): 279-292.

McElwee, C.D., 1982. Sensitivity Analysis and The Groundwater Inverse Problems, Groundwater 20(6): 723-735.

Miller, R.N., 2001. Assessment of Natural Attenuation at Two Manufactured Gas Plant Sites in Iowa. Master's Thesis, Iowa State University, Ames, IA.

USDA 1989. U.S. Department of Agriculture (USDA), Soil Conservation Service, Soil Survey of Cherokee County, Iowa, July 1989.

Widdowson, M.A., and Brauner, J.S., 2001. Numerical Simulation of a Natural Attenuation Experiment with a Petroleum Hydrocarbon NAPL Source. Ground Water, 39 (6): 939-951.

Wiedemeier, T.H., Wilson, J.T., Kampbell, D.H., Miller, R.N., and Hansen, J.E., 1995. Technical Protocol for Implementing Intrinsic Remediation with Long-Term Montoring for Natural Attenuation of Fuel Contamination Dissolved in Groundwater. Air Force Center for Environmental Excellence, Technology, Transfer Division, San Antonio, TX.

Wiedemeier, T.H., Rifai, H.S., Newell, C.J., and Wilson, J.T., 1999. Natural Attenuation of Fuels and Chlorinated Solvents in the Subsurface. John Wiley & Sons, Inc, New York.

Zhang, Y.K., Seo, B.M., Lovanh, N., Alvarez, P.J.J., and Heathcote, R., 2001. Report on Evaluation of Computer Software Packages for RBCA Tier-3 Analysis, Iowa Comprehensive Petroleum Underground Storage Tank Fund Board, Aon Risk Services, Inc., Des Moines, IA. <http://www.state.ia.us/dnr/organiza/wmad/lqbureau/ust/t3anl.doc>. (Date accessed: May 16, 2002)

Zheng, C., 1990. MT3D: A Modular Three - Dimensional Transport Model for Simulation of Advection, Dispersion and Chemical Reactions of Contaminants in Groundwater Systems. Kerr Environmental Research Laboratory, United States Environmental Protection Agency, Ada, Oklahoma.

Zheng, C., and Bennett, G.D., 1995. Applied Contaminant Transport Modeling, Theory and Practice. Van Nostrand Reinhold, a Division of International Thomson Publishing Inc., New York.

CHAPTER 5 CONCLUSIONS AND RECOMMENDATIONS

5.1 Conclusions

Natural attenuation of PAH and BTEX compounds was investigated at a FMGP site in Cherokee, Iowa. The strategy followed was to first characterize the geology, hydrogeology and contaminant plumes of site and then estimate the attenuation rates for various compounds using analytical and numerical methods. The objectives of this research were to:

1. Develop protocols for the use of Geoprobe direct push technologies to allow adequate development of geological and hydrogeological conceptual site models and optimizing groundwater monitoring for a MNA remedial approach.
2. Compare the capabilities of several publicly available groundwater flow/contaminant transport models (BIOSCREEN, BIOPLUME III and MODFLOW/MODPATH/RT3D) and select the model with the best overall capabilities for assessment of natural attenuation process at FMGP sites.
3. Use the selected model to model the groundwater flow and contaminant transport and to estimate the field-scale biodegradation rates at a specific site. Compare these rates to laboratory-scale biodegradation rates obtained in parallel studies by others or to published results.

The above three objectives were accomplished during the course of this research. The conclusions derived from the study are discussed below.

5.1.1. Site characterization

- Protocols were developed and applied for direct push electrical conductivity probing, groundwater and soil sampling, hydraulic conductivity testing using both pneumatic and slug method, and installation of pre-packed screen monitoring well for groundwater monitoring.
- Electrical conductivity push results matched fairly well with the bore hole geologic data of close-by monitoring wells. Electrical conductivity results showed high level of repeatability.

- Results of electrical conductivity indicated that the overlying loess layer nearly pinches out the underlying alluvium layer at the middle of the site and the pinch runs across the site in east-west direction. The material found in the pinch zone contained more silt and clay and had a hydraulic conductivity that was 3 orders of magnitude lower than the alluvium layer to the north and south of the pinch. Soil and groundwater sampling showed that groundwater flow was strongly affected by the pinch, and the nearly constant water heads found in the upgradient area at the site.
- Hydraulic conductivity at the site was found to vary by three orders of magnitude (0.12 – 400 ft/day) in the alluvium layer. Hydraulic conductivity results from Geoprobe dual push location HC5 (located between MW10 and MW11) matched the high hydraulic conductivity estimated in past for MW10 and MW11, indicating the capability of direct-push equipment to produce comparable results for hydraulic conductivity testing of conventional 2-inch monitoring wells.
- Pre-packed screen monitoring wells gave statistically similar concentrations as that of 2-inch monitoring well. The ease in installation, lower cost, minimal to no waste generation, and results equivalent to that by conventional site characterization techniques makes DPT an efficient method for natural attenuation application.
- The overall attenuation and biodegradation rate constants assuming first-order decay and using analytical solutions varied from 0.0058 d^{-1} - 0.011 d^{-1} and 0.0002 d^{-1} - 0.0022 d^{-1}, respectively, for BTEX and 0.013 d^{-1} - 0.022 d^{-1} and 0.00003 d^{-1} - 0.0003 d^{-1}, respectively, for PAHs (naphthalene, phenanthrene, acenaphthylene, and acenaphthene). Overall attenuation and biodegradation rate constants obtained at Cherokee site are smaller than the published values for these contaminants.
- Plots of contaminant concentrations at monitoring wells with time could not be used for rate constant estimations. However, the plots do show that the contaminant concentrations have decreased from values seen in 1993-1994 for

the eight target analytes indicating that the plume may not be stable, or at steady state.

- Plots of geochemistry supported the natural attenuation process occurring at site. Sulfate, nitrate concentrations in the contaminant plumes showed decrease in concentration from the background values while total iron concentration increased from background value, indicating denitrification, sulfate reduction, and iron reduction conditions prevailing at the site.

5.1.2. Groundwater flow and transport model comparison

- BIOSCREEN, BIOPLUME III (version 1.0) and MODFLOW/MODPATH/RT3D (GMS) were evaluated with respect to their capabilities to model the site geology and hydrogeology, stability of predicted hydraulic heads and concentrations, assumption, limitations and manner of application.
- BIOSCREEN cannot model sites with pumping wells, recharge, and vertical flow gradient. It assumes the aquifer to be isotropic, homogeneous and that sorption is linear and reversible. BIOSCREEN is intended more for simulating transport and biodegradation of petroleum compounds and not for sites with commingled contaminants.
- In BIOPLUME III (version 1.0), depth-averaged two-dimensional transport is assumed, bacterial growth is neglected and only hydrocarbon kinetics is considered in a heterogeneous and isotropic aquifer. Apart from these limitations and assumptions, various errors associated with the stability and application of the model were found such as inconsistent modeling results with identical input files, negative concentration results for contaminants indicating no zero concentration boundary condition for the contaminants, detachment of contaminant plume from the constant source, and over-prediction of contaminant migration in comparison to analytical model.
- RT3D coupled with MODFLOW was found to provide a better model than BIOPLUME III (version 1.0) and BIOSCREEN for groundwater flow and fate and transport of contaminants due to its 3-D modeling capability in a heterogeneous

and anisotropic aquifer with complex boundaries. In addition, it handles the microbial metabolism, its transport kinetics and provides consistent results for hydraulic heads and contaminant concentrations. RT3D can simulate instantaneous reaction, sequential electron donor-acceptor reactions, rate limited sorption reaction, and double Monod model and user definable reactions.

5.1.3. Groundwater flow and fate and transport of contaminants

- MODFLOW, MODPATH, and RT3D were used for groundwater flow modeling, tracking of particles emanating from the assumed source area, and transport study of: toluene and phenanthrene.
- The results of calibrated hydraulic heads using MODFLOW matched fairly well the observed hydraulic heads at the site (RMS error = 0.63). To account for the drop of 12.9-ft in the hydraulic heads between MW6 and MW8 it was assumed that the pinch is running between the two monitoring wells.
- Results of MODPATH showed the movement of particles in the south-southeast direction.
- While calibrating the simulated plume concentrations by RT3D against the observed concentrations, high RMS errors were found for all the contaminants except toluene.
- High concentrations observed around GWP13A and 13B and in some of the immediate downgradient groundwater probes indicated incomplete information on source extent and concentration.
- The transport modeling of phenanthrene when attempted by extending the source to the west of assumed source area gave low RMS error results. This indicated the possibility of contaminant source existing around GWP 22 and MW3.
- First-order biodegradation rate estimated for toluene and phenanthrene using modeling technique were 0.03 d^{-1} and 0.006 d^{-1}, respectively. The rates lie in the published range for the respective compounds but an order of magnitude higher than that calculated by Buscheck/Alcantar method.

- Result of the sensitivity analysis showed that biodegradation rate was the most critical input parameter in controlling the simulated concentrations and RMS error.

5.2. Recommendations for future work

Results of groundwater flow and contaminant transport modeling and site characterization were useful in providing evidence for natural attenuation and information on the presence of a pinch zone in the alluvium aquifer and possible extent of source area. However, there are data gaps that need to be filled. The true extent of the pinch zone, hydraulic heads and hydraulic conductivity at few more locations are needed. Extents and concentrations of both primary and potential secondary sources also need to be characterized. Higher concentrations observed in some of the downgradient wells and groundwater sampling locations than in the immediate upgradient water sampling locations are also of concern. That could be due to sample variability, as differences in concentrations were observed in the duplicate groundwater samples from same sampling depth at almost every location during August 2001 site characterization activity. Quarterly sampling of duplicate samples of groundwater is recommended to reduce the uncertainty in trends of contaminant concentrations with time and distance. This will also help in analyzing the stability of the contaminant plume as most of the statistical tests such as Mann-Whitney U test or Mann-Kendell test require at least eight consecutive contaminant concentration data. Required locations for EC, soil and groundwater pushes, pre-packed monitoring wells and hydraulic conductivity testing are presented in Figures E1 – E5. Once the source has been defined and the reason of high hydraulic head difference between MW6 and MW8 is determined, results of groundwater modeling should be re-assessed and transport modeling for remaining target analytes should be conducted. Also, more river elevation data is needed to provide more correct constant head boundary in the south.

APPENDIX A: BIOPLUME III (VERSION 1.0)

A1. BIOPLUME III (version 1.0), A REASONABLE SIMULATOR FOR NATURAL ATTENUATION?

A paper to be submitted to Journal of Groundwater Monitoring and Remediation

Rahul Biyani[1], Shane Rogers[1], Bruce Kjartanson[2], Say Kee Ong[2],

Abstract

The two-dimensional finite-difference natural attenuation simulator BIOPLUME III (version 1.0) was evaluated for reliability and consistency in predicting the fate and transport of organic contaminants in the study cases presented in the accompanying user manual. The study cases evaluated included both constant source and no-source non-attenuated hydrocarbon mass transport. Duplicate data files on two computers as well as data files generated by two independent users following the BIOPLUME III (version 1.0) user's manual tutorial were compared. Duplicate data files yielded results that were up to 35% and 50% different in contaminant concentrations in selected cells when simulated on two different computers for the cases of constant source and no-source, respectively. For the constant source case, BIOPLUME III (version 1.0) failed to preserve the source material through the entire simulation, resulting in the simulated detachment of a weak plume from the defined source material. When compared to an analytical solution, BIOPLUME III (version 1.0) grossly mis-predicted contaminant transport in the case of a constant source. Based on the results of this brief study, BIOPLUME III (version 1.0) should be re-evaluated for its efficacy and reliability in predicting natural attenuation of contaminants at contaminated sites.

A.1. Introduction

Natural attenuation is a non-evasive, non-destructive in-situ technique to reduce the concentration and mass of contaminants in the subsurface environment.

[1] Graduate Student, Department of Civil & Construction Engineering, Iowa State University, Ames, IA.
[2] Associate professor, Department of Civil & Construction Engineering, Iowa State University, Ames, IA.

It has become the most widely used remediation alternative at sites contaminated with petroleum hydrocarbons. Crucial to investigating natural attenuation as a remedial alternative is the ability to predict its efficacy over a reasonable time frame. A variety of models are available to predict the fate and transport of contaminants during natural attenuation, of which the most commonly used are BIOSCREEN, BIOPLUME III (version 1.0), and MT3D/RT3D.

BIOPLUME III (version 1.0) is a 2-D model for simulating natural attenuation of organic contaminants in groundwater due to advection, dispersion, sorption, and biodegradation. It is the result of a joint effort between the U.S. EPA and the U.S. Air Force to compile a natural attenuation simulator with a simple graphical user interface (GUI). The simple GUI is an attractive alternative to more complex models such as MT3D/RT3D, and since it can be downloaded from the U.S. EPA for free, its use as a learning tool in educational institutions and as a regulatory tool supporting site closure has increased in the past few years.

In attempting to use BIOPLUME III (version 1.0) to model contaminated sites, we have encountered several difficulties. We have reviewed the model based on the sample problems published in the accompanying manual (Rifai et al., 1998). In this article, we present the major inconsistencies, limitations, and flaws in the program we have encountered.

A.2. Methods

BIOPLUME III (version 1.0) was evaluated for the case of non-attenuated hydrocarbon mass transport with no source and a constant source as outlined by the tutorial in the user's manual. The evaluation of consistency was performed in two ways:

1. Two different users on two different computers (Pentium II – 350 MHz and Pentium I – 256 MHz) followed the tutorial separately and their simulations were compared –identified as Case 1.
2. The same input file was input into BIOPLUME III on the two different computers and the simulation output compared – identified as Case 2.

In Case 1, all input parameters were identical for both users, however slightly different x, y coordinates for the definition of the piezometric surface (isopleths), log points, boundaries, contaminant plume, and source area were input to the program. The x, y coordinates were slightly different, as the manual does not specify the exact locations for log points. Users tried to map the locations shown in Figure 3.2 on page 51 of the manual. For the second case, all factors were identical. Finally, the prediction from the BIOPLUME III (version 1.0) was compared to that of BIOSCREEN (Newell et al., 1996) (Developed for Air Force Center for Environmental Excellence (AFCEE) Technology Transfer Division, Brooks Air Force Base, Houston, Texas), a 3-D analytical solution to the transport equation for the same tutorial case.

A.3. Results

The BIOPLUME III (version 1.0) software is supplemented with a step-by-step manual that makes learning the model easy. It is a user-friendly program with a simple interface. However, the data input could be better if the program offered importing capabilities to define aquifer thickness, piezometric surface, contaminant plumes, or contaminant sources from well boring or sampling data. Although exporting data to spreadsheet programs is simple, the program offers no internal ability to compare field data to simulated data. The program also has a limit to which the grid network can be tightened (manual page no. 218). The manual suggests rewriting and recompiling the code to increase the grid size, if a tighter network is desired. There were some specific problems found in hydro-geologic model and contaminant model with constant source and no source.

A.3.1. Hydro-geologic Model

The initial piezometric surface as predicted by the kriging program in BIOPLUME III (version 1.0) was not stable. After defining the aquifer thickness, properties, and starting hydraulic heads, the ground water surface predicted upon kriging in the Case 2 had unwarranted dips and mounds in the hydraulic heads (Figure 1). Re-kriging the data seemed to supply more reasonable results.

Following simulation, the heads remained constant at the constant head boundaries, as expected. However, for the remaining cells, simulated hydraulic heads did not remain steady over time as suggested in the manual, indicating that the original hydraulic heads given in the example problem were not steady-state conditions for the site or the actual aquifer is not homogenous. Model results were consistent for the two users in Case 2 and were within approximately 1% of Case 1.

A.3.2. Contaminant Model – No Source

Tracking a contaminant plume over time without a source material present in the model resulted in a concentration profile that was different from that shown in page 64 of the manual. In fact, in Case 2, the users' plumes did not match either. For instance, the concentrations in the same grid element were nearly 150% higher for one user, as shown in Figure 2. Both users had negative concentrations down-gradient of the source, indicating there may be a lack of a lower bound to the concentration values. As with Case 2, results were different in the Case 1.

A.3.3. Contaminant Model - Constant Source

When the transport process was modeled using a constant source, the source was found to deplete with time for both Case 1 and 2(see Figure 3). Furthermore, the contaminant plumes predicted by the model were detached from the source in all cases, contrary to the results shown in the page 66 of the manual. It should be noted that the manual shows a source definition on page 66 that is larger than that requested in the text on page 65. Assuming this may be the reason for the differences, the source was redefined to the larger size, as shown in the manual. The plume was still detached from the source with the source depleting. As with the no-source contaminant case and with identical input files, we observed differences in predicted concentration values (up to 35%) and negative concentrations in grids downgradient of the source (up to 12 µg/L). The instability of the program was further observed when small changes in the source shape and size resulted in drastically different predictions of contaminant migration. By changing

the source to a rectangular shape instead of an oval shape given in the manual, the results still show source depletion with the reduction of width of the source.

A.3.4. Comparison with BIOSCREEN

Due to the problems associated with modeling a constant source in BIOPLUME III (version 1.0), the model was compared to an analytical solution to evaluate its performance. Using BIOSCREEN, a 3-D analytical solution, and the same parameters used in BIOPLUME III (version 1.0), an entirely different solution was realized (see Figure 4). BIOSCREEN, unlike BIOPLUME III (version 1.0), maintained the constant source and showed a consistent exponential depletion of the plume with distance, as expected. Furthermore, the total migration of the contaminant plume solved analytically by BIOSCREEN was much less than that of BIOPLUME III (version 1.0), suggesting problems in both the source definition and contaminant transport models of BIOPLUME III (version 1.0).

A.4. Conclusion

In summary, it was found that there may be errors associated with the use of BIOPLUME III (version 1.0) for modeling contaminant plumes at contaminated sites. Specifically, there were four primary errors associated with the program. First, BIOPLUME III (version 1.0) does not consistently model contaminant plumes, even when the input files are identical. Second, negative concentrations were obtained indicating that there was no zero concentration boundary condition for the contaminants across the site. Third, the model does not maintain the source as constant over time, resulting in errors in plume migration predictions primarily due to detachment from the source. Finally, in comparison to an analytical solution, the model seems to over-predict contaminant migration, resulting in contaminant plumes that stretch four times the distance predicted by the analytical model over a ten-year period in the BIOPLUME III manual's constant-source example. The errors associated with this model may call into question its stability and utility for making risk-based or regulatory decisions which may require consistent demonstration at different stations and confidence in the results.

A.5. References

Rifai, H.S., Newell, C.J., Gonzales, J.R, Dendrou, B., Dendrou, S., Kennedy, L., and Wilson, J.T., (1998). BIOPLUME III Natural Attenuation Decision Support System User's Manual Version 1.0 OSWER EPA/600/R-98/010. United States Environmental Protection Agency, Washington D.C.

Newell, C.J., McLeod, K.R., and Gonzales, J.R., 1996. BIOSCREEN Natural Attenuation Decision Support System User's Manual Version 1.3, June 1996. Air Force Center for Environmental Excellence Technology Transfer Division, Brooks Air Force Base, San Antonio, Texas.

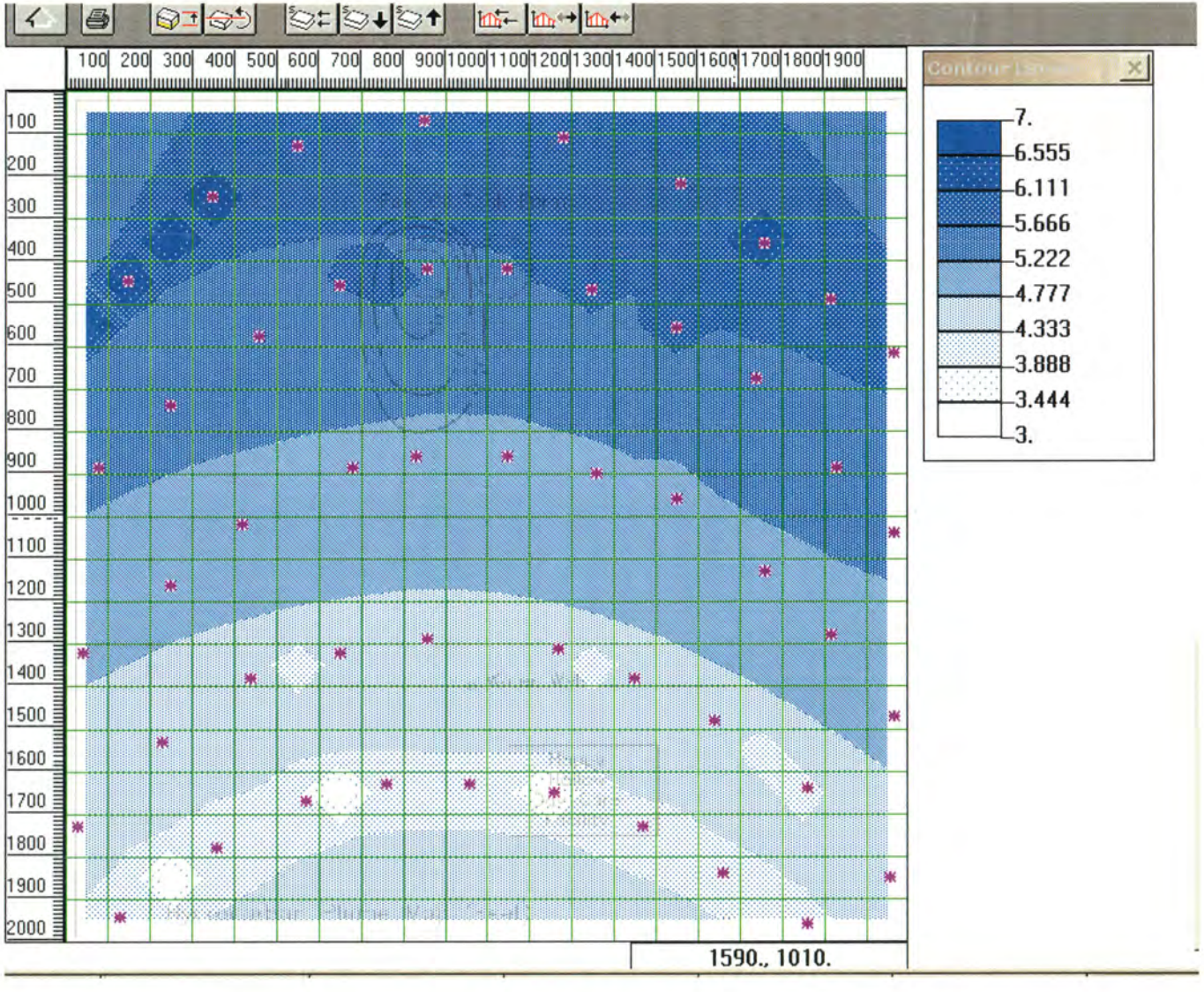

Figure A1. Dips and mounds observed in the hydraulic heads by both users following the manual (Case 2)

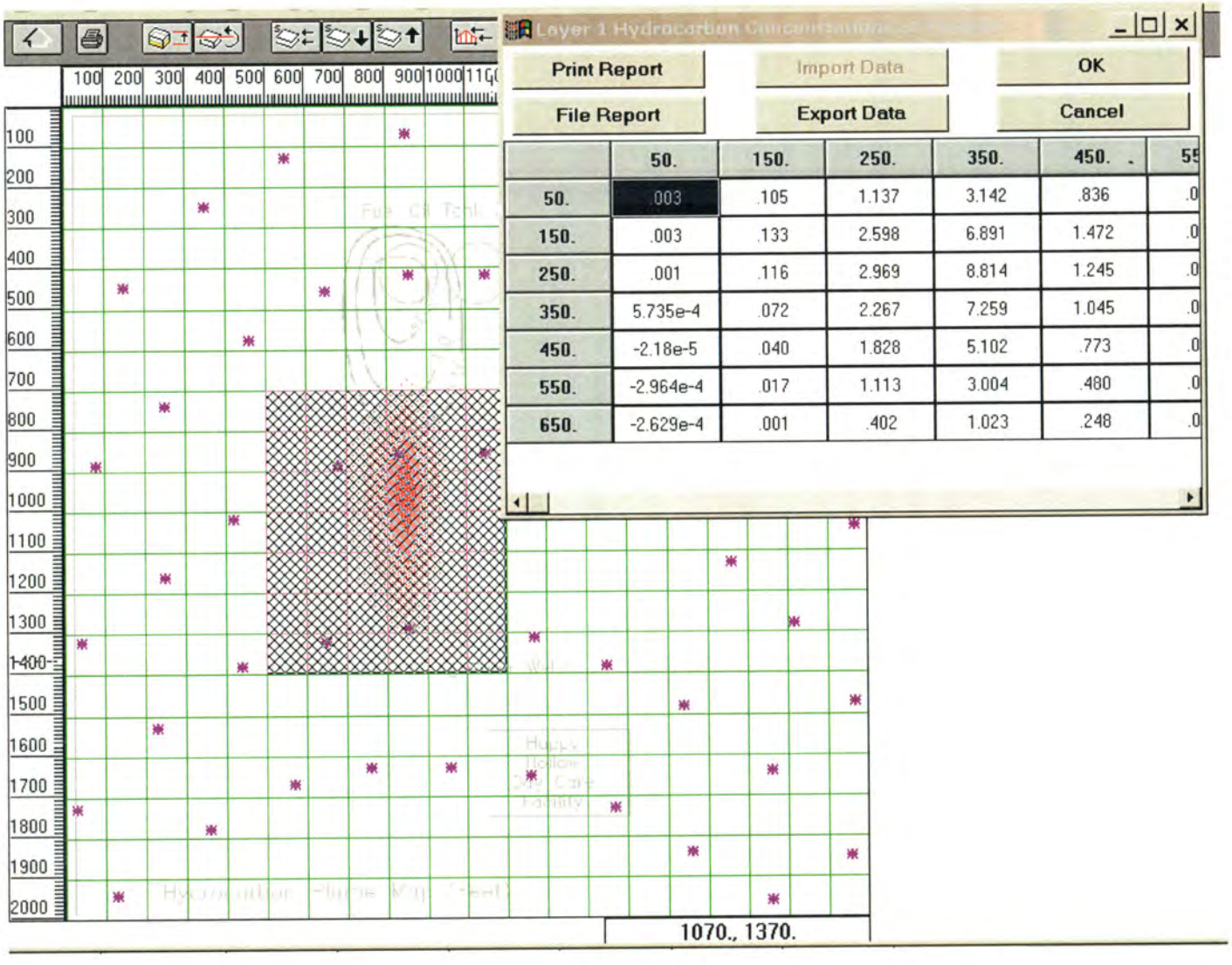

	50.	150.	250.	350.	450.	55
50.	.003	.105	1.137	3.142	.836	.0
150.	.003	.133	2.598	6.891	1.472	.0
250.	.001	.116	2.969	8.814	1.245	.0
350.	5.735e-4	.072	2.267	7.259	1.045	.0
450.	-2.18e-5	.040	1.828	5.102	.773	.0
550.	-2.964e-4	.017	1.113	3.004	.480	.0
650.	-2.629e-4	.001	.402	1.023	.248	.0

Figure A2.a. Result of running contaminant model - no source – user #1 (Case 2)

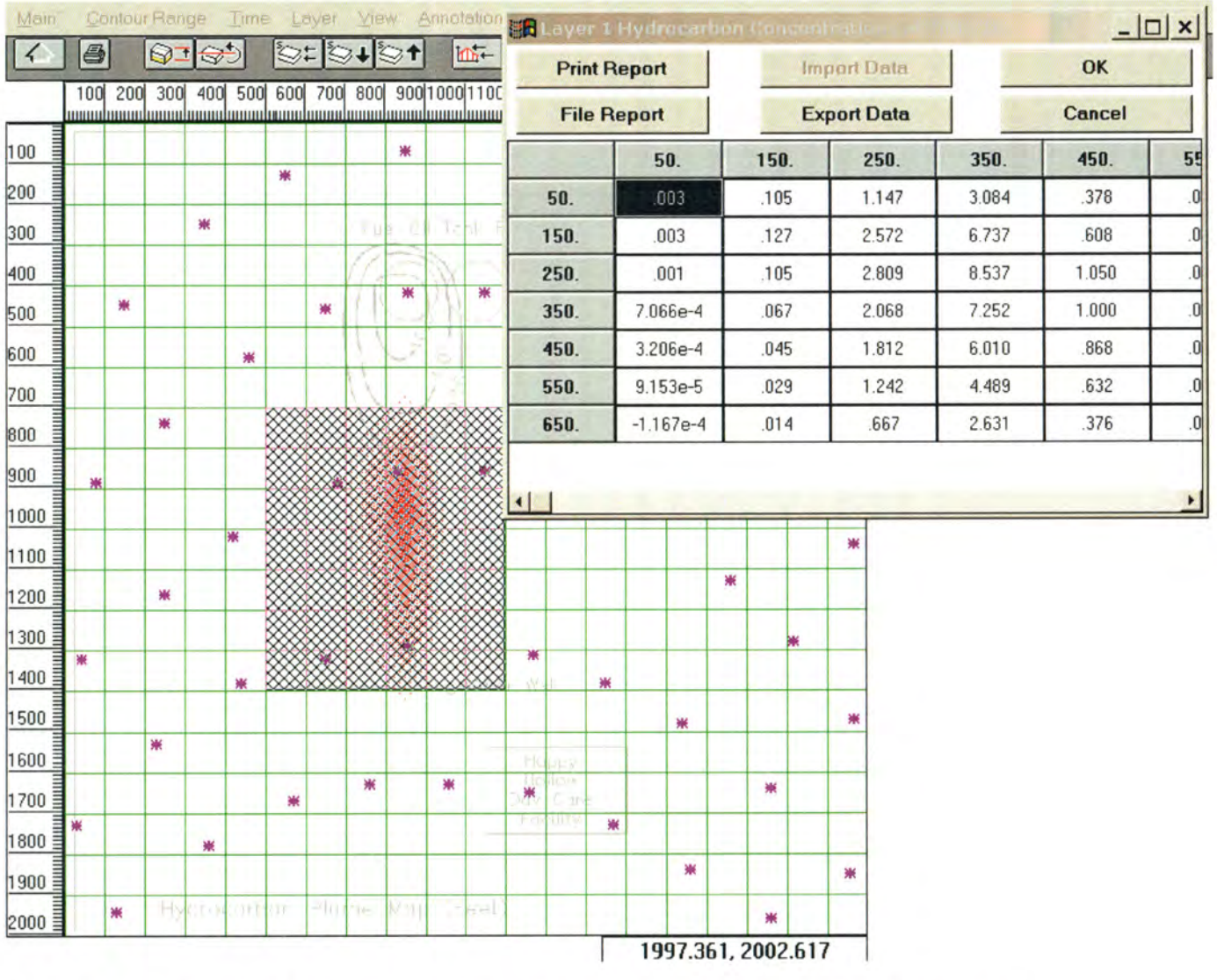

Figure A2.b. Result of running contaminant model – no source – user #2 (Case 2)

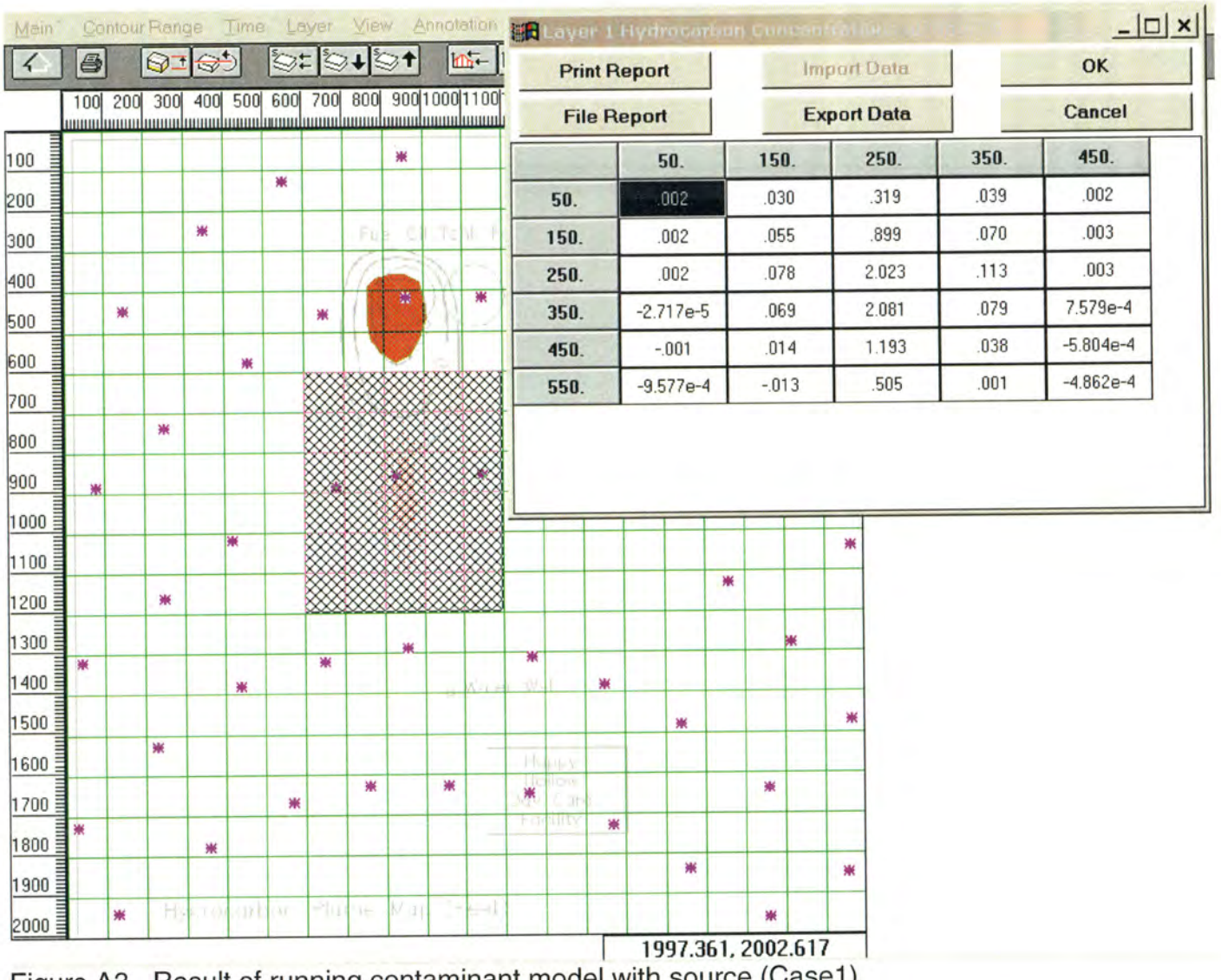

Figure A3. Result of running contaminant model with source (Case1)

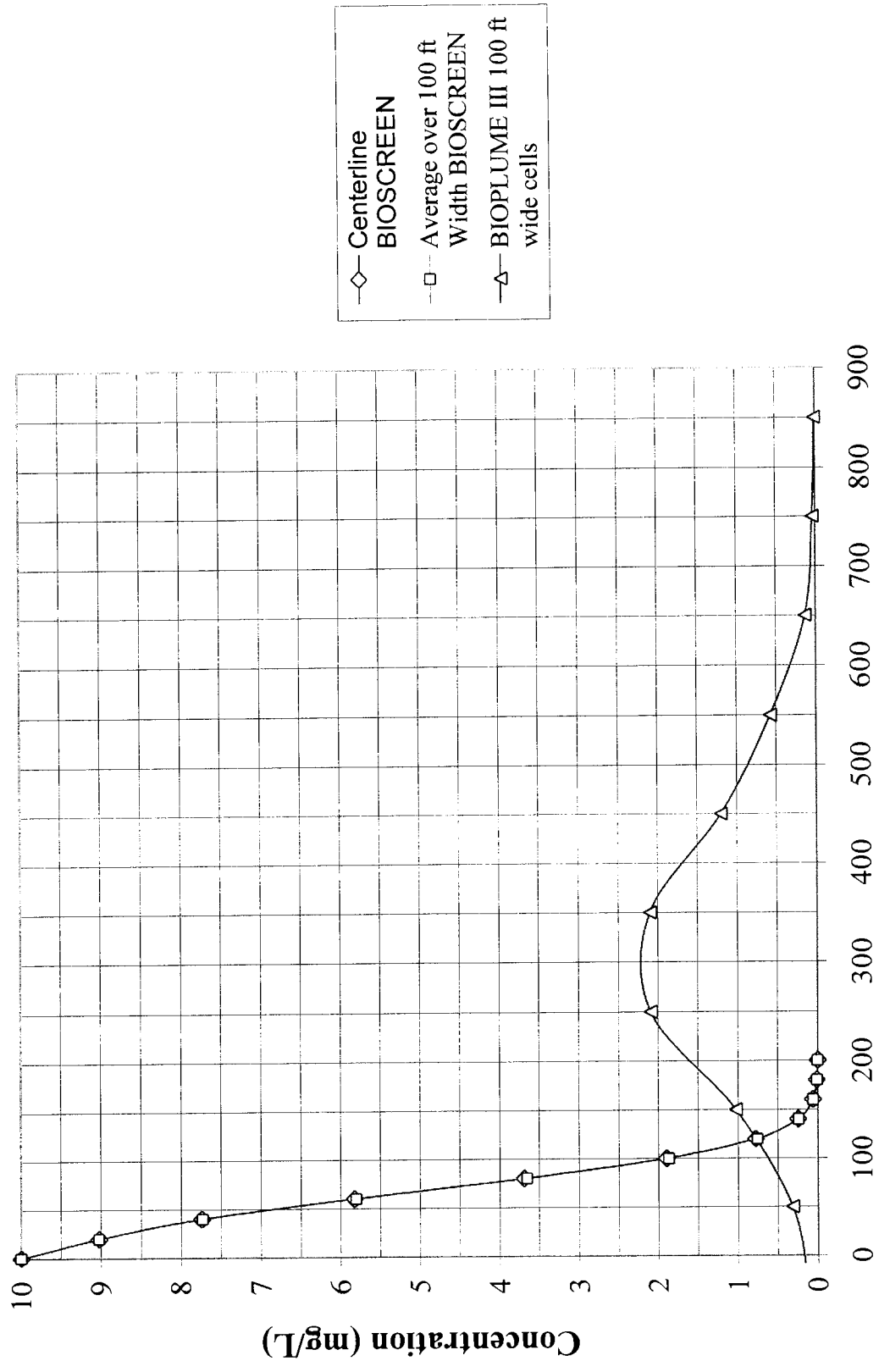

Figure A4. Comparison of BIOPLUME III results to BIOSCREEN

APPENDIX B: PAST DATA

Table B1. Groundwater elevation data at Cherokee FMGP site, Iowa

Monitoring Well	Coordinate (ft)		Groundwater Elevations (ft)										
	Northing	Easting	Nov-93	Mar-98	Jun-98	Sep-98	Jun-99	Nov-99	Jun-00	Nov-00	Jun-01	Aug-01	Average
MW-1	1126.7	1186.29	1176.26	1176.06	1176.36	1176.31	1176.52	1176.19	1176.15	1176.19	1176.41	1176.36	1176.28
MW-2	1137.8	1163.21	1176.29	1176.04	1176.38	1176.35	1176.53	1176.21	1176.18	1176.23	1176.37	1176.31	1176.29
MW-3	944.62	1046.5	1176.2	1176.05	1176.34	1176.31	1177.51	1176.17	1176.11	1175.98	1176.36	1176.3	1176.33
MW-4	1190.1	1165.62	1175.75	1176.08	1176.42	1176.36	1176.57	1176.28	1176.18	1176.27	1176.43	1176.36	1176.27
MW-5A	1014	1134.16	1175.7	1176.07	1176.36	1176.31	1176.53	1176.19	1176.14	1176.23	1176.43	1176.35	1176.23
MW-5B	1019.6	1134.59	1175.69	1176.04	1176.34	1176.29	1176.49	1176.19	1176.13	1176.17	1176.44	1176.37	1176.22
MW-6	931.32	1207.53	1175.7	1176	1176.35	1176.31	1176.37	1176.08	1176.08	1175.98	1176.27	NM	1176.13
MW-7	703.96	1022.71	NI	1158.97	1160.71	1158.05	1163.56	1157.56	1158.95	1158.25	1162.31	1159.22	1159.73
MW-8	919.14	1392.75	NI	1163.32	1163.85	1161.52	1164.91	1161.63	1161.93	1162.67	1166.04	1163.03	1163.21
MW-9	720.39	1203.82	NI	1159.42	1161.28	1158.43	1163.98	1158.06	1160.07	1159.23	1162.87	1159.85	1160.35
MW-10	636.7	1253.05	NI	1157.94	1159.52	1156.82	1162.8	1156.45	1157.74	1156.82	1161.08	1157.64	1158.53
MW-11	552.83	1310.98	NI	1157.95	1159.52	1156.81	1162.8	1156.44	1157.74	1156.82	1161.04	1157.61	1158.53
MW12	723.85	1376.74	NI	NI	NI	NI	NI	NI	NI	NI	NI	1157.71	1157.71
MW13A	827.9	1209.69	NI	NI	NI	NI	NI	NI	NI	NI	NI	1165.9	1165.90
MW13B	822.91	1209.68	NI	NI	NI	NI	NI	NI	NI	NI	NI	1163.52	1163.52

NM – Not measured
NI – Not installed

Table B2. Hydraulic conductivity data at Cherokee FMGP site, Iowa

Well Tested	Date of Testing	Method†	Soil Type	Screen Range (bgs) (ft.)	Screen Length (ft.)	Shape Factor (m)	Hydraulic Conductivity	
							B&V value (cm/sec)	Superslug Value (cm/sec)
MW1	1/29/92	both F/R	Alluvium	6.7-16.7	10	NA	8.03E-02*	NA
MW2	1/30/92	both F/R	Alluvium	9-17.9	9.9	NA	6.20E-02*	NA
MW3	1/31/92	both F/R	Alluvium/loess	8-19.7	9.7	NA	3.16E-02 *	NA
MW5	12/15/93	both F/R	Alluvium	19.8-29.5	9.7	NA	6.35E-02*	NA
MW7	6/22/94	both F/R	Alluvium	27-37	10	NA	4.10E-03*	NA
MW8	3/25/98	both F/R	Alluvium/till	28.2-33	4.8	5.23	2.16E-01**	2.07E-01
MW9	3/26/98	both F/R	Alluvium	25.2-30	4.8	5.23	1.60E-02**	1.53E-02
MW10	3/27/98	both F/R	Alluvium/till	37.2-42	4.8	5.23	9.24E-01**	1.30E-01
MW11	3/28/98	Rising	Alluvium/till	36.2-41	4.8	5.23	15.7E+01**	NS

† - F/R – both falling and rising head test
* - Black and Veatch, 1994
** - Black and Veatch, 1998
NA - Data not available
NS - Data not sufficient to calculate hydraulic conductivity value

APPENDIX C: SURVEYING DATA

Table C1. Raw surveying data from August 2001 site sampling event at Cherokee FMGP site, Iowa

Location	Northing (ft.)	Easting (ft.)	Elevation (ft.)
BM NE COR HDWALL	763.61	979.36	1165.94
BM W EDGE BRG/GT	590.67	1928.72	1181.3
CP	915.67	1264.96	0
CP NAIL NW	1180.11	1029.26	1192.04
CP NAIL SE	620.92	1522.3	1172.36
CP NAIL W	818.6	1039.78	1177.23
EC 2	932.12	1196.05	1176.65
EC 3	922.52	1389.38	1174.84
EC 4	849.64	1008.89	1179.15
EC 5	860.07	1040.86	1179.19
EC 6	900.06	1118.41	1176.76
EC 7	950.7	1257.08	1176.41
EC 8	782.69	1037.89	1174.82
EC 9	810.18	1122.99	1175.21
EC 10	862.68	1254.93	1175.65
EC 11	889.25	1321.79	1175.33
EC 12	1293.56	1117.41	1190.92
EC 13	1141.06	1293.52	1182.82
EC 14	1141.78	1207.64	1184.76
EC 15	1142.8	1153.65	1186.28
EC 16	1158.6	1078.63	1188.43
EC 17/GPW 19	1088.7	1032.39	1187.42
EC 18	1033.66	1089.22	1184.42
EC 19	953.45	1154.38	1177.9
EC 20	993.89	998.63	1182.09
EC 21	986.67	1126.02	1179.28
EC 22	982.57	1202.95	1178.24
EC 23	986.53	1258.61	1176.89
EC 24	700.6	930.9	1174.97
EC 25	620.92	1037.82	1172.31
EC 25A	616.34	1046.57	1172.38
GPW 1	843.08	988.81	1179.6
GPW 2	848.74	1008.68	1179.16
GPW 3	856.38	1039.46	1178.53
GPW 4	903.19	1124.87	1176.84
GPW 5	925.31	1191.17	1176.34
GPW 6	948.17	1254.11	1176.49

Table C1. Raw surveying data from August 2001 site sampling event at Cherokee FMGP site, Iowa (continued)

Location	Northing (ft.)	Easting (ft.)	Elevation (ft.)
GPW 7	950.35	1314.56	1175.55
GPW 8	781.63	1035.91	1174.77
GPW 9	808.34	1125.57	1175.15
GPW 10	842.59	1193.52	1174.86
GPW 11	860.36	1254.27	1175.61
GPW 12	891.18	1320.69	1175.19
GPW 13	909.65	1364.25	1174.85
GPW 14	1286.61	1117.03	1190.85
GPW 15	1141.17	1297.79	1182.73
GPW 16	1141.67	1211.91	1184.69
GPW 17	1142.29	1171.1	1185.98
GPW 18	1142.94	1072.09	1188.1
GPW 20	1029.25	1084.32	1184.36
GPW 21	957.92	1149.01	1178.2
GPW 22	999.22	996.52	1182.35
GPW 23	944.7	1046.54	1179.82
GPW 23	982.08	1048.75	1181.37
GPW 24	984.47	1130.18	1178.68
GPW 25	977.78	1202.22	1177.76
GPW 26	983.7	1262.29	1176.8
HC 1	1143.17	1304.43	1182.71
HC 2	810.96	1128.05	1175.2
HC 3	869.24	1311.58	1175.49
HC 4	863.49	1249.55	1175.64
HC 5	579.32	1254.34	1172.97
MW 1	1126.79	1086.44	1188.04
MW 1 ELEV.	1126.89	1086.4	1187.67
MW 2	1137.81	1163.26	1186.2
MW 2 ELEV.	1137.82	1163.14	1185.82
MW 3	720.36	1203.86	1173.35
MW 4	1190.13	1065.76	1189.18
MW 4 ELEV.	1190.06	1065.86	1188.73
MW 5A	1014.08	1134.24	1180.71
MW 5A ELEV.	1013.97	1134.26	1180.45
MW 5B	1019.67	1134.69	1181.02
MW 5B ELEV.	1019.59	1134.66	1180.72
MW 6	931.31	1207.54	1176.68

Table C1. Raw surveying data from August 2001 site sampling event at Cherokee FMGP site, Iowa (continued)

Location	Northing (ft.)	Easting (ft.)	Elevation (ft.)
MW 6 ELEV.	931.42	1207.56	1176.47
MW 6A	932.59	1201.44	1176.71
MW 6A ELEV.	932.57	1201.36	1176.34
MW 6B	931.63	1213.2	1176.58
MW 6B ELEV.	931.61	1213.08	1176.29
MW 6C	926.03	1206.74	1176.52
MW 6C ELEV.	926.04	1206.64	1176.15
MW 7	704.08	1022.7	1173.75
MW 7 ELEV.	704.16	1022.65	1173.51
MW 8	919.14	1392.75	1174.57
MW 10 ELEV.	636.78	1252.98	1172.48
MW 10 HORIZ.	636.7	1253.09	1172.82
MW 11	552.83	1310.98	1173.02
MW 12	723.85	1376.74	1173.06
MW 12 ELEV.	723.88	1376.72	1172.71
MW 13A	827.9	1209.69	1175.01
MW 13A ELEV.	828.03	1209.62	1174.7
MW 13B	822.91	1209.68	1174.94
MW 13B ELEV.	822.96	1209.7	1174.53
SS 1	1289.08	1118.2	1190.94
SS 1A	1141.42	1316.74	1182.52
SS 2	1142.92	1168.49	1185.85
SS 3	983.04	1051.71	1181.3
SS 4	1031.45	1084.33	1184.26
SS 5	983.67	1134.67	1178.83
SS 6	956.66	1153.77	1177.9
SS 7	980.21	1202.34	1177.98
SS 8	907.19	1128.24	1176.93
SS 9	920.04	1192.05	1176.08
SS 10	811.39	1129.22	1175.17
SS 11	847.99	1192.2	1175.04
SS 12	859.25	1258.17	1175.66
WATER LEVEL	513.23	1943.63	1158.26

APPENDIX D: FIELD DATA (AUGUST 2001)

D.1. Protocols for Hydraulic Conductivity Testing using Pneumatic Method

Steps for conducting the test

- Advance the dual tube probe rods into the ground. Once the desired depth is reached, add the distilled water to fill in the space between the outer and inner rods to prevent heaving.
- Remove the inner rods completely and retract the outer rods by approximately 2 feet. Lower the 2-foot screen to the bottom of the outer rods. Screen is tapped from above by rods to make sure that they fit properly into the bottom opening of outer rods (as shown in Figure 2.6).
- Perform the well development exercise as per Quality Assurance Project Plan prepared by Alliant Energy, 1999.
- Submerge the pressure transducer using the cable in the water column inside the outer rod. Data logger is attached to the other end of cable. Transducer should be kept a foot or two above the screen's top depending upon the distance between water table and screen top.
- Wait until the water level stabilizes (variation not more than +/- 0.05 inches in data logger reading).
- Attach the valve/gage assembly to the exposed push rod at the ground surface.
- Open the nitrogen gas or compressed air regulator and pressurize the air column above water. Monitor the air pressure using the pressure gauge attached with the regulator (as shown in Figure D17). Every 0.43-psi increase in the air pressure will give a drawdown of one foot in the water column.
- Pressure applied though gas or air depends on the length of water column and surrounding soil media. Once enough drawdown is created (one foot for loess and 10 feet for alluvium), depressurize the air column. Record the rise in water level with respect to time by the data logger attached to the transducer.
- Readings in the data recorder are exported to the software (Slugpoint).
- Repeat the test at least twice to verify the results.

D.2. Friedman's and Sign test (a non-parametric test) results for performance comparison of pre-packed screen monitoring wells 6A, 6B and 6C against 2-inch conventional MW6

MW6A, 6B, and 6C against MW6

XLSTAT version 5.1 - **Friedman's Test** - 5/23/02 at 9:11:34 AM
Data: workbook = BOOK1.xls / sheet = range = $K$26:$N$53 / 28 rows and 4 Columns.
Note: The calculation of the Friedman's χ^2 takes into account ties

Friedman's χ^2 (distributed as a Chi-square) observed value (df = 3): 2.150
P-value: 0.542
One-tailed test: the p-value is compared with the significance level alpha= 0.050

Friedman's χ^2 (distributed as a Chi-square) critical value (df = 3): 7.777

Decision:
At the level of significance alpha= 0.050 the decision is not to reject the null hypothesis (the absence of difference between the 4 groups).
In other words, the difference between the groups is **not significant**

XLSTAT version 5.1 - Comparing two paired samples - **Sign test / Two-tailed test**- 10/2/2002 at 5:32:55 PM

MW6A against MW6

Number of positive differences observed value: 6.000
P-value: 0.377
Two-tailed test: the p-value is compared with the significance level alpha/2= 0.025

Total significance level: alpha= 0.050
Decision:
At the total level of significance alpha= 0.050 the decision is not to reject the null hypothesis (absence of difference between samples)
In other words, the difference between samples is **not significant**

MW6B against MW6

Number of positive differences observed value: 4.000
P-value: 0.113
Two-tailed test: the p-value is compared with the significance level alpha/2= 0.025

Total significance level: alpha = 0.050
Decision:
At the total level of significance alpha = 0.050 the decision is not to reject the null hypothesis (absence of difference between samples)
In other words, the difference between samples is **not significant**

MW6C against MW6

Number of positive differences observed value: 3.000
P-value: 0.033
Two-tailed test: the p-value is compared with the significance level alpha/2= 0.025

Total significance level: alpha = 0.050
Decision:
At the total level of significance alpha = 0.050 the decision is to not reject the null hypothesis (absence of difference between samples)
In other words, the difference between samples is **not significant**

Table D1. Geoprobe groundwater monitoring mobile lab analysis results at Cherokee FMGP site, Iowa

Location	Sample Depth (ft.)	Geologic Unit at Midpoint	Ammonia (mg/L as N)	Nitrate (mg/L)	Nitrite (mg/L)	Dissolved Manganese (mg/L)	Ferrous Iron (mg/L)	Total Diss. Iron (mg/L)	Sulfate† (mg/L)	Sulfide (mg/L)
GPW-1	16	Alluvium ‡	0.02	0.9	0.003	NA	0.01	0.11	100	0.000
GPW-2	16	Alluvium	0.06	1.2	0.006	NA	0.00	0.00	100	0.001
GPW-3	18	Alluvium	BDL	0.5	0.006	NA	0.01	0.06	110	0.002
GPW-4	14	Alluvium	BDL	0.1	0.003	0.6	0.07	0.15	100	0.005
	19	Alluvium	0.20	0.1	0.002	1.1	0.17	0.22	100	0.005
GPW-5	12	Alluvium	0.08	0.1	0.003	0.8	0.01	0.02	130	0.001
	18	Till	0.02	0.4	0.009	2.0	0.14	0.25	120	0.001
GPW-6	12	Alluvium	0.02	1.1	0.017	1.9	0.01	0.03	140	0.003
	16	Alluvium	0.01	1.1	0.008	1.6	0.03	0.05	150	0.001
GPW-8	22	Alluvium	0.03	0.2	0.007	NA	0.01	0.06	130	0.012
GPW-9	24	Loess	0.01	1.2	0.006	NA	0.00	0.00	100	0.001
GPW-10	28	Alluvium ‡	BDL	0.5	0.006	NA	0.01	0.06	110	0.002
GPW-11	17	Loess	0.40	0.2	0.003	NA	1.02	2.35	110	0.009
	30	Alluvium	0.14	2.1	0.021	NA	0.41	0.59	150	2.46†
GPW-12	27	Loess	0.18	0.2	0.004	NA	3.5†	4.6†	230	0.003
GPW-13	27	Loess	BDL	0.3	0.001	NA	5.2†	8.8†	190	0.003
GPW-14	22	Alluvium	0.09	3†	0.013	NA	0.1	0.23	110	0.000
	32	Alluvium	0.02	14†	0.022	NA	0.09	0.46	100	0.001
GPW-15	15	Alluvium	0.02	0.5	0.005	0.0	0.00	0.03	90	0.000
	22	Alluvium	BDL	0.3	0.004	2.2	1.01	1.15	150	0.001
GPW-16	20	Alluvium	BDL	1.7	0.006	NA	0.02	0.02	110	0.000
	28	Alluvium	BDL	2	0.006	NA	0.10	0.15	100	0.001
GPW-17	18	Alluvium ‡	0.02	13†	0.007	NA	0.12	0.59	120	0.014
	28	Alluvium ‡	0.19	11†	0.005	NA	0.38	0.68	160	0.001

Table D1. Geoprobe groundwater monitoring mobile lab analysis results at Cherokee FMGP site, Iowa (continued)

Location	Sample Depth (ft.)	Unit	Ammonia (mg/L as N)	Nitrate (mg/L)	Nitrite (mg/L)	Dissolved Manganese (mg/L)	Ferrous Iron (mg/L)	Total Diss. Iron (mg/L)	Sulfate† (mg/L)	Sulfide (mg/L)
GPW-18	20	Alluvium	0.05	1.8	0.005	NA	0.00	0.34	100	0.014
	32	Alluvium	0.01	1.9	0.004	NA	0.02	0.03	100	0.002
GPW-19	18	Alluvium	0.02	10†	0.005	NA	0.00	0.00	100	0.014
	26	Alluvium	BDL	4†	0.023	NA	0.00	0.02	100	0.013
GPW-20	16	Alluvium	0.04	0.3	0.003	0.3	7.8†	9.1†	110	0.015
	27	Alluvium	BDL	1.4	0.28†	0.5	0.00	0.01	140	0.001
GPW-21	14	Alluvium	BDL	0.3	0.000	0.6	5.0†	5.4†	100	0.009
	20	Alluvium	BDL	0.2	0.043	2.7	0.13	0.15	100	0.002
GPW-22	12	Alluvium	0.05	0.6	0.033	0.3	0.8	0.91	100	0.005
	17	Alluvium	BDL	15†	0.009	0.2	0.27	0.34	110	0.002
GPW-23	15	Alluvium‡	0.03	0.3	0.005	0.6	2.11	3.3†	110	0.007
	20	Alluvium‡	BDL	17†	0.73†	0.5	0.22	0.38	220	0.001
GPW-24	16	Alluvium	2.1	0.4	0.005	0.6	0.3	1.37	90	0.000
	24	Alluvium	1.6	4.3†	1.49†	2.2	0.45	1.08	140	0.004
GPW-25	15	Alluvium	1.2	0.1	0.005	1.3	0.24	0.35	110	BDL
	20	Alluvium	0.2	2.0	0.048	2.5	0.52	0.67	90	0.004
GPW-26	14	Alluvium	0.13	4.5	0.019	2.0	0.09	0.03	100	0.004

BDL = Below detection limit
NA = Data not available
† = 10x dilution was required for analysis, dilution of sulfide may underestimate actual results
‡ = Approximate midpoint

Table D2. Monitoring well groundwater mobile lab analysis results at Cherokee FMGP site, Iowa

Location	Sample Depth (ft)	Geologic Unit at Midpoint	Ammonia (mg/L as N)	Nitrate (mg/L)	Nitrite (mg/L)	Dissolved Manganese (mg/L)	Ferrous Iron (mg/L)	Total Diss. Iron (mg/L)	Sulfate† (mg/L)	Sulfide (mg/L)
MW-1	11.4	Alluvium	BDL	14 †	0.006	NA	0.01	NA	NA	0.002
MW-2	32.0	Alluvium	BDL	2.3	0.005	NA	0.00	NA	90	0.002
MW-3	12.9	Alluvium	BDL	0.4	0.005	NA	3.8 †	NA	NA	0.005
MW-4	25.3	Alluvium	BDL	12 †	0.005	NA	0.02	NA	NA	0.005
MW-5A	9.2	Alluvium	BDL	1.8	0.029	NA	0.11	NA	NA	0.012
MW-5B	24.7	Alluvium	BDL	2.4	0.38 †	NA	1.46	NA	NA	0.003
MW-6	16.3	Alluvium	0.003	1.4	0.02	NA	0.36	NA	NA	0.006
GMW-6A			BDL	0.5	0.039	NA	0.01	0.03	100	0.000
GMW-6B			BDL	0.3	0.006	NA	0.03	0.15	110	0.001
GMW-6C			BDL	1.8	0.006	NA	0.89	1.32	120	0.004
MW-7	32.0	Alluvium	0.01	0.6	0.015	NA	7.4 †	NA	NA	0.003
MW-8	30.6	Alluvium	0.04	0.3	0.004	NA	1.74	NA	NA	0.004
MW-9	27.6	Alluvium	BDL	0.6	0.025	NA	0.28	NA	NA	0.032
MW-10	38.6	Alluvium	0.05	0.3	0.004	NA	6.0 †	NA	NA	0.001
MW-11	39.6	Alluvium	BDL	0.5	0.025	NA	0.03	NA	NA	0.000
GMW-13A			BDL	0.5	0.005	NA	0.85	NA	NA	0.001
GMW-13B			0.23	2.8	0.038	NA	0.65	NA	NA	1.93 †

BDL = Below detection limit
NA = Data not available
† = 10x dilution was required for analysis, dilution of sulfide may underestimate actual results
‡ = Approximate midpoint

Table D3. Flow-through cell readings for the Geoprobe groundwater samples at Cherokee FMGP site, Iowa

Location	Sample Depth (ft.)	Geologic Unit at Midpoint	Temperature (°C)	Dissolved Oxygen (mg/L)	Standard Redox Potential (Hydrogen Electrode) (mV)	Electrical Conductivity (µS/cm)
GPW-1	16	Alluvium ‡	15.5 / 20.9	3.0	133	809
GPW-2	16	Alluvium	18	1.1	105	867
GPW-3	18	Alluvium	17.6	1.2	81	853
GPW-4	14	Alluvium	17.2	1.8	41	702
	19	Alluvium	15.3	0.8	34	682
GPW-5	12	Alluvium	15.8	2.9	20	715
	18	Till	14.9	2.6	-179	841
GPW-6	12	Alluvium	16.3	5.1	55	984
	16	Alluvium	15.0	2.9	75	1090
GPW-8	22	Alluvium	NA	NA	NA	NA
GPW-9	24	Loess	NA	NA	NA	NA
GPW-10	28	Alluvium ‡	NA	NA	NA	NA
GPW-11	17	Loess	14.5	3.4	-33	1700
	30	Alluvium	16.2	2.3	-247	1302
GPW-12	27	Loess	NA	NA	NA	NA
GPW-13	27	Loess	12.95	0.6	-74	1537
GPW-14	22	Alluvium	NA	NA	NA	NA
	32	Alluvium	16.9	5.6	73	1327
GPW-15	15	Alluvium	19.2	0.7	30	1007
	22	Alluvium	16.1 / 19.8	0.9	-16	1250
GPW-16	20	Alluvium	15.8	0.9	13	1002
	28	Alluvium	15.9	0.6	-8	1016
GPW-17	18	Alluvium ‡	14.2	1.1	50	902
	28	Alluvium ‡	14.3	0.4	-14	857

Table D3. Flow-through cell readings for the Geoprobe groundwater samples at Cherokee FMGP site, Iowa (continued)

Location	Sample Depth (ft.)	Unit	Temperature (°C)	Dissolved Oxygen (mg/L)	Standard Redox Potential (Hydrogen Electrode) (mV)	Electrical Conductivity (µS/cm)
GPW-18	20	Alluvium	NA	NA	NA	NA
	32	Alluvium	14.6	4.4	40	1262
GPW-19	18	Alluvium	15.1	5.8	113	737
	26	Alluvium	14.5	1.7	111	824
GPW-20	16	Alluvium	NA	NA	NA	NA
	27	Alluvium	NA	NA	NA	NA
GPW-21	14	Alluvium	NA	NA	NA	NA
	20	Alluvium	NA	NA	NA	NA
GPW-22	12	Alluvium	NA	NA	NA	NA
	17	Alluvium	NA	NA	NA	NA
GPW-23	15	Alluvium ‡	NA	NA	NA	NA
	20	Alluvium ‡	NA	NA	NA	NA
GPW-24	16	Alluvium	NA	NA	NA	NA
	24 [2.]	Alluvium	NA	NA	NA	NA
GPW-25	15	Alluvium	NA	NA	NA	NA
	20	Alluvium	NA	NA	NA	NA
GPW-26	14	Alluvium	NA	NA	NA	NA

NA = Data not available
‡ = Approximate midpoint
* = Dropping Slowly
** = Dropping Fast
1, 2 = Air was being mixed with the water

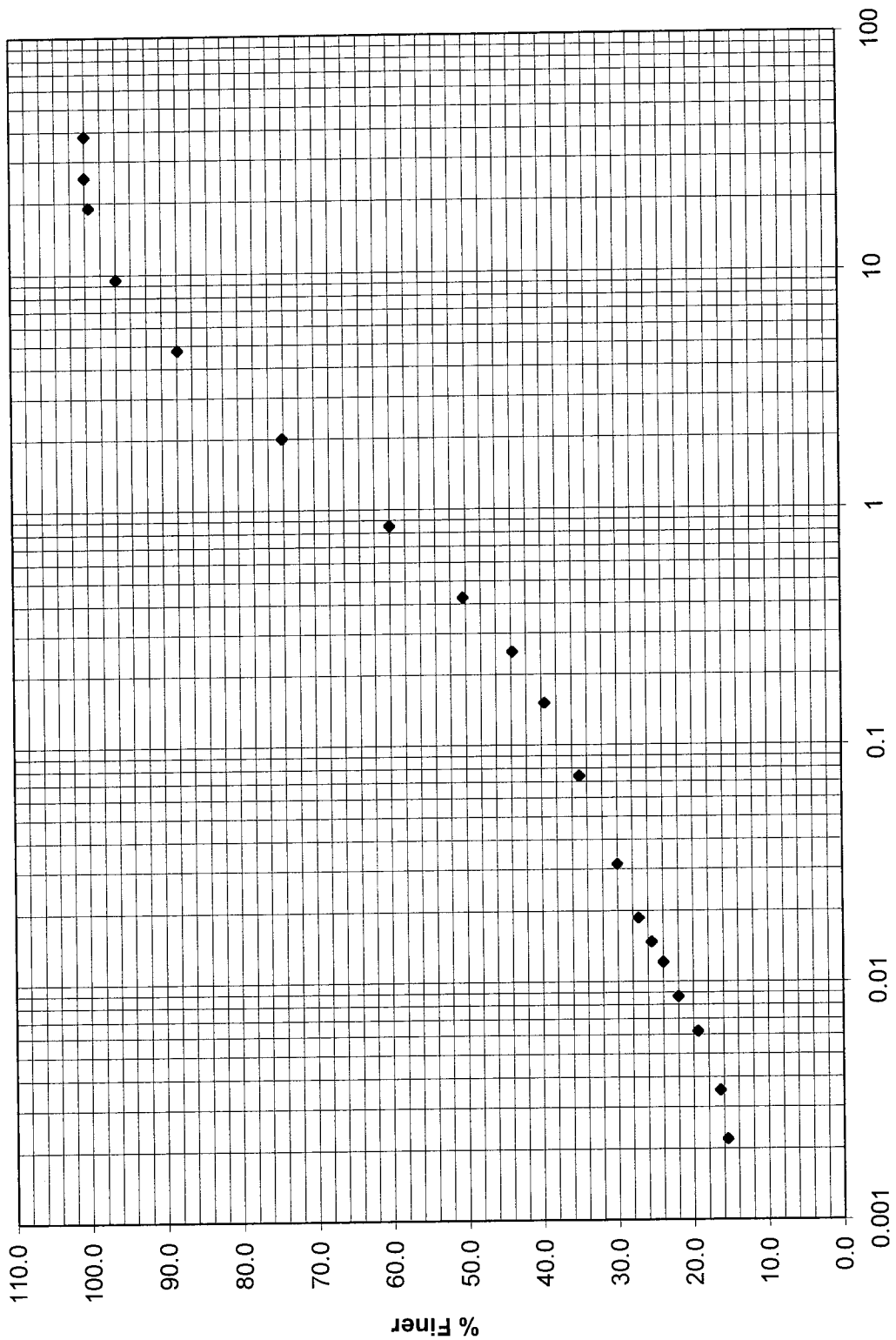

Figure D1. Grain-size distribution curve for soil sampling location – SS2

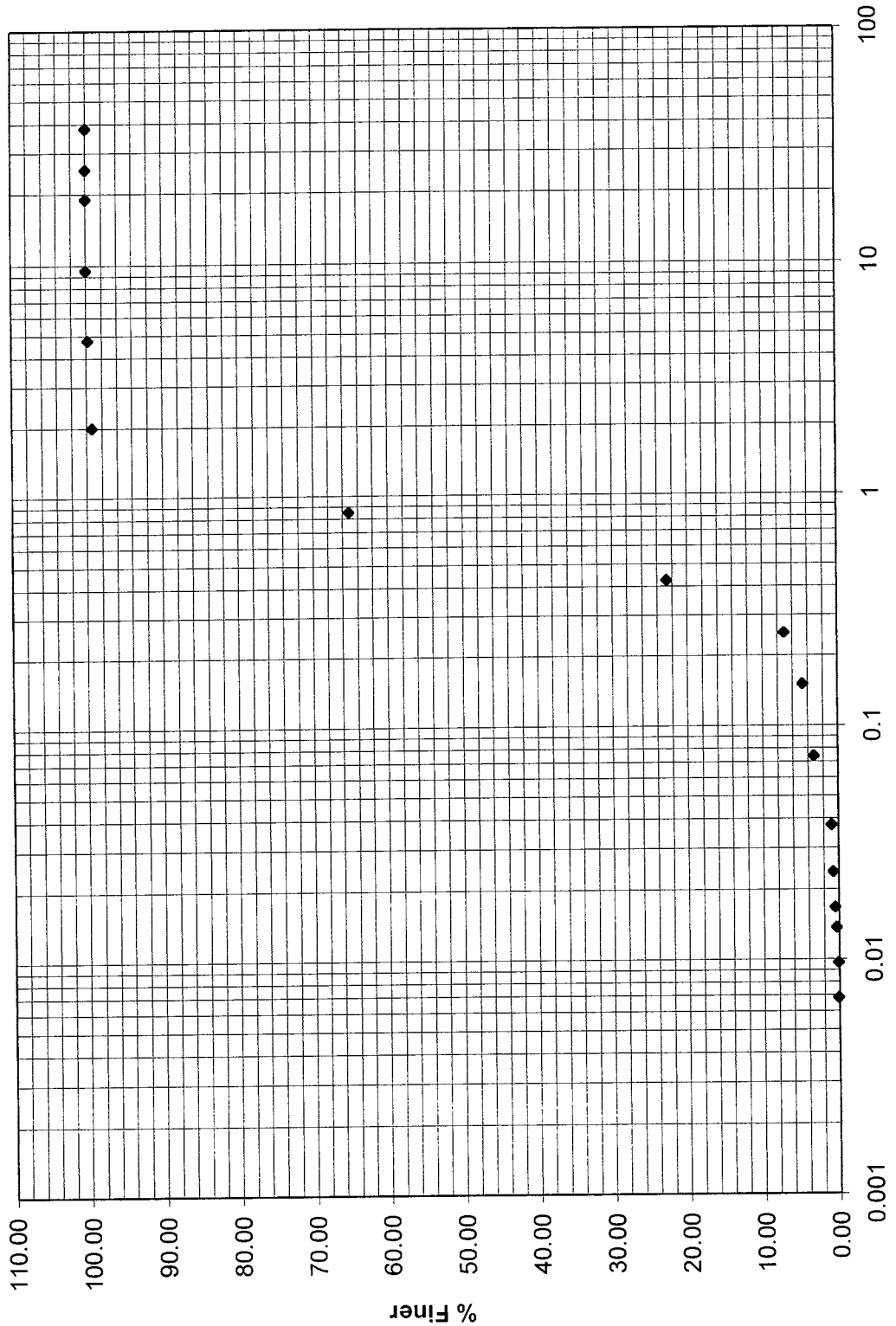

Figure D2. Grain-size distribution curve for soil sampling location - HC5

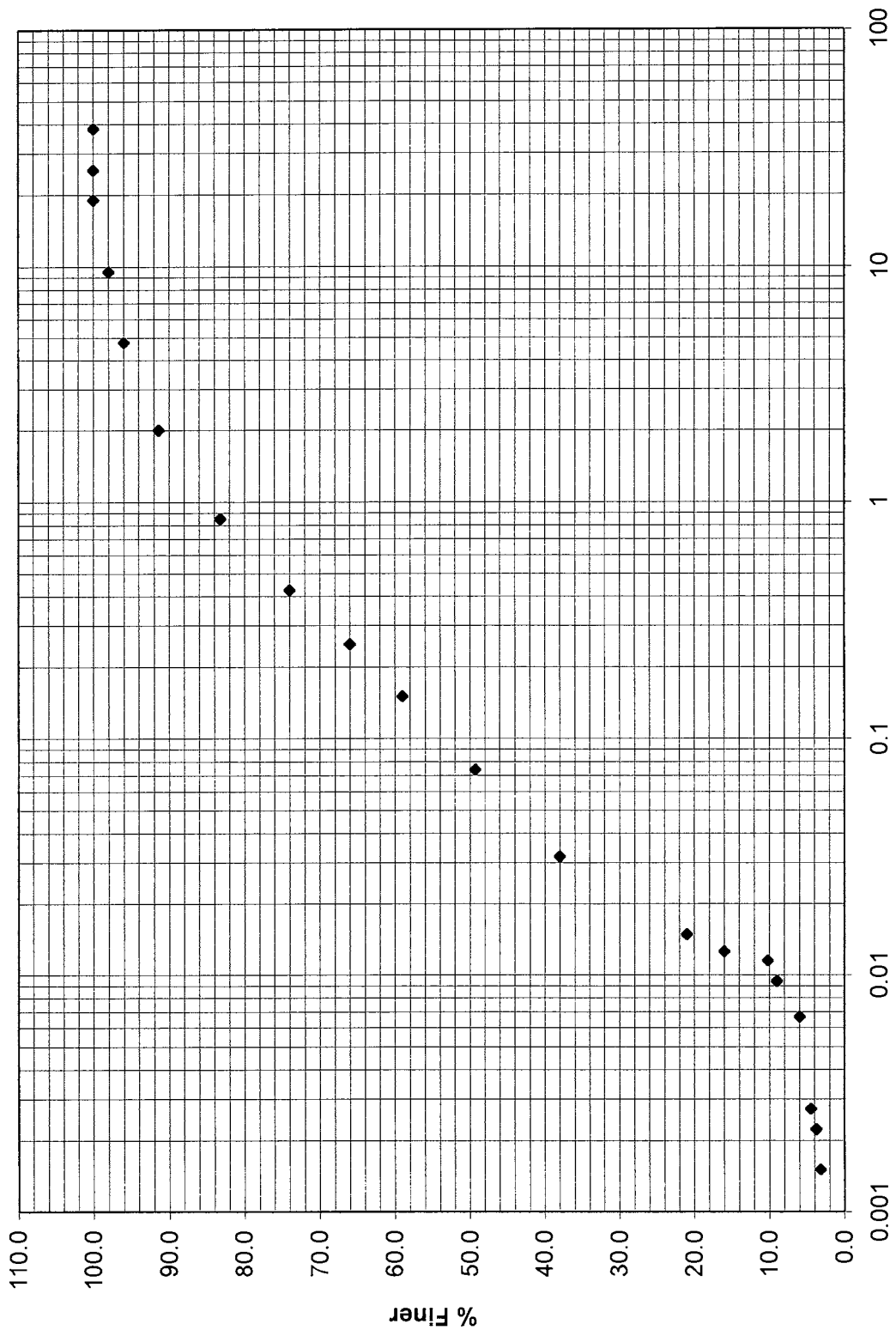

Figure D3. Grain-size distribution curve for soil sampling location – SS10

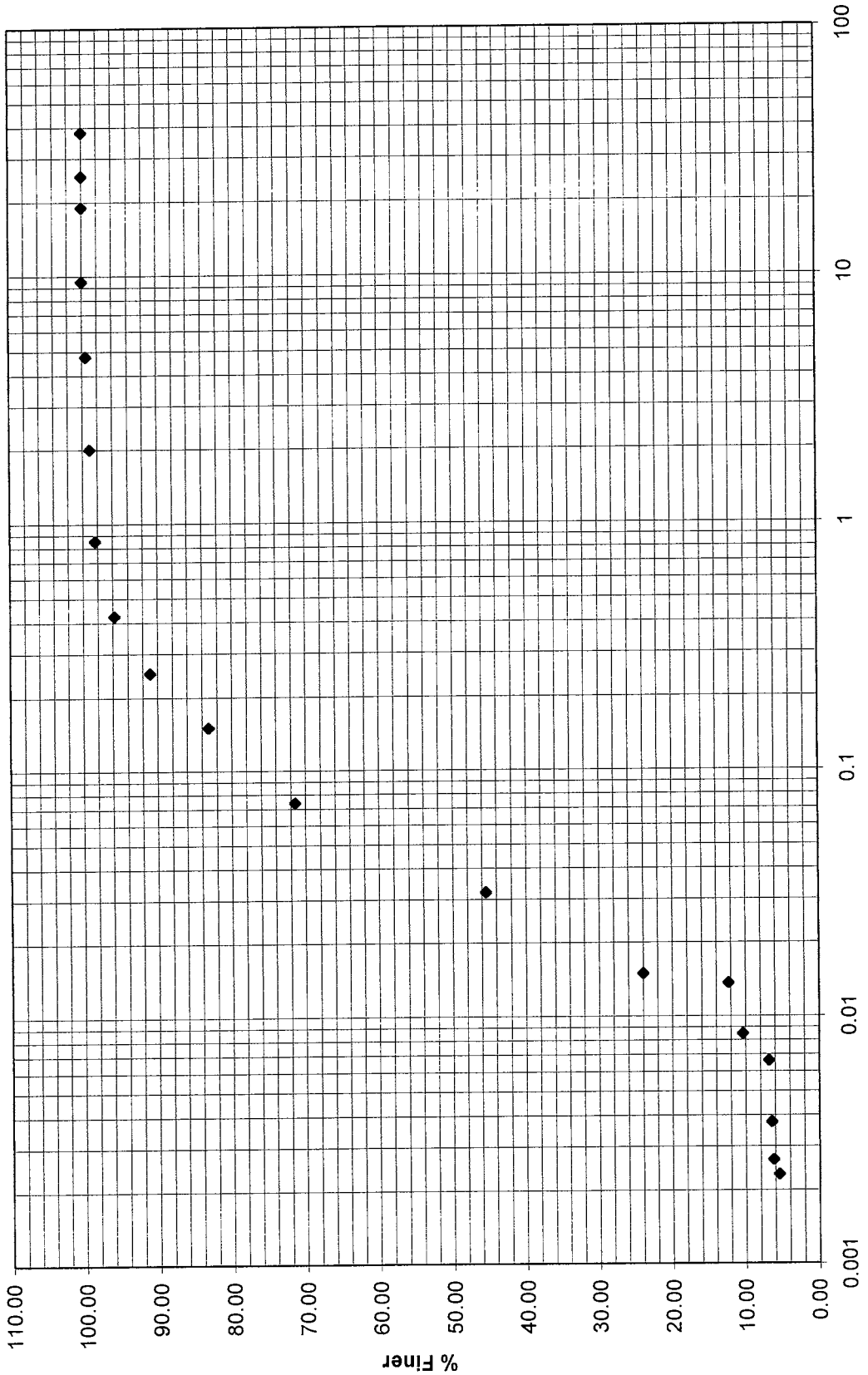

Figure D4. Grain-size distribution curve for soil sampling location - SS12

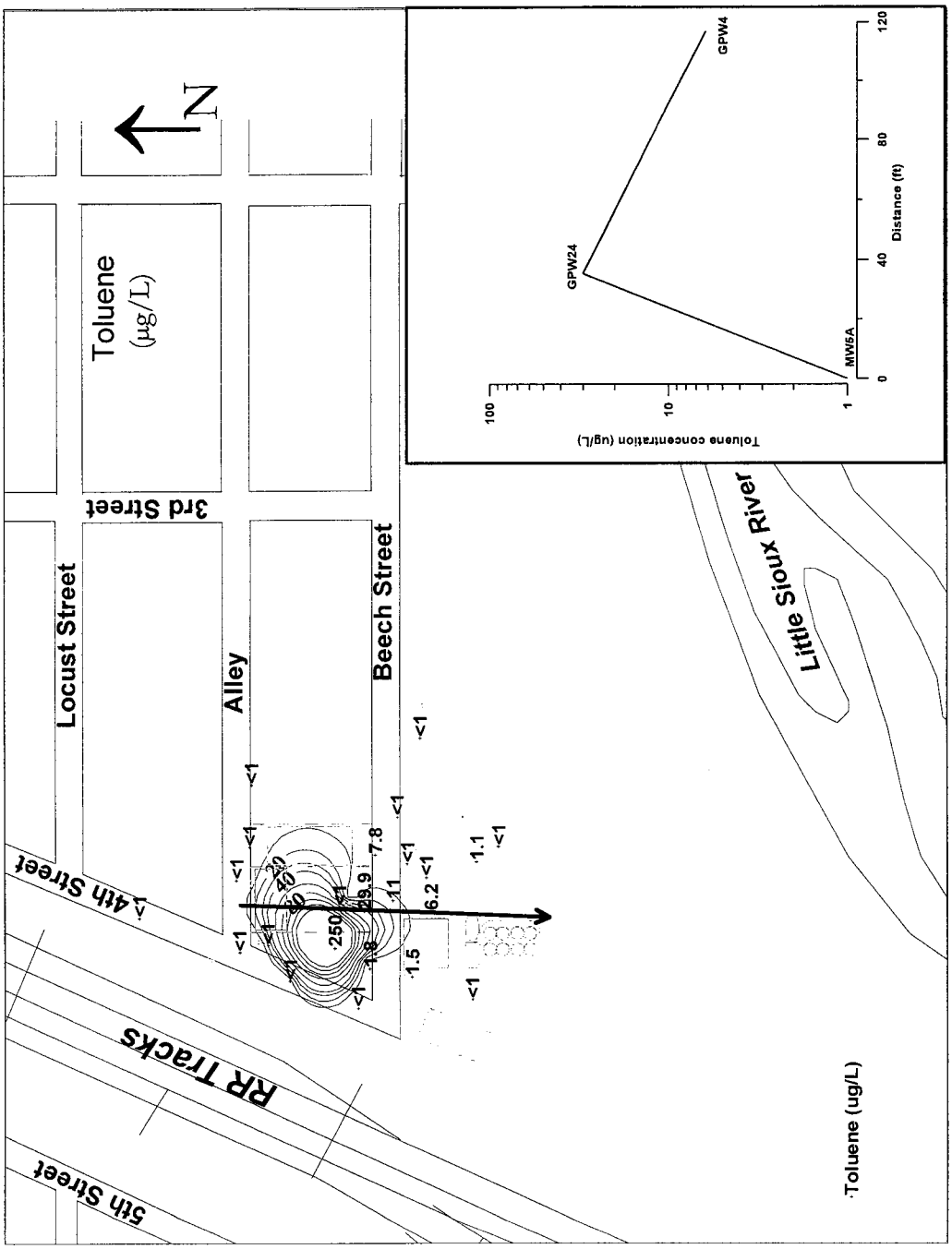

Figure D5. Contours of toluene concentration in the upper half of the aquifer (August 2001 data)

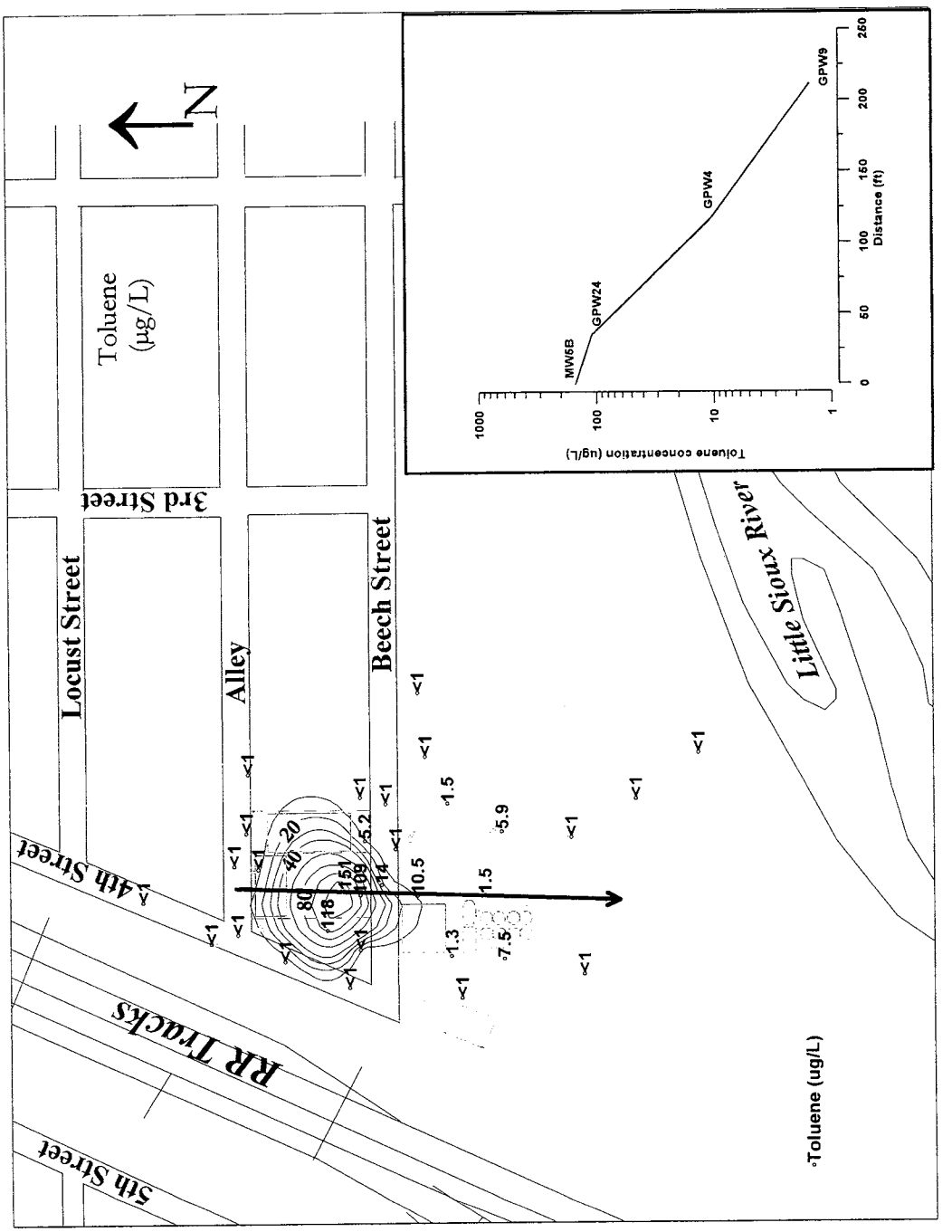

Figure D6. Contours of toluene concentration in the lower half of the aquifer (August 2001 data)

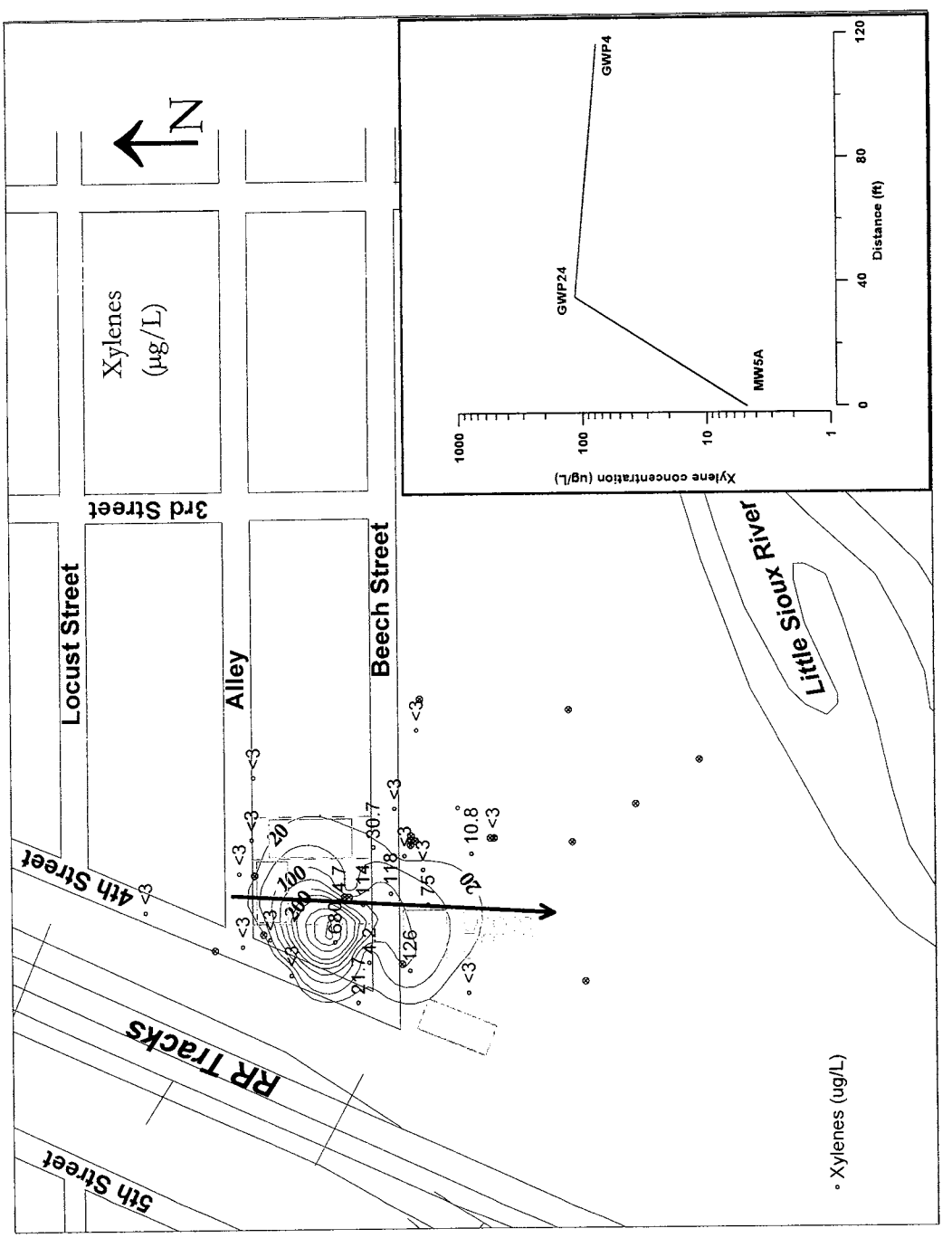

Figure D7. Contours for xylene concentration in the upper half of the aquifer (August 2001 data)

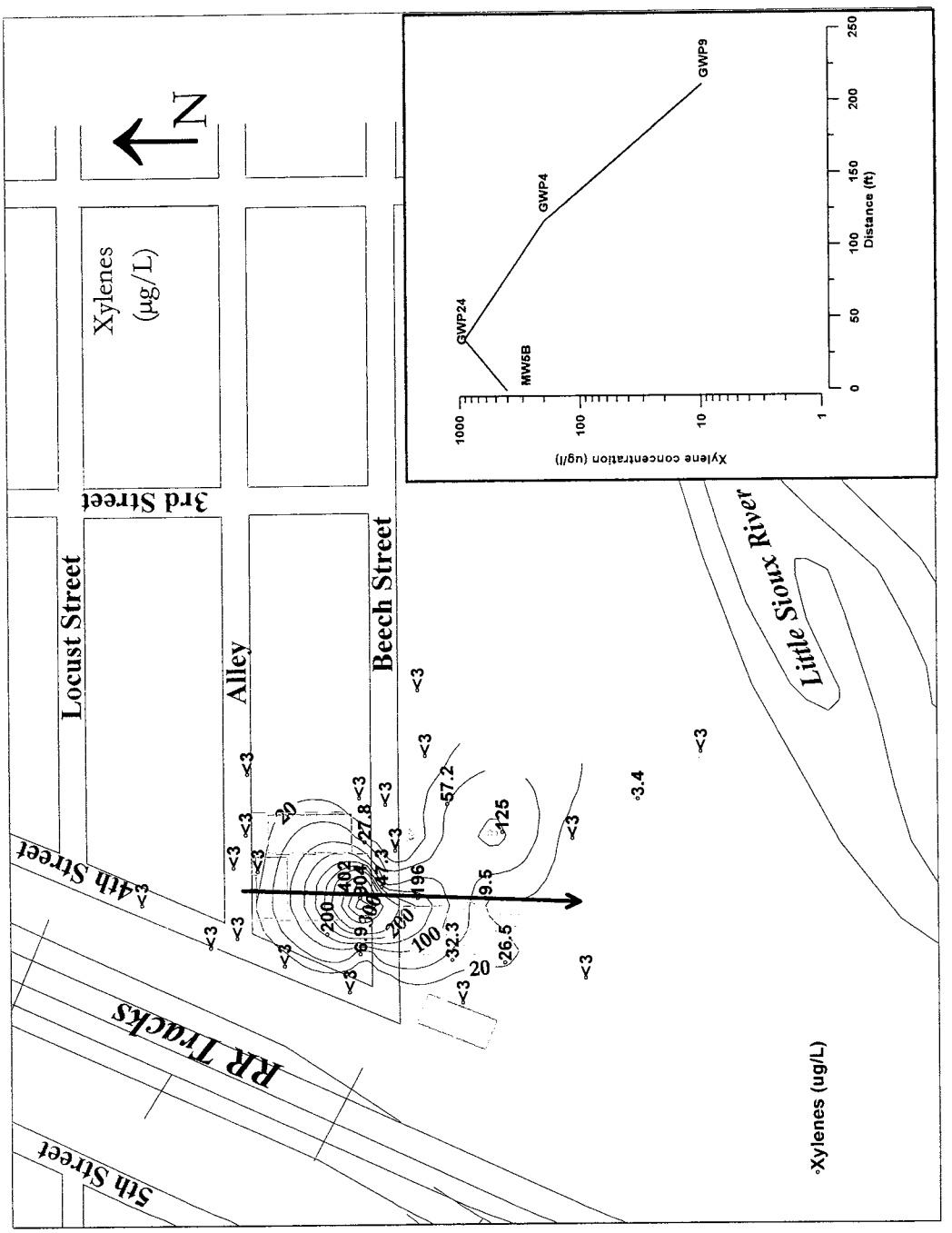

Figure D8. Contours of xylene concentration in the lower half of the aquifer (August 2001 data)

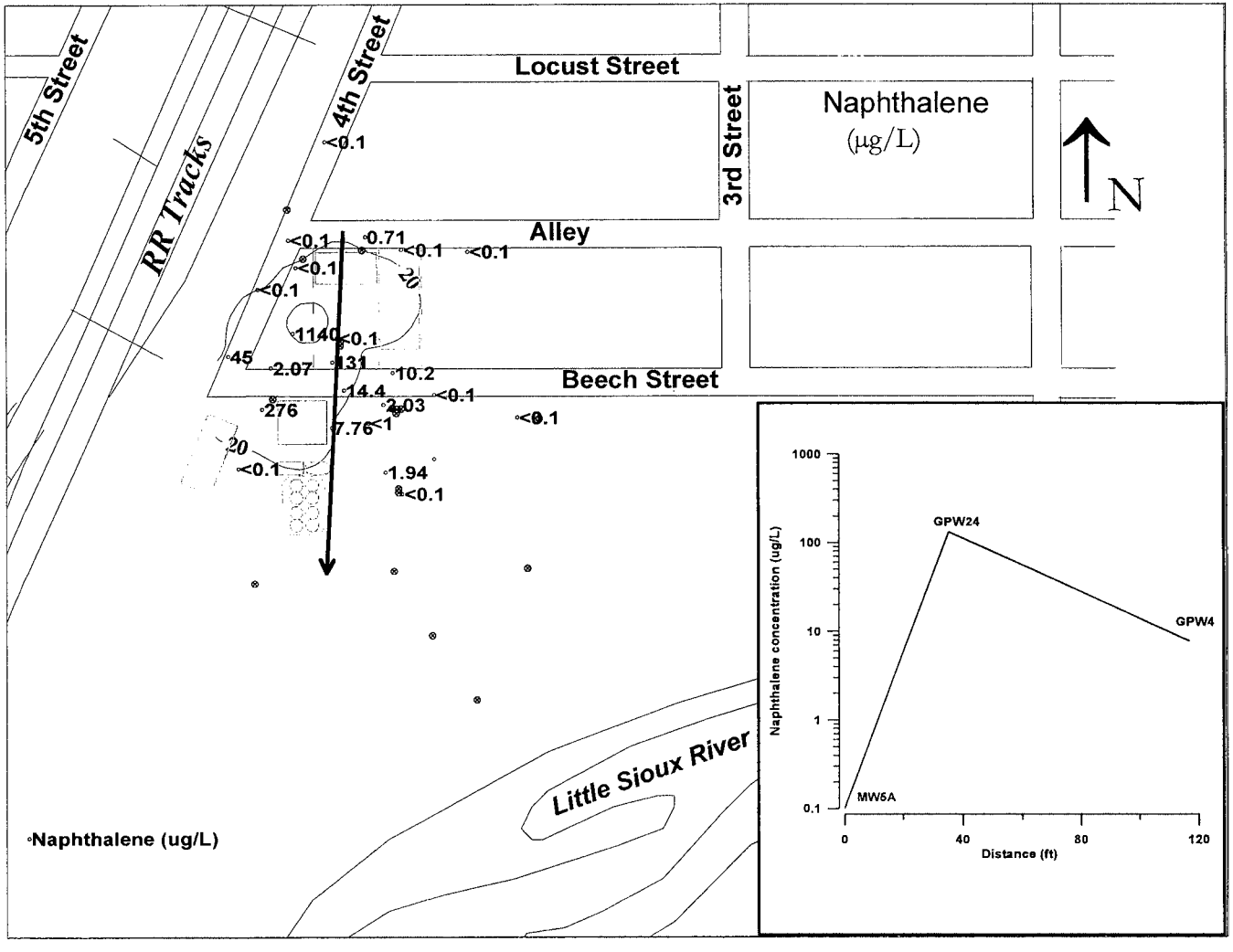

Figure D9. Contours of napthalene concentration in the upper half of the aquifer (August 2001 data)

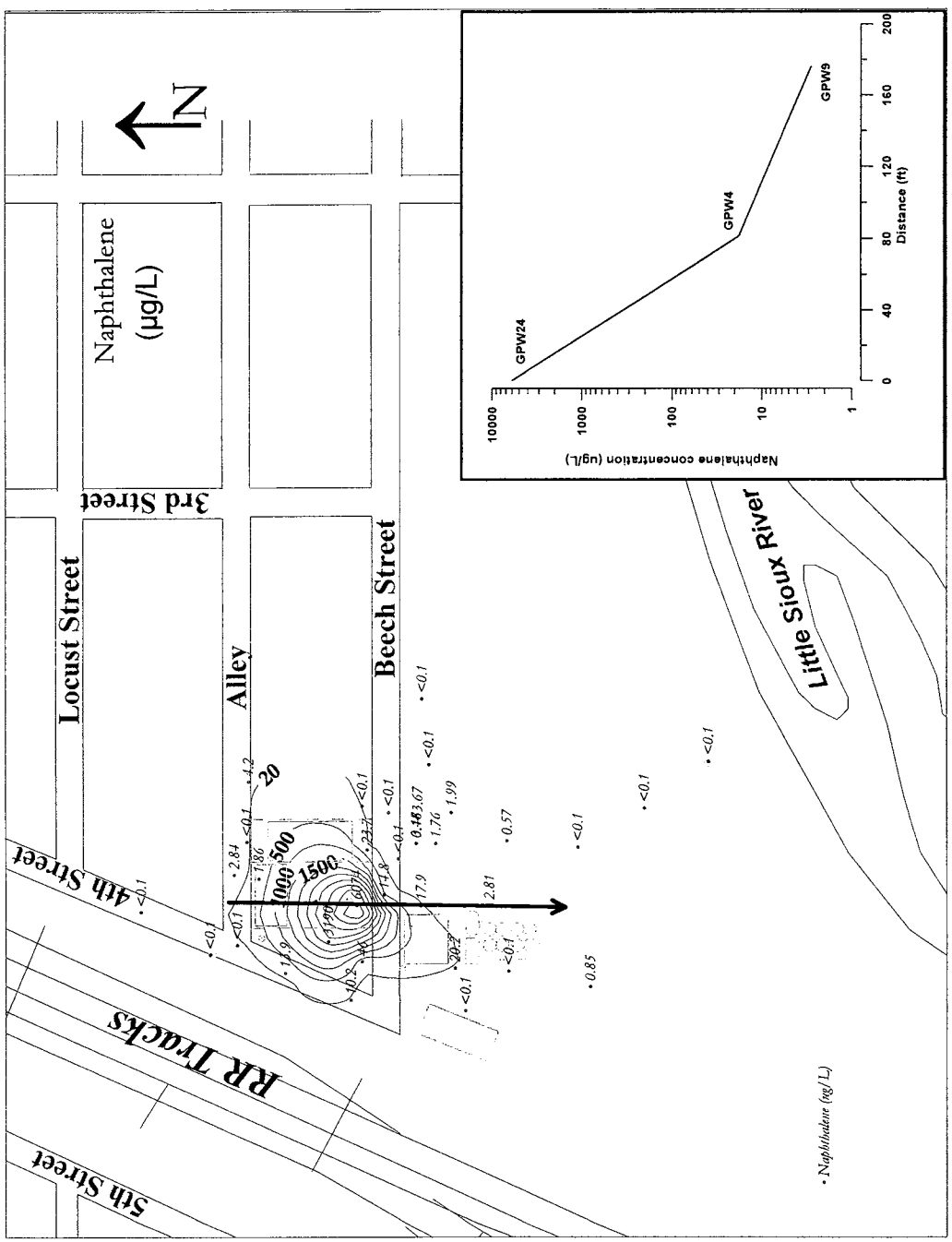

Figure D.10. Contours of napthalene concentration in the lower half of the aquifer (August 2001 data)

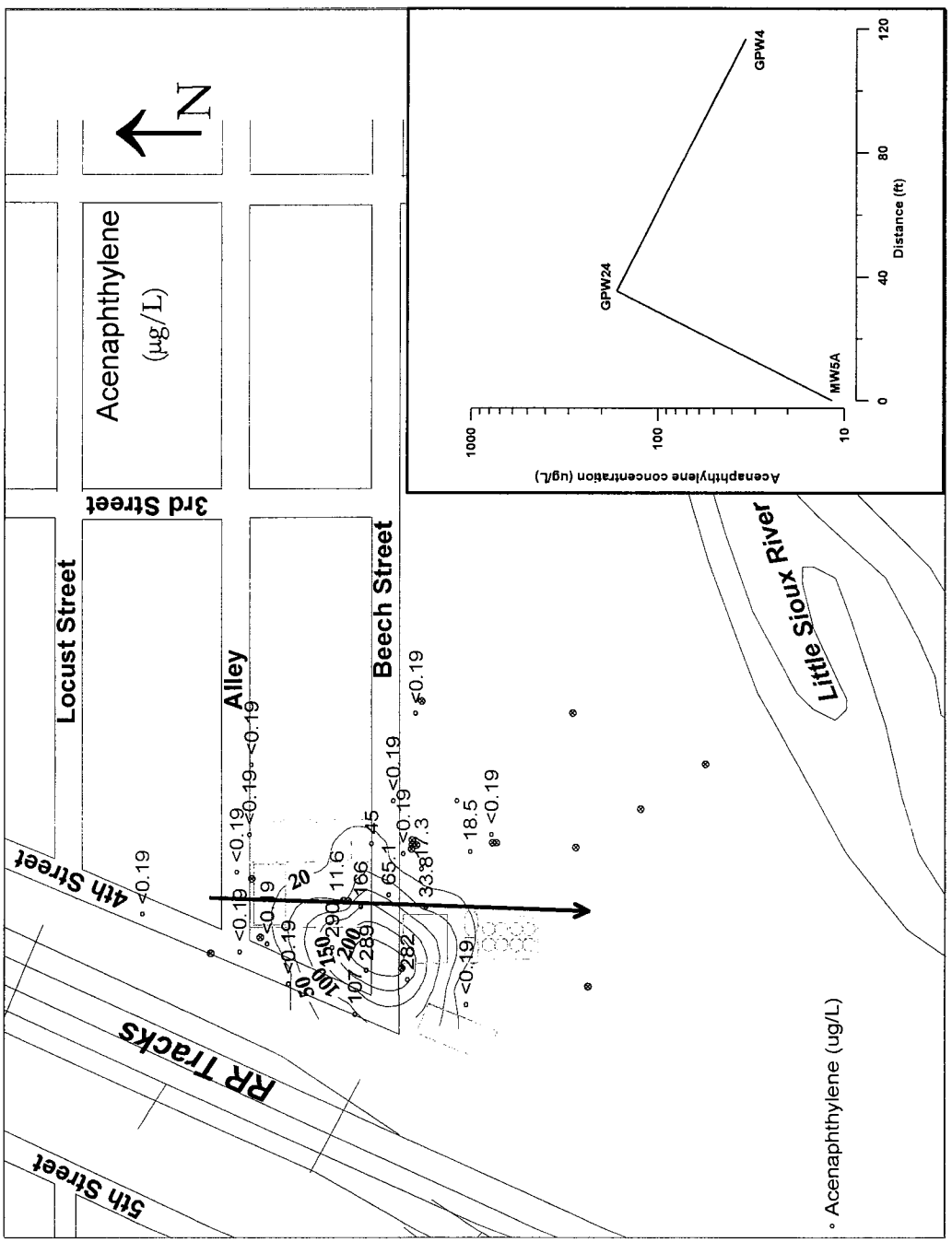

Figure D11. Contours of acenaphthylene concentration in the upper half of the aquifer (August 2001 data

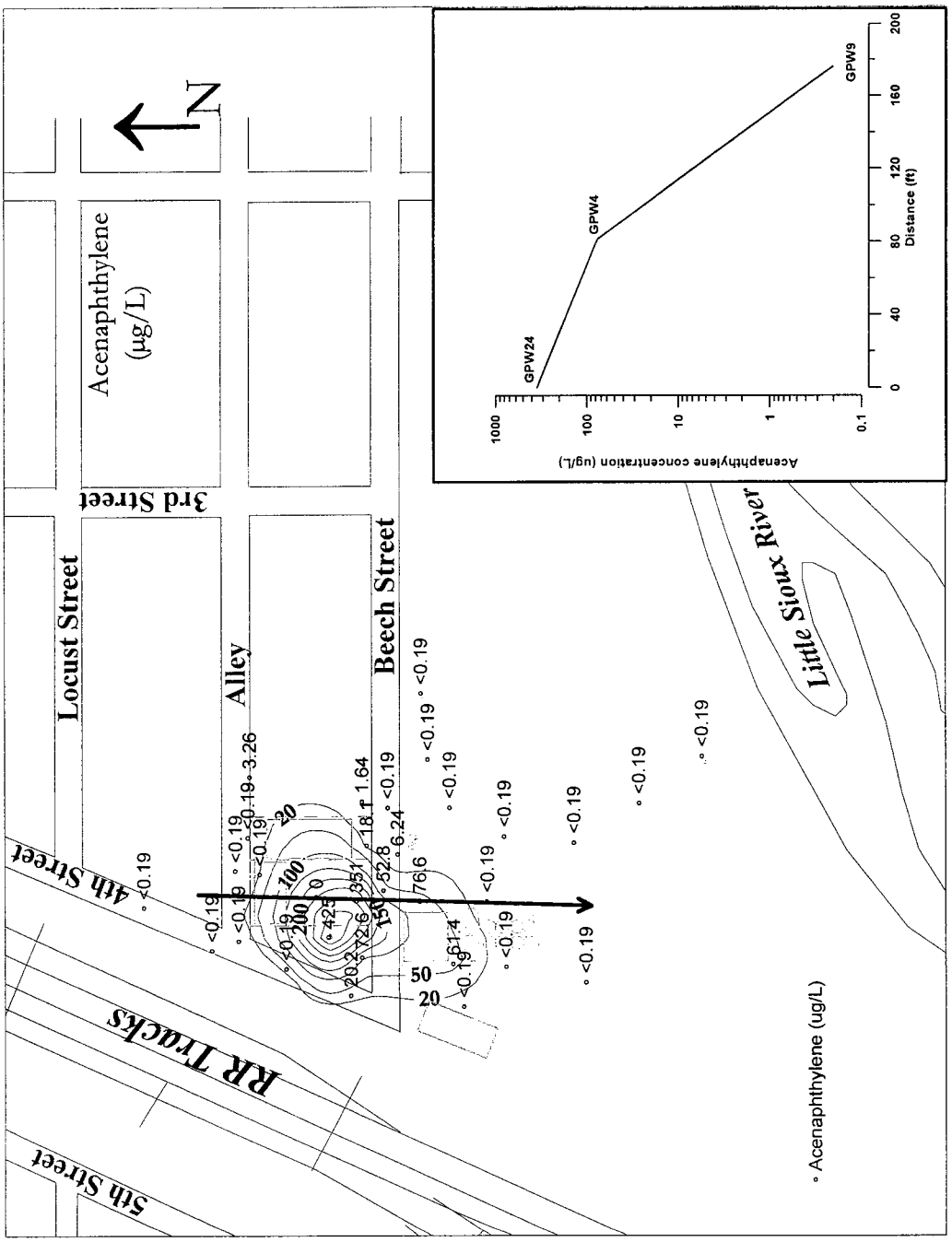

Figure D12. Contours of acenaphthylene concentration in the lower half of the aquifer (August 2001 data

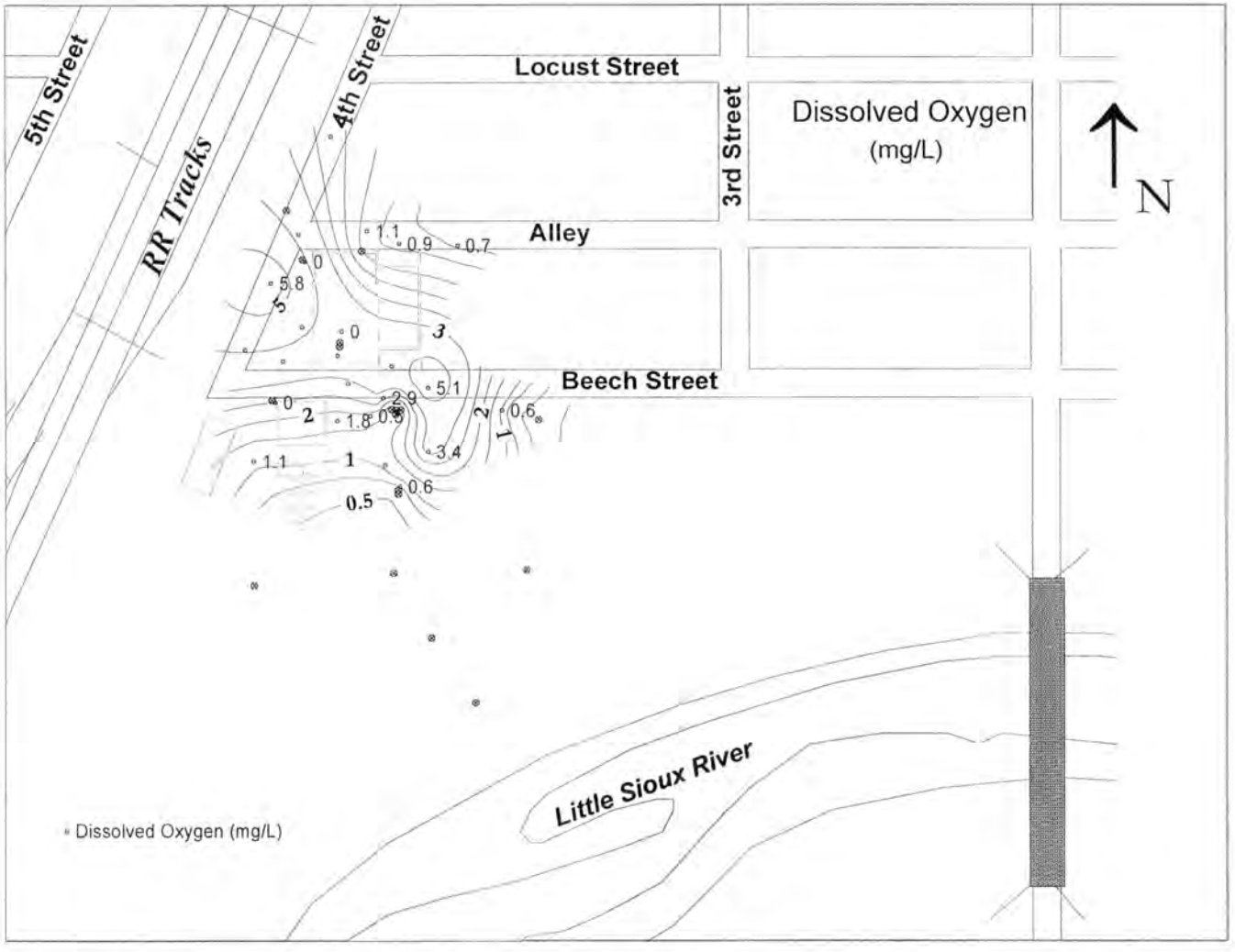

Figure D13. Contours of dissolved oxygen concentration in the upper part of the aquifer (August 2001 data)

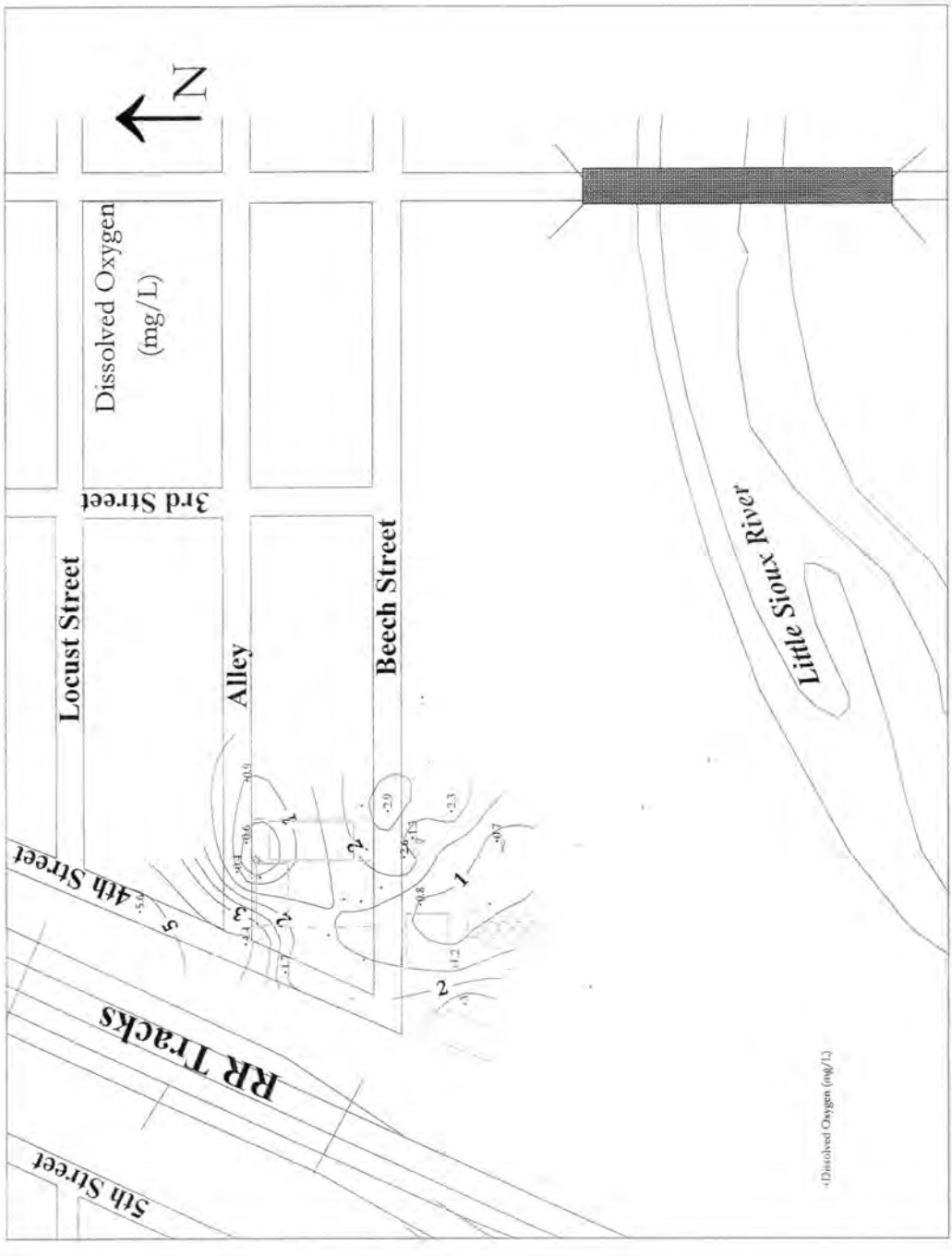

Figure D14. Contours of dissolved oxygen concentration in the lower half of the aquifer (August 2001 data)

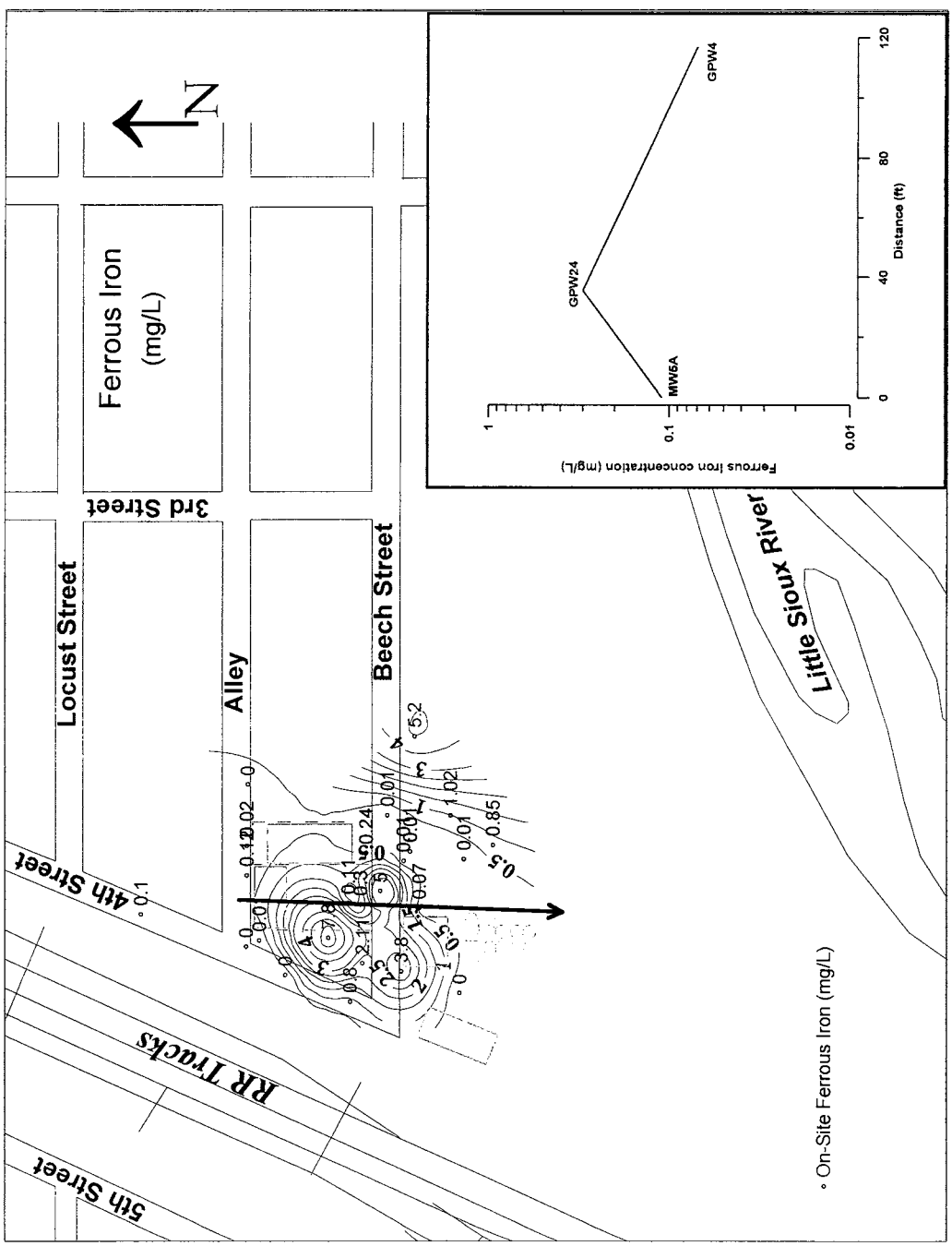

Figure D15. Contours of ferrous iron concentration in the upper half of the aquifer (August 2001 data)

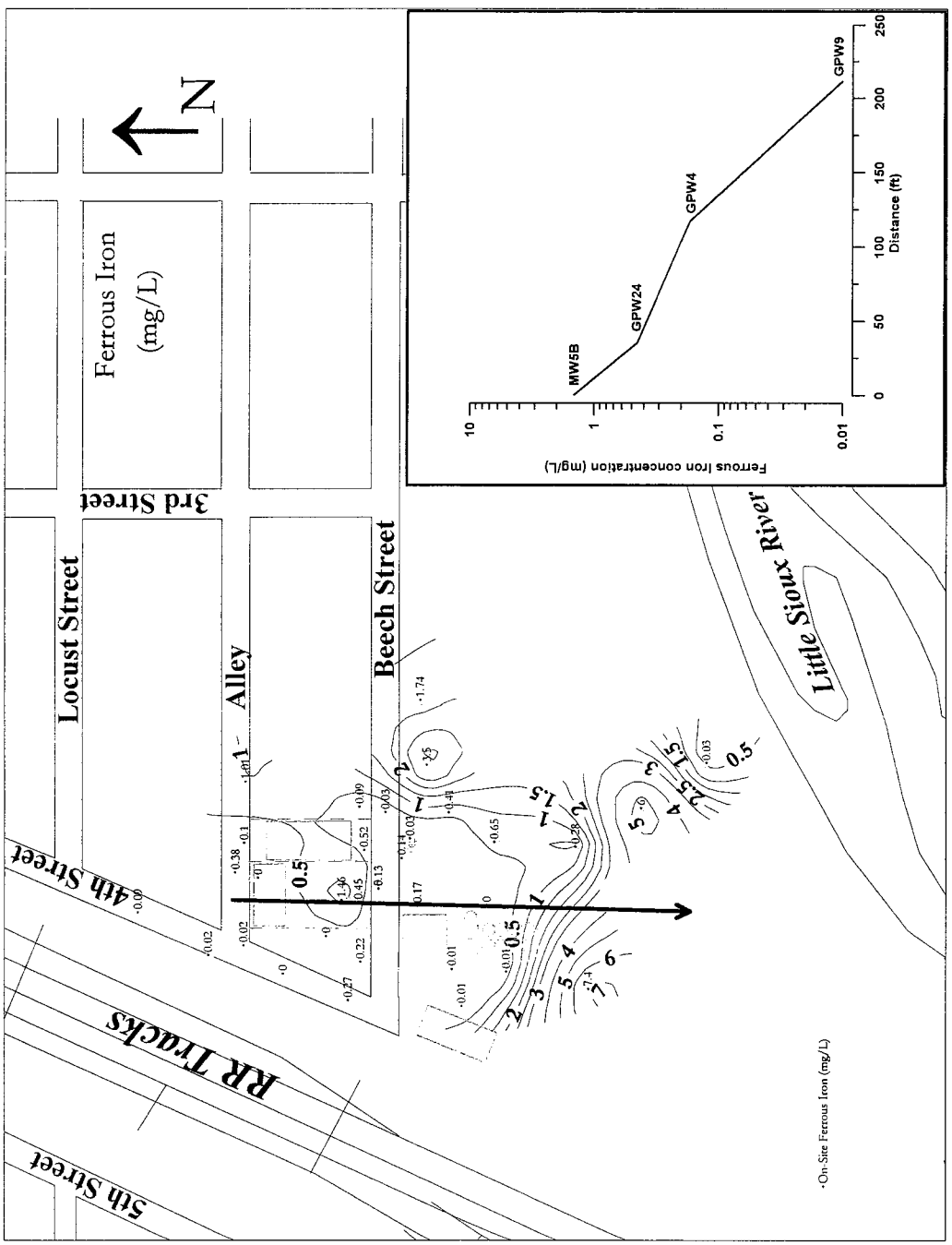

Figure D16. Contours of ferrous iron concentration in the lower half of the aquifer (August 2001 data)

Figure D17. Image showing the pneumatic method in use at Cherokee FMGP site, Iowa

APPENDIX E: FUTURE TEST LOCATIONS

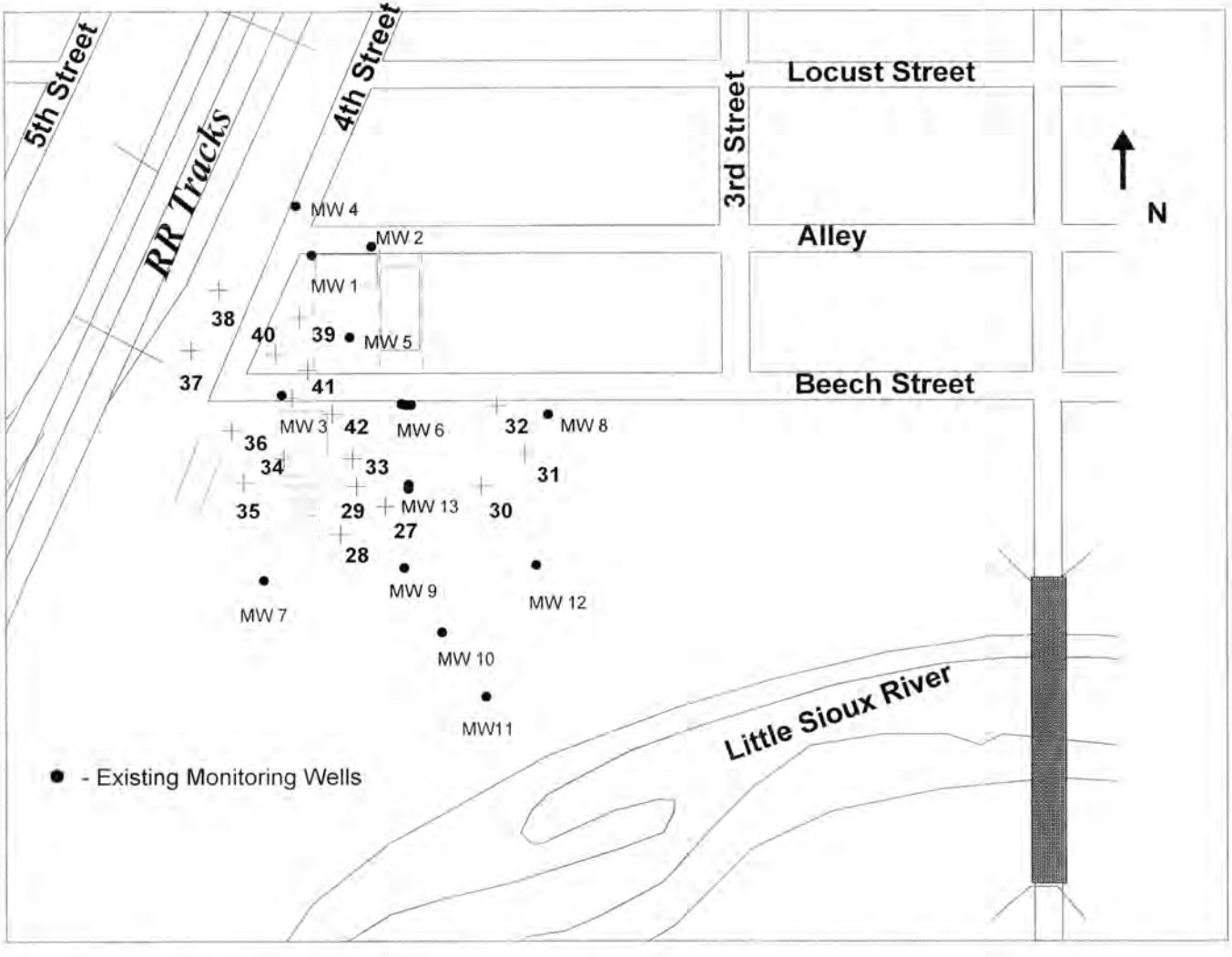

Figure E1. Proposed EC push locations for phase II site investigation at Cherokee FMGP site, Iowa

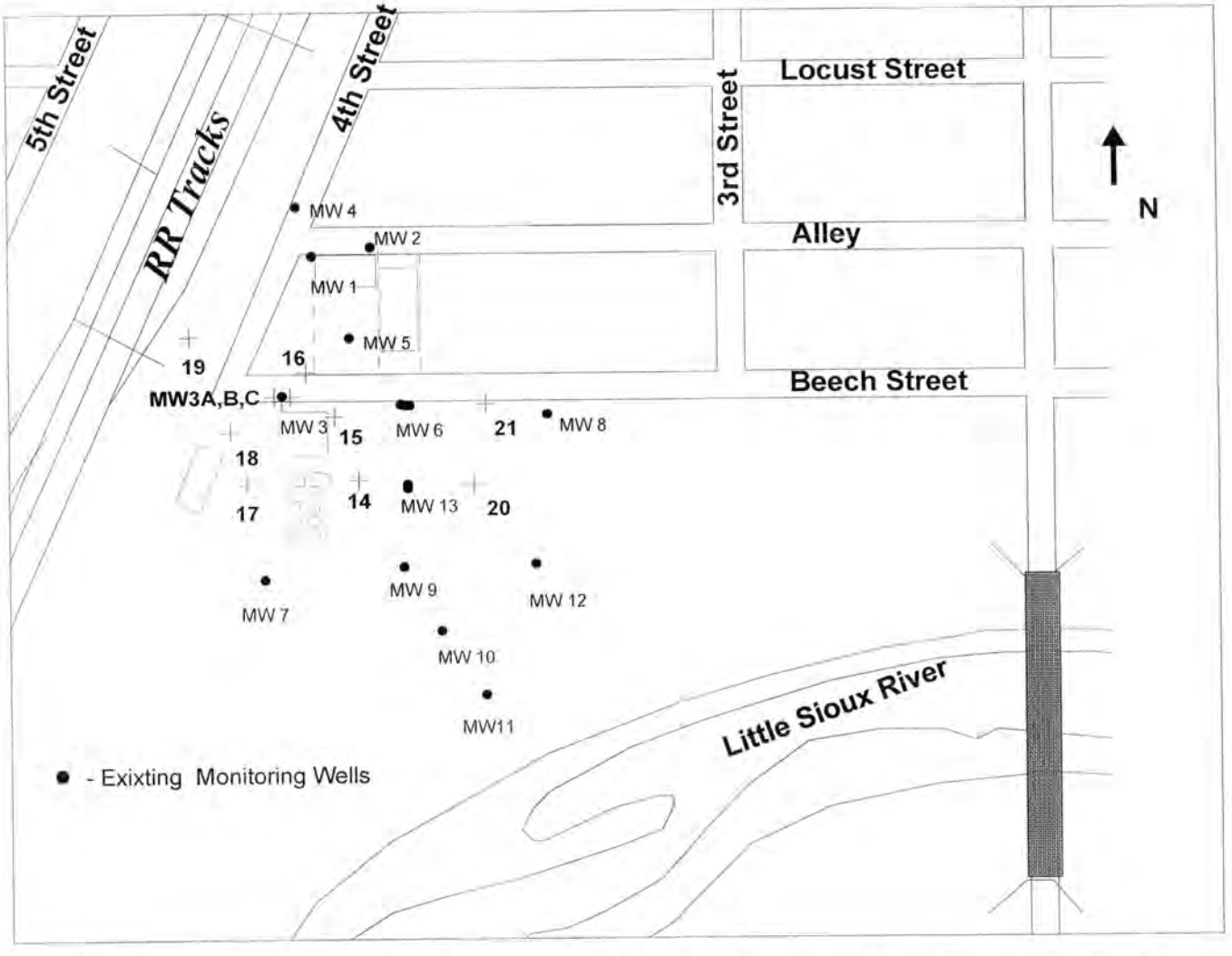

Figure E2. Proposed pre-packed screen monitoring well (GPMW) locations for phase II of site investigation at Cherokee FMGP site, Iowa

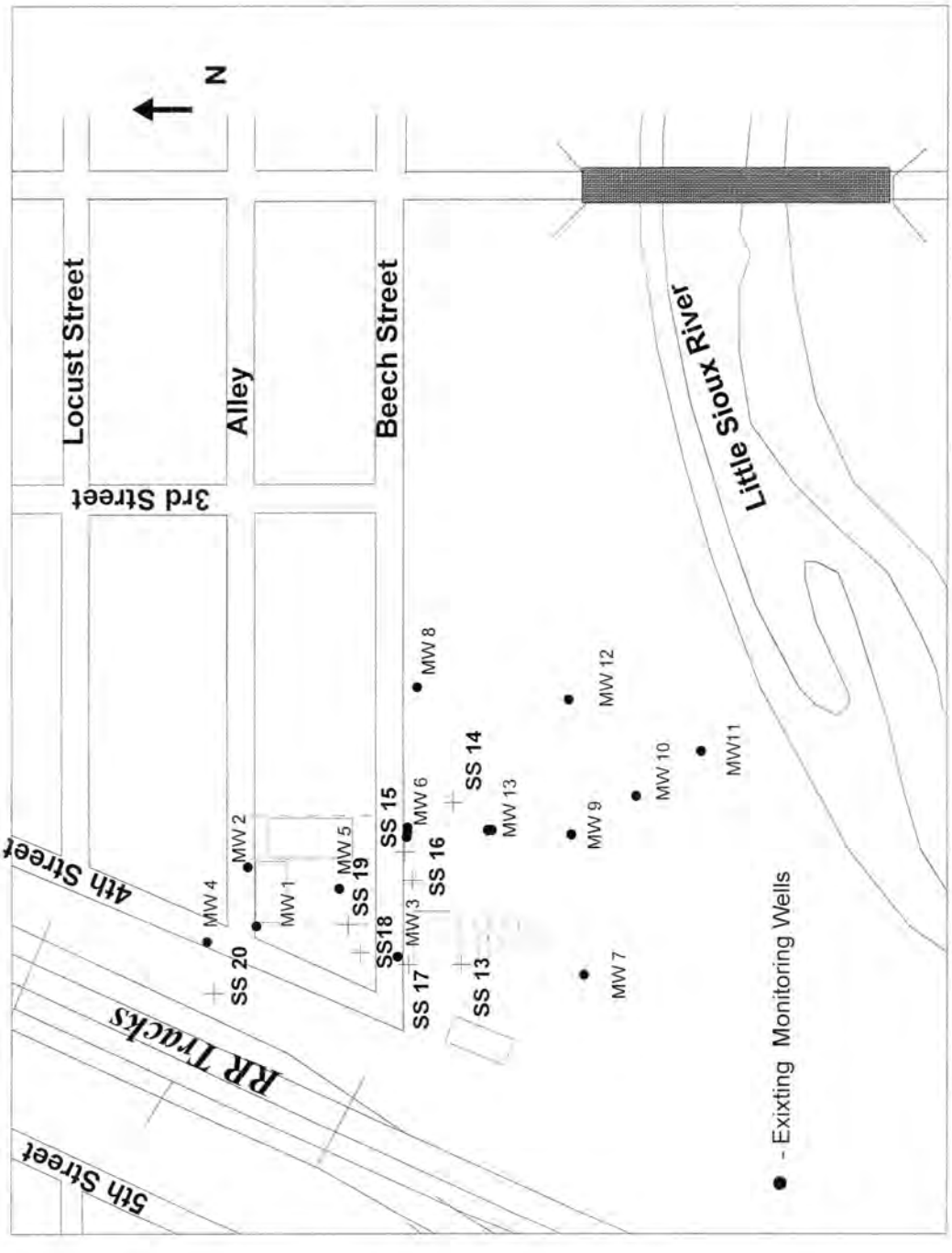

Figure E3. Proposed soil sampling locations for phase II of site investigation at Cherokee FMGP site, Iowa

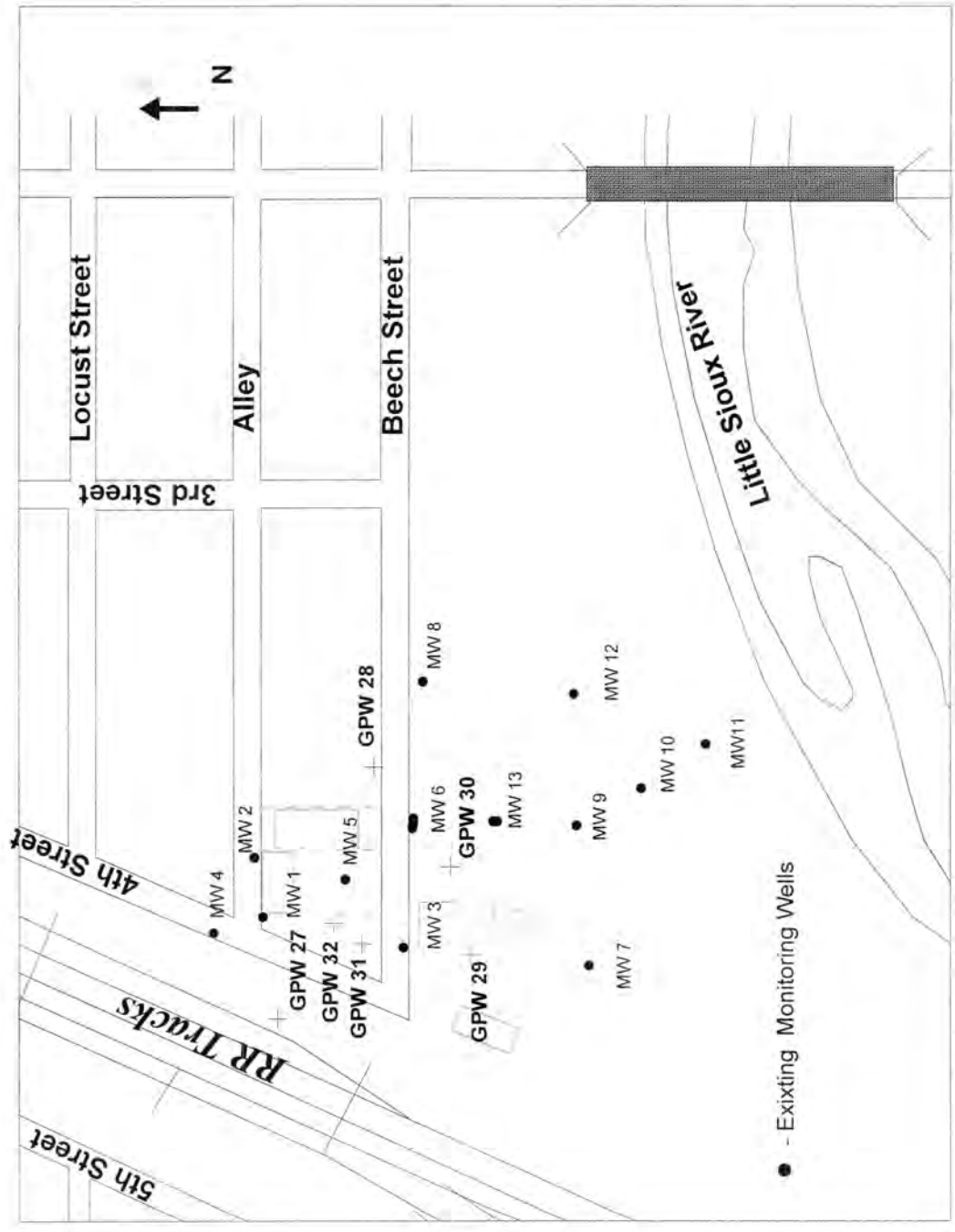

Figure E4. Proposed groundwater sampling locations for phase II of site investigation at Cherokee FMGI site. Iowa

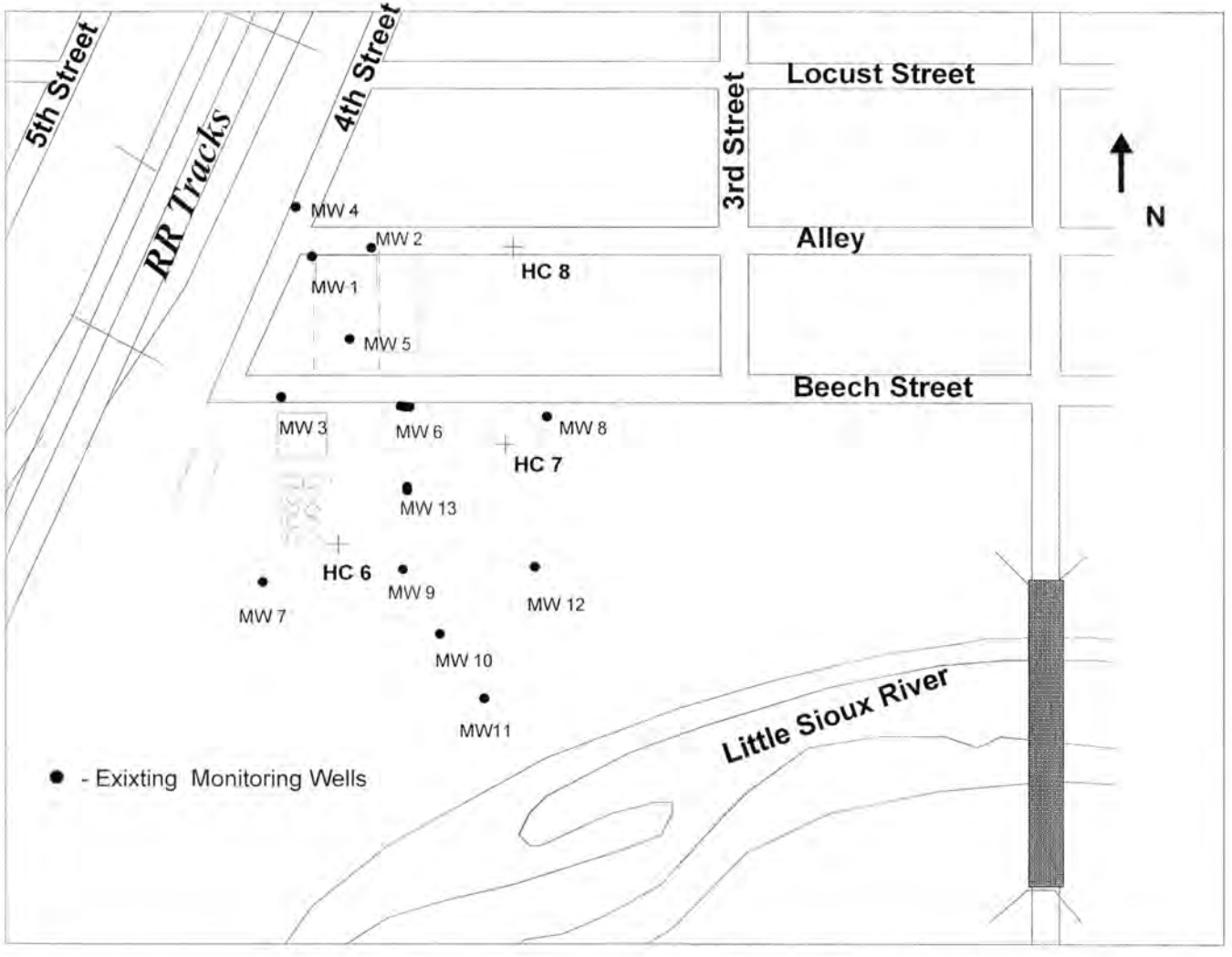

Figure E5. Proposed hydraulic conductivity test locations for phase II of site investigation at Cherokee FMGP site. Iowa

APPENDIX F: MODELING

Table F1. Top elevations of soil layers at Cherokee FMGP site, Iowa

Location	x-coordinate (ft)	y-coordinate (ft)	TOL[1] (ft)	TOA1[2] (ft)	TOA2[3] (ft)	TOT[4] (ft)
EC2	1196.05	932.12	1174.4	1165.9	1162.5	1159.1
EC3	1389.38	922.52	1170.8	1147.8	1144.6	1141.3
EC4	1008.89	849.64	1177.2	1166.7	1163.7	1160.7
EC5	1040.86	860.07	1178.4	1166.7	1162.2	1157.7
EC6	1118.41	900.06	1175.6	1167.3	1161.5	1155.8
EC7	1257.08	950.7	1174.4	1165.9	1161.9	1157.9
EC8	1037.89	782.69	1169.8	1156.3	1154.1	1151.8
EC9	1122.99	810.18	1173	1157.7	1153.5	1149.2
EC10	1254.93	862.68	1172.2	1147.7	1144.9	1142.2
EC11	1321.79	889.25	1171.3	1147.8	1147.1	1146.3
EC12	1117.41	1293.56	1189.7	1187.2	1170.5	1153.9
EC13	1293.52	1117.41	1181.8	1176.8	1167.3	1157.8
EC14	1207.64	1141.78	1183.8	1176.8	1165.3	1153.8
EC16	1078.63	1158.6	1183.4	1167.4	1167.4	1151.4
EC17	1032.39	1088.7	1186.9	1176.4	1167.4	1158.4
EC18	1089.22	1033.66	1184.4	1175.4	1165.4	1155.4
EC19	1154.38	953.45	1176.4	1169.4	1162.7	1155.9
EC20	998.63	993.89	1181.6	1176.1	1164.3	1152.6
EC21	1126.02	986.67	1178.5	1171.3	1162.3	1153.3
EC22	1202.95	982.57	1173.2	1170.2	1163.6	1156.9
EC23	1258.61	986.53	1175.9	1168.9	1164.6	1160.4
EC24	930.9	700.6	1171.8	1149.5	1144.4	1139.3
EC25A	1046.57	616.34	1172.4	1147.9	1142.6	1137.4
MW1	1086.4	1126.8	1183	1182.9	1171	1159
MW2	1163	1137	1182	1181.9	1169.5	1157
MW3	1046.54	944.7	1177.5	1169.3	1163.1	1156.8
MW4	1065.76	1190.13	1186.7	1178.9	1169	1159.1
MW5	1134.69	1019.67	1176.2	1173.7	1162.5	1151.3
MW6	1207.56	931.42	1174.3	1167	1161.5	1156
MW7	1022.65	704.16	1169.5	1148.5	1142.5	1136.5
MW9	1203.86	720.36	1169.9	1148.4	1145.9	1143.4

Table F1. Top elevations of soil layers at Cherokee FMGP site, Iowa (continued)

Location	x-coordinate (ft)	y-coordinate (ft)	TOL[1] (ft)	TOA1[2] (ft)	TOA2[3] (ft)	TOT[4] (ft)
MW10	1252.98	636.78	1167.5	1148.5	1143	1137.5
MW11	1310.98	552.83	1166.5	1155	1143.3	1131.5
GWP A1	990.5	827.1	1169.1	1163.5	1161.5	1159.5
GWP A2	1121.9	828.9	1169.5	1162	1158	1154
GWP A3	1216.9	831.6	1168.9	1146.9	1145.7	1144.4
GWP A4	1307.4	833.2	1172.2	1148.7	1145	1141.2
GWP A5	1403.4	833.1	1171.5	1147	1145.5	1144
GWP A6	883.4	822.1	1173.2	1167.7	1165.1	1162.5
GWP B1	1112.5	728.5	1171.4	1146.4	1144.9	1143.4
GWP B2	1215.8	729.8	1170.1	1146.7	1140.7	1134.6
GWP B3	1318.9	732	1167.9	1151.6	1143.7	1135.7
GWP B4	1422.4	733.2	1170.5	1147	1141	1135
GWP C2	1217.5	627.8	1170.5	1151.5	1143.5	1135.5
GWP C3	1321.8	630.2	1165.6	1150.6	1142.8	1135
GWP D1	931.9	924.1	1174.6	1170.6	1167.7	1164.8
GWP D2	1335.6	931.2	1167	1155	1148.8	1142.5
Artificial1*	1186	1080	1179	1173	1164	1155
Artificial2*	1332	1065	1178	1160	1155.5	1151
Artificial3*	1457	662	1170	1147	1141	1135
Artificial4*	1391	603	1167	1147	1141	1135
Artificial5*	1186	522	1167	1150	1141	1132
Artificial6*	1075	456	1168	1147	1139	1131
Artificial7*	1097	560	1168	1147	1139.5	1132
Artificial8*	1127	655	1172	1152	1143.5	1135
Artificial8*	863	933	1174	1170	1167	1164

[1]- Top of loess layer
[2]- Top of shallow aquifer layer
[3]- Top of deeper aquifer layer
[4]- Top of till layer
*- Fake pushes generated for smooth interpolation of layers elevations

Table F2. Comparison of simulated and observed piezometric heads with recharge as input parameter

Monitoring Well Location	Simulated Head (ft)	Observed Head (ft)	Difference (ft)	Square of Difference
MW1	1176.32	1176.28	0.04	0.0016
MW2	1176.32	1176.29	0.03	0.0009
MW3	1176.17	1176.33	-0.16	0.0256
MW4	1176.33	1176.27	0.06	0.0036
MW5B	1176.3	1176.22	0.08	0.0064
MW6	1176	1176.13	-0.13	0.0169
MW7	1159.8	1159.73	0.07	0.0064
MW8	1164	1163.21	0.79	0.624
MW9	1159.75	1160.35	-0.6	0.36
MW10	1158.09	1158.53	-0.44	0.1936
MW11	1158.08	1158.53	-0.44	0.1936
MW12	1158.14	1157.7	0.43	0.185
MW13B	1167.4	1165.9	1.5	2.25
			Total square of difference=	3.86
			Root mean square of difference=	0.54

Table F3. Linear sorption coefficients (K_d, ml/g) for BTEX and PAH compounds with depth at soil sampling location

Location			**SS2(L*)**	**SS2(A**)**	**SS2(A)**	**SS5(A)**	**SS5(A)**	**SS6(L)**	**SS6(A)**	**SS6(A)**
Depth			**4-8**	**18-20**	**24-26**	**12-14**	**16-18.5**	**6-8**	**12-14**	**16-18**
f_{oc}(%)			**0.29**	**0.25**	**0.2**	**0.8**	**0.3**	**3.05**	**2.6**	**0.35**
Compound	**log K_{ow}**	**K_{oc} (ml/g)**								
Benzene	2.12	83	0.24	0.21	0.17	0.66	0.25	2.53	2.16	0.29
Toulene	2.73	300	0.87	0.75	0.60	2.40	0.90	9.15	7.80	1.05
Ethylbenzene	3.15	1100	3.19	2.75	2.20	8.80	3.30	33.55	28.60	3.85
Xylene (p-xylene)	3.26	240	0.70	0.60	0.48	1.92	0.72	7.32	6.24	0.84
Naphthalene	3.37	1300	3.77	3.25	2.60	10.40	3.90	39.65	33.80	4.55
Acenapthlene	4	4500	13.05	11.25	9.00	36.00	13.50	137.25	117.00	15.75
Acenapthylene	3.7	2500	7.25	6.25	5.00	20.00	7.50	76.25	65.00	8.75
Anthracene	4.45	14000	40.60	35.00	28.00	112.00	42.00	427.00	364.00	49.00
Fluorene	4.18	7300	21.17	18.25	14.60	58.40	21.90	222.65	189.80	25.55
Phenanthrene	4.46	14000	40.60	35	28	112	42	427	364	49
Fluoranthene	4.9	38000	110.20	95	76	304	114	1159	988	133
Pyrene	4.88	38000	110.20	95	76	304	114	1159	988	133
Chrysene	5.61	200000	580	500	400	1600	600	6100	5200	700
Benzo(a)anthracene	5.6	1300000	3770	3250	2600	10400	3900	39650	33800	4550
Benzo(b)fluoranthene	6.06	550000	1595	1375	1100	4400	1650	16775	14300	1925
Benzo(k)fluoranthene	6.06	550000	1595	1375	1100	4400	1650	16775	14300	1925
Benzo(a)pyrene	6.06	5500000	15950	13750	11000	44000	16500	167750	143000	19250
Dibenzo(a,h)anthracene	6.8	3300000	9570	8250	6600	26400	9900	100650	85800	11550
Ideno(1,2,3-cd)pyrene	6.5	1600000	4640	4000	3200	12800	4800	48800	41600	5600
Benzo(g,h,i)perylene	6.51	1600000	4640	4000	3200	12800	4800	48800	41600	5600

Table F3. Linear sorption coefficients (K_d, ml/g) for BTEX and PAH compounds with depth at soil sampling location (continued)

Location			SS8(L)	SS8(A)	SS8(A)	SS10(L)	SS10(A)	SS12(L)	SS12(L)	HC5(L)	HC5(A)
Depth			8-10	10-12	16-18	12-13.5	16-18	8-10	16-18.5	12-16	22-26
f_{oc}(%)			0.3	0.2	0.15	2.6	2.9	0.7	3.9	0.35	0.3
Compound	log K_{ow}	K_{oc} (ml/g)									
Benzene	2.12	83	0.249	0.17	0.12	2.16	2.41	0.58	3.24	0.29	0.25
Toluene	2.73	300	0.9	0.60	0.45	7.80	8.70	2.10	11.70	1.05	0.90
Ethylbenzene	3.15	1100	3.3	2.20	1.65	28.60	31.90	7.70	42.90	3.85	3.30
Xylene (p-xylene)	3.26	240	0.72	0.48	0.36	6.24	6.96	1.68	9.36	0.84	0.72
Naphthalene	3.37	1300	3.9	2.60	1.95	33.80	37.70	9.10	50.70	4.55	3.90
Acenapthene	4	4500	13.5	9.00	6.75	117	130.50	31.50	175.50	15.75	13.50
Acenapthylene	3.7	2500	7.5	5.00	3.75	65	72.50	17.50	97.50	8.75	7.50
Anthracene	4.45	14000	42	28.0	21	364	406	98	546	49	42
Fluorene	4.18	7300	21.9	14.6	11	189.8	211.7	51.1	284.7	25.6	21.9
Phenanthrene	4.46	14000	42	28	21	364	406	98	546	49	42
Fluoranthene	4.9	38000	114	76	57	988	1102	266	1482	133	114
Pyrene	4.88	38000	114	76	57	988	1102	266	1482	133	114
Chrysene	5.61	200000	600	400	300	5200	5800	1400	7800	700	600
Benzo(a)anthracene	5.6	1300000	3900	2600	1950	33800	37700	9100	50700	4550	3900
Benzo(b)fluoranthene	6.06	550000	1650	1100	825	14300	15950	3850	21450	1925	1650
Benzo(k)fluoranthene	6.06	550000	1650	1100	825	14300	15950	3850	21450	1925	1650
Benzo(a)pyrene	6.06	5500000	16500	11000	8250	143000	159500	38500	214500	19250	16500
Dibenzo(a,h)anthracene	6.8	3300000	9900	6600	4950	85800	95700	23100	128700	11550	9900
Ideno(1,2,3-cd)pyrene	6.5	1600000	4800	3200	2400	41600	46400	11200	62400	5600	4800
Benzo(g,h,i)perylene	6.51	1600000	4800	3200	2400	41600	46400	11200	62400	5600	4800

* - Loess

** - Alluvium

Table F4. Retardation Coefficient for BTEX and PAH compounds with depth at soil sapling location

Location	SS2(L*)	SS2(A**)	SS2(A)	SS5(A)	SS5(A)	SS6(L)	SS6(A)	SS6(A)
Depth	**4-8**	**18-20**	**24-26**	**12-14**	**16-18.5**	**6-8**	**12-14**	**16-18**
Compound								
Benzene	1.63	2.31	2.05	5.21	2.58	7.58	14.67	2.84
Toluene	3.26	5.75	4.80	16.20	6.70	24.79	50.40	7.65
Ethylbenzene	9.29	18.42	14.93	56.73	21.90	88.23	182.13	25.38
Xylene (p-xylene)	2.81	4.80	4.04	13.16	5.56	20.03	40.52	6.32
Naphthalene	10.80	21.58	17.47	66.87	25.70	104.09	215.07	29.82
Acenapthene	34.93	72.25	58	229	86.50	357.85	742	100.75
Acenapthylene	19.85	40.58	32.67	127.67	48.50	199.25	412.67	56.42
Anthracene	106.56	222.67	178.33	710.33	267.00	1111.20	2306.33	311.33
Fluorene	56.04	116.58	93.47	370.87	139.70	579.89	1203.07	162.82
Phenanthrene	106.56	222.67	178.33	710.33	267	1111.20	2306.33	311.33
Fluoranthene	287.52	602.67	482.33	1926.33	723	3014.40	6258.33	843.33
Pyrene	287.52	602.67	482.33	1926.33	723	3014.40	6258.33	843.33
Chrysene	1509	3167.67	2534.33	10134.33	3801	15861	32934.33	4434.33
Benzo(a)anthracene	9803	20584.33	16467.67	65867.67	24701	103091	214067.67	28817.67
Benzo(b)fluoranthene	4148	8709.33	6967.67	27867.67	10451	43616	90567.67	12192.67
Benzo(k)fluoranthene	4148	8709.33	6967.67	27867.67	10451	43616	90567.67	12192.67
Benzo(a)pyrene	41471	87084.33	69667.67	278667.67	104501	436151	905667.67	121917.67
Dibenzo(a,h)anthracene	24883	52251	41801	167201	62701	261691	543401	73151
Ideno(1,2,3-cd)pyrene	12065	25334.33	20267.67	81067.67	30401	126881	263467.67	35467.67
Benzo(g,h,i)perylene	12065	25334.33	20267.67	81067.67	30401	126881	263467.67	35467.67

Table F4. Retardation Coefficient for BTEX and PAH compounds with depth at soil sapling location (continued)

Location	SS8(L)	SS8(A)	SS8(A)	SS10(L)	SS10(A)	SS12(L)	SS12(L)	HC5(L)	HC5(A)
Depth	**8-10**	**10-12**	**16-18**	**12-13.5**	**16-18**	**8-10**	**16-18.5**	**12-16**	**22-26**
Compound									
Benzene	1.78	2.05	1.7885	6.6108	16.24	2.5106	9.4162	1.7553	2.577
Toluene	1.6474	4.80	3.85	21.28	56.10	6.46	31.42	3.73	6.7
Ethylbenzene	3.34	14.93	11.45	75.36	203.03	21.02	112.54	11.01	21.9
Xylene (p-xylene)	9.58	4.04	3.28	17.224	45.08	5.368	25.336	3.184	5.56
Naphthalene	2.872	17.47	13.35	88.88	239.77	24.66	132.82	12.83	25.7
Acenapthene	11.14	58.00	43.75	305.2	827.50	82.9	457.3	41.95	86.5
Acenapthylene	36.1	32.67	24.75	170	460.17	46.5	254.5	23.75	48.5
Anthracene	20.5	178.33	134	947.4	2572.33	255.8	1420.6	128.4	267
Fluorene	110.2	93.47	70.35	494.48	1341.77	133.86	741.22	67.43	139.7
Phenanthrene	57.94	178.33	134	947.4	2572.33	255.8	1420.6	128.4	267
Fluoranthene	110.2	482.33	362	2569.8	6980.33	692.6	3854.2	346.8	723
Pyrene	297.4	482.33	362	2569.8	6980.33	692.6	3854.2	346.8	723
Chrysene	297.4	2534.33	1901	13521	36734.33	3641	20281	1821	3801
Benzo(a)anthracene	1561	16467.67	12351	87881	238767.67	23661	131821	11831	24701
Benzo(b)fluoranthene	10141	6967.67	5226	37181	101017.67	10011	55771	5006	10451
Benzo(k)fluoranthene	4291	6967.67	5226	37181	101017.67	10011	55771	5006	10451
Benzo(a)pyrene	4291	69667.67	52251	371801	1010167.67	100101	557701	50051	104501
Dibenzo(a,h)anthracene	42901	41801	31351	223081	606101.00	60061	334621	30031	62701
Ideno(1,2,3-cd)pyrene	25741	20267.67	15201	108161	293867.67	29121	162241	14561	30401
Benzo(g,h,i)perylene	12481	20267.67	15201	108161	293867.6667	29121	162241	14561	30401

* - Loess

** - Alluvium

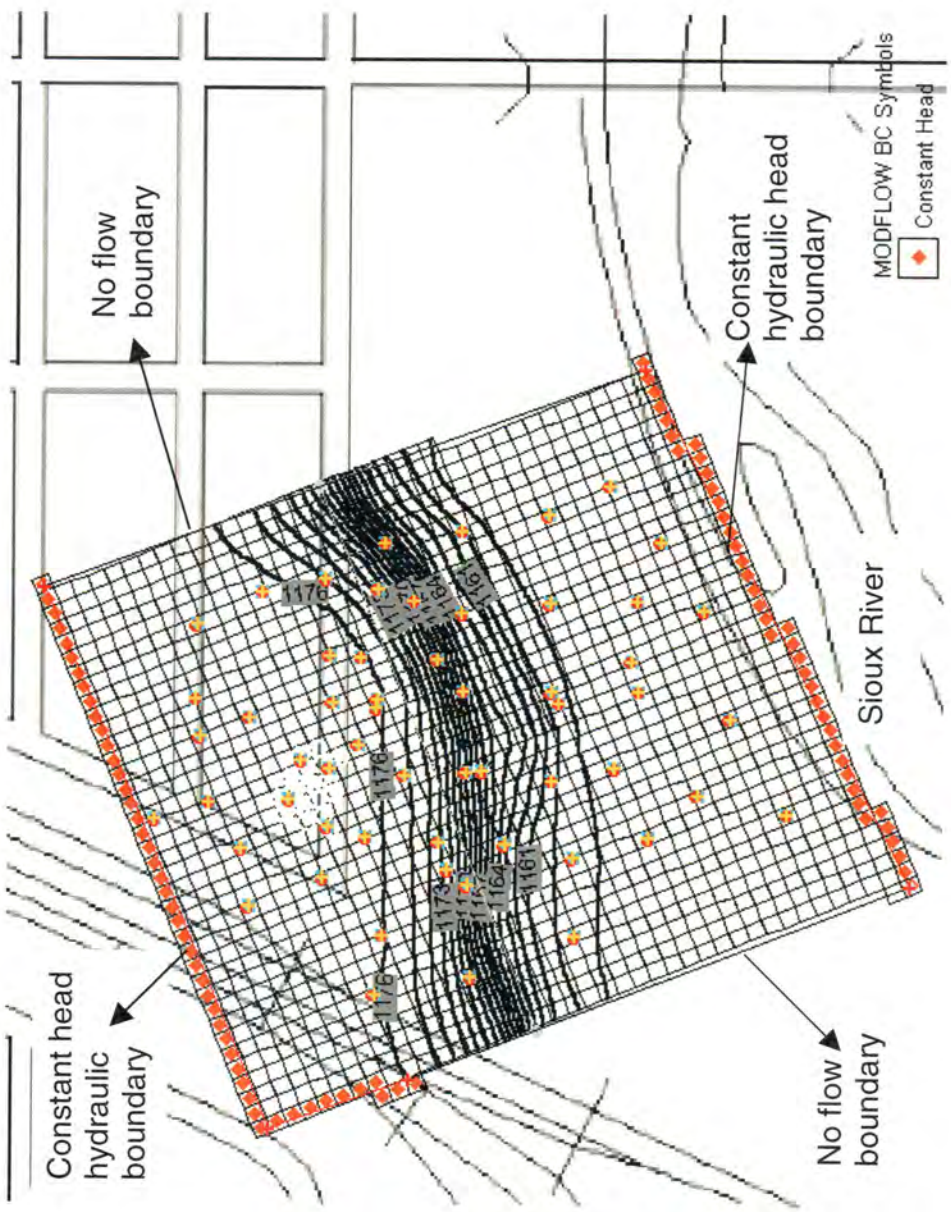

Figure F1. Hydraulic heads as simulated by MODFLOW with recharge as input parameter